Latitudinal variation in the demography and life history of a temperate marine herbivorous fish *Odax pullus* (Labridae)

By

Elizabeth Danièle Laman Trip

A thesis presented in fulfilment of the requirements for the degree of
Doctor of Philosophy
School of Biological Sciences
University of Auckland, 2009

Abstract

This thesis examined latitudinal variation in the demography and life history of a temperate marine herbivorous fish, *Odax pullus* (Labridae). Over 1000 individuals were collected at six locations across ~13^{o} of latitude, and an age-based approach was used to establish the patterns of variation in growth rate, size-at-age, development rate (size- and age-at-maturity and -at-sex change), life span, and rate of physiological ageing. Firstly, an otolith-based ageing procedure was developed following successful validation of the daily and annual periodicity of opaque zone formation, and histological analysis of the reproductive biology of *O. pullus* was combined with sex-specific demographic information to establish a diagnosis of monandric protogynous sex change. Secondly, a "biota-environment linkage" approach was used to explore the patterns of geographic variation in life history and the effects of potential underlying environmental factors (sea surface temperature, species density, habitat and food availability, exposure, and extrinsic mortality). Significant latitudinal trends in growth, body size, development, and longevity were identified along a broad North – South gradient, with individuals growing slower, maturing and changing sex later, achieving larger body sizes and living longer at higher latitudes. The main effects of latitude on the phenotypic response of life histories were related to the latitudinal gradient in environmental temperature. Species density and habitat (food) availability also affected the responses in body size and development, and these effects were detected on a local spatial scale. Comparison with a temperate carnivorous labrid, *Notolabrus fucicola*, revealed no differences in the response of growth, body size, development and life span to temperature in the two species with contrasting diets, thus providing no support for the hypothesis of a temperature constraint on herbivory at high latitudes in *O. pullus*. Lastly, the processes underlying latitudinal changes in life span were investigated in the context of the oxidative stress hypothesis of ageing and of the predictions of the Metabolic Theory of Ecology, and the age-pigment neurolipofuscin was quantified in older *O. pullus* individuals to assess the rate of oxidative damage accumulation across latitudes. Neurolipofuscin accumulation rate increased with temperature, indicating that a slower rate of ageing contributed to greater life expectancies at colder temperatures.

Acknowledgements

First and foremost, I would like to thank my three supervisors (in alphabetical order): Prof Howard Choat (James Cook University, Townsville, Australia), Assoc Prof Kendall Clements (University of Auckland, New Zealand) and Prof David Raubenheimer (Massey University, Auckland, New Zealand). I would like to thank them for giving me the opportunity to work on this project, their help in the collection of my samples and for their support throughout my PhD. I would particularly like to thank Howard for his invaluable contribution during the analysis and writing of my thesis, and for his help and support throughout the years. Secondly, I would like to thank the Royal Society of New Zealand Marsden Fund for funding this research and my scholarship. I also received a University of Auckland International Fees Bursary and additional financial support from the University of Auckland – School of Biological Sciences, which I am extremely grateful for.

Second, I would like to thank Jethro Johnson, whose PhD research on the nutritional ecology of *Odax pullus* was concurrent with my work. I would like to thank Jethro for his invaluable help and friendship at all steps of this work, from the collection of samples, organisation of field trips, analysis, and endless discussions and input during the write up. Working with you has been a pleasure; we have made a great team! Many people have also provided invaluable help. Special thanks go to Matt Sheehy (University of Leicester, UK) for advice and help on the histology of lipofuscin; Malcolm Haddon (CSIRO, Hobart, Australia) for reviewing my excel macros; Min Liu (University of Hong Kong, China) for advice and help on the interpretation of transitional gonads; Anthony Hickey (University of Auckland) for discussions on the rate of ageing; Ashley Williams (James Cook University, Australia) for advice on the estimation of size- and age-at-maturity; Jennifer Chen (University of Auckland) and Sue Reilly (James Cook University, Townsville, Australia) for help with the preparation of histological sections; Adrian Turner (University of Auckland) for help with fluorescence microscopy; Maren Wellenreuther (University of Lund, Sweden) for help with the Fetch Effect program; Tim Sippel and Louis Ranjard (University of Auckland) for help with retrieving the sea surface temperature data; Emma Marks, Todd Denis and Kathy Ruggiero (University of Auckland) for help with statistics; Vivian Ward (University of Auckland) for the maps; Ian McDonald (University of Auckland) for the brain photograph; and Mary Sewell (University of Auckland) for discussions along the way. This work has also involved a substantial amount of field work, so thank you to all people involved in the collection of our

samples: Brady Doak and Murray Birch who skippered the Hawere on our numerous trips around the Hauraki Gulf and up north; John Hum from Southern Pursuit Charters and Martin Holmes from Catamaran Sailing & Launch Charters (Malborough Sounds); Rob Swale and Ian Baines from Jewel Charters (Stewart Is and Fiordland); Morris Skeggs from Happy Motoring (Invercargill); and Schannel Van Dijken, Arthur Cozens, Murray Birch, Brady Doak, Lindsey White, and Zoe Hilton for help onboard various of our field trips. And thank you to everyone here at the Marine Lab.

Last but not least, I would like to thank my family and friends both in New Zealand and in France: to my partner Karl Jensen, for his relentless support over the last four years; to my parents Brigitte & Michael, my brother Guillaume, my sister Karen and brother-in-law Henri, and my grand-parents Andrée & Serge Boussard, and Frans & Vicki Laman Trip, who have supported me, and much much more, throughout my life; and to all my friends here in Auckland and back home in France. Finally, a special thank you to my dearest friend of 25 odd years Eva Masson: we will sit together as two old ladies one day!

Table of contents

List of figures

List of tables

Chapter 1. General Introduction

Many ectotherm organisms are distributed over wide geographical ranges, which cover extensive gradients in environmental conditions, including physical (*e.g.* temperature, habitat) and biological parameters (*e.g.* population density, food availability). A critical factor affecting ectotherm life history is environmental temperature, which varies over geographical gradients of latitude. Yet, the response of ectotherm life history over latitudinal gradients of temperature, particularly body size, largely remains a "life history puzzle" (Stearns and Koella, 1986; Stearns, 1989; 1992; Berrigan and Charnov, 1994; Angilletta *et al.*, 2004; Charnov and Gillooly, 2004; Kingsolver and Huey, 2008). Marine ectotherms offer great advantages in the study of how temperature influences life history. Not only is there increasing understanding of the mechanisms that underlie variation in ectotherm life histories over latitudinal gradients of temperature (Kingsolver and Huey, 2008), but marine ectotherms often occupy continuous latitudinal gradients over broad geographical scales. Furthermore, the biological effects of temperature on ectotherms are pronounced, as their internal temperature is directly dependent upon, and varies with, that of the environment (poikilothermia).

Life history theory predicts delayed maturity at a *smaller* size in environments that retard growth (Stearns, 1992). Conditions that may retard growth include decreasing rearing temperatures, increasing species density, decreasing habitat "quality", or increasing "nutrient stress" (Stearns, 1992). However, the effect of temperature across geographical gradients of latitude on the response of ectotherm life history traits differs from the effect of other factors affecting growth. Indeed, colder rearing temperatures at higher latitudes result in delayed maturity at a *larger* body size (Atkinson, 1994). Understanding the mechanism(s) underlying this "life history puzzle" represents a challenging task (Kingsolver and Huey, 2008), and is of particular concern because of its significance to our understanding of natural population dynamics (*e.g.* size and age structures, sexual maturation schedules, reproductive output, life spans).

Critical life history traits include growth rate, size- and age-at-maturity, final body size, size- and age-specific mortality, and individual life spans, among others (Stearns, 1992). These are tied by a number of trade-offs, including these between age-at-maturity and adult mortality (life span), between somatic growth and reproduction, and between reproductive

effort and survival (Roff, 1984; Stearns, 1989; Kozlowski, 1992; Stearns, 1992; Roff, 2000; Roff and Fairbairn, 2007). The presence of life history trade-offs implies that understanding the response of ectotherm life history to environmental temperature gradients will require empirical information on the relationship between life history traits, primarily body size, rate of reproductive development, and mortality schedules, and how their interaction is affected across gradients of latitude (Partridge and Sibly, 1991; Stearns, 1992; Charnov, 1993; Kingsolver and Huey, 2008).

The relationship between body size and latitude (temperature) has been the focus of life history studies for more than a century, and, in ectotherms, is widely referred to as the Temperature-Size Rule (TSR) (Bergmann, 1847; Mayr, 1956; James, 1970; Stearns, 1992; Atkinson, 1994; Partridge and French, 1996; Atkinson and Sibly, 1997; Blackburn *et al.*, 1999; Kingsolver and Huey, 2008; Angilletta, 2009). The TSR predicts slower growth, delayed maturity at a larger size, and larger final size in colder rearing environments (Atkinson 1994). In fish, examples supporting this pattern are numerous, although examination over wide spatial scales of the relationship between life history traits and latitude rarely encompasses all of the above mentioned life history parameters simultaneously. Emerging research, largely based on widely distributed tropical fish species, often examines latitudinal gradients in growth rate, adult body size and longevity, and commonly demonstrates faster growth, larger adult body sizes, and/or increased longevities at higher latitudes (*e.g.* Meekan *et al.*, 2001; Choat and Robertson, 2002; Choat *et al.*, 2003; Robertson *et al.*, 2005). Changes in reproductive development rates over gradients of latitude are often examined independently of growth and life spans, however, showing increased egg size, and greater reproductive output at higher latitudes (*e.g.* Kokita, 2003; Kokita, 2004; but see Ruttenberg *et al.*, 2005). Data on age-and size-at-maturity in the context of life history across gradients of latitude are comparatively scarce, although experimental data show that temperature directly increases development rate, and thus reduces the time spent at each developmental stage (Martell *et al.*, 2005).

In fish, examination of patterns of variation in somatic growth is further complicated in that growth rate has shown contradictory responses to temperature. While some species grow slower to achieve a larger size at higher latitudes (TSR) (Atkinson, 1994; Rochet, 2000; Heibo *et al.*, 2005), a number of species of fish display counter-gradient variation in growth, and grow faster to achieve a larger size at higher latitudes (*e.g.* Conover and Present, 1990;

Conover *et al.*, 1997; Arendt and Wilson, 1999; Imsland *et al.*, 2000; Yamahira and Conover, 2002; Robertson *et al.*, 2005). Counter-gradient variation in growth is most likely to evolve under particular selective pressures, particularly those associated with increased over-wintering juvenile mortality, which often result from shorter growing seasons at higher latitudes (Conover and Present, 1990; Conover and Schultz, 1995; Schultz *et al.*, 2002; Yamahira and Conover, 2002). However, the possibility of fast growth at higher latitudes is of particular significance as growth rate directly affects size- and age-at-maturity (Berrigan and Charnov, 1994).

Development rate (*e.g.* age-at-maturity) is also directly related to adult mortality (longevity), as shorter life spans select for earlier age-at-maturity (Stearns 1992). There is growing evidence that faster growth and larger body sizes at higher latitudes are associated with a consistent pattern of intra-specific variation in longevity over latitudinal gradients of temperature, with fish living longer at higher latitudes (Meekan *et al.*, 2001; Robertson *et al.*, 2005). However, this pattern directly contradicts the prediction that faster growth is associated with reduced life spans (Metcalfe and Monaghan, 2003). In ectotherms, natural mortality is thought to have a physiological basis dependent on environmental temperature and reproductive rate. Recent work suggests that oxidative stress, *i.e.* the relationship between aerobic energy generation through respiration and cellular damage generated by the by-products of oxygen metabolism, might play a significant role in shaping population life spans (Monaghan *et al.*, 2009) and may be directly involved in the trade-off between reproduction and mortality rate (Harshman and Zera, 2007). Oxidative damage is at the basis of the "rate-of-living theory" or "free-radical hypothesis of ageing", which predicts that, as metabolic rate of ectotherms decreases at lower environmental temperatures, the production of free-radicals and thus of cellular damage through oxidative stress are reduced, resulting in a slower rate of senescence and increased life spans at higher latitudes. This hypothesis has been successfully used to examine differences in longevity across species adapted to different temperature environments (*e.g.* Philipp *et al.*, 2005a; Philipp *et al.*, 2005b; Philipp *et al.*, 2006). However, comparatively little has been done to explore the patterns of variation in life span in natural populations of species distributed over large spatial scales. Examination of the relationship between physiological ageing, mortality (life span), growth rate, and development rate will provide useful insights into the life history trade-offs underpinning the mechanisms of variation in longevity, growth rate and development over latitudinal gradients of temperature.

This thesis uses an integrative age-based approach to examine the predictions of life history theory over an environmental gradient of latitude, by exploring age- and size-based demographics in a widely distributed temperate reef fish, *Odax pullus* (Perciformes, Labridae). There are four primary reasons why *O. pullus* is an ideal species for such an analysis. Firstly, *O. pullus* is endemic to, and distributed throughout New Zealand (with the exception of the Three Kings Islands), thus allowing sampling 1) over a broad latitudinal gradient spanning over ~15^{o} of latitude, and 2) over a species' entire distributional range. The latter point is particularly significant in the context of variation in somatic growth at the extremities of a species' geographical range (Munday *et al.*, 2008). Sampling over the entire species' range is seldom possible in life history studies over large latitudinal gradients. Secondly, variation in adult size has been described for the study species, from an average of 45 cm Total Length (TL) in northern New Zealand to a maximum of 70cm TL in more southern regions (Clements, 2003). Thirdly, the protogynous (sex reversal from female to male) sexual ontogeny of *O. pullus* (Ritchie, 1969; Crabb, 1993) allows estimation of developmental rates between two key life history stages, sexual maturity and sex change. Lastly, recent work has demonstrated a key role for nutrition in mediating the trade-off between longevity and reproduction in terrestrial ectotherms (insects) (Lee *et al.*, 2008; Maklakov *et al.*, 2008). *O. pullus* is exclusively herbivorous as an adult after a short carnivorous post-settlement juvenile stage (Clements and Choat, 1993), thus allowing for examination of life history phenomena in the context of the species' nutritional ecology.

Two of the most important factors affecting growth in fish are temperature and diet (Munday *et al.*, 2008), and, although life history theory predicts contradicting effects from each factor independently (Berrigan and Charnov, 1994), the interactive effect of food and temperature is rarely considered over gradients of latitude (Kingsolver *et al.*, 2006; Stillwell *et al.*, 2007). As herbivores are not well represented amongst fishes, with less than 5% of marine and freshwater species living on an herbivorous diet (Horn, 1989), the majority of life history studies have primarily dealt with carnivorous or omnivorous species. As a result, little is known of how an herbivorous diet may affect growth, body size, development, and associated life histories, and in particular of how these life history parameters respond over a large latitudinal gradient of temperature. If the digestion of an herbivorous diet is constrained by temperature, as suggested in Gaines and Lubchenco (1982), Harmelin-Vivien (2002), Behrens (2005), Floeter *et al.* (2005), and Behrens and Lafferty (2007), we may hypothesise that nutrient acquisition in herbivorous fishes will be impaired at colder temperatures. In this

case, higher latitude environments will provide conditions of "nutrient stress", or low nutrient availability, which are likely to retard growth (Jones, 1986; Martell *et al.*, 2005). As a result, we may expect individuals living at higher latitudes to grow slower and display delayed maturity at a *smaller* size (Stearns, 1992; Berrigan and Charnov, 1994). This implies the possibility however, that the patterns of variation in life history traits over a latitudinal gradient of temperature in *O. pullus* may be compromised by the effect of a temperature constraint on the digestion of an herbivorous diet. This thesis examines the hypothesis that the life history of an herbivorous fish will be impacted by temperature at high latitudes by contrasting the patterns of latitudinal variation in life history traits of the study species, *O. pullus*, to that of a closely related carnivorous species, *Notolabrus fucicola* (Labridae). *N. fucicola* is distributed across New Zealand, occurs in the same costal reef kelp habitats as *O. pullus*, and is exclusively carnivorous throughout its life span (Denny and Schiel, 2001). Their overlapping geographical distribution, body sizes, habitat, ecology and phylogenetic background, and contrasting feeding regimes, provide an ideal opportunity for the comparison of the response in life history traits of an herbivorous fish with that of a carnivorous species over a large latitudinal gradient of temperature.

In overview, this thesis addresses two primary issues: firstly, that of the response of ectotherm life history traits to environmental temperature over a wide gradient of latitude, and secondly, that of the demographic performance (*i.e.* potential for growth, reproduction and survival) of an herbivorous ectotherm in a marine environment, ranging from warm (18^{o}C) to cold (13^{o}C) temperate. To address these issues, three lines of approach were taken. First, an age-based approach allowed estimation of key life history traits specifically growth rate, development rate (sexual maturation and sex change) and mortality (life span). Second, the demographic response of *O. pullus* was examined in the context of the predictions of ectotherm life history theory, in response to both temperature and nutrient stress. And third, a comparative approach was used to contrast the response in life history traits across latitudes of an herbivorous species with that of a closely related carnivore. The study species *O. pullus* and *N. fucicola* were sampled at six locations across New Zealand. I first establish the relationship between size and age in *O. pullus*, and develop a robust ageing method for the study species, for both adult and juvenile age classes, based on sectioned sagittal otoliths (Chapter 2). The relationship between size and age, and validation of the ageing method for *N. fucicola* were established elsewhere (Ewing *et al.*, 2003). Chapter 3 establishes the pattern of sexual development in *O. pullus* (for *N. fucicola*, see Denny and Schiel 2002), and

examines the relationship between size, age, sex, sexual maturation and sex change. Chapters 2 and 3 establish the fundamental demography of *O. pullus*, thus providing essential information at the basis of the comparative analysis of size- and age-based life history traits across locations sampled (Chapter 4). Chapter 4 relates all extracted life history parameters of *O. pullus* and *N. fucicola* to environmental temperature, latitude, species abundance, habitat availability and exposure. Specifically, Chapter 4 examines the patterns of latitudinal variation in body size at different life history stages (sexual maturity, sex reversal, adult size), somatic growth rate and the relationship between growth rate and age, development rate (age at sexual maturity and at sex change), and mortality rate (longevity). Chapter 4 thus provides insight into the trade-offs underpinning variation in life history traits over latitudinal gradients of temperature in the context of the species' nutritional ecology. In Chapter 5, I explore the patterns of latitudinal variation in longevity of *O. pullus* by examining the relationship between environmental temperature and the rate of senescence ("oxidative stress hypothesis of ageing"), and by relating those estimates to the observed patterns of variation in growth and development rates.

Study species

The study species *Odax pullus* (odacine) and *Notolabrus fucicola* (pseudolabrine) represent two tribes of reef fishes within the family Labridae (Perciformes). The Labridae are the second largest family of marine fishes, and have recently been established as a monophyletic group (Clements *et al.*, 2004; Westneat and Alfaro, 2005). These species are thus phylogenetically associated but differ in terms of their nutritional ecology, *O. pullus* being an herbivore while *N. fucicola* is a carnivore.

O. pullus (also known as butterfish, greenbone, or marari) is endemic to New Zealand, and is distributed from Cape Reinga (172.6^{o}E, 34.4^{o}S) at the northern tip of the North Island of New Zealand down to the Antipodes Islands southeast of the southern tip of the South Island of New Zealand (179^{o}E, 49.5^{o}S), spanning a gradient of ~15^{o} of latitude (Francis, 2001). It is abundant across its range, and lives primarily within the first twenty meters of the water column on moderately exposed rocky temperate reefs. *O. pullus* is primarily found on coastal rocky reefs amidst kelp, and is most closely associated with the pheophytes *Ecklonia radiata*, *Carpophyllum spp*, *Lessonia spp*, and *Macrocystis spp*, on which it feeds. *O. pullus*

is exclusively herbivorous as an adult after a short carnivorous post-settlement juvenile stage (Clements and Choat, 1993).

N. fucicola (also known as banded wrasse, yellow-saddled wrasse, or purple wrasse) is distributed across southeastern Australia and New Zealand (Russell, 1988). In New Zealand, *N. fucicola* is present from the Three Kings Islands (172.1^{o}E, 34.1^{o}S), north of the North Island, down to the Snares and Chatham Islands (48ºS, 166.4ºE) (Francis, 2001). It is abundant across its range, and lives primarily within the first ten to twenty meters of the water column on moderately exposed to exposed rocky temperate reefs. *N. fucicola* is a gonochoristic (separate sexes) temperate labrid (Denny and Schiel, 2002). *N. fucicola* is exclusively carnivorous, and preys principally on invertebrates including bivalves, crabs, isopods and amphipods (Denny and Schiel, 2001).

Chapter 2. Age estimation of *Odax pullus* (Labridae): otolith microstructure, validation of increment periodicity, and position of the first annual band

2.1 Introduction

Chronological age of organisms is one of the most important biological variables (Campana, 2001). Its estimation is the basis for acquiring a wide range of biological information. This includes growth trajectories, longevity, growth and mortality rates, population age structure, and key life history transitions including age-specific changes in growth rate, and the timing of recruitment, sexual maturation, and sexual ontogeny. These variables provide core information for a variety of disciplines, from population ecology to stock management and assessment, and species conservation.

As the majority of fishes are poikilotherms, we may expect their demography and life histories to be influenced by a range of environmental variables. A predominant feature of this is that shown by the relationship between environmental temperature and body size, somatic growth, and development rate (Atkinson, 1994). Latitudinal gradients of body size have been shown for a number of temperate and tropical fish species, with larger body sizes at higher latitudes (Conover, 1990; Meekan *et al.*, 2001; Choat and Robertson, 2002; Choat *et al.*, 2003; Robertson *et al.*, 2005; Ruttenberg *et al.*, 2005). Moreover, emerging evidence shows a negative correlation between environmental temperature and life span, with individuals living longer in colder environments (Robertson *et al.*, 2005; Ruttenberg *et al.*, 2005; Trip *et al.*, 2008).

In fishes, a number of structures have been used to estimate age, including scales, vertebrae, fin rays, and bones (Campana, 2001). Otoliths (ear bones) are the most reliable and widely used calcified structures (Secor *et al.*, 1995). There are two primary reasons for this. Firstly, in contrast to skeletal structures (vertebrae, scales, bones), otolith growth is often decoupled from somatic growth (Reznick *et al.*, 1989; Francis *et al.*, 1993; Campana, 2001). A corollary of this is that otolith growth is continuous throughout the life span; this is reflected in the linear positive correlation between otolith weight and age seen in species with either a continuous or an asymptotic form of growth (Boehlert, 1985; Pawson, 1990; Fletcher, 1991; Francis and Campana, 2004). Secondly, as otoliths grow within the isolated

environment of the semi-circular canals, they are thought to grow in relative independence from external environmental conditions (Campana, 2001). The combination of these features makes otoliths a reliable candidate for estimating age in fish in which somatic growth is expected to vary with environmental conditions, and for recording of maximum age.

The need for validation of the accuracy (or closeness to the true value) and precision (or reproducibility of estimates) of any ageing method has been stressed by a number of authors (Beamish and McFarlane, 1983; Campana, 2001). Misinterpretation of ageing structures has lead to a number of misinformed fisheries management decisions, most often as a result of under-estimation of longevity and over-estimation of growth rate, with consequences on the sustainability of a number of commercially important species. Well-known examples include orange roughy *Hoplostethus atlanticus* (Tracey and Horn, 1999), and sablefish *Anoplopoma fimbria* (Beamish and McFarlane, 1987), along many others (Summerfelt and Hall, 1987). Considerable progress has been made in the reliability of estimation of age in fish in the past two and a half decades (Begg *et al.*, 2005). While validation of absolute age remains the most accurate method, most studies rely on the periodicity of growth increment formation, on both an annual and a daily scale (Campana, 2001). When applied across age classes and combined with the validation of the position of the first growth increment, this provides accurate estimates of age (Beamish and McFarlane, 1983; Campana, 2001). These are of particular significance to the younger and older age classes, which are the most critical age groups for the estimation of growth rate and longevity, respectively.

Four primary issues arise from the previous studies on age and growth of *Odax pullus* (Ritchie, 1969; Crabb, 1993; Bader, 1998; Paul *et al.*, 2000). Firstly, in all cases, age was estimated using scales and whole otoliths, both of which structures have been shown to lead to a number of ageing errors, in particular those of underestimation of age in older fish (Beamish and McFarlane, 1987). Secondly, even though authors have acknowledged the need for validation of the ageing methods, no validation studies were undertaken. Thirdly, all age and growth estimates to date are based solely on adult individuals, with no data available on the early growth of the study species. Fourthly, identification of the first annual growth increment was uncertain, and, consequently, the reliability of the estimation of age one has been questioned (Ritchie, 1969; Paul *et al.*, 2000).

Misinterpretation of the position of the first annual growth increment directly affects estimation of maximum age and growth rate, and has been shown to lead to consistent ageing errors (*e.g.* Francis and Stevens 2000, Natanson et al. 2001 in Campana 2001). Two innermost increments have been observed in the ageing structures of butterfish, including fin spines, scales and otoliths (Ritchie, 1969; Paul *et al.*, 2000). The innermost opaque zone observed was named 'annulus 0' in Paul et al. (2000). Ritchie (1969) interpreted this opaque zone as representing the first annual ring, and the resulting growth trajectory showed a small size at age one and a fast continuous form of growth reaching no asymptotic size by maximum age (Fig. 2.1). This differed markedly from the form of growth found by Bader (1998) and Paul et al. (2000), in which 'annulus 0' was not taken as age one, and which resulted in a comparatively faster estimate of growth rate between the ages of zero and one year (larger size-at-age one), and a slower continuous form of growth (Fig. 2.1). Paul et al. (2000) attempted to clarify the position of the first annual growth increment using Ritchie's growth back-calculation procedure on scales. Their results suggest that the innermost increment or increment '0' is not the first annual growth increment. However, the authors concluded that the nature of this first check mark or increment could not be resolved unless examination of known-age juvenile fish was undertaken. No juvenile individuals of *O. pullus* have been examined to date.

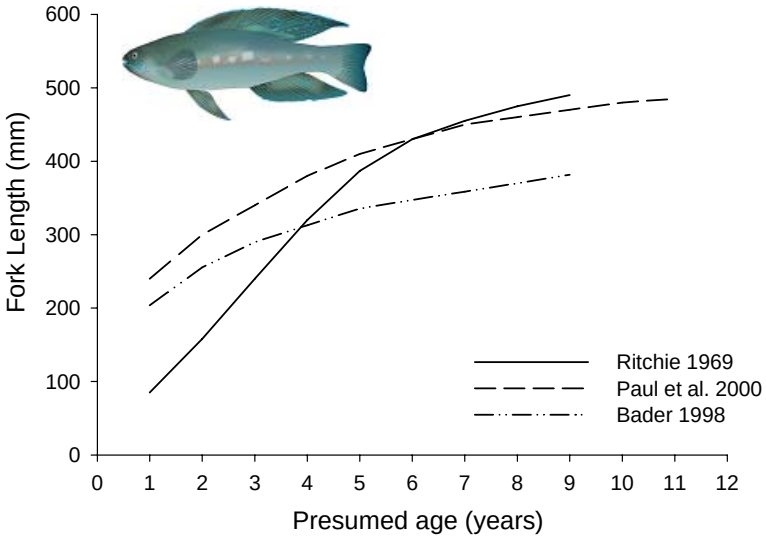

Fig. 2.1: Form of the growth trajectories shown in the previous studies of size-at-age in *Odax pullus*. Length in Bader (1998) was converted from Standard Length (SL) to Fork Length (FL) using the SL-FL relationship in the present thesis.

The primary aim of this chapter is to provide a robust ageing procedure using sectioned sagittal otoliths in the study species *O. pullus*, and to generate size-at-age (growth) trajectories based on a validated ageing method. Specifically, this chapter aims at providing (1) a validation of the timing and periodicity of otolith growth increment formation in fish with more than one increment formed, (2) a validation of daily otolith increment formation, (3) a validation of the position of the first growth increment directed at clarifying the nature of 'annulus 0', and (4) assessment of the form of growth of the study species in the Hauraki Gulf, New Zealand, based on a validated ageing method. Also, this chapter aims at providing a detailed description of the otolith-processing method. Results of the ageing method and validation procedure are discussed in the context of growth modelling and estimation of growth rate.

2.2 Materials & methods

All age estimates in this study are based on thin sections of sagittal otoliths (Secor *et al.*, 1995).

The terminology used for the alternating zones seen in the ageing structures of *O. pullus* was inconsistent across the five previous studies examining age in *Odax pullus*. In this thesis I will use the term *opaque zone* (a zone which appears dark under transmitted light) for what has been referred to as the "winter growth", "black", "dark" or "hyaline" zone; and a *translucent zone* (which appears transparent or bright under transmitted light) for what has been called the "opaque", "white" or "summer growth" zone (Ritchie, 1969; Crabb, 1993; Bader, 1998; Paul *et al.*, 2000). A combination of one opaque and one translucent zone forms one *growth increment*, which forms the unit of enumeration of age.

A total of 447 fish were sampled in the Hauraki Gulf for size and age information. All fish, except those used for validation of daily increments, were collected by spearing in the Hauraki Gulf, northern New Zealand (35.9 - 36.6^{o}S; 174.7 - 175.9^{o}E). Each fish was brought back onboard the boat for immediate processing. Otoliths were dissected out by slicing open the top of the cranium and exposing the brain. After removal of the brain, the sagittal pair of otoliths was extracted from the otic capsules, rinsed in 70% ethanol, and stored dry in 96-well plates. Each fish was measured to the nearest millimeter Fork Length (FL).

One sagitta from each pair of otoliths was chosen randomly and weighed to the nearest 10^{-7} gram (0.0001mg) using a UMX5 Metler Toledo ultra-microbalance. A transverse section through the nucleus was obtained by grinding down both anterior and posterior ends of the otolith, thus yielding a thin transverse section containing the nucleus.

For grinding, each sagitta was positioned on a glass slide so that the nucleus was sitting just below the edge of the slide, and the antero-posterior axis was oriented perpendicularly to the edge of the slide. "Crystalbond™" thermoplastic cement was used to mount the otolith on the slide by melting the cement on a hotplate. The anterior end of the otolith was then ground on a "GF4 Gemmasta Facetting Machine" diamond polishing wheel, using P400-grade wet and dry sandpaper. Secondly, the half sectioned otolith was then mounted ground-face down, allowing for the posterior end of the otolith to be ground down, until rings could be distinguished between the nucleus and the outer margin of the otolith. The section was then covered with Crystalbond before reading.

Otoliths of sagittal weight less than 0.001mg were processed as described above, with P800-grade wet and dry sandpaper to grind down both anterior and posterior ends. Additionally, sections were further polished after each cut using 12µm (yellow) and 3µm (pink) aluminium oxide lapping film. Particular care was taken to achieve a balance between the readability of the rings concentric to the nucleus and of those close to the edge of the otolith. During sectioning, each sagitta was observed at 100x-magnification under transmitted light, until the thin section was judged to have reached the appropriate balance.

Periodicity and timing of opaque zone formation

Validation of increment periodicity and examination of the timing of opaque zone formation were undertaken using Edge Type Analysis (ETA) (Manickchand-Heileman and Phillip, 2000; Ewing *et al.*, 2003; Pears *et al.*, 2006). The presence of an opaque or a translucent zone on the growing edge of the otolith was recorded, and the frequency of opaque zones for each month was plotted over a two year cycle. The *otolith edge*, where the presence or absence of an opaque or a translucent zone was recorded, refers to the outer rim of the otolith on the ventral side of the sectioned otolith.

A total of 304 sagittal otoliths of *Odax pullus* were collected in the Hauraki Gulf, New Zealand (35.9 - 36.6°S; 174.7 - 175.9°E) over a period of two years of consecutive sampling from February 2006 to January 2008. The number of monthly samples collected is summarized in Table 2.1. Thirty-eight of the otoliths collected were less than one year old and were not included in the analysis for validation of annual increment periodicity.

Table 2.1: Monthly sampling effort of *Odax pullus* in the Hauraki Gulf from February 2006 to January 2008, showing the number of individuals collected.

Month	2006	2007	2008	*Total*
January		13	18	*31*
February	38			*38*
March		13		*13*
April	6	16		*22*
May	32			*32*
June	12	14		*26*
July	11			*11*
August	30	21		*51*
September	4	14		*18*
October	14			*14*
November	13	13		*26*
December	12	10		*22*
Total	*172*	*114*	*18*	*304*

The following protocol was established for analysis of edge types (Campana, 2001). Firstly, sections were randomized so as to conceal from the examiner the identity and the month of origin of each sample; secondly, the ETA was performed on separate age groups; thirdly, the distribution of observed frequencies of edge types across months was statistically tested against a uniform distribution to avoid subjectivity in the results; and lastly, the relationship between, on the one hand, the proportion of otoliths showing an uncertain edge and, on the other, month sampled, age and sample size was examined. As sample sizes for each month were not sufficient to validate increment periodicity for each age class separately, some age classes were pooled to achieve adequate sample size across months sampled, and validation was performed for three groups of age classes separately. Age groups on which

ETA was performed were as follows: individuals aged one and two were pooled to form age group 1-2 (total sample size of 93 otoliths), individuals aged three and four were pooled together to form age group 3-4 (total sample size of 120 otoliths), and all individuals aged five and above were pooled to form age groups 5+ (total sample size of 53 otoliths). ETA was subsequently performed on all age groups together.

For each fish, a sagittal thin section was photographed under a dissecting microscope with transmitted light at 40x- or 50x-magnification using a SciTech Insight-Spot camera. Digital images of the sections were then allocated a random number. During analysis of each sectioned sagitta, the edge type was assigned to one of the following three categories: (1) translucent, (2) opaque or (3) uncertain. A section was categorized as having a translucent edge when a bright zone (as seen under transmitted light) could be observed between the last opaque zone (which appears black under transmitted light) and the edge of the otolith (Fig. 2.4 A & B). Conversely, a section was considered to have an opaque edge when no translucent zone could be identified between the last opaque ring and the outer edge of the otolith (Fig. 2.4 C & D). Reference photographs showing otolith margins with a translucent edge and an opaque edge are presented in Fig. 2.4. All sections for which the edge type was not readily interpretable were recorded as uncertain.

Observed frequency distributions of otoliths showing an opaque edge (percent otoliths with an opaque edge over the total number of otoliths edges analysed each month) were plotted per month for each year sampled (2006 & 2007), for all age groups examined. Monthly occurrences of opaque edge types were then analysed by comparing the observed distributions to a uniform distribution for circular data (Rayleigh's Test; Zar, 1999). The null hypothesis H_0 tested was that opaque edge types were uniformly distributed across months; the alternative hypothesis H_A was that there is a mean population direction in the distribution of opaque edge types across months. Assumption of a unimodal distribution (von Mises distribution) was met. To achieve adequate sample sizes in each month for both years sampled, data were pooled across age groups in both 2006 and 2007, respectively, and Rayleigh's Test was performed separately for each year. Statistical package "Oriana 2.02e" for circular statistics was used for the analyses.

Throughout this thesis, it is assumed that periodicity will not vary with geographical location, and that opaque zone formation follows the same pattern of periodicity at all

locations sampled across New Zealand (as shown for Lethrinus miniatus in Williams *et al.*, 2005).

Otolith microstructure

To validate the daily pattern of increment formation in juvenile otoliths, a field-based oxytetracycline (OTC) tagging experiment was undertaken. On 14th April 2008, seven juvenile *Odax pullus* were caught with hand nets in Looking Glass Bay, Fiordland, New Zealand (44.9 - 46.1°S; 166.6 - 167.2°E). Size of juveniles captured ranged between 68 and 102 mm FL. Upon capture, all fish were kept in fresh seawater, and anaesthetised with clove oil. Each fish was then weighed to the nearest gram, and injected with a solution of OTC (5mg OTC / 1mL of 1.7% saline solution) at 50mg of tetracycline per kg of fish (Hernaman *et al.*, 2000). After injection, the fish were returned to fresh seawater. All seven fish recovered after injection. Thereafter the water was changed and a supply of food and shelter was given daily. Food and shelter was fresh *Lansburgia sp.* (Phaeophyceae) covered in epiphytes including hydroids, red seaweeds, and small crustaceans. The fish were kept for four days, and euthanised on the 18th April with an overdose of clove oil. Each individual was then frozen at -20°C for subsequent processing in the laboratory.

In the lab, all fish were measured to the nearest millimeter, and weighed to the nearest gram. Otoliths were dissected out, cleaned and stored dry in eppendorf tubes, wrapped in aluminum foil, and kept in a light-proof jar. Otoliths were then weighed to the nearest 10^{-7} g, and processed as detailed above for juvenile otoliths (sagittal weight < 0.001mg). The total number of increments was read under a compound microscope at 100x-magnification. Precision of readings was checked by examining the correlation between otolith weight and number of increments, on the assumption of a linear increase in otolith weight with age (Boehlert, 1985; Pawson, 1990; Fletcher, 1991; Francis *et al.*, 2005).

Sections were then exposed to a Ultra-Violet (UV) light source, and viewed through a green filter; green emission wavelengths were found to produce the best results for revealing the presence of a fluorescent mark. The margin of all otoliths was viewed at 100x-magnification with immersion oil, and digital images were taken at the otoliths' edges using a Leica DC500 camera. For each otolith, two images were taken of the exact same frame (using image analysis software "AnalySis" - Soft Imaging System). One image was taken under

transmitted light, and the second image was taken under UV light. Marginal increments visible under transmitted light were highlighted using image analysis software GIMP 2.2, and the annotated layer was subsequently pasted onto the UV image to observe the positioning of the increments in relation to the fluorescent mark. The number of increments visible between the start of the fluorescent band and the outer margin of the otolith was enumerated (Thorrold and Milicich, 1990; Welsford, 2003). This procedure was repeated four times around the otolith's edge where a concordance was found between presence of the OTC fluorescent mark and interpretable marginal increments. The mean (+- SE) number of rings visible between the OTC mark and the otolith edge was calculated, and compared to the number of days the fish were held between OTC injection and euthanasia (four days).

Determination of the position of first annual increment

Determination of the position of the first annual opaque zone was undertaken following three separate methods.

Firstly, otolith radius of "age 1-cohort" individuals (i.e. juveniles born during the spawning season previous to the year sampled) caught at the time of opaque zone formation was measured (Campana 2001). The mean radius was then compared to that of the first three opaque zones (named 'zone 0', 'zone 1', and 'zone 2', as described in Paul et al. 2000) seen in otoliths sections of older individuals (Ewing *et al.*, 2003).

Opaque zone formation occurred between September and December in older individuals, and peaked in November (see results of timing and periodicity of opaque zone formation in section 2.3). We can expect the first annual growth increment to be laid down at the same time of year (Williams *et al.*, 2005). A total of twenty-three juvenile individuals (size range 87 to 282 mm FL) were sampled in the Hauraki Gulf between September and December over three years of sampling (2005 to 2008).

In order to identify individuals that belonged to the "age-1 cohort", age was determined for each individual (age range 115 to 393 days), and approximate hatch date was assessed through estimation of the length of the spawning season by plotting mean monthly Gonado-Somatic Index (GSI; $GSI = \frac{Gonad\ Weight}{Gutted\ Weight} \times 100$) of Hauraki Gulf females. This suggested that spawning occurred between July and November, and peaked in August (with

mean GSI = 5.99% +- 0.65 SE). Accordingly, it was estimated that the age of any "age-1 cohort" juvenile, *i.e.* individual born during the previous spawning season (July to November; year *x*) and caught during opaque zone formation (September to December; year *x+1*), could theoretically range from a minimum of 9 months (0.75 years) to a maximum of 1.5 years. A total of nine individuals aged less than nine months were consequently excluded from the analysis.

The maximum distance between the primordium (center of the nucleus) and the edge of the sectioned otolith (maximum transverse radius) was then measured for each "age-1 cohort" individual to the nearest micrometer using image analysis software ImageJ 1.37v. Similarly, the distance between the primordium and the outer edge of each of the first three opaque zones: 'zone 0', 'zone 1' and 'zone 2', was then measured to the nearest micrometer in transverse sagittal sections of 50 randomly selected otoliths aged three years or more.

Otolith radii of "age-1 cohort" individuals were then compared to the radii measured for each of the three opaque zones in a one-way Analysis of Variance (ANOVA), and homogeneous groups were identified in pair-wise comparisons using Tukey's HSD Test. To avoid auto-correlation in the data tested (i.e. the maximum transverse radius to 'zone 0' in a given otolith section is likely to be correlated with the value of the radius measurement found for 'zone 1' in the same otolith; this will apply similarly to the measurement of 'zone 2' radius in that given section), each of the 50 otoliths used in the analysis was randomly assigned to one of the three zone categories ('zone 0', 'zone 1' or 'zone 2'), so that no two measurements compared in the analysis were obtained from the same otolith section. The "ANOVA" module in Statistica 7.1 was used in the analysis. Assumptions of normality and homogeneity of variance were checked graphically by examining the spread of the observed values and residuals within each group and the relationship between group means and variance.

Secondly, monthly progression of otolith radius of juvenile individuals of known age 0+ and 1+ year was followed over an annual cycle. Thirty-nine *O. pullus* juveniles aged 0+ year (size range 87 to 218 mm FL; age range 115 to 309 days), and thirty-nine individuals aged 1+ year (size range 147 to 315 mm FL; age 1 year), were sampled in the Hauraki Gulf over a period of 2.5 years, from August 2005 to January 2008 (except for three fish collected previously in 1996 & 1997). Samples collected were pooled by month across years in order to have samples within each month of the year and adequate sample sizes for each month. For

each individual, age was determined in days or years, and the maximum transverse radius (maximum distance between the primordium and the edge of the otolith) of sagittal sections was measured to the nearest micrometer using image analysis software ImageJ 1.37v. The mean radii were then plotted for each month for both age cohorts. Results were then graphically related to the mean radii estimated for "age-1 cohort" individuals at the time of opaque zone formation, 'zone 0', 'zone 1' and 'zone 2', respectively.

Lastly, the mean age range at which the first inner opaque zone ('zone 0') was laid down was estimated by counting the number of daily increments between the primordium and the inner and outer edges of 'zone 0', respectively. Six individual otolith sections (age range 1 to 3 years) were selected, among samples collected in the Hauraki Gulf between August 2005 and January 2008, in which the presence of 'zone 0' coincided with interpretable daily increments between the primordium and both the inner and the outer edges of the first opaque zone. The number of daily increments was counted under transmitted light using a compound microscope at 100x-oil magnification and mean age range was estimated.

Enumeration of age

Annual increments were counted under a stereo-dissector with transmitted light, and daily rings were counted under a high-power microscope at 100x-oil magnification with transmitted light. Three separate readings were performed for each otolith sectioned. In the case of annual increments, the following protocol was used for enumeration of age. Count 1 was carried out upon sectioning, while count 2 was completed from digital photographs after validation of the position of ring 1. Count 3 was completed under stereo-dissector with transmitted light as in count 1 with the addition of ring 1 being known. Counts 2 and 3 were accomplished each without prior knowledge of results of previous counts. Age was then estimated as follows: when all three counts were identical, the reading was taken as the final estimate of age; when two out of the three readings coincided, the coinciding value was taken as the final age estimate; and when the three counts differed each by one year, the mean value of the three readings was taken as the final age estimate. When readings deviated by more than one year, a fourth reading was done. If the reading coincided with any of the previous readings that value was taken as the final age estimate, however if the fourth reading differed from all other previous readings, the second otolith if available was processed and read, or

else the individual was not included in the age-based analyses. In the case of daily increments, age was estimated as the mean value of the three independent counts. All counts of both annual and daily increments were performed without prior knowledge of fish size, otolith weight or sex.

Precision of age estimates

All readings were made by one reader. Precision of age estimates was estimated using two separate methods.

Firstly, the mean coefficient of variation (CV) for the age readings performed was estimated from the average CV across all individuals aged. The CV was calculated for each individual fish as follows: $CV_j = 100\% \times \frac{\sqrt{\sum_{i=1}^{R} \frac{\left(x_{ij}-x_j\right)^2}{R-1}}}{x_j}$, where CV_j is the coefficient of variation of age readings for fish j, X_{ij} is i^{th} age reading for fish j, X_j is the mean age estimate across all readings, and R is the number of readings (Campana, 2001). Mean CV for each age class was then plotted to examine the presence of an age-bias in the precision of age estimates.

Secondly, correlation between sagittal weight and estimated age was examined using correlation analysis (Pears *et al.*, 2006). The "correlation matrix" module in Statistica 7.1 was used for the analysis.

Growth modelling

Age and size (Fork Length, FL) estimates were plotted to examine growth of *O. pullus* from the Hauraki Gulf (New Zealand). Growth was modelled by fitting size-at-age data with the following two growth functions: (i) the von Bertalanffy Growth Function (VBGF) and (ii) the re-parameterised equation of the VBGF (rVBGF) (Francis, 1988). Both the VBGF and rVBGF functions were used in order to (i) test the rVBGF as a tool for modelling growth and (ii) assess the biological relevance of the parameters of mean size-at-age generated by the re-parameterised version of the VBGF. The VBGF also provided

parameter estimates that were in line with those presented in previous studies of growth in *O. pullus*.

The generalised equation of the VBGF, which is traditionally used to describe growth in fish (Cerrato, 1990; Chen *et al.*, 1992) is expressed as follows:

$$L_t = L_\infty \left[1 - e^{-K(t-t_0)}\right],$$

where L_t is estimated mean size-at-age t, L_∞ is mean asymptotic size, K is a curvature parameter and t_0 is the age at which the fish have a theoretical size of zero.

Francis' (1988) re-parameterised version of the VBGF (*e.g.* Moulton *et al.*, 1992; Welsford and Lyle, 2005; Trip *et al.*, 2008) is based on the following three parameters L_τ, L_ω and L_μ, which express expected mean body size at three arbitrary ages τ, ω and μ. Ages τ and μ are chosen arbitrarily within the range of the data set so as to cover the growth over the majority of the life span, and ω is determined by the average age of τ and μ. The rVBGF is described as:

$$L_t = L_\tau + \frac{(L_\mu - L_\tau)\left(1 - r\left(2\frac{t-\tau}{\mu-\tau}\right)\right)}{1-r^2};$$

where $r = \frac{L_\mu - L_\omega}{L_\omega - L_\tau}$, and L_t is the average size-at-age t to be predicted by the model, provided that: $L_\mu < L_\omega < L_\mu$ and $(L_\mu - L_\omega) \neq (L_\omega - L_\tau)$, limitations that affect both the generalised and the re-parameterized VBGF. Age τ was chosen as one year, age μ as nine years, and age ω was then calculated to be five years, as size data at these three ages were well represented in the dataset and those ages covered growth of *O. pullus* over the majority of its life span in the Hauraki Gulf. Consequently, parameters of the rVBGF model resulted in estimates of mean size-at-age one L_1, five L_5, and nine L_9.

For both growth functions fitted to the observed size and age data, the best-fit model was estimated by minimizing the negative log of the likelihood, assuming a normal probability density function (Kimura, 1980; Haddon, 2001; Trip *et al.*, 2008). For comparison of expected mean size-at-age between the two models used, the rVBGF parameter values of expected mean sizes at ages one, five and nine were compared with: (1) the values found for the rVBGF parameters and with (2) mean size-at-age based on the original size data.

2.3 Results

Validation of periodicity and timing of opaque zone formation

Edge Type Analysis (ETA) revealed that the proportion of *Odax pullus* otolith samples with an opaque zone forming on the growing edge varied across months, and peaked at the same time of year for all age groups analysed. The observed pattern was consistent in both years examined, suggesting an annual pattern of periodicity of opaque zone formation.

In age group 1-2, the proportion of otoliths showing an opaque zone on the growing edge reached 50% in October 2006 and peaked at 75% in November 2006; in November 2007, 100% of otoliths examined showed an opaque edge (Fig. 2.2 a). In age group 3-4, 50% of otoliths examined showed an opaque growing edge in September 2006, which increased to 60% in October 2006 and peaked at 75% in November 2006; a similar pattern was found in 2007, with 75% of otoliths showing an opaque zone on the growing edge in September, 100% in November and 71% in December 2007 (Fig. 2.2 b). In age group 5+, the proportion of otoliths showing an opaque growing edge peaked at 100% in both November and December 2006, and reached 100% in September 2007, 67% in November 2007 and 100% in December 2007 (Fig. 2.2 c). These results suggest that (1) the proportion of otoliths with an opaque growing edge peaked in November in all age groups in both years examined (even though in age group 5+ in 2007 opaque zone formation peaked at 100% from September to December), and (2) that the range of months over which opaque zone formation occurred varied between September and December in all age classes and both years examined. From January to August (included), the proportion of otoliths with an opaque growing edge ranged between 0 and 40%, and averaged 8.4%.

A similar pattern of opaque zone formation was found when examining all age groups together and when comparing the timing of opaque zone formation between years sampled (Fig. 2.2 d). Monthly occurrence of otoliths with an opaque zone forming on the growing edge differed significantly from a circular uniform distribution in both years sampled, suggesting that there was a mean population direction in the observed frequency distribution of opaque zones across months. This was consistent for both 2006 and 2007 (Rayleigh's Test, $p < 0.001$, Table 2.2). The direction of the mean mode of the observed frequency distributions showed that opaque zone formation peaked in November in both years sampled

(Table 2.2; Fig. 2.3), confirming the patterns suggested by all three age classes examined separately.

The proportion of otoliths displaying an uncertain edge (25 otoliths; 9% of otoliths examined) showed no correlation with age ($p = 0.908$; $r = - 0.04$), month of sampling ($p = 0.141$; $r = - 0.45$), or sample size ($p = 0.634$; $r = 0.12$), suggesting no bias in the presence of otoliths with an uncertain edge during the analyses.

In overview, results of the ETA showed that, for all age groups examined, the timing of opaque zone formation peaked during the austral spring in November, and occurred from September to December. Opaque zone formation peaked at the same time of year in both years examined, indicating that one opaque zone is formed each year in spring and that together with a translucent zone, the enumeration of increments in the otoliths of *O. pullus* may be used as an estimate of age in years. These results validate the annual pattern of opaque zone formation in the sagittal otoliths of *O. pullus*.

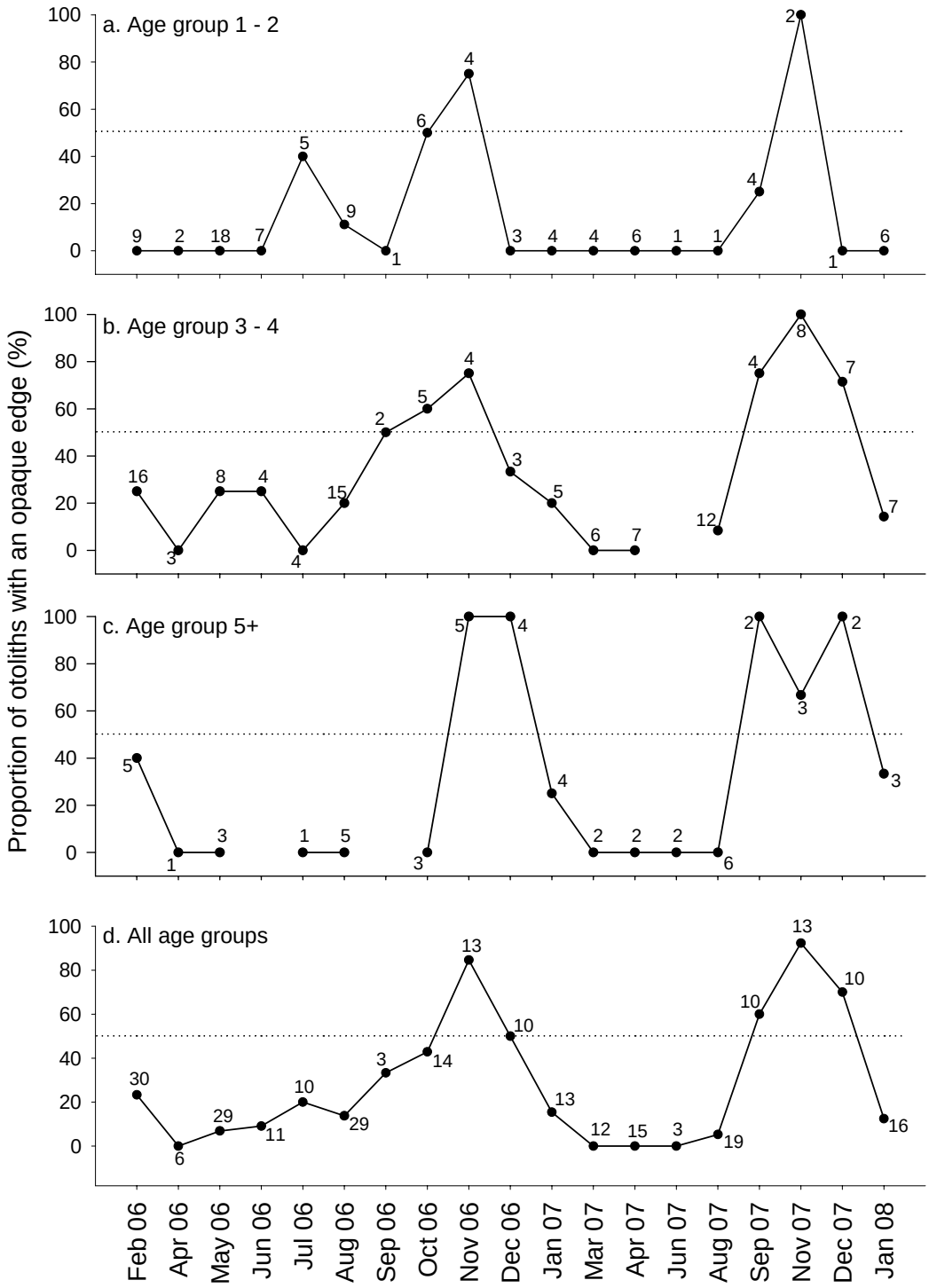

Fig. 2.2: Periodicity of opaque zone formation in sagittal otoliths of *Odax pullus* in the Hauraki Gulf. Two-year cycle of monthly occurrence of sagittal otoliths with an opaque zone forming on the growing edge, from February 2006 to January 2008, for three separate age groups (graphs a, b, c) and for all age groups pooled (graph d). Dotted line shows position of 50% opaque edges, and number labels show sample size.

Table 2.2: Results of Rayleigh's Test comparing the monthly occurrence of *Odax pullus* otoliths with an opaque edge type to a circular uniform distribution in both years sampled. H_0: occurrence of opaque edge types is uniform across months; H_A: occurrence of opaque edge types is not uniform, i.e. there is a mean population direction (shown in Mean month column). N is total number of otoliths examined for each year. Z is Rayleigh's statistic, and *p* shows significance at 0.05 level.

Year sampled	N	Z	*P*	Mean month
2006	168	94.999	*< 0.001*	November
2007	98	152.884	*< 0.001*	November

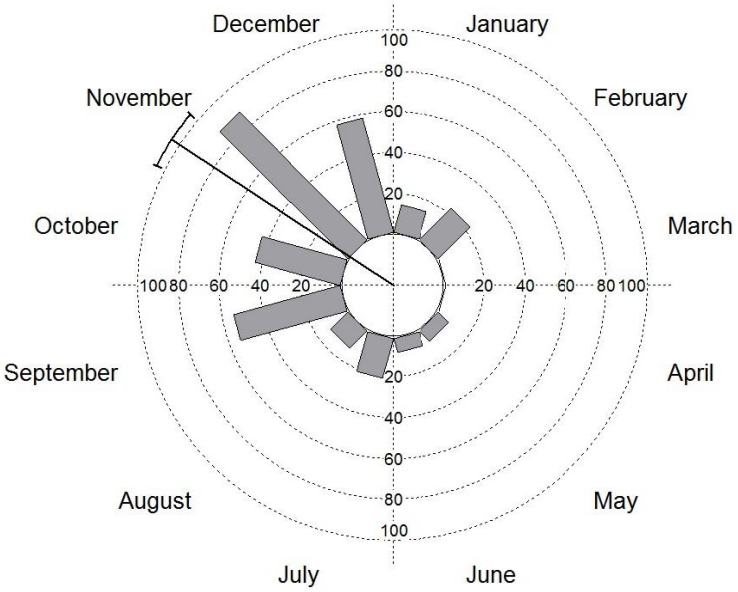

Fig. 2.3: Timing of opaque zone formation of *Odax pullus* in the Hauraki Gulf. Monthly occurrence of sagittal otoliths showing an opaque zone forming on the growing edge (%). Bold line shows mean mode of frequency distribution across months (+- 95% CI).

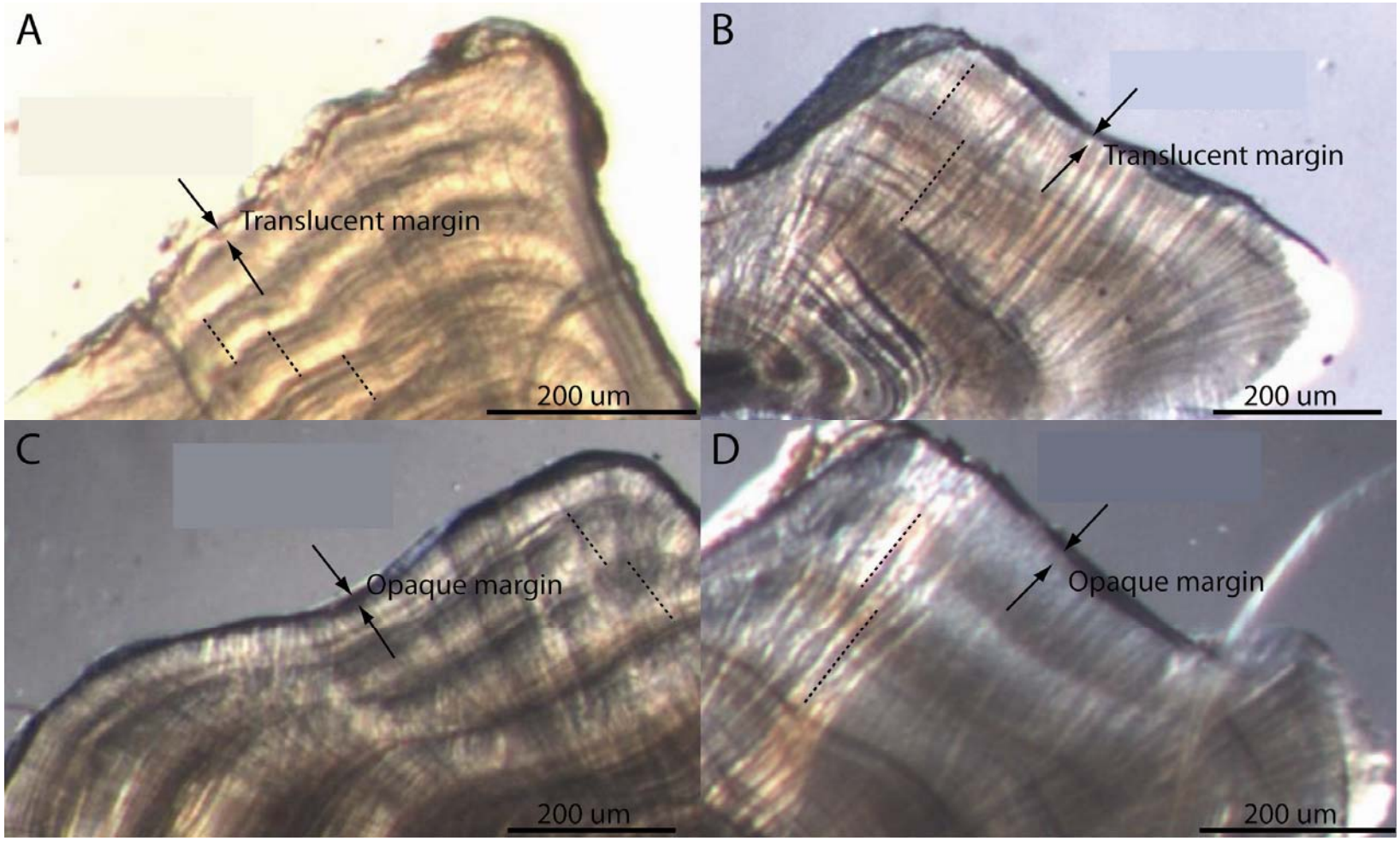

Fig. 2.4: Reference photomicrographs of (A, B) translucent and (C, D) opaque margins of otolith thin sections used for Edge Type Analysis in the validation of periodicity of opaque zone formation in *Odax pullus*. Otoliths are viewed under transmitted light at 40x (photos B, C, D) or 50x (photo A) magnification. Arrows indicate the position of the otolith margin. Dotted lines illustrate the position of completed annual increments.

Otolith microstructure – validation of daily increment formation

Two juvenile *Odax pullus* showed clear marginal increments coinciding with a visible OTC fluorescing mark (Fig. 2.5). The remaining five individuals used in this experiment showed either an OTC mark that was not defined clearly enough or the OTC mark did not coincide with clear interpretable marginal increments. For both individuals showing positive results in the OTC experiment, the mean number of increments counted between the inner margin of the OTC mark and the outer margin of the otolith was 4 (+- 0.125 SE) (Table 2.3). This coincided with the number of days the fish were held captive between injection of OTC and sacrifice (four days). These results validate the daily pattern of increment deposition in juvenile sagittal otoliths of *O. pullus*, and illustrate that one micro-increment may be interpreted as one day of age.

There was a significant correlation between sagittal weight and estimated age across all seven juvenile fish sampled ($r = 0.97$; $p < 0.001$) (Fig.2.6).

Table 2.3: Results of oxytetracycline (OTC) experiment on seven juvenile *Odax pullus*, showing total number of increments visible from the nucleus to the otolith margin, otolith weight (OW), size (Fork Length), presence or absence of a OTC mark, mean number of increments (±Standard Error) laid between time of injection of OTC and euthanasia, and the range of increments observed between OTC mark and otolith margin. OTC mark indicates whether a fluorescing band was visible under UV light which coincided with adequate interpretability of marginal increments.

Fish	Total increments	OW (mg)	Size (FL, mm)	OTC mark	Increments (+-SE)	Increments range
1	199	0.2187	93	Yes	4 (+-0)	4
2	139	0.1147	68	Yes	4 (+-0.193)	4-5
3	224	0.2332	102	No	-	-
4	220	0.2162	88	No	-	-
5	151	0.1508	75	No	-	-
6	225	0.2293	102	No	-	-
7	199	0.2103	95	No	-	-
Total					4 (+-0.125)	4-5

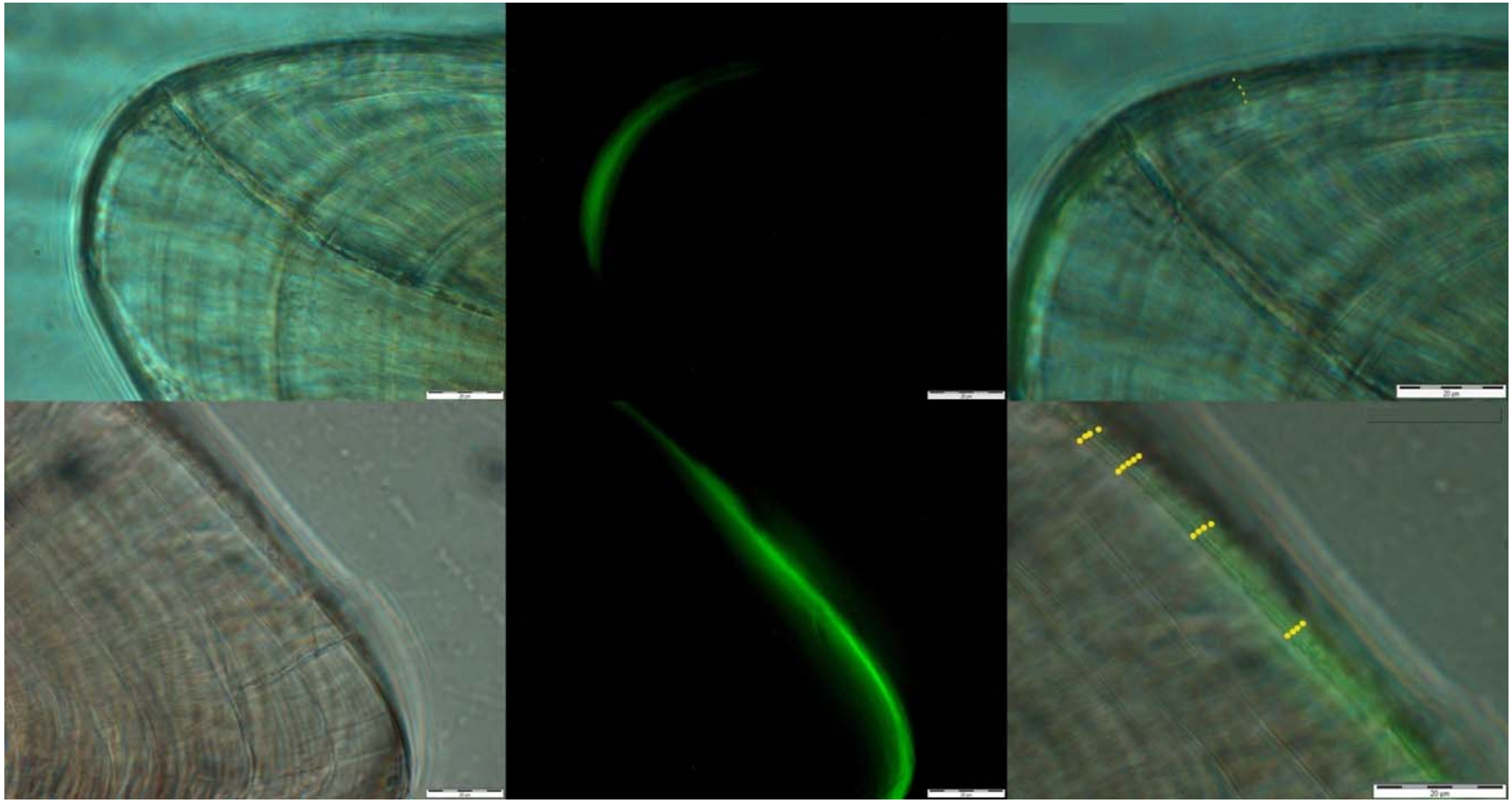

Fig. 2.5: Sectioned sagittal otoliths of two juvenile *Odax pullus* injected with oxytetracycline (OTC) for validation of daily increment deposition. Each row shows the same frame of one otolith seen under different light sources (all images taken at x100 objective). Left-hand panel shows otolith margin seen under transmitted light, center panel shows otolith margin under UV light, and right-hand panel is an expanded image of the overlay of the two previous images with the marginal increments visible highlighted with a yellow dot. Scale bars represent 20μm.

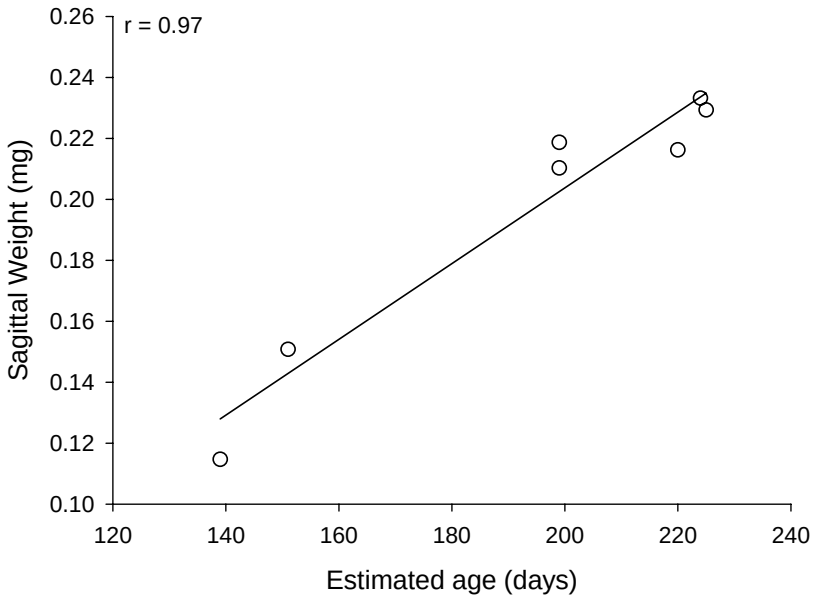

Fig. 2.6: Correlation between sagittal weight and estimated age of juvenile *Odax pullus* used in the oxytetracycline validation experiment. Least-squares linear function $y = -0.0448 + 0.0012x$ is presented.

Determination of the position of the first annual ring

Mean maximum otolith radius measured for the "age-1 cohort" individuals caught at the time of opaque zone formation (between September and December) suggested that the first annual opaque zone in otoliths of *Odax pullus* in the Hauraki Gulf was laid down at an average distance from the center of the nucleus of 632.83 μm +/- 23.84 SE (n = 14) (Fig. 2.7). Mean transverse radii estimated for 'zone 0', 'zone 1', and 'zone 2' are presented on Fig. 2.8.

Comparison of otolith radii measured between "age-1 cohort", 'zone 0', 'zone 1' and 'zone 2' using one-way ANOVA revealed a significant difference in otolith radius between the groups (Table 2.4; $F_{3, 58} = 64.837$, $p < 0.001$), with radii of 'zone 0' and 'zone 1' on average 34.2% smaller and 35.3% larger than 'zone 1', respectively. Pair-wise comparisons (Tukey's Test) showed that mean transverse otolith radii of "age-1 cohort" otoliths at the time of opaque zone formation and 'zone 1' together formed a homogeneous group, while 'zone 0' and 'zone 2' were significantly different from all other otolith radii (Fig. 2.9).

Monthly progression of mean maximum transverse radius of otolith sections of individuals aged 0+ and 1+ year showed that the smallest mean transverse radius was found

in December, which coincides with the end of the spawning season, and that mean radius increased each month from December onwards in both Young-Of-the-Year (YOY) individuals (aged 0+ years) and 1 year-old individuals (Fig. 2.10A). Monthly growth in otolith radius coincided with a monthly increase in body size (fork length) (Fig. 2.10B). In November, which corresponds to the peak timing of opaque zone formation, the radius of individuals aged 0+ met that of individuals aged 1+, and overlapped with the mean radius found for "age-1 cohort" juveniles caught at the time of opaque zone formation and with that of 'zone 1'.

Estimation of mean age at which 'zone 0' occurs was undertaken by counting the number of daily increments observed between the primordium and the inner and outer edges of 'zone 0', respectively. This revealed that the inner edge of 'zone 0' appeared on average after 80 days of age, and that the outer edge of 'zone 0' was concluded on average after 132 days of age. This suggested that 'zone 0' was laid down on average between the ages of 0.22 and 0.36 years.

These results suggest that the first annual growth increment in *O. pullus* can be expected to be laid down at a mean distance from the primordium of 632.83 μm +/- 23.84 SE in the Hauraki Gulf, and that 'zone 1', which corresponds to the second innermost opaque zone identified in older otoliths sections, is the opaque band that corresponds to one year of age. In turn, this signifies that 'zone 0', the innermost opaque ring, is laid down before the first birthday, and does not correspond to age 1, thereby confirming the hypothesis suggested by Paul et al. (2000).

Table 2.4: Results of ANOVA comparing otolith radius (μm) of "age-1 cohort" juvenile *Odax pullus* caught at the time of opaque zone formation (September to December) to otolith radius of ring types 'zone 0', 'zone 1', and 'zone 2' found in older individuals.

Effect	SS	MS	df	F	*p*
Intercept	21570129	21570129	1	3197.705	*<0.001*
Ring	1312083	437361	3	64.837	*<0.001*
Error	391239	6746	58		

Fig. 2.7: Photomicrograph of a thin section of sagittal otolith of an "age-1 cohort" juvenile *Odax pullus* caught in November in the Hauraki Gulf, showing formation of the first annual opaque zone. P shows position of the primordium (center of the nucleus); and line shows the position of the maximum transverse radius (mean radius +- SE).

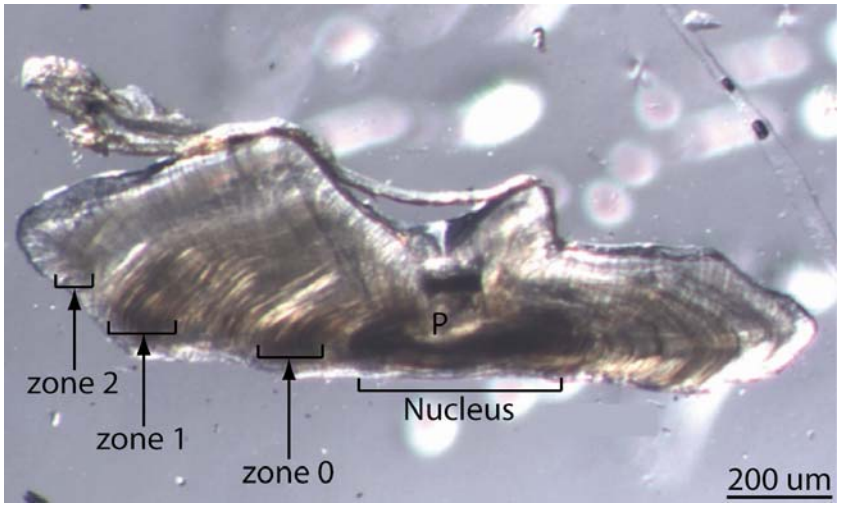

Fig. 2.8: Thin section of sagittal otolith of *Odax pullus* in the Hauraki Gulf viewed under transmitted light, showing the position of the three ring types 'zone 0', 'zone 1' and 'zone 2'. P indicates position of the primordium (centre of the nucleus). Mean maximum transverse sagittal radii of 'zone 0', 'zone 1' and 'zone 2' were 378.06 µm +/- 11.02 SE (n = 16), 574.66 µm +/- 21.76 SE (n = 16), and 777.74 µm +/- 24.58 SE (n = 16), respectively.

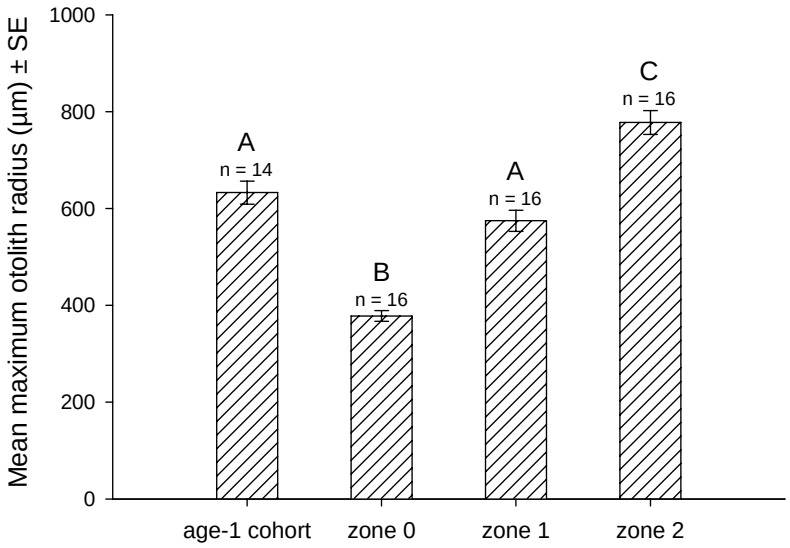

Fig. 2.9: Comparison of mean otolith radius of 'age-1 cohort' juvenile *Odax pullus* caught at the time of opaque zone formation with mean otolith radius of the first three opaque zones 'zone 0', 'zone 1' and 'zone 2' of older individuals (shown in Fig.2.8). Labels show homogeneous groups (Tukey's Test), and sample size n.

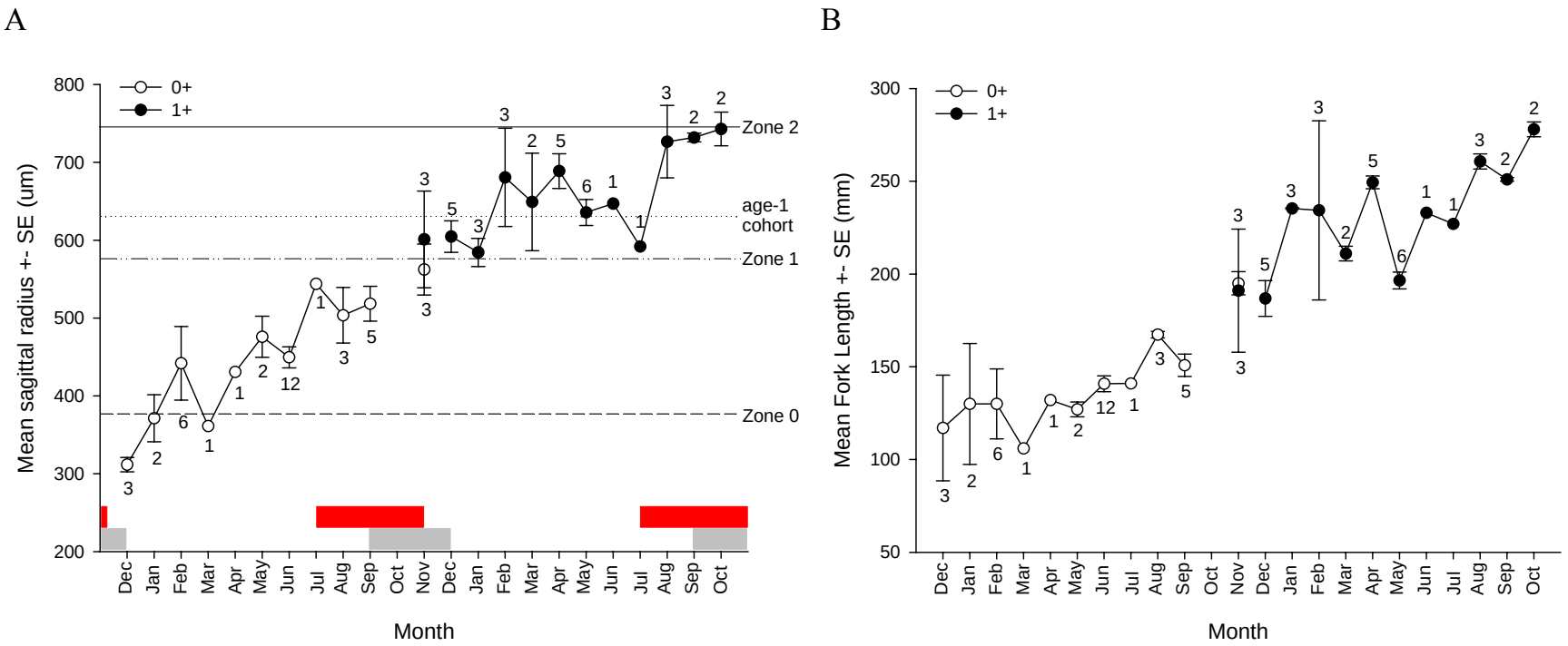

Fig. 2.10: Monthly progression of (A) mean otolith radius and (B) mean body size of Young-of-the-Year (age 0+ years; open circles) and one year old (black circles) juvenile *Odax pullus* in the Hauraki Gulf. Dotted line shows the position of the mean transverse radius of "age-1 cohort" juveniles caught at the time of opaque zone formation, dashed line shows the position of the mean transverse radius of 'zone 0', dashed-and-dotted line shows the position of the mean transverse radius of 'zone 1', and solid line shows the position of the mean transverse radius of 'zone 2'. Grey-shaded areas show timing of opaque zone formation, and red-shaded areas show timing of spawning season.

Precision of readings

The mean coefficient of variation (CV) of age readings across all otolith sections of *Odax pullus* aged was 8.7% +/- 0.5 SE, which corresponds to an Average Percent Error (APE) value of 6.3% (see regression equation between CV and APE in Campana 2001). This value coincides with that found across studies using CV and/or APE as an estimate of precision (mean CV across literature reviewed in Campana (2001) was 7.6 % +/- 1.5 SE), suggesting a satisfactory level of precision in the readings of age from otolith sections in the study species. Examination of the percent variation between readings across age classes revealed that readings of individuals aged less than one year appeared significantly more variable than those of individuals aged one year or more, as may be expected from the inherently larger variance associated with increment counts in number of days than in number of years (Fig. 2.11).

There was a significant positive correlation between otolith weight and estimated age ($r = 0.94$; $p < 0.001$) (Fig. 2.12), which was consistent with the expected linear increase in otolith weight with age (Fletcher, 1991; Francis *et al.*, 2005).

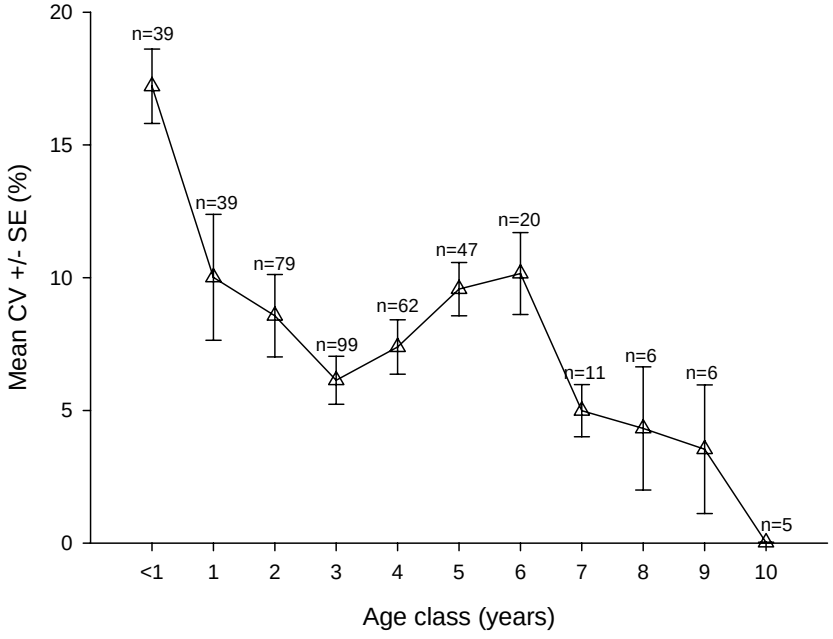

Fig. 2.11: Mean coefficient of variation (CV) of age readings for *Odax pullus* in the Hauraki Gulf per age class. Error bars show Standard Error (SE), and labels show sample size.

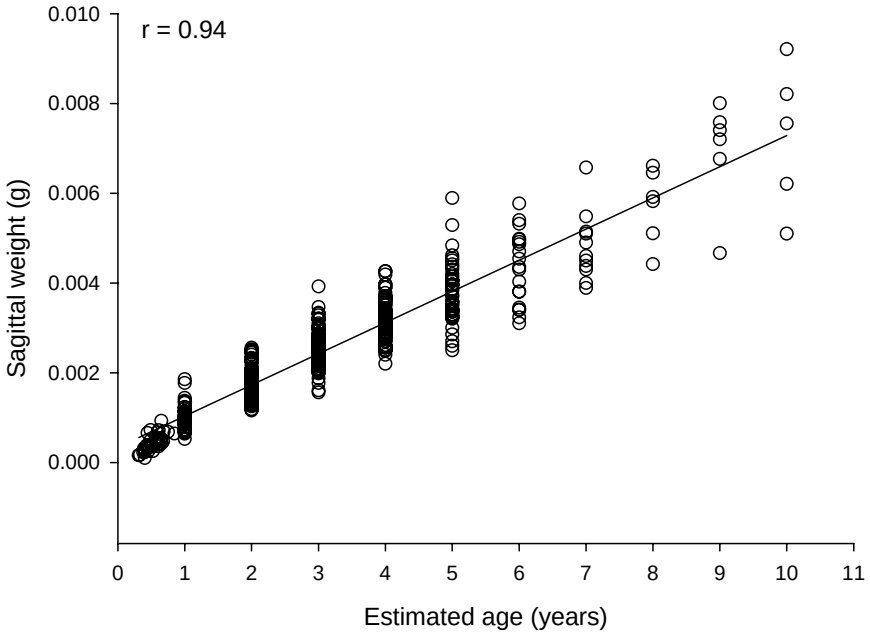

Fig. 2.12: Correlation between sagittal weight and age (n = 436) of *Odax pullus* in the Hauraki Gulf. Least-squares linear function $y = 0.0003 + 0.0007x$ is presented.

Relationship between size and age

Examination of the relationship between size and age of *Odax pullus* in the Hauraki Gulf revealed an asymptotic form of growth and fast early growth, with individuals reaching 70% of mean asymptotic size by the age of two years and achieving a maximum age of eleven years (Fig. 2.13). Best-fit parameter values of VBGF and rVBGF growth trajectories fitted were L_∞ = 457.36 mm FL (asymptotic size), K = 0.517 (curvature coefficient), and t_0 = - 0.23 (age at which fish have a theoretical body size of zero), and L(1) = 214.35 mm FL (mean size-at-age one), L(5) = 426.01 mm FL (mean size-at-age five), and L(9) = 450.29 mm FL (mean size-at-age nine), respectively. Comparison of mean size-at-age estimates at the ages of one, five, and nine years showed that the rVBGF parameter values did not differ significantly from estimates of mean size-at-age as predicted by the best-fit VBGF trajectory, and from estimates of mean size-at-age as calculated from original size and age data (Fig. 2.14). These results indicate that the rVBGF provides reliable estimates of mean size-at-age for the study species.

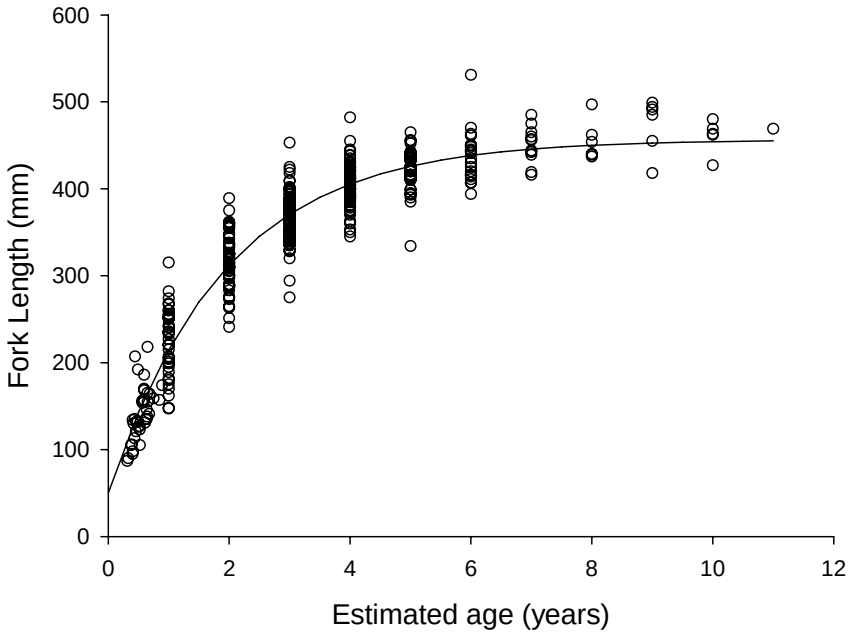

Fig. 2.13: Size-at-age of *Odax pullus* in the Hauraki Gulf, showing the best-fit re-parameterized von Bertalanffy Growth Function (n = 437).

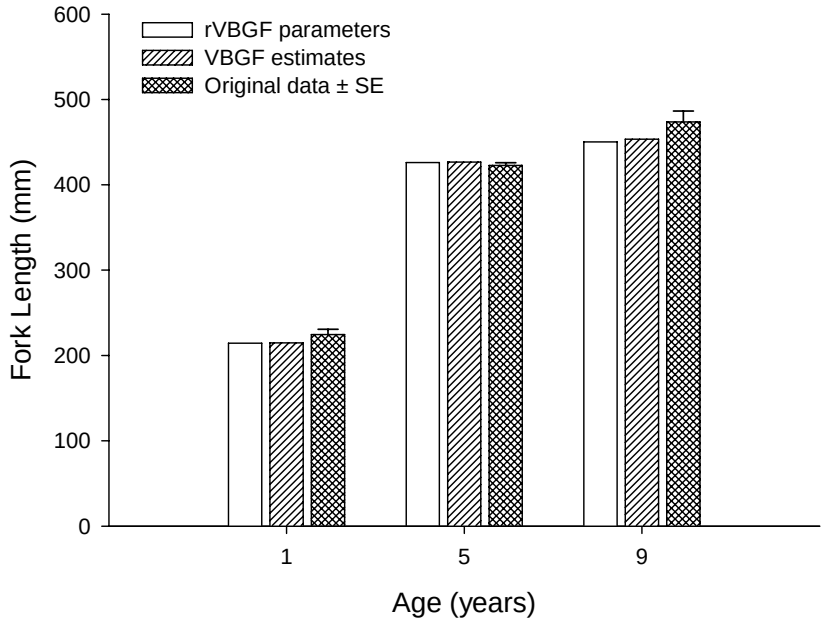

Fig. 2.14: Comparison of estimates of mean size-at-age *of Odax pullus* from the Hauraki Gulf at the ages of one, five, and nine years obtained from: (i) the re-parameterized von Bertalanffy growth function (rVBGF) parameters, (ii) expected size-at-age predicted by the best-fit VBGF model, and (iii) mean size-at-age as calculated from the original size and age data (presented with Standard Error bars).

2.4 Discussion

Analysis of otolith sections of *Odax pullus* in the Hauraki Gulf revealed a clear pattern of alternating opaque and translucent bands running concentrically from the nucleus to the otolith edge. This coincides with the pattern found in otoliths across most fish species (Summerfelt and Hall, 1987; Secor *et al.*, 1995; Begg *et al.*, 2005). Analysis of the periodicity and timing of opaque zone formation revealed an annual pattern. One opaque zone formed each year examined during the austral spring between September and December peaking in November. The timing and periodicity of opaque zone formation found in the study species coincides with the pattern found for a number of fish species in temperate marine environments of the southern hemisphere (Beckman and Wilson, 1995). Field validation of daily increment formation in juvenile individuals revealed that one growth increment was formed on a daily basis in the otoliths aged less than one year, as expected in larval and juvenile fish (Pannella, 1971). The position of the first annual growth increment was determined (mean distance between otolith nucleus and outer margin of first annual opaque zone of 632.83 μm +/- 23.84 SE). This allowed clarification of the nature of 'annulus 0', which was laid down between an average of 80 and 132 days of age, and which, accordingly, did not represent year one. Together, these results provide the basis for the analysis of age in *O. pullus*, and form a reliable ageing procedure using sectioned sagittal otoliths. Examination of the relationship between the resulting age estimates and size for the study species in the Hauraki Gulf, showed a maximum age of eleven years, and a determinate growth trajectory, which coincides with the form of growth found for a number of related Labrid species (*e.g.* Choat *et al.*, 1996).

Analysis of the position of the first annual opaque zone in the otoliths of *O. pullus* revealed that age one corresponds to the second innermost opaque zone present in the otoliths sections of the study species. This result is significant as misinterpretation of the position of the first annual growth increment leads to a constant ageing error by at least one year, and ultimately results in an over- or under-estimation of somatic growth rate, maximum age (longevity), and all related age-based demographic parameters. In the present study, *O. pullus* was found to display a mean body size of 214.35 mm FL by the age of one year. This finding falls within the range of values previously found for individuals of the same age in Bader (1998) and Paul *et al.* (2000) (~204 and ~240 mm FL, respectively). In contrast, these results differ from those presented in Ritchie (1969) (~85 mm total length at the age of one year).

Differences in growth rate and body size may be expected when comparing growth trajectories among populations living at different latitudes. However, determination of the age at which 'annulus 0' is laid down in *O. pullus* and of the position of the first annual increment in the present study suggests that the use of 'annulus 0' as age one in Ritchie (1969) resulted in an under-estimation of size-at-age one, as well as an under-estimation of maximum age achieved. These results illustrate the significance of the determination of the position of the first annual growth increment and the effect of misinterpretation of the first annulus on the resulting estimates of growth rate and size-at-age, in particular in the early parts of the life span.

Examination of the relationship between size and age of *O. pullus* revealed a form of growth that differed markedly from that found in the previous studies of growth in butterfish (Ritchie, 1969; Bader, 1998; Paul *et al.*, 2000). The growth trajectory generated from the validated ageing method revealed a comparatively faster rate of growth in the early part of the life span, and a relatively more determinate form of growth (Fig. 2.15). *O. pullus* in the Hauraki Gulf achieved on average 70% of their mean asymptotic size by the age of two years, and 90% by the age of four years. As compared to the results found in Ritchie (1969), this difference in the form of growth may be explained by the difference in the interpretation of the position of the first annual growth increment, as mentioned above, as well as by the use of back-calculated lengths based on scales to estimate growth (see Francis, 1990 for a review of back-calculation of fish length). In contrast, Bader (1998) and Paul *et al.* (2000) excluded 'annulus 0' from their age counts, as in the present study, and fitted the traditional VBGF, but found comparatively lower values of K and higher values of t_0, both indicative of little curvature in the growth curve and low rates of growth in the early parts of the life history (Table 2.5). A low curvature parameter suggests a sample bias rather than a biologically meaningful interpretation, as shown in Berumen (2005). In both cases (Bader, 1998; Paul *et al.*, 2000), growth trajectories fitted to the sampled size-at-age information were constructed with one individual aged one year, as opposed to thirty-nine individuals aged less than one year and thirty-nine individuals aged one year old in the present study. The absence of juvenile individuals when constructing a growth trajectory directly affects the accuracy and precision of estimates of the derived demographic parameters, in particular that of the von Bertalanffy growth function (VBGF) parameters L_∞, K and t_0 (Kritzer *et al.*, 2001; Berumen, 2005). Berumen (2005) used four species of butterflyfish (Chaetodontidae) to show that exclusion of juvenile individuals from each data set resulted in (1) overestimation of mean

asymptotic size L_{∞}, (2) underestimation of the curvature parameter K, and (3) overestimation of theoretical age at size zero t_0. Together, these parameter estimation errors generated a form of growth that did not represent the actual from of growth of the study species (see figure 1 in Berumen, 2005). This in turn directly affects estimates of growth rate, mortality rate, and mean maximum size (Kritzer *et al.*, 2001). Comparison of the VBGF parameters found in Bader (1998) and Paul *et al.* (2000) to those generated from this study shows that the K values are significantly lower and that the t_0 values are significantly greater (Table 2.5), illustrating that the absence of individuals in the lower end of the age range directly affects the reliability of the growth estimates.

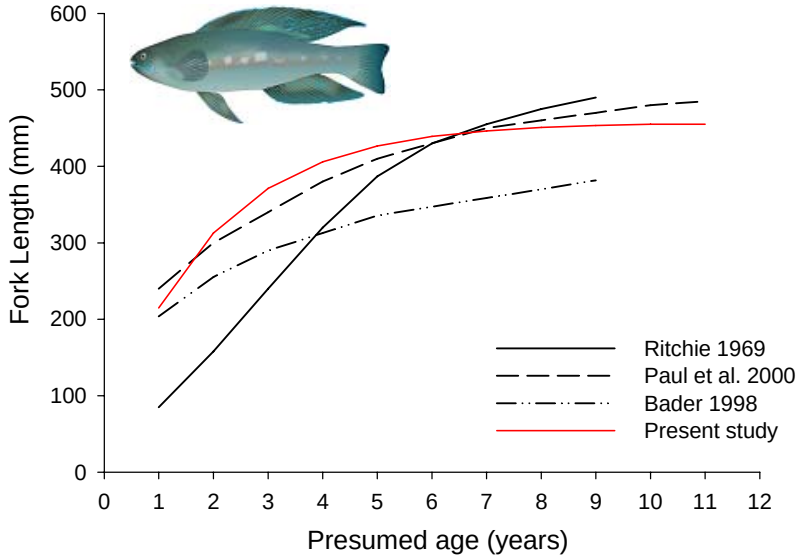

Fig. 2.15: Comparison of growth trajectories of previous size-at-age studies of *Odax pullus* with the form of growth found for the study species in the present study.

Table 2.5: Summary table showing results from the present study and those found in the previous studies on growth in *Odax pullus*, comparing: (1) the number of fish aged less than one year and the number of fish aged 1 year included in the samples; and (2) the von Bertalanffy growth function (VBGF) parameters. $L\infty$ represents mean asymptotic size, K is the curvature parameter, and t_0 represents theoretical age at which size equals zero (x-intercept), often used as an approximation for pelagic larval phase duration.

Reference	*No fish aged < 1 year*	*No fish aged 1 year*	*VBGF parameters*		
			L∞ (mm; FL)	*K*	*t_0 (years)*
Bader (1998)	0	1	365	0.22	-2.4
Paul *et. al* (2000)	0	1	518	0.23	-1.7
Present study	39	39	457	0.52	-0.23 (84 days)

The re-parameterized von Bertalanffy Growth Function (rVBGF) was proposed by Francis (1988) to improve the biological interpretability of the traditional VBGF parameters. Indeed, their relevance has often been questioned (Knight, 1968; Roff, 1980; Schnute and Fournier, 1980; Craig, 1999), in particular that of the VBGF curvature parameter *K*, which has often been wrongly interpreted and used as a measure of growth rate (Cerrato, 1991). The parameters of the rVBGF equation generate estimates of mean size-at-age, which are inherently more meaningful. Furthermore, the biological significance of the rVBGF parameters allows for a direct comparison of mean size-at-age and is of particular significance when comparing growth between populations (*e.g.* Welsford and Lyle, 2005; Trip *et al.*, 2008). In this study, the value of the parameters estimated from the rVBGF (*L(1)*, *L(5)*, and *L(9)*) were compared to the expected size-at-age obtained from the traditional VBGF and to actual mean size-at-age as calculated from the original data set at the same ages of one, five and nine years. No differences were found in the expected mean sizes at all three ages examined, as could be expected from two related models (Francis, 1988), and no differences were found between the estimated rVBGF value of *L(1)*, *L(5)*, and *L(9)* and mean values generated from the original size-at-age data, suggesting that the rVBGF model parameters adequately estimated mean size-at-age. These findings demonstrate that the parameters of the rVBGF equation can be interpreted directly as estimates of expected mean size-at-age. As the parameters yielded from the rVBGF model have greater biological relevance than those of the traditional VBGF model, the use of the rVBGF model will be preferred for the study of growth throughout this thesis.

These results demonstrate a number of critical aspects concerning the study of age and growth. Firstly, misinterpretation of the position of the first annual growth increment directly affects the resulting estimates of size-at-age, somatic growth rate and maximum age. This result illustrates the need for including the position of the first annual increment in validation procedures of ageing methods as proposed by Campana (2001). Secondly, these results show the importance of including juvenile individuals when modelling growth and estimating somatic growth rate as shown by Kritzer *et al.* (2001) and Berumen (2005). Covering the entire extent of the age and size ranges of a study species will be critical when estimating somatic growth rate and related demographic traits. Thirdly, the choice of a growth model to establish the relationship between size and age directly affects the biological interpretability of growth parameter estimates. This will be particularly relevant when comparing growth and related age-based demographic traits among populations of

individuals, for example between geographical populations along a latitudinal gradient, or between sexes within given populations, and when establishing patterns of variation in body size, growth rate, longevity, and development rate across gradients of latitude. In this case, a main concern is that the parameters extracted from the models need to provide reliable, comparable, and biologically relevant, information.

Chapter 3. Reproductive biology of the protogynous temperate wrasse *Odax pullus* (Labridae) in the Hauraki Gulf, New Zealand

3.1 Introduction

The ability to change sex is common amongst teleost fishes (Sadovy and Liu, 2008). The ontogeny of sex change may vary across families and genera (reviewed in Sadovy and Liu, 2008), but also within species (Munday *et al.*, 2006b). Such flexibility in sexual ontogeny is thought to optimise individual reproductive value within variable environmental conditions (Munday *et al.*, 2006a; Angilletta, 2009), and significant advances have been made as to our understanding of the underlying mechanisms driving the processes and timing of sex reversal (Allsop and West, 2003b; Allsop and West, 2003a; Munoz and Warner, 2003; Allsop and West, 2004; Buston *et al.*, 2004; Munday *et al.*, 2006a; Munday *et al.*, 2006b).

The Labridae, with a total of eighty-two genera and around six hundred species (Westneat and Alfaro, 2005), display a wide range of patterns in sexual ontogeny, from gonochorism (separate sexes) to sequential hermaphroditism (sex change) (Sadovy and Liu, 2008). Many labrid species exhibit protogynous (female-to-male) sex reversal, which has been confirmed in twenty-one genera to date. While functional protogyny has been shown in many labrid tribes (Reinboth, 1962; 1967; 1968; 1970; Choat and Robertson, 1975; Reinboth, 1975; Robertson and Warner, 1978; Warner and Robertson, 1978), patterns of sexual ontogeny of odacine labrids are poorly understood. As it has been suggested that temperate environments at higher latitudes may provide less favourable thermal conditions for the underlying physiological processes of sex change (Sadovy and Liu 2008), the odacines are a potentially interesting group in this context. This chapter examines the reproductive biology of the odacine labrid *Odax pullus*.

Diagnosis of the sexual ontogeny of labrid species has proven to be complex. This results primarily from a mismatch between reproductive function (gonochorism vs. sex change) and gonad microstructure. In particular, testes that possess the morphological characteristics of previous female identity (Sadovy and Shapiro, 1987) and that, as such, are considered to be the product of protogynous sex-reversal, may not have passed through a

functional female stage (Liu and Sadovy, 2009). Males may be derived from immature bisexual individuals (Hamilton *et al.*, 2008), or directly from an immature female phase (Denny and Schiel, 2002). This is further complicated by the presence within many labrid species of two male development pathways (Reinboth, 1962; 1967; Choat and Robertson, 1975). Depending on local population structure, some males develop directly from a juvenile gonad (primary males) while others are the result of sex reversal of functional females (secondary males) (Shapiro and Rasotto, 1993; Munday *et al.*, 2006b). The complexity of diagnosis of sexual ontogeny in labrid species raises a number of critical points. Firstly, establishing the schedules of sexual maturation and of sex reversal (size- and age-at-maturity and -at-sex change) will be necessary for the diagnosis of reproductive function. This may be challenging in temperate environments however, as the diagnosis of female spawning history may be hindered in conditions where females undergo long inter-spawning intervals. Secondly, examination of the gonad structure of immature juvenile individuals will be critical for the assessment of male and female ontogeny (Liu and Sadovy, 2009). Thirdly, histological examination of gonad structure will need to i) cover all sexual development stages (*i.e.* across the size and age ranges), and ii) be associated with demographic information on the relationship between size, age and sexual identity.

Prior examination of sexual ontogeny and reproductive function in *O. pullus* has suggested the presence of protogyny (Ritchie, 1969; Crabb, 1993; Bader, 1998). Evidence supporting this is based on (i) the presence of a sex-specific size and age distribution, with males occurring in the larger size- and older age- classes (Crabb, 1993; Bader, 1998), and (ii) the presence of an ex-ovarian lumen, of primary oocytes in developing testicular tissue, and of peripheral sperm sinuses (Crabb, 1993; Bader, 1998). However, the reliability of these diagnostic features as evidence for functional protogyny has been questioned (Liu and Sadovy, 2004; Sadovy and Liu, 2008; Liu and Sadovy, 2009). In particular, no evidence of prior female function in testes displaying female histological features has been found to adequately support the hypothesis of protogynous sex reversal in this species. The general aim of this study is to examine the sexual ontogeny and development of *O. pullus* in the Hauraki Gulf, northern New Zealand. Specifically, I first examine the morphology and microstructure of male and female gonads across the species' size and age range at the sampling location, including juvenile individuals. Secondly, I combine histological and demographic information in order to establish the relationship between gonad microstructure, size, and age. This allows establishing the patterns of male and female recruitment into the

population and the schedules of reproductive development and sexual maturation. Thirdly, I examine the histology of testis microstructure for the presence of prior female reproductive function, in order to assess the ontogeny of male function and establish the reproductive biology of the study species.

3.2 Materials & Methods

Sample collection

A total of 319 individuals of *O. pullus* were sampled in the Hauraki Gulf of New Zealand (35.9 - 36.6°S; 174.7 - 175.9°E) (Fig. 3.1). Fish were collected monthly over two and a half consecutive years between August 2005 and January 2008 (Table 3.1).

Fish were sampled by spearing and processed within one hour of collection. Fork Length (FL), Gutted Weight (GW), and gonad weight were recorded for each fish to the nearest millimetre, ten grams and gram, respectively. The sagittal pair of otoliths was removed, rinsed in 70% ethanol, and stored dry. Whole gonads were removed and placed in FAAC, a formalin-based fixative (formaldehyde 4%, glacial acetic acid 5%, calcium chloride 1.3%; Pears et al. 2006). After a minimum period of two weeks, fixed gonads were transferred into 70% ethanol before histological processing.

Table 3.1: Monthly sampling effort of *Odax pullus* in the Hauraki Gulf from August 2005 to January 2008, showing the number of individuals collected. * shows samples that had been frozen prior to being fixed – histology of these samples allowed determination of sex but not assessment of sexual maturity.

Month	2005	2006	2007	2008	*Total*
January			14	19	*33*
February		39			*39*
March			13		*13*
April		6	16		*22*
May		32			*32*
June		12	14		*26*
July		11			*11*
August	4*	9 + 20*	4 + 14*		*51*
September		4	14		*18*
October		14			*14*
November	4	13	13		*30*
December	7	13	10		*30*
Total	*15*	*173*	*112*	*19*	*319*

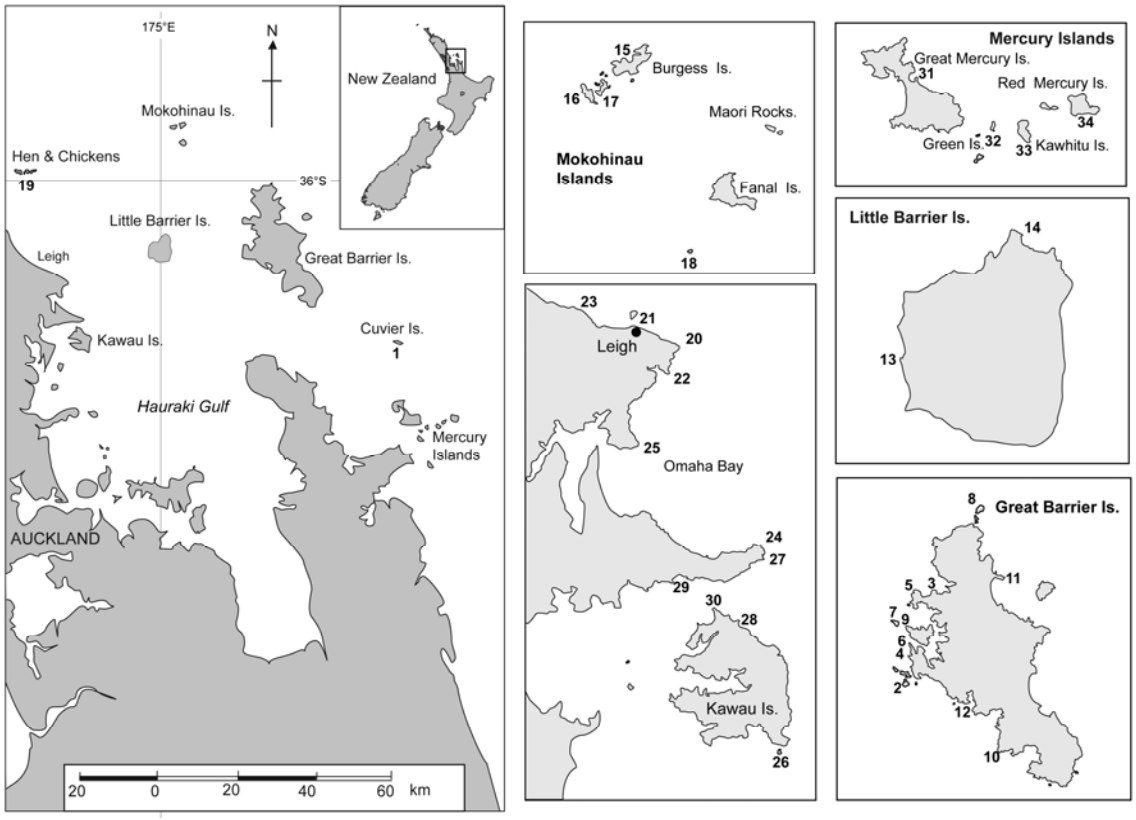

Fig. 3.1: Map showing sampling locations of *Odax pullus* in the Hauraki Gulf, New Zealand, with detailed maps of sampling sites at each island group (Cuvier Is (1), Great Barrier Is (2-12), Little Barrier Is (13-14), Mokohinau Islands (15-18), Hen & Chickens Islands (19), Leigh/Omaha Bay (20-25), Kawau Is (26-30), Mercury Islands (31-34)).
Legend: 1: Cuvier Island; 2: Broken Is, 3: Catherine Bay, 4: Grey Group, 5: Maunganui Point, 6: Motu Rako, 7: Motuhaku Is, 8: Needles Point, 9: Nelson Is, 10: Shag Point, 11: Waikaro Point, 12: Whangara Is, 13: Lion Rock, 14: Ngatamahina Point, 15: House Bay, 16: the Gardens, 17: Sentinel Cove, 18: Navire Rock, 19: Hen & Chicks Is, 20: Cape Rodney, 21: Goat Is, 22: Maori Is, 23: Okakari Point, 24: Takatu Point, 25: Ti Point, 26: Challenger, 27: Elephant Rock, 28: Fairchild Reef, 29: Jones Bay, 30: Kawati Point, 31: Coralie Bay, 32: Green Is, 33: Kawhitu Is, 34: Red Mercury Is.

Gonad histology

Gonads were blotted dry and weighed whole (including both lobes) to the nearest 10^{-4} gram. One gonad lobe was selected randomly, and a transverse section through the medial region was taken for histological processing. All gonad samples were embedded in paraffin wax, sectioned at 7 μm, mounted on glass slides and stained with Gill's Haematoxylin and Eosin stain (H&E stain).

In order to examine the consistency of gonad development across the length of the gonad lobe as well as across gonad lobes, two sub-sample procedures were followed. (i) A subset of 39 gonad samples (collected November to April) was serially sectioned in the anterior, medial and posterior regions of the tissue to examine the consistency of gonad development along the gonad length. (ii) In a sub-sample of 10 gonads (collected in March), both lobes were sectioned to examine the consistency of reproductive diagnosis across gonad lobes analysed. Analysis of the sub-sampled histological sections showed no variation in diagnosis of sexual identity or reproductive status among gonad regions sampled and between lobes sectioned. Consequently, transverse sectioning of the medial region of one randomly chosen gonad lobe was considered to provide representative information for diagnosis of reproductive developmental stage and sexual identity of each gonad.

All histological sections were examined under a high power microscope with transmitted light. For each section, sexual identity, reproductive activity and spawning history were assessed. Examination of the slides was blind with respect to fish identity, age, or size. Stages of oocyte development were classified by the latest non-atretic stage present in the tissue, as follows: stage I – chromatin nucleolar stage, stage II – peri-nucleolar stage, stage III – cortical alveoli stage (formation of yolk vesicle precursors), stage IV – vitellogenic (yolk) stage, and stage V – hydrated stage (West, 1990). Oocyte atresia was identified following criteria presented in Hunter and Macewicz (1985), and the presence of α-stage atretic vitellogenic oocytes and of brown bodies was recorded. The latest and most abundant spermatogenetic stage present was used to identify the developmental stage of each testis (Grier, 1981). Gonads were classified as one of the following four categories: (i) "female", when oogenic tissue was present throughout the section, (ii) "male", when spermatogenic tissue was observed throughout the section, (iii) "early-transitional", when atretic vitellogenic (or later stages) oocytes and/or post-ovulatory follicles could be seen within developing testicular tissue, and (iv) "late-transitional", when the simultaneous presence of primary

oocytes (pre-vitellogenic stages chromatin nucleolar and peri-nucleolar) and spermatogenic tissue (spermatogonia to spermatozoa) was observed, and no signs of previous spawning as a female (post-ovulatory follicles and / or atretic vitellogenic oocytes) could be seen (Sadovy and Shapiro, 1987; Sadovy and Liu, 2008). The presence in ovaries of intra-lamellar muscle bundles, atretic vitellogenic oocytes, and post-ovulatory follicles was recorded, and their incidence across months was established to examine their relationship to the timing of post-spawning events. When appropriate, these criteria were used in the diagnosis of female spawning history (Adams and Choat, 2002; Liu and Sadovy, 2004). Criteria used in the diagnosis of gonad sexual identity, reproductive activity, developmental stage, and spawning history are summarized in Table 3.2.

Size- and age-frequency distributions of males and females were established (frequency of males or females per size or age class as a proportion of the total number of individuals collected). Evidence for putative protogynous sex change was assessed using criteria developed in Sadovy and Shapiro (1987) and Sadovy and Liu (2008). A critical factor was to correctly identify transitional individuals, a key criteria of interest being the presence or absence of atretic vitellogenic (or later stage) oocytes (AVOs). A subset of sections identified as early-transitional, mature inactive (resting) female, spawning female (with stage V oocytes) and post-spawning female (with AVOs) was unstained for H&E, and re-stained for identification of glycoproteins, a primary constituent of yolk, using Periodic-Acid Schiff (PAS) and Haematoxilin (counter-stain) (Wallace and Selman, 1981). In order to establish the ontogeny of testis development, the organisational microstructure of juvenile gonads was examined (Liu and Sadovy, 2009), and testis microstructure was compared to that of ovaries (Shapiro and Rasotto, 1993). Male gonads were further examined to: (i) determine the position of sperm sinuses (central duct situated dorsally indicative of primary male development, versus peripheral ducts indicative of secondary male development), and (ii) to check for the presence of a membrane-lined lumen (indicative of ex-ovarian lumen) and lamellar structure.

Reproductive seasonality

Timing and duration of the spawning season was assessed based on the period of highest female reproductive activity. Reproductive activity was evaluated from monthly

variation in the gonadosomatic index (GSI). GSI was calculated using weight of both ovaries (gonad weight) as a proportion of gutted body weight, as follows: $GSI\ (\%) = \frac{Gonad\ weight\ (g)}{Gutted\ weight\ (g)} * 100$.

Mean monthly GSI was estimated for mature and immature females and the GSI profile examined across months sampled. GSI was plotted with mean monthly sea surface temperature (SST) recorded in the Hauraki Gulf across both years sampled.

The timing of the formation of intra-lamellar muscle bundles (ILMB), post-ovulatory follicles (POF) and atretic vitellogenic oocytes (AVO) was examined by plotting the frequency of ovaries showing ILMBs, POFs, or AVOs, respectively, across months.

Size- and age-at-maturity

Estimation of size- and age-at-maturity was performed based on females collected during the spawning season (Pears *et al.*, 2006). Females with inactive ovaries (stage I & II oocytes only) during the spawning months were immature, and females displaying stage III (cortical alveoli stage) to stage V (hydrated stage) oocytes during the spawning season were mature.

Size- and age-at-maturity were estimated by calculating the size and age at which 50% of females were mature (proportion of mature females relative to the total number of females within each size or age class). For each female, information used was size (Fork Length FL in mm), age (in years), and maturity (immature or mature). A logistic function was fitted to the non-linear relationship between maturity (dependent variable, *y*-axis) and size or age (independent variable, *x*-axis) respectively, following Moore et al. (2007) and Williams et al. (2008). The best-fit logistic model was estimated by minimising the negative log of the likelihood based on a probability density function with a binomial distribution (Haddon, 2001). The logistic function used is of the form: $P_a = \frac{1}{1+ e^{(-\ln(19)*\frac{(a - a_{50})}{(a_{95} - a_{50})})}}$, where P_a is the proportion of mature females in size or age class a, a_{50} is the size or age at which 50% of females are mature, and a_{95} is the size or age at which 95% of females are mature. Parameters estimated were size-at-50% maturity L_{50}, size-at-95% maturity L_{95}, age-at-50%

maturity T_{50}, and age-at-95% maturity T_{95}. Size classes were based on 50 mm increments, and age classes were based on one year increments.

95% confidence intervals (CI) were estimated for each parameter value of a_{50} and a_{95} using a bootstrapping procedure (Moore *et al.*, 2007). The data were randomly re-sampled 1000 times with replication. For each re-sampled data set, the logistic function was fitted and the best-fit combination of parameters a_{50} and a_{95} was estimated as described above. 95% percentile confidence intervals were calculated using the as 2.5 and 97.5 percentiles of the bootstrap estimates (Haddon, 2001).

Sex-specific growth

An additional 108 fish (total of 427 fish) were sampled for size-at-age information; these additional individuals were sexed macroscopically. Based on the histological diagnosis of sexual identity of reproductively active males and females processed in this study, the error associated with macroscopic identification of sexual identity was calculated as 0.8%, and considered negligible. Sagittal otoliths were processed, and age was estimated as described in Chapter 2 (section 2.2). Size-at-age data was modeled separately for males and females using the re-parameterized equation of the von Bertalanffy growth function (rVBGF) (Francis, 1988) as described in Chapter 2 (section 2.2, *"Growth modelling"*). Best-fit rVBGF models were estimated for each sex separately by minimizing the negative log of the likelihood assuming a normal probability density function (Kimura, 1980; Haddon, 2001; Trip *et al.*, 2008). The rVBGF parameters yielded estimates of mean size-at-age one ($L(1)$), five ($L(5)$) and nine ($L(9)$) for females, and of mean size-at-age five ($L(5)$) and nine ($L(9)$) for males (no males were present in year one age class). A Likelihood Ratio Test (LRT) was used to compare the growth of males and females (Cerrato, 1990). The LRT statistic *D* was estimated as follows: $D = -2 * (\log \frac{L_\omega}{L_\Omega})$, where L_ω is the maximum likelihood of the data under the null hypothesis of no difference in growth between males and females, and L_Ω is the maximum likelihood of the data under the alternative hypothesis that growth of males and females is better represented by two separate models. The null hypothesis of no difference in growth between the sexes was rejected at $\alpha = 0.05$ if *D* exceeded the value of $\chi^2(q)$, with q being the difference in the number of parameters under the two hypotheses (*i.e.* $q = 3$ for coincident curves) ($\chi^2_{0.05}(3) = 7.81$).

Table 3.2: Description of histological features used in the diagnosis of sexual development, including gonad sexual identity, reproductive activity, and spawning history. ILMB: intra-lamellar muscle bundle, AVO: atretic vitellogenic oocyte; POF: post-ovulatory follicle; BB: brown body.

Gonad tissue	Sexual identity	Reproductive activity	Most advanced gamete stage present	Spawning history
Oogenic tissue only	Female	Inactive	Pre-vitellogenic oocytes: Chromatin nucleolar (stage I) and/or peri-nucleolar (stage II) oocytes	➢ No AVOs: - Thin ovary wall, small cross-sectional area → <u>Immature</u> - Spawning history could not be diagnosed → <u>Undetermined</u> ➢ AVOs present: ILMBs & BBs and thick ovary wall may be present → <u>Mature</u>
		Ripening 1	Cortical alveoli (stage III) oocytes	
		Ripening 2	Vitellogenic (stage IV) oocytes	Mature
		Spawning	Hydrated oocytes (stage V), POFs, BBs, and/or ILMBs may be present	
		Post-spawning	AVOs present, BBs, degenerating hydrated oocytes (stage V) in ovarian lumen, all oocyte stages present	
Both oogenic and spermato-genic tissues present	Early transitional	Inactive	Peri-nucleolar oocytes (stage II), spermatogenic crypts developing (spermatocyte is most advanced stage present), degenerating vitellogenic (or later stage) oocytes, prominent central membrane-lined lumen	Signs of prior spawning as a functional female: AVOs, POFs
	Late transitional	Inactive male	spermatogenic crypts (spermatogonia and spermatocytes most abundant), sperm sinuses may be present, central lumen present	No signs of prior spawning as functional female (no AVOs, no POFs)
		Active male	Peri-nucleolar stage oocytes present (stage II), all stages of spermatogenesis present, spermatozoa abundant, sperm sinuses developed and filling with spermatozoa, central lumen may be present	
Spermat-ogenic tissue only	Male	Inactive	Spermatogonia crypts abundant, spermatocytes and/or spermatides may be present, sperm sinuses empty	Remnant of central lumen may be present
		Ripening	Spermatides and spermatozoa most abundant, sperm sinuses filling with spermatozoa	
		Spawning	Spermatozoa stage most abundant, sperm sinuses packed with spermatozoa	

3.3 Results

Sex-specific demography: size, age, growth and mortality of males and females

Size and age information were collected for a total of 324 females and 91 males of *Odax pullus* in the Hauraki Gulf, New Zealand. Examination of sex-specific size and age frequency distributions showed that the size and age range of males overlapped with that of the larger and older females, resulting in a distinct bi-modal distribution in both size and age (Fig. 3.2). Males were distributed in the larger (350 to 549 mm FL) and older (3 to 9 years) size and age classes, while females were present across the size and age range of the study species. The largest individual sampled was 531 mm FL (male, 6 years old and 2030 g GW), and the oldest individual collected was 11 years old (female, 469 mm FL & 1120 g GW). Sex-specific size and age distributions were confirmed by the presence of significantly different distributions in both size (Kolmogorov-Smirnov Test; $p < 0.01$) and age (Kolmogorov-Smirnov Test; $p < 0.01$) between the sexes. These results suggest the presence of a differential pattern of recruitment between the sexes to explain the patterns of sex-specific size and age distributions. Two alternative scenarios were considered throughout the following analyses of gonad function and morphology: (i) delayed sexual maturity in males relative to females, males maturing directly from an immature juvenile stage at a larger body size and at an older age than females, and (ii) secondary male development pathway, males maturing first as functional females and undergoing protogynous sex reversal before maturing as functional males (protogynous sex change).

There was no difference in growth between the sexes (Likelihood Ratio Test; $D = 0.0823;; \ df = 3; \ p = 0.99$), suggesting no difference in either growth rate or mean adult body size between the sexes (Fig. 3.3). The rVBGF parameter values found to best represent size-at-age of males and females provided estimates of mean size-at-age one ($L(1)$) of 214.1 mm FL, mean size-at-age five $L(5)$ of 426.8 mm FL, and mean size-at-age nine $L(9)$ of 455.4 mm FL (Fig. 3.3). Individuals achieved 47% of mean adult body size by the age of one and reached 85% of mean adult body size by the age of 3.5 years, indicating the presence of fast early somatic growth. Males occurred from the age of three years and at 83% of asymptotic body size (smallest male sampled was 376 mm FL).

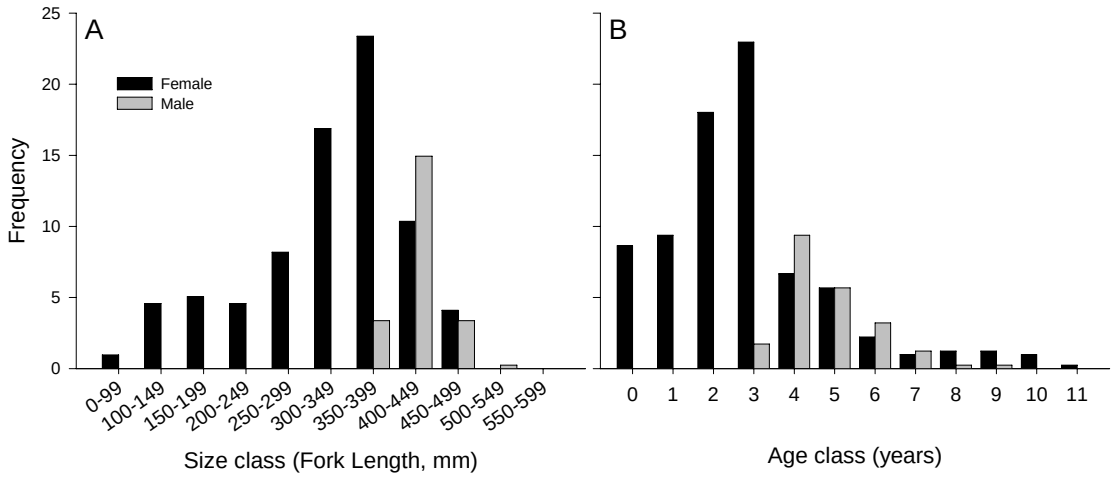

Fig. 3.2: (A) Size- (n = 415) and (B) Age-frequency distribution (n = 405) of males (grey bars) and females (black bars) *Odax pullus* from the Hauraki Gulf.

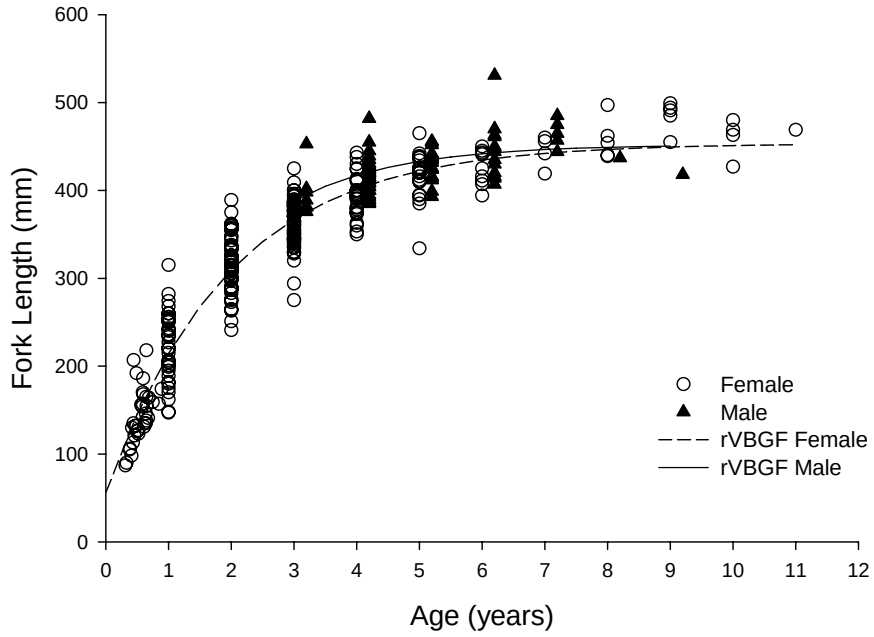

Fig. 3.3: Sex-specific growth trajectories of *Odax pullus* from the Hauraki Gulf, showing size-at-age of males (n = 88) (black triangle) and females (n = 317) (white circle), and sex-specific best-fit re-parameterized von Bertalanffy Growth Function (rVBGF).

Reproductive seasonality, oocyte development and female reproductive output

Examination of gonadosomatic index (GSI) of females across months sampled from August 2005 to January 2008 revealed that relative gonad weight of mature females significantly increased between July and November and peaked in August in both years examined (Fig. 3.4 A). Monthly variation in female GSI coincided with the pattern of variation in relative gonad weight of males across months sampled (Fig. 3.4 B). These results coincide with the frequency distribution of post-ovulatory follicles (POF), which provide evidence of recent spawning, and were present in ovaries between July and November, and of atretic vitellogenic oocytes (AVO), which occurred between July and February (Fig. 3.5 A). Months during which GSI was highest coincided with those where mean sea surface temperature (SST) was lowest in both years sampled. These results suggest that spawning activity of *Odax pullus* in the Hauraki Gulf occurs during the austral winter and spring months, between July and November, and peaks in August.

Intra-lamellar muscle bundles (ILMB) in mature ovaries first occurred in August, during the most active month of the spawning season. Frequency of ILMB peaked in January shortly after spawning had ceased, and ILMB were present in less than 3% of mature ovaries in the months leading to the next annual spawning event (Fig. 3.5 B). These results suggest that the presence of ILMBs were related to post-spawning events and could be used in the diagnosis of spawning history of females to help distinguish between immature (never spawned) and mature (spawned) females.

Oocyte growth started in March, with an increasing percentage of mature ovaries showing cortical alveoli oocytes (stage III) from March to June, peaking immediately prior to the start of the spawning season (Fig. 3.6). Vitellogenesis was initiated at the start of the spawning season in July, when oocytes of all mature females had reached the vitellogenic (stage IV) or hydrated (stage V) stages of oocyte maturation, indicating that females were near spawning. 65% of active females contained hydrated oocytes in August, which coincided with the month of peak of spawning activity. From September to November, a gradually increasing percentage of mature females showed receding ovaries and peri-nucleolar oocytes (stage II), which coincided with an increase in the frequency of ovaries showing post-ovulatory follicles and atretic vitellogenic oocytes (Fig. 3.5 A). These results suggest that, while spawning spanned from July to November, not all sexually mature females participated equally over the duration of the spawning season. Comparison of size

and age of mature inactive and active females sampled between September and November revealed that mature inactive females (showing receding ovaries after recent spawning) were smaller (range of 241 to 409 mm FL) and younger (range of 1 to 4 years old) than females showing reproductively active ovaries from September to November (size range 370 to 469 mm FL, and age range 3 to 10 years old), suggesting that larger older females contributed for a comparatively longer period of time than smaller younger females over the length of the spawning season.

Examination of the relationship between ovary weight (as a proxy for estimation of reproductive output, see Pears et al. 2006) and size and age of mature active females showed a significant exponential relationship with body size ($r^2 = 0.61$, $p < 0.001$) (Fig. 3.7 A), and a significant linear positive relationship with age ($r^2 = 0.63$, $p < 0.001$) (Fig. 3.7 B), suggesting that a small increase in female size will result in an exponential increase in gonad weight, that larger and older females will display significantly greater ovary weights and reproductive outputs than smaller and/or younger spawning females, and that age is a significant predictor of ovary weight, with older females producing greater reproductive output (greater fecundity) than younger females. Mapping of ovary weight onto the relationship between body size and age of mature spawning females revealed that larger and older females (> 400 mm FL and > 5 years) displayed the heaviest ovaries (Fig. 3.8). These results suggest that large old females are significant breeders and that they contribute comparatively greater amounts of reproductive output than young small reproductive females. All important breeding females displayed body sizes above the minimum legal size limit and appear vulnerable to extrinsic mortality.

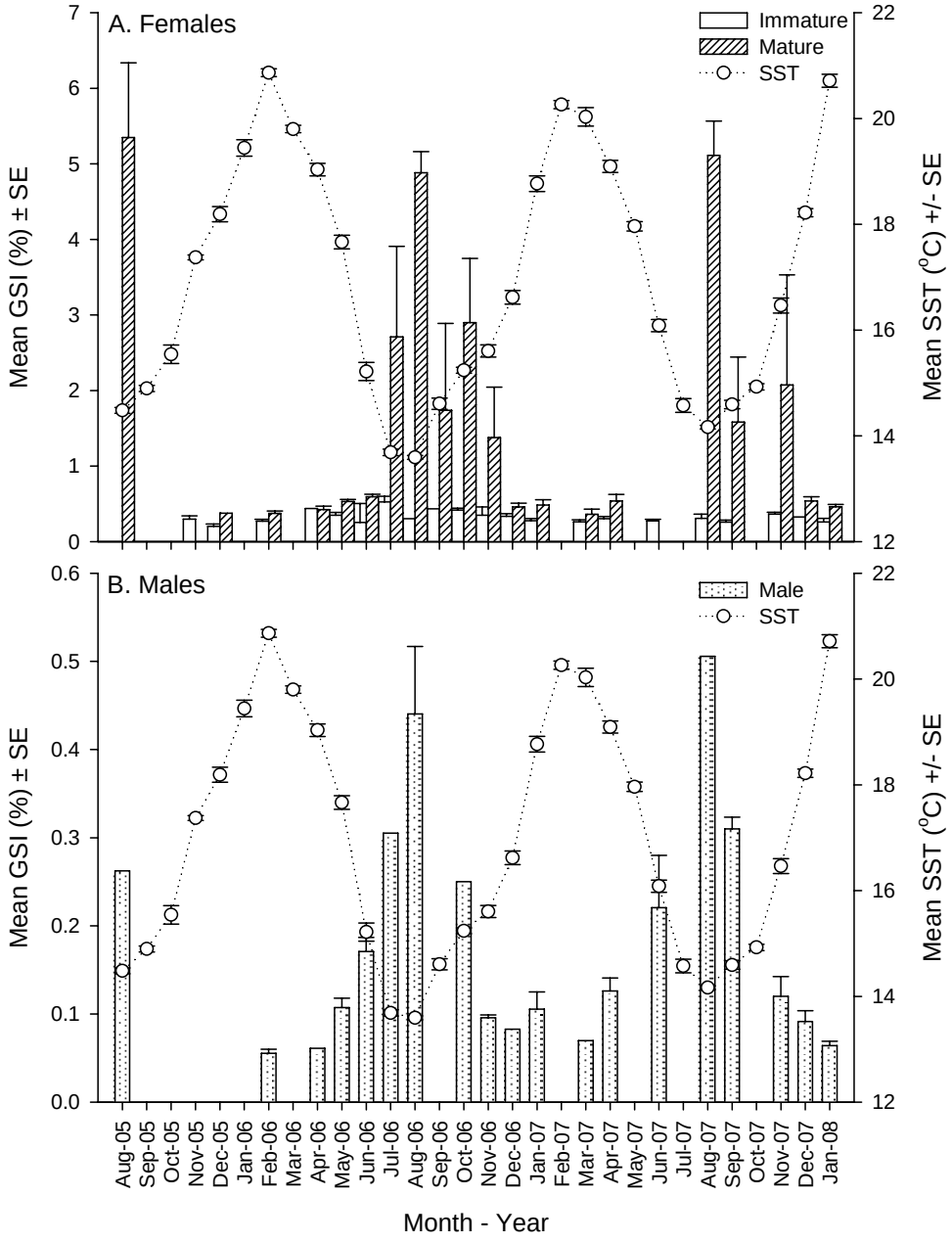

Fig. 3.4: Mean monthly variation in relative gonad weight (gonadosomatic index; GSI) of *Odax pullus* in the Hauraki Gulf, showing variation in reproductive activity of (A) immature (n = 94) (open bars) and mature females (n = 138) (shaded bars), and (B) males (n = 49) (dotted bars). Local mean sea surface temperature (SST) (in degrees Celsius ^{o}C) recorded across months sampled between August 2005 and January 2008 is shown on the right-hand *y*-axis.

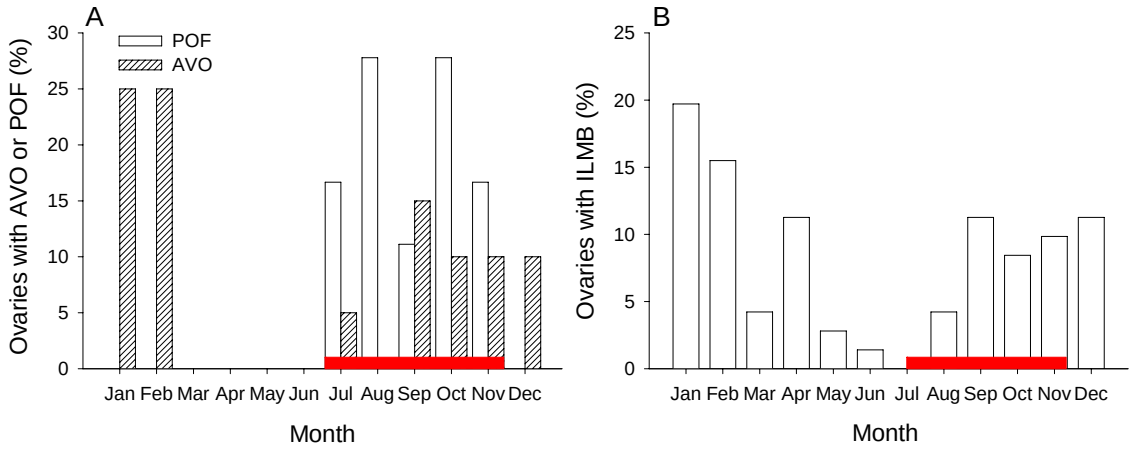

Fig. 3.5: Frequency distribution of (A) post-ovulatory follicles (POF) (n = 18) and atretic vitellogenic oocytes (AVO) (n = 20), and (B) intra-lamellar muscle bundles (ILMB) (n = 71) found across months in mature ovaries of *Odax pullus* from the Hauraki Gulf. Frequency estimates shown were calculated by combining both years sampled. Red horizontal bars show timing and duration of spawning.

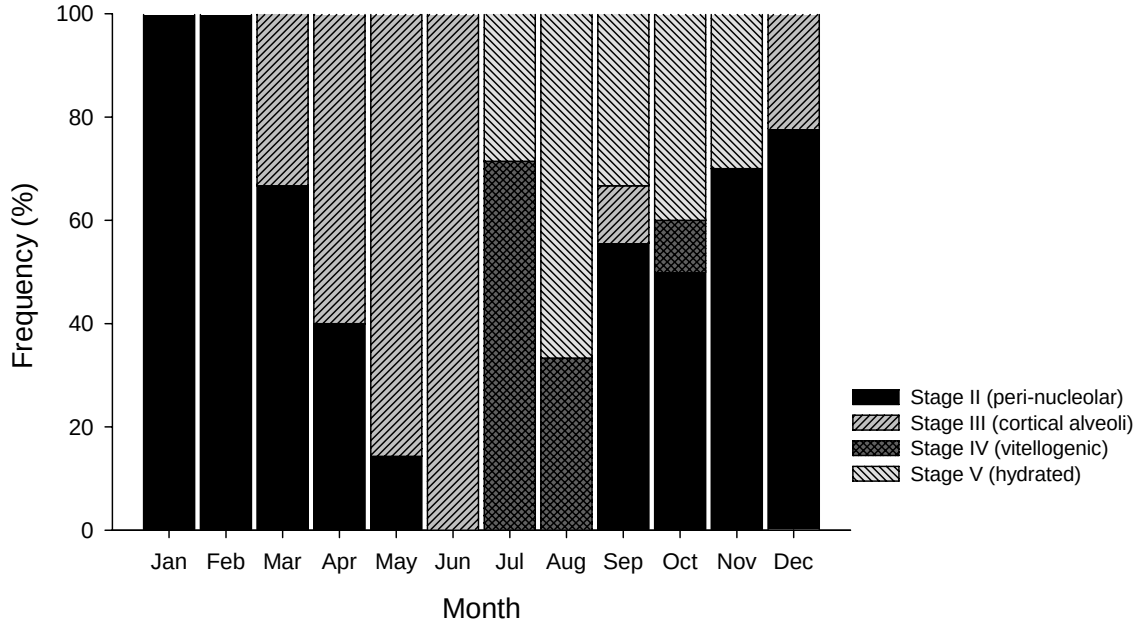

Fig. 3.6: Monthly progression of oocyte development (based on the most advanced stage present) in ovaries of mature *Odax pullus* females (n = 144) from the Hauraki Gulf.

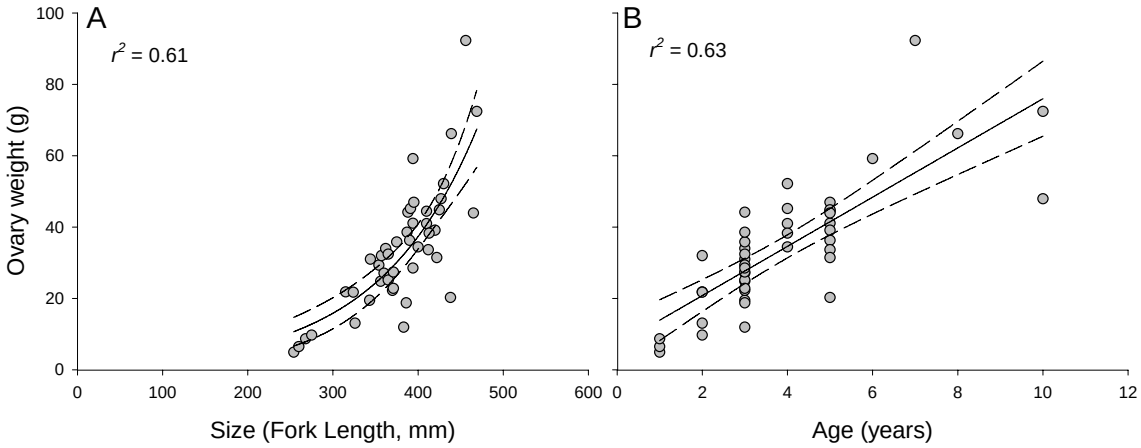

Fig. 3.7: Variation in ovary weight (as a proxy for reproductive output) with (A) size, and (B) age of *Odax pullus* from the Hauraki Gulf. Least-regressions are presented with 95% confidence intervals: (A) $y = 1.21\ (\pm 0.58\ s.e.) * e^{0.0086\ (\pm 0.0012\ s.e.)\ x}$ and (B) $y = 7.00\ (\pm 3.54\ s.e.) + 6.90\ (\pm 0.81\ s.e.)x$.

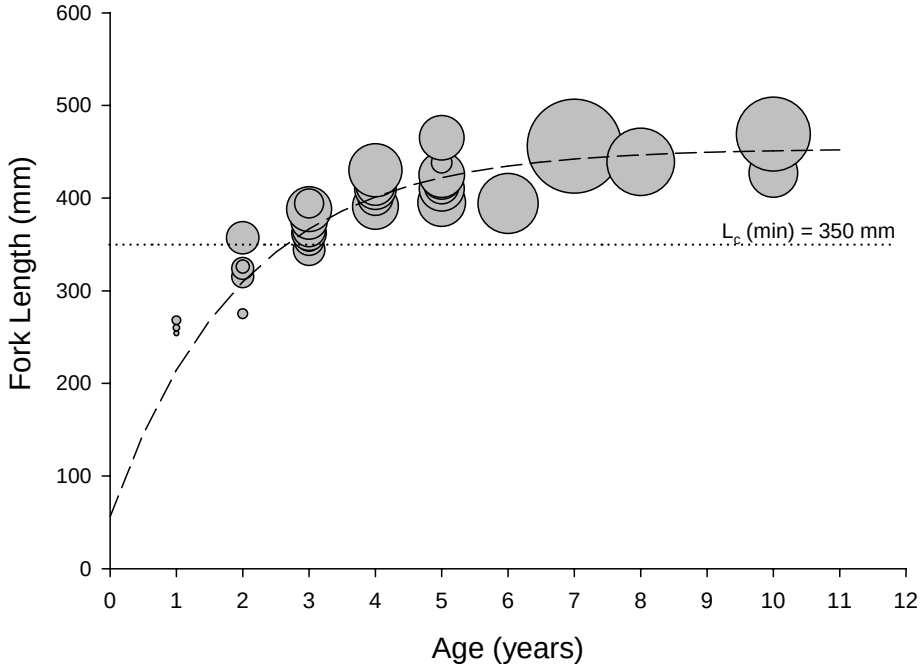

Fig. 3.8: Size-at-age of mature *Odax pullus* spawning females (n = 45) from the Hauraki Gulf, showing relative ovary weight (circle size) as a measure of female contribution to reproductive output. Best-fit growth trajectory (re-parameterized von Bertalanffy Growth Function) is shown. Horizontal dotted line shows minimum legal size of capture for *O. pullus* (L_c (min)).

Size- and age-at-maturity

Size and age at which 50% of females were sexually mature were estimated at 240.7 mm FL [95% percentile CI 228.7 – 264.8] (Fig. 3.9A), and at 1.2 years [1.1 – 1.5] (Fig. 3.9B), respectively. These results indicate that reproductive growth occurred at the time of somatic growth, between 52 and 59% of asymptotic body length ($L(9)$), and between 10 and 14% of maximum age (11 years). Size and age at which 95% of females were sexually mature were 297.9 [280.3 – 317.2] mm FL, and 1.9 [1.6 – 2.2] years, respectively, suggesting that the majority of females were sexually mature by the time 60 to 70% of adult body size was reached, and 16 to 20% of the total life span. Reproductive life of females was therefore estimated to span between a minimum of 8.7 years to a maximum of 9.3 years, representing a duration of 79 to 85% of total female longevity. The smallest mature active female was 241 mm FL in body length, and the youngest mature active female was one year of age. Immature females collected during the reproductive season were on average smaller, with body lengths ranging between 135 and 335 mm FL, and younger, with ages ranging between one and three years, than mature active females.

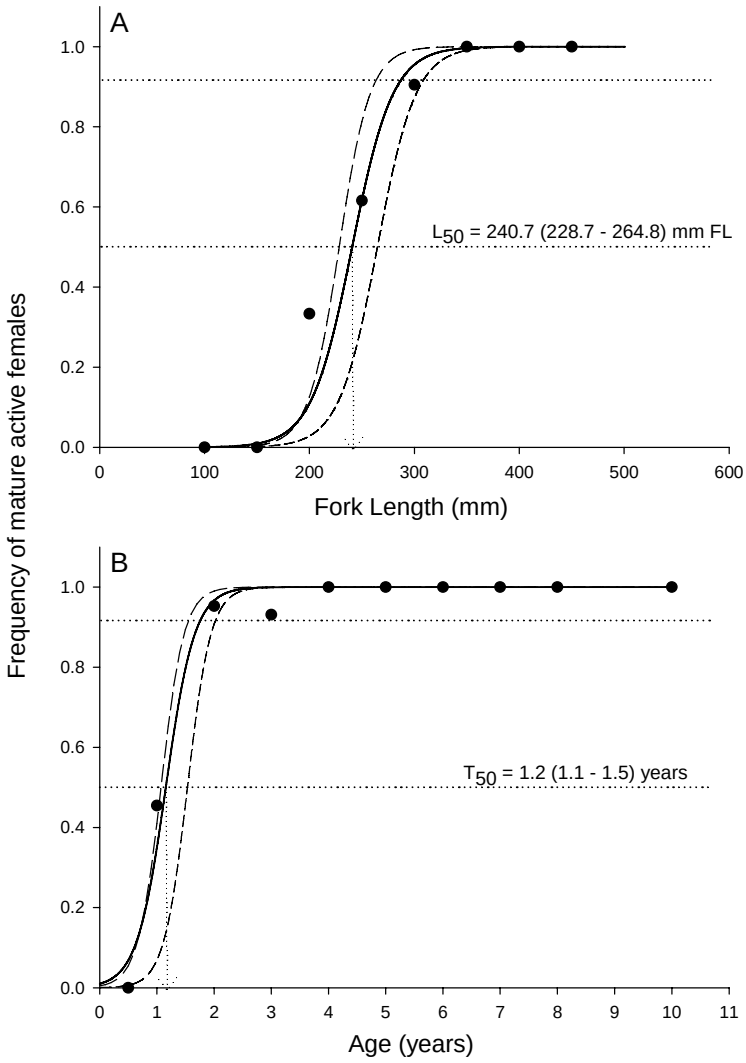

Fig. 3.9: Size- and age-at-maturity of *Odax pullus* in the Hauraki Gulf. Frequency of mature active females collected during the spawning season (July to November incl.) per (A) size (n = 97) and (B) age (n = 96) class. The logistic curves (continuous lines) are shown with 95% percentile confidence intervals (CI) (dashed lines) and observed frequency data (closed circles). Dotted lines indicate size (L_{50}) and age (T_{50}) (with 95% CI) at which 50% of females are mature.

Gonad structure and developmental stages

Analysis of gonad histology was performed for a total of 309 *Odax pullus* individuals from the Hauraki Gulf, New Zealand. A total of 250 (80.9%) gonad sections exclusively showed ovarian tissue, and 51 sections (16.5%) exclusively displayed testicular tissue, resulting in a significantly female-biased sex ratio across histological samples examined

(4.9:1, n = 309, Chi-square, $p < 0.001$). Eight sections showed both developing spermatogenic tissue and primary oocytes (transitional individuals) (2.6%).

Females

All transverse sections of ovaries showed a lamellar structure. Lamellae were tightly packed in immature (Fig. 3.11 a) and mature inactive females (Fig. 3.11 i), and filled the ovarian lumen in spawning females (Fig. 3.11 e). Nests of germ cells and early meiotic primordial cells were commonly observed within the lamellar membrane of inactive ovaries (Fig. 3.11 b). The ovarian lumen was lined by a membrane-like layer, and appeared filled with stage V (hydrated stage) oocytes in spawning females, and with degenerating stage V oocytes in post-spawning and some mature inactive (resting) females (Fig. 3.11 e, g, i), suggesting that the ovarian lumen is used as an egress for oocytes during spawning. All ovaries were externally lined with a muscular wall, which varied in thickness across females sampled, with a thin ovarian wall in immature and spawning females, and a comparatively thicker ovarian wall in most mature inactive females.

(i) Immature females

36% of females were diagnosed as immature (never spawned). Immature females were aged between 0.3 and three years, and occurred from 90 to 385 mm FL in body length (Fig. 3.10 a). Ovarian lamellae of immature females were packed with pre-vitellogenic oocytes (chromatin nucleolar and peri-nucleolar stages) (Fig. 3.11 b). Immature females were collected across all months sampled.

(ii) Mature females (ripening, spawning, post-spawning and resting)

57.6% of females were mature (spawning or showing signs of previous spawning episodes), and these were observed between 215 and 499 mm FL, and between 1 and 10 years of age (Fig. 3.10 b). Spawning history of 6.4% of females could not be reliably identified (undetermined inactive females); these females were sampled outside of the spawning season, and showed body lengths ranging from 288 to 426 mm FL, and were aged between 1 and 5 years old. Pre-vitellogenic oocytes were present in ovaries at all stages of ovarian maturation. Vitellogenic oocyte growth was initiated in March with the appearance of cortical alveoli stage oocytes (stage III) in ripening females (Fig. 3.11 d). Vitellogenesis started in July, and vitellogenic (stage IV) and hydrated (stage V) oocytes were observed in

spawning females over the length of the spawning months (July to November) (Fig. 3.11 f). All stages of oocyte growth were present in ovaries of active spawning females, suggesting the presence of multiple spawning events for each active female during the spawning months (batch spawning). Post-spawning ovaries showed α-stage atresia of vitellogenic oocytes and displayed a disorganized lamellar structure (Fig. 3.11 g, h). Numerous degenerating hydrated oocytes were present in the lumen, and prominent intra-lamellar muscle bundles and numerous post-ovulatory follicles were observed within the lamellae. Lamellae of mature inactive (resting) females were dominated by pre-vitellogenic (stages I & II) oocytes, and displayed intra-lamellar muscle bundles (Fig. 3.11 j). Mature resting females collected between November and January (immediately following completion of the spawning season) displayed some atretic vitellogenic oocytes within the lamellae, and numerous degenerating hydrated oocytes in the ovarian lumen (Fig. 3.11 i).

Males

Body length of males ranged between 376 and 482 mm FL, and males were aged between 3 and 9 years (Fig. 3.10 d). No small or young males were observed across the 309 gonad samples examined. Testes were tightly packed with spermatogenic tissue and presented a lobular structure. All testes were externally lined with a thick muscular wall. Sperm ducts were consistently distributed at the periphery of the testicular tissue in both inactive and active males, and no dorsal sperm ducts were found (Fig. 3.12). The peripheral sperm sinuses were membrane lined, and appeared to form from within the external layer of the developing spermatogenic tissue (*e.g.* Fig. 3.13 d), although in fully developed inactive or active males sperm sinuses appeared to be merged with the gonad wall (*e.g.* Fig. 3.12 b, d, h). Sperm sinuses were filled with mature sperm in active males suggesting that peripheral sperm sinuses are used for the egress of sperm during spawning (Fig. 3.12 d). 31% of testes (aged 3 – 6 years, and body length 393 – 455 mm FL) showed a membrane-lined central lumen, filled with connective tissue and / or brown bodies (Fig. 3.12 e, f). Spermatogonia were prominent across the testicular tissue of inactive males, which were collected between November and February (Fig. 3.12 a, b). Sperm sinuses were developed but empty in inactive males, and appeared to fill with spermatozoa in ripening males (Fig. 3.12 c, d). All stages of spermatogenesis were observed in ripening males; however spermatogonia and spermatocytes were most abundant (Fig. 3.12 c, d). The testes of spawning males were dominated by spermatids and spermatozoa, and few spermatogonia were present (Fig. 3.12

h). Ripening males were collected between February and June, and spawning males were found from June to November. This timing coincides with that of oocyte development in females, and indicates that both sexes are sexually active across the length of the spawning months.

Transitional individuals

Eight transverse gonad sections revealed the simultaneous presence of spermatogenic and oogenic tissue (Fig. 3.13). Size and age distribution of transitional individuals ranged from 359 – 418 mm FL and from 2 – 4 years old (Fig. 3.10 c). Transitional individuals were absent from the smaller size and younger age classes, and were found from October to February. Oocytes observed within the developing spermatogenic tissue were pre-vitellogenic oocytes including chromatin-nucleolar (stage I) and peri-nucleolar (stage II) (Fig. 3.13 b, d). No atretic vitellogenic oocytes undergoing α-atresia were found within the developing spermatogenic tissue. The most advanced stage of spermatogenesis present varied across individuals however spermatogonia and spermatocytes were the most abundant stages in 75% of gonad tissues sampled. Sperm sinuses were not present in these sections, and a prominent central membrane-lined lumen was observed containing abundant connective tissue and brown bodies (Fig. 3.13 a). Degenerating stage V (hydrated) oocytes were identified within the central lumen of two of these sections (see Fig. 3.14 for histological validation of these structures and analysis of transitional sections). These two were diagnosed as early-transitional individuals, while the remaining four were identified as being late-transitionals. In the remaining 25% of transitional gonads examined, all stages of spermatogenesis, including spermatozoa, were present, sperm sinuses were fully developed and filling with spermatozoa (Fig. 3.13 c). These were diagnosed as being active ripening males, and were collected in February. Mean body length of transitional individuals (n = 6), excluding active males with primary oocytes (n = 2), was 384.3 mm FL (+/- 8.6 SE), and mean age was 3.0 years (+/- 0.3 SE).

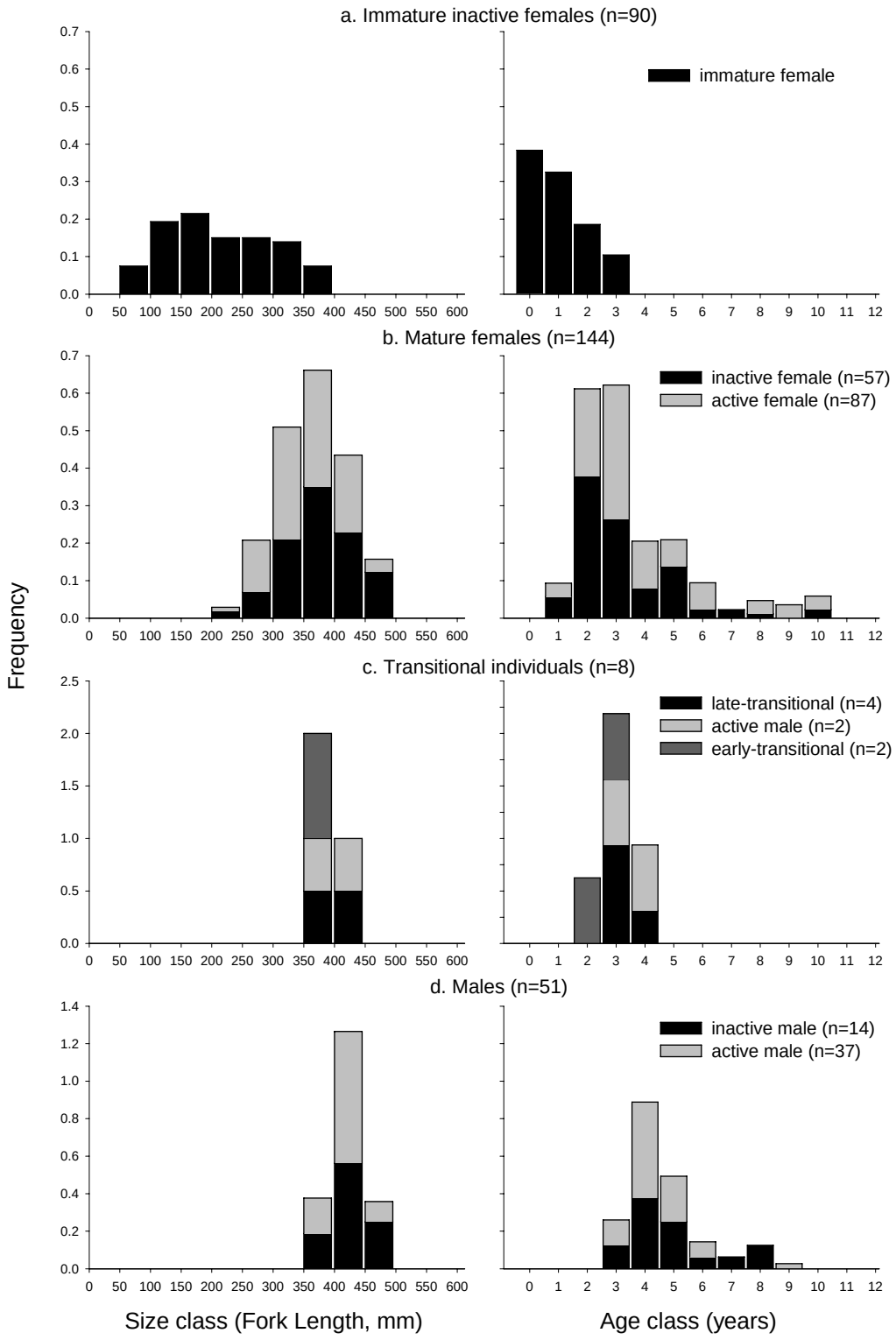

Fig. 3.10: Size and age frequency distributions of (a) immature inactive females, (b) mature inactive and active females (ripening, spawning or post-spawning), (c) transitional individuals, and (d) inactive and active males of *Odax pullus* in the Hauraki Gulf. Frequency is calculated relative to the total number of individuals sampled at each developmental stage.

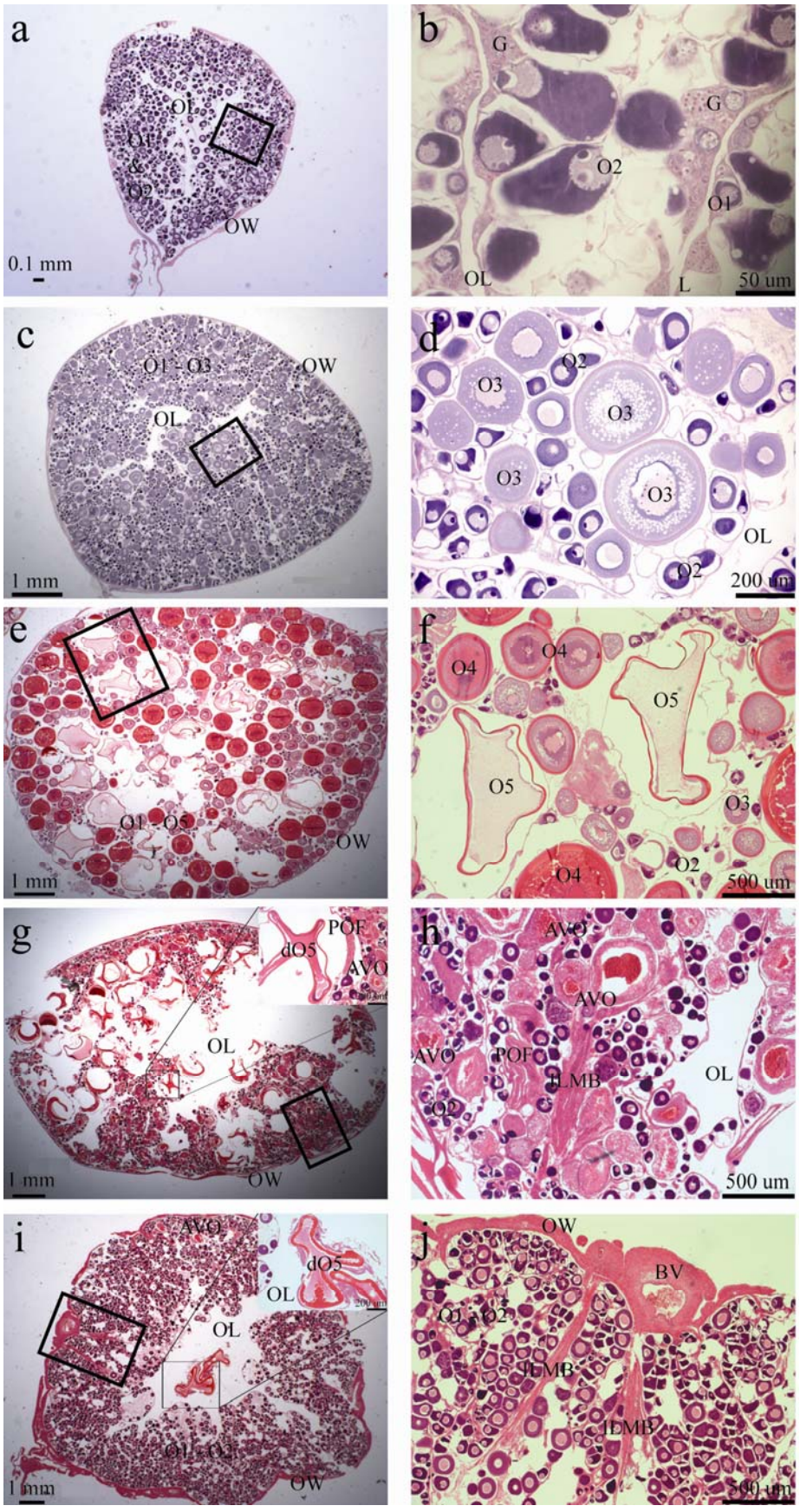
a
O1
O2
&
O3
OW
0.1 mm
b
G
G
O2
O1
OL
L
50 um
c
O1 - O3
OW
OL
1 mm
d
O2
O3
O3
O3
O3
OL
O2
200 um
e
O1 - O5
OW
1 mm
f
O4
O4
O5
O5
O3
O2
O4
500 um
g
POF
dO5
AVO
OL
1 mm
OW
h
AVO
AVO
AVO
POF
LMB
OL
O2
500 um
i
AVO
dO5
OL
OL
O1 - O3
1 mm
OW
j
OW
BV
O1 - O2
LMB
LMB
500 um

Fig. 3.11 (page 63): Photomicrographs of transverse histological sections of ovaries of *Odax pullus* in the Hauraki Gulf, showing ovary structure (left hand panel; figures a, c, e, g, i) and detail of characteristic features (right hand panel; figures b, d, f, h, j) at four stages of ovary development.
(a – b) immature ovary of juvenile female (192 mm FL, 0.49 year old, caught in November) with detail of proliferating germ cells (G) at base of ovarian lamellae (L);
(c – d) mature ripening female (336 mm FL, 2 years old, caught in May) with detail of cortical alveoli (stage III) oocytes (O3);
(e –f) mature spawning female (357 mm FL, 2 years old, caught in August) with detail of vitellogenic (O4) and hydrated oocytes (O5);
(g – h) mature post-spawning female (383 mm FL, 3 years old, caught in September) with detail showing degenerating hydrated (stage V) oocyte (dO5), post-ovulatory follicles (POF), atretic vitellogenic oocytes (AVO), and intra-lamellar muscle bundles (ILMB);
(i – j) mature inactive (resting) female (375 mm FL, 2 years old, caught in October) with detail of proliferating primary oocytes (O1 & O2) and intra-lamellar muscle bundles (ILMB).
BV: blood vessel; OW: ovarian wall; OL: ovarian lumen.
Sections are stained with Haematoxylin & Eosin.

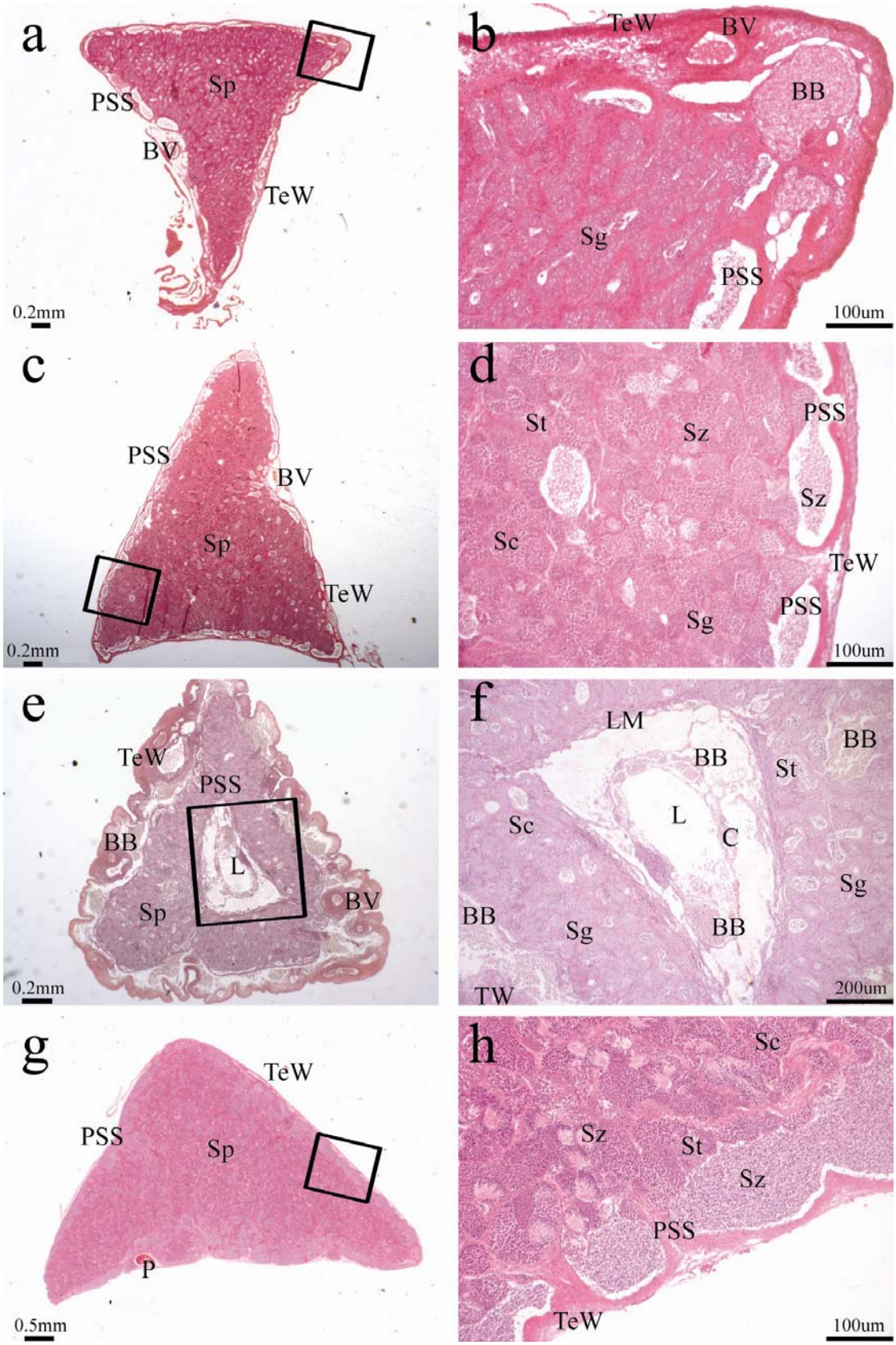
a
PSS
Sp
BV
TeW
0.2mm
b
TeW
BV
BB
Sg
PSS
100um
c
PSS
BV
Sp
TeW
0.2mm
d
St
Sz
PSS
Sz
Sc
TeW
Sg
PSS
100um
e
TeW
PSS
BB
L
Sp
BV
0.2mm
f
LM
BB
BB
St
Sc
L
C
Sg
BB
Sg
BB
TW
200um
g
TeW
PSS
Sp
P
0.5mm
h
Sc
Sz
St
Sz
PSS
TeW
100um

Fig. 3.12 (page 65): Photomicrographs of transverse histological sections of testes of *Odax pullus* in the Hauraki Gulf, showing testis structure (left hand panel) and detail of characteristic features across testis developmental stages (right hand panel).
(a – b): Inactive testis of mature male (7 years old, 457 mm FL, collected in January), showing abundance of spermatogonia (Sg) and empty peripheral sperm sinuses (PSS).
(c – d): Active testis of mature ripening male (5 years old, 440 mm FL, collected in June), showing all stages of spermatogenesis.
(e – f): Active testis of ripening male with remnant of central lumen (L) (4 years old, 425 mm FL, collected in February) showing the lumen membrane (LM), abundant connective tissue (C) and brown bodies (BB).
(g – h): Active testis of mature spawning male (5 years old, 441 mm FL, collected in September) showing peripheral sperm sinuses packed with spermatozoa (Sz). TeW: testis wall. Sections were stained with Haematoxylin & Eosin.

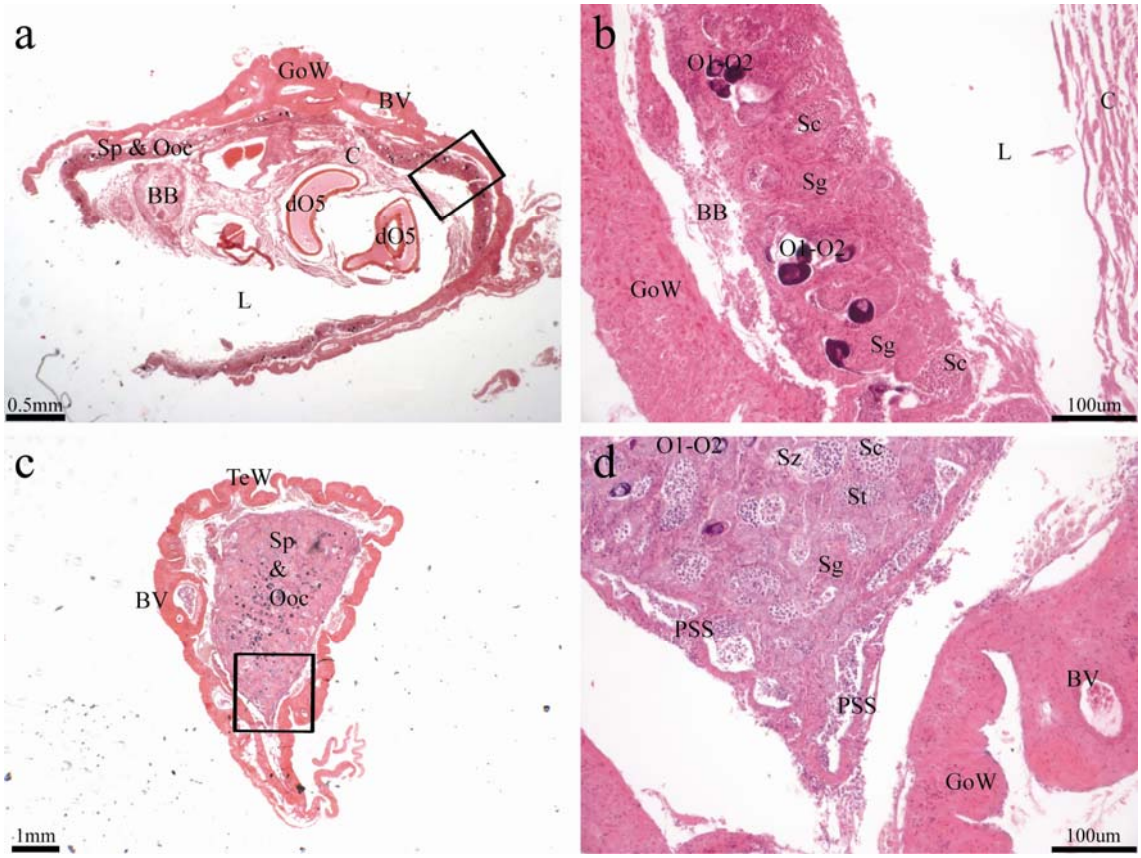

Fig. 3.13: Photomicrographs of transverse histological sections of *Odax pullus* gonads in the Hauraki Gulf with both spermatogenic and oogenic tissue, showing gonad structure of (a, b) an early-transitional individual and (c, d) of a late –transitional (ripening male).
BB: brown body; BV: blood vessel; C: connective tissue; dO5: degenerating stage V (hydrated) oocyte; GoW: gonad wall; L: lumen; Ooc: oogenic tissue; O1: chromatin-nucleolar (stage I) oocyte; O2: peri-nucleolar (stage II) oocyte; PSS: peripheral sperm sinuses; Sc: spermatocyte; Sg: spermatogonia; St: spermatid; Sz: spermatozoa; Sp: spermatogenic tissue; TeW: testis wall. Sections were stained with Haematoxylin & Eosin.

Ontogeny of testis development, and size- and age-at-sex change

The central lumen of two early-transitional individuals displayed distinct hydrated oocyte-like structures (Fig. 3.14 a). Similar hydrated oocyte-like structures were found in the ovarian lumen of mature resting females (Fig. 3.14 c). The cytoplasm and envelope of these structures both stained positively to Periodic Acid Schiff (PAS), indicating the presence of glycoprotein elements, a primary component of vitellogenin (Fig. 3.14 b, d). Vitellogenin is a female-specific hepatic protein which forms a precursor to the formation of yolk during vitellogenesis (McMillan, 2007). Glycoprotein elements are also characteristic of the chorion (zona pellucida), which develops specifically in vitellogenic oocytes (McMillan, 2007). Staining of these structures was consistent with that found in degenerating hydrated oocytes in post-spawning females (Fig. 3.14 e, f), and in vitellogenic and hydrated oocytes in spawning females (Fig. 3.14 g, h). These results suggest that the structures found in the lumen of early-transitional individuals and mature resting females match the structure and composition of degenerating hydrated (stage V) oocytes and, consequently, are likely to be related to post-spawning events and hence to prior female function. The two early-transitional individuals displaying degenerating hydrated oocytes within their central lumen may therefore be diagnosed as undergoing functional sex reversal, as defined by the presence of degenerating hydrated oocytes (indicating prior female function) within developing spermatogenic tissue (Sadovy and Liu 2008). This implies the presence of functional protogynous sex change in *O. pullus*. Early-transitional individuals were collected in October and November, displayed body lengths of 359 and 379 mm FL, and were aged 2 and 3 years old (Fig. 3.10 c). Size- and age-at-sex change were estimated from the mean body size and age of transitional individuals, at 369 mm FL (+/- 10 SE) and age-at-sex change of 2.5 years old (+/- 0.5 SE), which correspond to 82% of adult body size and 23% of maximum age.

Examination of the relationship between size and age of immature females and transitional individuals (including early- and late-transitional individuals) showed an overlap in size and age between the two developmental stages in the upper size and age range of immature females (Fig. 3.15). However, some transitional individuals occurred in size and age classes where immature females were absent, suggesting that not all transitional individuals may be ontogenetically related to immature females (Fig. 3.15). Mean size and age of early-transitional individuals were 369 mm FL (+/- 10 SE) and 2.5 years old (+/- 0.5 SE) (n = 2). In contrast, size- and age-at-maturity (50% female maturity) occurred at 240.7

mm FL [95% percentile CI 228.5 – 264.8] and at 1.2 years old [1.1 – 1.5], suggesting that female-to-male transition occurs at a significantly larger size and older age than that of female sexual maturity. Size and age of the smallest male overlapped with that of the transitional individuals (Fig. 3.15).

22.7% of active females collected from September to November showed receding ovaries with atretic vitellogenic oocytes, suggesting that they ceased spawning after peak spawning activity in August. Females showing receding ovaries were those displaying relatively smaller body sizes (329.7 mm FL +/- 12.4 SE) and younger age classes (2.4 years +/- 0.2 SE) as compared with that of spawning females (416.2 mm FL +/- 10.1 SE and 4.6 years +/- 0.6 SE). While the mean body size of receding females tended to be comparatively smaller than the mean size of transitional individuals, mean age of receding females coincided with that found for transitional individuals. These results suggest the possibility that, during a spawning season, younger functional females may participate in spawning until peak spawning is achieved, and that these females may subsequently undergo ovary regression before changing sex. In this case, comparatively older and larger females may continue to spawn after September and these individuals are likely to remain female. Furthermore, males were significantly larger than females at the age of three years (ANOVA, $F_{1, 98} = 12.682$, $p < 0.001$), even though no difference in adult body size or somatic growth rate was found between the sexes. Three year old females ranged in size between 275 and 425 mm FL, and three year old males ranged between 376 and 453 mm FL, suggesting that the females changing sex into males are those that have reached a larger body size by the age of three years. Transitional individuals were found in October and November, suggesting that sexual transition from functional female to male may start during the second half of the spawning season after peak spawning activity.

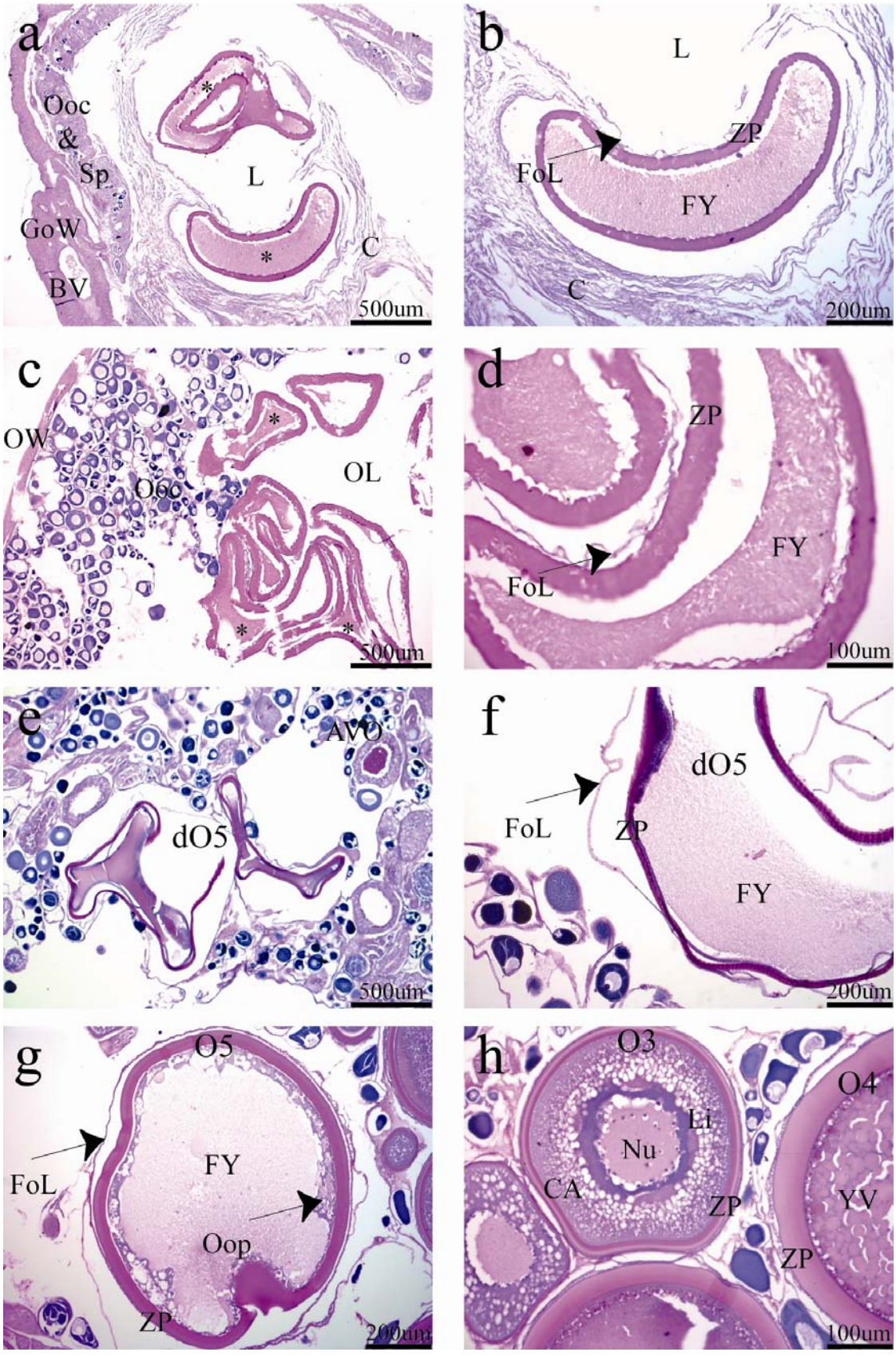
a
Ooc
&
Sp
GoW
BV
L
C
500um
b
L
ZP
FoL
FY
C
200um
c
OW
OL
Ooc
500um
d
ZP
FY
FoL
100um
e
AVO
dO5
500um
f
dO5
FoL
ZP
FY
200um
g
O5
FoL
FY
Oop
ZP
200um
h
O3
O4
Li
Nu
CA
ZP
YV
ZP
100um

Fig. 3.14 (page 69): Histological identification of structures found in the central lumen of early-transitional *Odax pullus* individuals and mature females (indicated by * on figure) in the Hauraki Gulf. Photomicrographs of transverse sections of gonads of (a – b) an early-transitional individual, (b – c) a mature resting female, (c – d) a post-spawning female showing degenerating hydrated oocytes and atretic vitellogenic oocytes, and (e – f) a spawning female showing vitellogenic and hydrated oocytes.
AVO: atretic vitellogenic oocyte; C: connective tissue; CA: cortical alveoli vesicle; dO5: degenerating stage V (hydrated) oocyte; FoL: follicle layer; FY: fluid yolk; GoW: gonad wall; L: lumen; Li: Lipid vacuoles; Nu: nucleus; Ooc: oogenic tissue; Oop: ooplasm; OL: ovarian lumen; OW: ovarian wall; O3: stage III (cortical alveoli); O4: stage IV (vitellogenic) oocyte; O5: stage V (hydrated) oocyte; Sp: spermatogenic tissue; YV: yolk vacuole; ZP: zona pellucid (chorion). Sections were stained with Periodic Acid Schiff (PAS) & Haematoxylin.

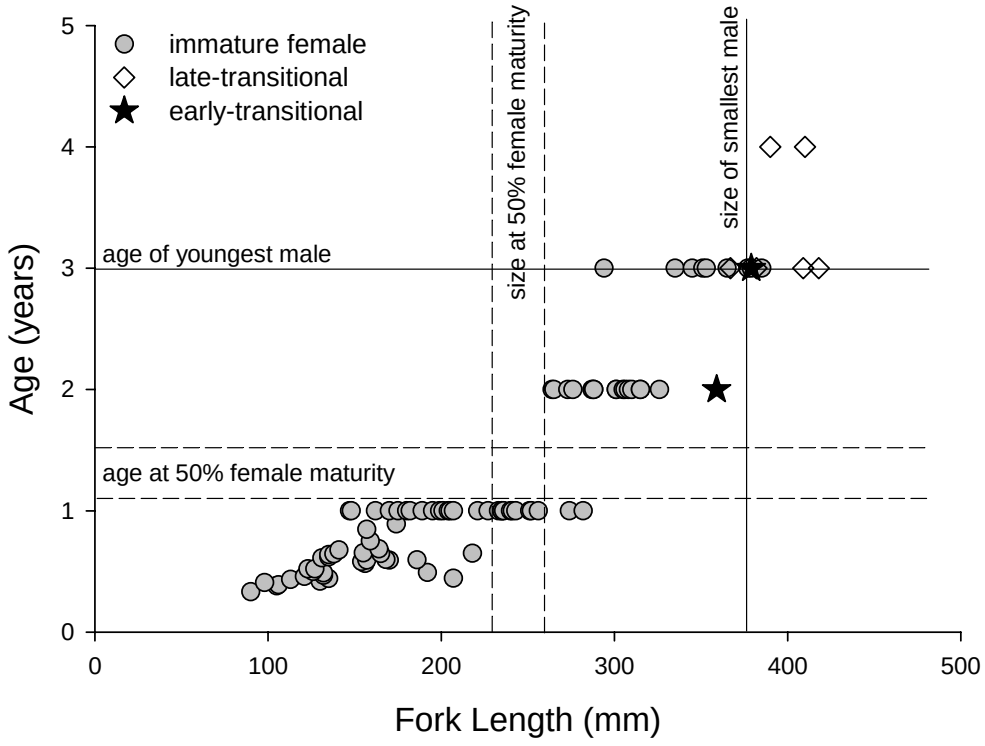

Fig. 3.15: Relationship between size and age of immature females (n = 90), early-transitional individuals (n = 2) and late-transitional individuals (n = 6) of *Odax pullus* in the Hauraki Gulf. Dashed lines show the confidence regions of estimated size and age at 50% female maturity and continuous lines show size and age of the smallest male sampled.

3.4 Discussion

Results of this study on the reproductive biology and demography of males and females of *Odax pullus* in the Hauraki Gulf, New Zealand, are consistent with the diagnostic features of monandric protogyny, whereby all males are the result of functional sex change of mature females (Sadovy and Shapiro, 1987). This coincides with the most commonly found pattern of sexual ontogeny amongst labrid fishes, as described in numerous other labrid species (Choat and Robertson, 1975; Robertson and Warner, 1978; Warner and Robertson, 1978). Not all *O. pullus* females changed sex into males, however, as seen by the overlapping size and age structures of males and females in the larger and older size and age classes. Furthermore, the oldest individual sampled was female (11 years old). Females changing sex into males underwent sex reversal at an estimated ~82% of adult body size and at ~23% of maximum age. Transitional individuals contained mixed male and female tissue as seen in most labrid species (undelimited type II, Sadovy and Shapiro 1987). Males, early- and late-transitional individuals were absent from the smaller size and younger age classes, and males first occurred in the population at a minimum body length of 376 mm FL and at 3 years of age, indicating the presence of a single male development pathway (monandry) in the Hauraki Gulf population sampled. In contrast, all individuals present in the small and young size and age classes were immature females, suggesting that all individuals undergo an immature female phase before maturing as females. Sexual maturation of females occurred within the first 10-15% of the life span, indicating a reproductive life extending close to 90% of the life span. Female maturation coincided with a period of fast initial growth, implying the presence of simultaneous somatic and reproductive growth. There was no difference in growth between the sexes, indicating no difference in the costs (in terms of growth) of reproduction and/or gonad maturation between the sexes. *O. pullus* spawned in the Hauraki Gulf during the austral winter and spring months between July and November, peaking in August, which coincides with the spawning season of other temperate labrids in New Zealand (*e.g. Notolabrus fucicola*, Denny and Schiel, 2002). Sex reversal appeared to start during the second half of the spawning season, after peak spawning activity.

Diagnosis of sex change can be problematic, particularly because of the difficulties associated with identifying transitional individuals (undergoing sex reversal), which provide the most reliable source of evidence for the presence of sex change (Sadovy and Shapiro, 1987; Sadovy and Liu, 2008). In the case of protogynous sex change, Sadovy and Shapiro

(1987) and Sadovy and Liu (2008) recommended that histological evidence of female-to-male sex reversal should meet the strict criterion of the presence of atretic vitellogenic oocyte(s) (AVO), which confirm prior female function, within developing testicular tissue. Transitional gonads of *O. pullus* displayed primary oocytes within developing spermatogenic tissue, and no AVOs were diagnosed. Degenerating hydrated oocytes were identified in the lumen of some of these transitional individuals. These structures were also found in the ovarian lumen of mature resting females, and closely matched the staining properties of hydrated oocytes found in spawning and post-spawning females, thereby suggesting the presence of prior female function in the early-transitional individuals identified. Gonad microstructure of early-transitional individuals of *O. pullus* closely resembled that of the closely related California sheephead, *Semicossyphus pulcher*, a temperate protogynous hypsigenyine in which similar degenerating hydrated oocytes were found in the lumen of transitional individuals and mature resting females (see Figs. 5 & 6 in Warner, 1975). Histological identification of transitional individuals allowed diagnosis of functional female-to-male sex reversal in *O. pullus*.

Similarly, no AVOs were found within transitional gonad tissue of a number of protogynous temperate labrid species (Warner, 1975; Barrett, 1995; Gillanders, 1995; McBride and Thurman, 2003; Coulson *et al.*, 2009). In contrast, AVOs are comparatively more common within developing testicular tissue of transitional individuals in sub-tropical and tropical species as seen in some labrid examples (*e.g.* Cheilinus undulatus in Sadovy *et al.*, 2003; Xyrichthys novacula in Candi *et al.*, 2004) and other related taxa (*e.g.* Young and Martin, 1982; Fennessy and Sadovy, 2002; Asoh and Yoshikawa, 2003). The greater difficulty of identifying AVOs in transitional gonads of temperate species may be explained by the transient nature of oocyte atresia, in particular at the α-stage, and by the difficulty of identifying β- to γ-stage atretic oocytes (Hunter and Macewicz, 1985). This issue is of particular relevance to temperate species in which spawning is restricted to a limited number of months. As oocyte atresia can be observed during spawning and until shortly after spawning has ceased (Hunter and Macewicz, 1985), we may expect the seasonal pattern of spawning to be reflected in the presence of AVOs, as shown here in *O. pullus*. This suggests that the detection of oocyte atresia in gonads of transitional individuals may be impaired in temperate species, and that as a result, meeting the histological requirements for the diagnosis of functional sex change based on the presence of AVOs may not always be satisfied.

Instead, many authors have relied on the simultaneous presence of degenerating primary oocytes within developing testicular tissue, in combination with an ex-ovarian lumen, a lamellar structure of the testis, the presence of peripheral sperm sinuses and sex-specific size frequency information, to diagnose the presence of protogynous sex reversal (Barrett, 1995; Gillanders, 1995; McBride and Johnson, 2007; Coulson *et al.*, 2009). The diagnosis of protogynous sex change in *O. pullus* was confirmed by examining the relationship between size, age and gonad microstructure in the early parts of the life history of the study species. Some transitional *O. pullus* individuals were found to be larger and/or older than immature females, a pattern which does not meet expected size and age distributions of transitional individuals developing directly from an immature female phase, as seen in the gonochoristic scarine *Bolbometopon muricatum* (Hamilton *et al.*, 2008). In contrast, size and age of transitional individuals of *O. pullus* overlapped with the size and age distributions of mature females, confirming that transitional individuals may develop from mature females. These results illustrate that combining size-at-age information with histological analysis of gonad structure provides a powerful tool for the diagnosis of sexual ontogeny, particularly in cases where identification of the histological criteria necessary for evidence of functional sex change may be challenging.

Males of *O. pullus* occurred in the larger and older size and age classes, a pattern which coincides with the expected sex-specific size- and age-distributions of many protogynous species (Ghiselin, 1969; Warner, 1984; Sadovy and Shapiro, 1987). In many cases however, male-biased size distributions are often associated with sex-specific patterns of growth, with males achieving greater body sizes (for a given age) than females as a result of (i) faster initial growth (Munday *et al.*, 2004), (ii) a growth spurt at the time of sex reversal (Munday *et al.*, 2009), or (iii) a combination of these two mechanisms (Walker *et al.*, 2007). No differences in adult body size and growth rate were found between males and females in *O. pullus*, with males and females reaching similar mean maximum sizes. Male function is often considered to be less costly than that of females, and the general view of a trade-off between growth and reproduction has lead to assume that females that change sex into males subsequently have more energy available to allocate towards the function of somatic growth at the time of sex reversal. Energy expenditure in males may increase, however, as a result of behavioural costs, in particular those associated with reproductive and mating behaviours. *O. pullus* is a haremic-mating species, whereby males dominate a group of females within a restricted feeding area. This suggests that males of *O. pullus* may spend a significant amount

of energy maintaining their spawning territory and/or group(s) of females. Male *O. pullus* have also been shown to spend less time feeding than females (Clements, 1985), and females display a shift in the nutritional composition of their diet over the spawning months, a pattern which was not seen in males. These behavioural features associated with male reproductive function may generate costs that are reflected in terms of growth, and these costs may underlie the patterns of male growth in the study species. Furthermore, male-biased sexual size dimorphism often reflects the presence of high intrasexual competition amongst males, whereby greater size of males increases access to females (size-advantage model; Ghiselin, 1969; Warner, 1984). The absence of male-biased sex-specific differences in adult size in *O. pullus* suggests that male size in this species may not play a critical role in determining the reproductive success of males, and/or that local conspecific density and distribution patterns may provide conditions of low intrasexual competition in the study species.

The absence of sex-specific growth in *O. pullus* does not exclude the possibility that females changing sex into males are those growing faster initially within a given age class (Munday *et al.*, 2004; Walker *et al.*, 2007), and males of *O. pullus* at the age of three years were on average larger than females, suggesting that individuals undergoing sex reversal may be those growing faster during the initial part of the life history. If the females that change sex are those that grow faster initially, we may expect them to reach size-at-sex change at a younger age than those growing comparatively slower. Ovary weight increased with age of *O. pullus* females, indicating that older females contribute comparatively greater amounts of reproductive output than younger females. As a result, faster growing females will reach size-at-sex change earlier and will display comparatively smaller ovary size than older females of the same size. We may hypothesise that older (slower growing) females in *O. pullus* will defer sex change to younger females (faster growing) within the group, and that increasing female reproductive output with age may underlie the presence of non-sex changing females in this species. Female age and condition have been shown to increase larval survival (Berkeley *et al.*, 2004; Meekan *et al.*, 2006), and if larval survival and fecundity increase with female size and age, we may expect strong selection for maintaining larger and older females within a given population. This hypothesis meets the argument at the basis of the size-advantage hypothesis (SAH; Munoz and Warner, 2003), which predicts that larger females within a given social grouping will defer sex change to smaller females within the group, when their reproductive value (which considers the balance between current and future reproductive success) is higher than that of the sum of all other female members of the social

group, and this is associated with a size-fecundity skew. Back-calculation of male and female individual growth trajectories will be essential in order to disentangle the relationship between growth and the mechanisms of sex reversal in *O. pullus*.

This study provides the first comprehensive analysis of the reproductive biology and demography of an odacine labrid species, and contributes to a better understanding of the reproductive biology of temperate labrids. In particular, this study illustrates the significance of combining size and age information with detailed gonad microstructure for the diagnosis of sexual ontogeny, particularly in cases where the diagnosis of sex change is challenging. Further examination of the reproductive biology and sex-specific demography of odacine labrids should extend to include the closely related species residing in temperate Australian waters (*e.g. Heteroscarus acroptilus*, *Olisthops cyanomelas*).

Chapter 4. Latitudinal effects on the demography and life history of a temperate marine herbivorous fish, *Odax pullus* (Labridae)

4.1 Introduction

Thermal environments vary over space or time. This generates selective pressures on organisms' life histories that may lead to the evolution of phenotypic plasticity in life history traits (Angilletta, 2009). Thermal heterogeneity is particularly significant for ectotherms distributed over wide geographical gradients. Many marine fishes, including those associated with reefs, have broad geographical distributions. In species associated with shallow reef environments, distributions are usually linked to coastal habitats, and frequently cover extensive latitudinal gradients. This is characteristic of many temperate water species, which often display distributions that extend from warm subtropical to cold high latitude reef systems, resulting in exposure to significant gradients of temperature.

Animals with wide geographical ranges often display systematic gradients in body size (Angilletta 2009). The response of body size to temperature gradients has received extensive attention for more than a century and is widely referred to as Bergmann's Rule (but see Blackburn *et al.*, 1999). Bergmann's rule was initially intended to describe a generalization observed across species and has since been extended to describe intraspecific variation in body size with latitude (Rensch, 1938; Mayr, 1956), and has been widely applied to ectotherms (Ray, 1960; Atkinson, 1994). In many examples, individuals reach a larger body size in colder environments at higher latitudes (or altitudes) (Bergmann, 1847; Atkinson, 1994; Sibly and Atkinson, 1994; Kingsolver and Huey, 2008). Changes in body size have profound effects on associated life history traits. In particular, body size will directly affect size-at-maturity and fecundity, two life history parameters that contribute significantly to lifetime reproductive success (Roff, 1992; Stearns, 1992; Charnov, 1993).

In many ectothermic taxa, larger body size under colder rearing conditions at higher latitudes is coupled with delayed maturity at a larger body size (Ray, 1960; Atkinson, 1994; Angilletta, 2009) (but see Mousseau, 1997; Ashton and Feldman, 2003). This 'near-universal' response of ectothermic maturation rates to environmental temperature over

gradients of latitude is widely referred to as the Temperature-Size Rule (TSR) (Atkinson, 1996). While advances have been made as to the theoretical underpinnings of the TSR ("Hotter is smaller" hypothesis) (Kingsolver and Huey, 2008), the mechanisms remain elusive (Partridge *et al.*, 1994; Perrin, 1995; Partridge and French, 1996; van der Have and de Jong, 1996; Atkinson and Sibly, 1997). Before a general explanation can be found, there is a need to (i) examine species- and population-specific patterns (Atkinson, 1996), and (ii) to use approaches that integrate a range of environmental, physiological, and/or ecological factors as potential drivers underlying the phenotypic plasticity and/or evolution of demographic and life history traits over geographical gradients of temperature (Angilletta, 2009).

The effect of temperature on body size and maturation rates contrasts with that of other factors that reduce growth rate, such as a reduction in food availability, which results in differing reaction norms of both adult body size and size- and age-at-maturity. These differences are at the basis of the "life history puzzle" identified in Berrigan and Charnov (1994). In many ectotherms, individuals grow more slowly, mature later at a smaller body size, and reach a smaller adult body size in conditions of low food availability or high nutrient stress (Stearns, 1992; Berrigan and Charnov, 1994; Atkinson and Sibly, 1997). Berrigan and Charnov (1994) proposed that the relationship between growth rate and adult body size provides a means to predict the shape of the reaction norm for size- and age-at-maturity to these two environmental cues. If environmental temperature is the primary driver underlying maturation rates, then reduced growth rates at higher latitudes will result in delayed maturity at a larger size and larger final body size. In contrast, if food availability is the primary factor affecting the rate of somatic growth, reduced growth in conditions of low food availability will result in delayed maturity at a smaller size and smaller ensuing adult body size (Berrigan and Charnov, 1994).

The contrasting effects of temperature and food availability on ectotherm reaction norms are significant in the context of widely distributed marine herbivorous ectotherms. A common view is that herbivorous fishes are penalized in cold environments due to an inability to process and assimilate plant food at low temperatures. This is the basis of a hypothesis that herbivory in marine ectotherms is subject to a physiological constraint on the digestion of algal material at high latitudes (Horn, 1989; Harmelin-Vivien, 2002; Behrens, 2005; Floeter *et al.*, 2005; Behrens and Lafferty, 2007). This view originated in Gaines and Lubchenco (1982), and was proposed as one of several hypotheses for the lower relative

species diversity and abundance of herbivorous fishes in cold water systems. This hypothesis is based on the premise that low temperatures limit the capacity to process algal matter (Horn, 1989), because (i) herbivorous fishes are unable to meet metabolic demands at high latitudes due to a presumed 'low quality' diet (*e.g.* Behrens and Lafferty, 2007), (ii) the fermentative processes associated with the digestion of algal material are restricted at low temperatures (*e.g.* Behrens, 2005), and (iii) feeding rates decrease with temperature, thus limiting the amount of food that can be processed at high latitudes (*e.g.* Floeter *et al.*, 2005; Smith, 2008). If such digestion-related constraints on herbivory exist at low temperatures, this would be equivalent to a reduction in resource (food/nutrient) availability for herbivores living at high latitudes. In this case, we would expect individuals living on a herbivorous diet at colder latitudes to grow slower and achieve smaller body sizes (Berrigan and Charnov, 1994).

An alternative view considers the mechanistic processes that underlie the impacts of temperature and body size on metabolic rate. Metabolic rate increases with body size and temperature, and influences the rate of resource uptake and thus the amount of energy available for allocation to growth, reproduction and maintenance (Brown *et al.*, 2004). Reduced metabolic rates in individuals living at colder temperatures will be associated with lower rates of resource uptake for a given body size, and will be correlated with lower maintenance costs. This implies that greater amounts of energy may be available for growth in individuals living at colder temperatures, as this energy will not be involved in the underlying costs of high metabolic rates. This approach, which underlies the more general Metabolic Theory of Ecology, predicts that larger body size at higher latitudes may be a result of a direct effect of temperature and body size on metabolic rate. An assumption is that the responses of metabolic and resource uptake rates to temperature will be independent of diet, and will be applicable to both herbivores and carnivores.

This chapter addresses the following two questions. Firstly, what are the demographic responses of an ectothermic herbivore over a broad latitudinal gradient of temperature? Secondly, is this response consistent with the hypothesis of a temperature-constraint on herbivory at high latitudes? The predictions of Berrigan and Charnov (1994) provide a framework to address these issues. Specifically, if growth is reduced at lower temperatures as a result of a constraint on herbivory at higher latitudes ('temperature-constraint' hypothesis), we may expect the responses in growth and maturation rates of an ectothermic herbivore to reflect those predicted for reductions in food availability at colder latitudes. Comparison of

these life history responses with a species living on a non-herbivorous diet will be informative as the effects of environmental temperature are likely to result in contrasting patterns of variation in body size and maturation rates at higher latitudes between an herbivore and a non-herbivore. Alternatively, if the digestion of an herbivorous diet is not constrained by temperature at higher latitudes, we may expect two species living on contrasting diets to display similar responses over latitudinal gradients of temperature. In this case, an herbivorous and a non-herbivorous species are likely to both reflect the effects of temperature on ectotherm developmental rates ("Hotter is smaller" hypothesis).

I first explore the patterns of variation of the study species in demographic and life history traits across latitudes and relate these to environmental temperature, species abundance, exposure, habitat availability and fishing effort, which may all affect growth, body size and age structures, and development rates. Secondly, the possibility of a temperature-constraint on herbivory at high latitudes is examined by (i) exploring the response in growth, body size and maturation rates of *Odax pullus* in the context of the predictions presented in Berrigan and Charnov (1994), and (ii) comparing the responses of life history traits of *O. pullus* over a latitudinal gradient of temperature with that of a closely related carnivore, *Notolabrus fucicola*. The responses in growth rate, body size, development rate (size- and age-at-maturity) and longevity of *N. fucicola* to environmental temperature are expected to meet the predictions of the TSR ("Hotter is smaller"; Fig. 4.1 A). In contrast, the response of *O. pullus* to temperature over a wide gradient of latitude is expected to reflect the predictions of (1) a physiological constraint on herbivory if *O. pullus* individuals grow slower, mature later at a smaller body size and reach a smaller adult body size at colder temperatures (higher latitudes) ('temperature-constraint' hypothesis; Fig. 4.1 B); or (2) the TSR if individuals grow slower, mature later at a larger body size, and reach a larger adult body size at higher latitudes ("Hotter is smaller"; Fig. 4.1 A). In this case, no differences are expected in the slopes of the thermal reaction norms for body size and maturation rates between the two study species, a scenario which would argue against the presence of a temperature constraint on herbivory at high latitudes.

Intraspecific density represents a potentially confounding factor. The physiological constraint hypothesis (Gaines and Lubchenco, 1982) predicts that, as herbivores are constrained in their digestion of algal material at colder temperatures, numbers of *O. pullus* will be decreasing with increasing latitude, and that greater densities of the herbivorous *O.*

pullus will be found at lower latitudes (warmer temperatures). If densities of *O. pullus* were found to be significantly higher at low latitudes then intraspecific competition might obscure the trends in size and growth predicted by the physiological constraint hypothesis. If, however, demography and population densities are independent of nutritional status as argued in a mechanistic hypothesis relating temperature and metabolic rate, then we would not expect systematic reductions in the density of herbivores relative to carnivores with decreasing temperature. For this reason the sampling design included estimates of density at high, intermediate and low latitude localities for both the herbivorous and carnivorous species in association with the full repertoire of demographic data.

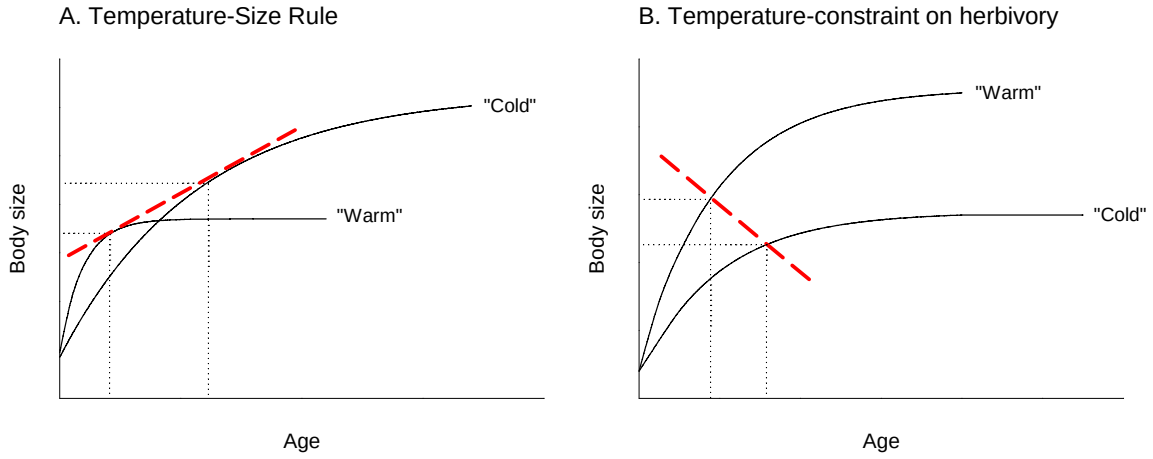

Fig. 4.1: Diagram illustrating the predicted response of growth (solid black line), body size (*y*-axis), development (thermal reaction norm for size- and age-at-maturity; dashed red line), and longevity (*x*-axis), over a latitudinal gradient of temperature ("warm" indicates low latitudes; "cold" indicates high latitudes), in the context of (A) ectotherm life history theory over environmental gradients of temperature (Temperature-Size Rule: "Hotter is smaller"), and (B) the hypothesis of a temperature-constraint on herbivory at high latitudes. Non-herbivorous species are predicted to follow the patterns of variation described in (A). Adapted from Stearns (1992) and Berrigan and Charnov (1994).

4.2 Materials & Methods

Sampling

A total of 1064 individuals of *Odax pullus* were collected at six locations across New Zealand spanning a gradient of 13° of latitude: Karikari Peninsula, Hauraki Gulf, Wellington, D'Urville Island (Malborough Sounds), Fiordland, and Stewart Island (Fig. 4.2). A total of 450 *Notolabrus fucicola* were collected at the following six locations, spanning a latitudinal gradient of 13° degrees: Three Kings Islands, Hauraki Gulf, Wellington, D'Urville Island (Malborough Sounds), Fiordland, and Stewart Island (Fig. 4.2). Sample sizes are presented in Table 4.1.

Fish were sampled by spearing and processed within one hour of collection. Standard Length (SL), Fork Length (FL), Total Weight (TW), and Gutted Weight (GW) were recorded for each fish to the nearest millimetre and ten grams, respectively. The sagittal pair of otoliths was removed in all samples collected, rinsed in 70% ethanol, and stored dry. Gonad tissue was collected for a sub-sample of 634 *O. pullus* and 202 *N. fucicola* individuals (Table 4.1). Whole gonads were dissected out, weighed to the nearest gram, and placed in FAAC, a formalin-based fixative (formaldehyde 4%, glacial acetic acid 5%, calcium chloride 1.3%; Pears et al. 2006), before histological processing. Samples for which gonads were not collected for histology were sexed macroscopically (except 20 individuals from the Hauraki Gulf which were not sexed). Error associated with macroscopic sexing was estimated as 0.8% (see Chapter 3 – section 3.2 for details), and considered negligible.

Estimation of age

Age was estimated from sectioned sagittal otoliths for all individuals sampled. Methods used for otolith sectioning and enumeration of age are detailed in Chapter 2 (section 2.2). One opaque zone (as seen under transmitted light) was formed each year in sagittal otoliths of individuals aged one year or more, and one increment was deposited daily in sagittae of individuals aged one year or less in both species examined. Validation of ageing methods are presented in Chapter 2 (section 2.2 & 2.3) for *O. pullus*, and in Ewing *et al.* (2003) and Welsford (2003) for *N. fucicola*.

Fig. 4.2: Map of sampling locations of *Odax pullus* and *Notolabrus fucicola* across New Zealand.

Table 4.1: Sampling of *Odax pullus* and *Notolabrus fucicola* across New Zealand. Summary table showing longitude/latitude coordinates at each sampling location, mean annual sea surface temperature (SST, in degrees celcius ^{o}C), amplitude of mean monthly temperature difference between the warmest and coldest months (Δ SST, in ^{o}C), total samples sizes collected, number of gonad samples collected, and month/year when gonad samples were taken. (*) indicates presence of active females in the sample, showing samples for which size- and age-at-maturity could be estimated. (†) indicates presence of transitional individuals in the sample, showing samples for which size- and age-at-sex change could be estimated. *O. pullus* does not occur at the Three Kings Islands.

Location	Longitude / latitude	Mean annual SST (Δ SST)	N total (N gonad samples)		Date gonads sampled
			O. pullus	*N. fucicola*	
Three Kings Is	172.1^{o}E, 34.1^{o}S	17.1 (5.3)	-	111 (0)	-
Karikari	173.7^{o}E, 35^{o}S	17.8 (5.5)	44 (41)	0 (0)	Mar 2006
Hauraki Gulf	175.3^{o}E, 36.3^{o}S	17.6 (6.4)	447 (319*†)	75 (60*)	Monthly, 2005-2008
Wellington	174.7^{o}E, 41.3^{o}S	14.5 (5.2)	68 (0)	34 (0)	-
D'Urville Is	173.9^{o}E, 40.7^{o}S	14.7 (5.3)	125 (104†)	68 (63)	Jan-Feb 2007 & 2008
Fiordland	166.9^{o}E, 45.5^{o}S	13.7 (4.2)	55 (47)	26 (24)	Apr 2008
Stewart Is	167.9^{o}E, 47^{o}S	12.1 (3.6)	325 (123*†)	136 (55*)	Dec 2006 & 2007
N total			*1064 (634)*	*450 (202)*	

Modelling of growth

Growth of *O. pullus* and *N. fucicola* was estimated for all populations sampled by examination of the relationship between size (Fork Length, FL) and age. Size-at-age data were fitted with Francis' (1988) re-parameterized equation of the von Bertalanffy Growth Function (rVBGF) (Francis, 1988; Moulton *et al.*, 1992; Welsford and Lyle, 2005; Trip *et al.*, 2008). Details of the form of the rVBGF function are described in Chapter 2 (section 2.2). The best-fit model was estimated for each population by minimizing the negative log of the likelihood, given a probability density function with a normal distribution (Kimura, 1980; Haddon, 2001). rVBGF parameters estimated for *O. pullus* were $L(1)$, $L(5)$, and $L(9)$, providing estimates of mean body size-at-ages one, five and nine years. For *N. fucicola*, rVBGF parameters estimated were $L(1)$, $L(9)$, and $L(17)$, generating estimates of mean body size-at-ages one, nine, and seventeen years. Choice of the ages used to estimate rVBGF parameter values was designed for intraspecific comparison of mean size-at-age across populations sampled, and was thus aimed at representing the length of the life span across the shortest lived population within each species. Choice of the age values used for parameter estimation did not affect the form of the resulting growth trajectories in any of the populations of the two species examined.

When few or no individuals aged one year or less were collected within a sample (Table 4.2), an estimated value of size-at-settlement (*i.e.* size at theoretical age zero, *y*-intercept of size-at-age plots) of 15.5 mm FL was added to the data (*N. fucicola*). This estimate was based on results of minimum size at settlement of *N. fucicola* in Tasmania found in Welsford et al. (2004) of 10.4 mm Standard Length (SL) and was transformed to Fork Length (FL) using the SL-FL relationship of the present data.

Table 4.2: Number of individuals in each population of *Odax pullus* and *Notolabrus fucicola* sampled that were aged: 1) less than one year and 2) one year old, showing samples in which a constraint was used to fit the rVBGF and VBGF models to the size-at-age data (shown by asterisk *). 3K: Three Kings Islands; KA: Karikari Peninsula; HG: Hauraki Gulf; WE: Wellington; DU: D'Urville Island; FD: Fiordland; SI: Stewart Island.

		3K	KA	HG	WE	DU	FD	SI
O. pullus	N (<1year)	-	4	39	0	7	8	14
	N (=1 year old)	-	3	39	5	29	5	24
N. fucicola	N (<1year)	6	-	0*	0*	0*	0*	1
	N (=1 year old)	15	-	1	0	3	2	1

For each species at each location, variance around rVBGF parameters $L(1)$, $L(5)$ and $L(9)$ for *O. pullus*, and $L(1)$, $L(9)$ and $L(17)$ for *N. fucicola* was estimated using a bootstrapping technique following Gotz et al. (2008). Size-at-age data for each population were re-sampled 1000 times with replication and maintaining population age structure. Means were bias-adjusted and 95% percentile confidence intervals (CIs) were calculated from the sorted bootstrap estimates (Haddon, 2001; Gotz *et al.*, 2008).

Growth rate

Instantaneous growth rate (IGR) was estimated in the initial part of the life span at ages 6 months, 1, 1.5, 2, 2.5, and 3 – 8 years (adapted from Robertson *et al.*, 2005). IGR was calculated as follows: $IGR = K * (L_\infty - L_t)$, where K and L_∞ are best-fit von Bertalanffy Growth Function (VBGF) parameters, and L_t is expected size-at-age t (Porch *et al.*, 2002). The VBGF was fitted by minimising the negative log of the likelihood given a normal probability density function, as described for modelling of growth using the rVBGF. No differences were found in expected size generated by the VBGF and rVBGF growth

functions (see also Chapter 2, section 2.3). In *N. fucicola*, where few or no individuals aged one year or less were sampled (Table 4.2), VBGF were fitted to size-at-age data by constraining the best-fit function to be equal or less than 50 mm at settlement (at theoretical age zero) (Kritzer *et al.*, 2001; Berumen, 2005).

So as to obtain growth rate estimates that were comparable across species and locations, estimates of IGR were scaled to expected body size-at-age *t*, as follows: $G = \frac{IGR}{L_t}$, where G $(year^{-1})$ is relative instantaneous growth rate. *G* provides a measure of growth rate per unit of body size (in terms of fork length) at a given age.

Estimation of longevity and adult body size

Mean maximum age T_{max} (longevity) and mean maximum body size L_{max} (adult body size) were calculated for each population as the average age (in years) of the 10% oldest individuals for *O. pullus* and the 25% oldest individuals for *N. fucicola*, and the average body size (fork length, in mm) of the 10% largest individuals found within each sample of *O. pullus* and the 25% largest individuals of *N. fucicola*, respectively (adapted from Trip et al. 2008). Mean maximum age and size were calculated on a greater proportion of the sample in *N. fucicola* to account for comparatively lower sample sizes than that in *O. pullus* (Claisse *et al.*, 2009). For each species at each location, variance around parameters T_{max} and L_{max} was estimated using a bootstrapping technique following Gotz et al. (2008). Age and size data for each population were re-sampled with replication so as to obtain 1000 estimates of T_{max} and L_{max}. Mean maximum age and size were bias-adjusted, and 95% percentile confidence intervals (CIs) were calculated from the sorted bootstrap estimates (Haddon, 2001; Gotz *et al.*, 2008).

Size- and age-at-maturity

Gonad histology was performed for a total of 836 individuals (Table 4.1). Details of histological processing of gonad samples are described in Chapter 3 (section 3.2). Sexual identity, reproductive development, and spawning history of *O. pullus* were assessed based

on criteria developed in Chapter 3 (Table 3.2). Reproductive development of *N. fucicola* was assessed based on criteria developed in Denny and Schiel (2002).

Estimation of size- and age-at-maturity based on females collected outside of the spawning months has been shown to produce biased estimates as a result of the difficulties associated with establishing spawning history in reproductively inactive ovaries (Pears *et al.*, 2006). Size- and age-at-maturity were therefore estimated in populations displaying signs of spawning activity at the time of sampling, as established by the presence in ovaries of vitellogenic oocyte growth (stages IV to V) and/or of oocyte α-atresia indicating immediate or recent spawning, respectively. Spawning activity was found for both study species at two of the locations sampled, in the Hauraki Gulf (July to November, Chapter 3) and Stewart Island (August to January, Paul, 1998). Size- and age-at-maturity were estimated at those two locations, by calculating the size and age at which 50% of females were mature (proportion of mature females relative to the total number of females within each size or age class) (Moore *et al.*, 2007; Williams *et al.*, 2008). Fitting of the logistic function is described in Chapter 3 (section 3.2). 95% confidence intervals (CI) were estimated for each parameter value of L_{50} (size-at-maturity) and T_{50} (age-at-maturity) using a bootstrapping procedure (Moore *et al.*, 2007), as described in Chapter 3 (section 3.2).

Size- and age-at-sex change

Two independent methods were used to estimate size- and age-at-sex change in *O. pullus*.

Firstly, mean size and age of transitional (undergoing female-to-male sex reversal) individuals was calculated. Transitional individuals were found at three locations, Hauraki Gulf, D'Urville Island, and Stewart Island. Histological criteria used for evidence of sexual transition are detailed in Table 3.2 (Chapter 3, section 3.2). Separate one-way analyses of variance (ANOVA) and post-hoc comparisons (Tukey's Test) were used to identify significant differences across locations.

Secondly, a logistic regression approach was used to estimate size and age at which 50% of sex changing females have undergone sex reversal (Williams *et al.*, 2008). However, examination of sex-specific size and age distributions of *O. pullus* at each location sampled

showed that, while some females changed sex to being functional males, others remained female. This was accounted for in the form of the logistic function used by modifying the expected frequency of being male from a value of 1 (in the case where all females change sex into males) to the observed frequency of males (x) within in each size or age class, as follows: $P_a = \frac{x}{1+e^{\left(-\ln(19)*\frac{(a-a_{50})}{(a_{95}-a_{50})}\right)}}$, where P_a is the predicted proportion of sex changing females in size or age class a, x is the observed frequency of males within each size or age class, a_{50} is the size or age at which 50% of sex changing females have changed sex, and a_{95} is the size or age at which 95% of sex changing females have changed sex. Parameters estimated were size-at-50% sex change L_{sc50}, size-at-95% sex change L_{sc95}, age-at-50% sex change T_{sc50}, and age-at-95% sex change T_{sc95}. Size classes were based on 50 mm increments (fork length), and age classes were based on one year increments.

The best-fit logistic model parameters were estimated by minimising the negative log of the likelihood based on a probability density function with a binomial distribution (Haddon, 2001). 95% confidence intervals (CIs) were estimated for each parameter value of L_{sc50}, L_{sc95}, T_{sc50}, and T_{sc95} using a bootstrapping procedure (Moore *et al.*, 2007). The data were randomly re-sampled 1000 times with replication. For each re-sampled data set, the logistic function was fitted and the best-fit combination of parameters was estimated as described above. 95% percentile CIs were calculated from the 2.5 and 97.5 percentiles of the bootstrap estimates, and means were bias-adjusted (Haddon, 2001).

Reproductive effort

In order to explore the effect(s) of delayed maturity on female reproductive growth, the relationship between ovary weight (as a proxy for reproductive output) of reproductively active females and female body size (fork length) and age was examined across populations sampled in the Hauraki Gulf and Stewart Island for both *O. pullus* and *N. fucicola*.

Environmental factors

Sea surface temperature

Mean monthly sea surface temperature (SST) data were obtained from satellite-derived temperatures. Satellite-derived SST data have been shown to be reliable estimators of in-situ near shore SST over broad spatial scales (Smale and Wernberg, 2009). Satellite-SST data were retrieved from the National Oceanographic and Atmospheric Administration (NOAA) CoastWatch Program ("BloomWatch360") for each of the seven locations sampled (Three Kings Is, Karikari, Hauraki Gulf, Wellington, D'Urville Is, Fiordland, and Stewart Is; http://coastwatch.pfel.noaa.gov/coastwatch/CWBrowserWW360.jsp?get). Long term SST estimates were generated from mean monthly SST between January 1985 and December 2007.

Four SST measures were considered (Table 4.3). Firstly, mean annual SST was calculated as an average SST across all months at each site sampled. Secondly, the amplitude of the variation in mean monthly SST (Δ SST) was estimated as the difference in temperature between the warmest and coldest months of the year. Lastly, the minimum and maximum mean SSTs were coldest and warmest temperatures recorded for each location, respectively. Correlation analysis across all four SST measures showed significant pair-wise correlations (Table 4.3), and mean annual SST was chosen to describe temperature.

Mean annual SST decreased significantly with latitude (Correlation analysis; $R = 0.97$, $p < 0.001$).

Table 4.3: Pair-wise correlations amongst sea surface temperature (SST) variables: mean annual SST (Mean SST), amplitude of temperature variation between coldest and warmest months (Δ SST), minimum SST and maximum SST, showing Pearson's correlation coefficient and significance value.

Variable	Mean SST	Δ SST	Max SST	Min SST
Mean SST	-			
Δ SST	0.88 *($p < 0.01$)*	-		
Max SST	0.99 *($p < 0.001$)*	0.91 *($p < 0.01$)*	-	
Min SST	0.99 *($p < 0.001$)*	0.81 *($p < 0.05$)*	0.98 *($p < 0.001$)*	-

Abundance estimates

Abundance estimates of *O. pullus* and *N. fucicola* were obtained by J. Howard Choat at the following sampling locations: Karikari Peninsula, Hauraki Gulf, D'Urville Is, and Stewart Is. Counts were recorded for each species along 30x10m belt transects on scuba. A total of 14 – 37 replicate belt-transects were conducted within each region, and mean abundance estimates were calculated per 300 m^2. Abundance estimates were additionally obtained for *O. pullus* from the Poor Knights Islands, which have been a no-take marine reserve since 1981, to estimate abundance in the long-term absence of recreational or commercial fishing. Abundance estimates at the Three Kings Is (*N. fucicola*) and in Wellington (*O. pullus* and *N. fucicola*) were obtained from Table III in Choat and Ayling (1987), and in Fiordland (*O. pullus* and *N. fucicola*) from Fig. 25 in Schiel and Hickford (2001). These studies were chosen based on their similarity in sampling units and count methods to the present study. Abundance estimates are presented in Appendix 1.

Habitat

O. pullus and *N. fucicola* both occur on shallow rocky reef beds covered with macroalgal assemblages of large brown seaweeds (Francis, 2001). Available algal habitat cover for both study species was obtained from Shears and Babcock (2007). Total percent occurrence (% quadrats in which each algal species were recorded) of the following fucoidean and laminarian algal species was used (see Appendix 5 in Shears and Babcock 2007): *Carpophyllum maschallocarpum*, *C. flexuosum*, *Margineriella boryana*, *Lessonia variegata*, *Ecklonia radiata*, and *Macrocystis pyrifera*. These species were selected as primary representatives of preferred habitat of *O. pullus* across New Zealand (unpublished data); *N. fucicola* habitat coincides with that of *O. pullus* but also extends over sandy substrata across reefs. Locations used as representatives of sampling sites of the present study were: Cape Karikari (Karikari), Mokohinaus Is and Leigh (mean value; Hauraki Gulf), Wellington (Wellington), Long Is (D'Urville Is), Doubtful Sound and Preservation Inlet (mean value; Fiordland), and Patterson Inlet and Port Adventure (mean value; Stewart Is). No data were available at the Three Kings Is.

Exposure (fetch)

Exposure of each location to prevailing winds and resulting wave action was calculated by estimating fetch (Wellenreuther *et al.*, 2008). Fetch is a measure of the distance to land of a given point, and was calculated over a maximum distance of 300km for each 20^{o} angle around each location. Fetch was assessed using the "Fetch Effect Analysis" program (Pickard, 2000). A GPS coordinate recording was taken for each site where one or more fish were collected. Total fetch ("sum fetch") was calculated for each collecting site and averaged across sites within each sampling region to obtain an estimate of mean total fetch for all seven sampling locations (Three Kings Is, Karikari, Hauraki Gulf, Wellington, D'Urville Is, Fiordland, and Stewart Is).

Fishing effort

Estimates of fishing effort were obtained for *O. pullus* from the latest New Zealand Ministry of Fisheries report (2008). Estimates of commercial fishing effort were based on reported domestic landings from 2001-02 to 2006-07, and recreational fishing effort was estimated from surveys conducted between 1991 and 1994. Recreational fishing effort is assumed to have either remained similar to, or be greater than, values obtained from these surveys dating back fifteen years. Total estimated fishing effort was calculated as the sum of both commercial and recreational fishing effort estimates (in tonnes). Information used is available from: http://fpcs.fish.govt.nz/science/documents/plenary/BUT_FINAL%2008.pdf, and is presented in Table 4.4 (also see Appendix 2).

There is no recreational or commercial fishing for *N. fucicola* at any of the locations sampled across New Zealand.

Table 4.4: Reported commercial landings of *Odax pullus* between 2001 – 2007 (overall mean per year +/- SE, in tonnes), estimated recreational harvest (per year, data based on surveys undertaken between 1991 and 1994), and total estimated annual fishing effort for each location sampled. Information presented is based on the 2008 New Zealand Ministry of Fisheries report(http://fpcs.fish.govt.nz/science/documents/plenary/BUT_FINAL%2008.pdf). The Poor Knights Islands have been a no-take marine reserve since 1981. All estimates are presented in tonnes per year.

Location	Fishstock	Reported commercial landings (+/- SE)	Estimated recreational harvest	Total estimated fishing effort
Karikari Peninsula	BUT 1	1.83 (+/- 0.40)	10	11.83
Poor Knights Is	BUT 1	0	0	0
Hauraki Gulf	BUT 1	1.83 (+/- 0.40)	10	11.83
Wellington	BUT 2	54.67 (+/- 3.07)	80	134.67
D'Urville Is	BUT 7	25.5 (+/- 0.7)	15	40.5
Fiordland	BUT 5	30.67 (+/- 3.66)	10	40.67
Stewart Is	BUT 5	30.67 (+/- 3.66)	10	40.67

Analysis

Geographical variation in life history, and effect of environmental factors (temperature, abundance, habitat, exposure, and fishing)

A "biota-environment linkage" (BEL) approach was used to explore the patterns of geographic variation in life history and the effects of potential underlying environmental factors (Clarke, 1993; Clarke and Ainsworth, 1993; Clarke *et al.*, 2008). This non-parametric multivariate approach aims at estimating the contribution of environmental factors to explaining the observed variation in biological data.

First, variation in life history traits across locations sampled was explored using Principal Component Analysis (PCA). Given the number of samples (six locations) over which the ordination of biological variables was performed, care was taken to minimise the potential effects of over-fitting, which occur when the number of variables examined exceeds the number of samples. Here, nineteen (*O. pullus*) and fifteen (*N. fucicola*) life history variables were identified (Table 4.5). Correlation amongst variables also generates random noise, thus reducing the power of a model to explain any true variation in the data. To minimise these effects, a set of criteria was developed for selecting a group of relevant life history variables for inclusion in the analysis. The aim was two-fold: to remove the most

redundant life history variables, and to keep all relevant demographic information. Variables were first categorised according to the type of information provided. Four information categories were identified: (i) age, (ii) size, (iii) growth rate, and (iv) development rate, with the aim of retaining at least one life history variable within each of these four categories. Secondly, a correlation matrix was constructed across all nineteen (*O. pullus*) and fifteen (*N. fucicola*) life history variables, and when two variables were correlated by more than 75% within a given category, only one of the two correlated variables was selected for inclusion into the analysis. A total of eight (*O. pullus*) and six (*N. fucicola*) variables were retained for the PCA (Table 4.5). Variables were checked for the presence of skewed distributions across locations using pair-wise correlation plots (Draftsman plots), but no transformations of the life history variables were required. All six populations of *O. pullus* sampled, and all but the Three Kings Is population of *N. fucicola* (Three Kings Is was excluded for lack of habitat availability information) were included in the analysis. All variables were normalised to a common scale.

Second, the contribution of environmental factors to explaining the patterns of variation in life history traits across locations was examined using rank correlation analysis (global BEST test; Clarke *et al.*, 2008). Environmental factors examined were: mean annual Sea Surface Temperature (SST, ^{o}C), abundance (individuals/300m^2), habitat (total % occurrence of preferred macroalgal species), exposure (fetch, kms), and fishing effort (tonnes, *O. pullus* only). Rank correlation analysis was performed between the life history (biotic) and environmental (abiotic) similarity matrices for all possible combinations of single or subsets of environmental variables ($(2^p - 1)$ combinations possible, with p = number of environmental variables). The single or subset of environmental variables that best correlated with the life history similarity matrix was selected based on the highest correlation coefficient (ρ_i). Rank correlation was based on Spearman's correlation coefficient, and resemblance matrices were constructed from Euclidean distances. All data were normalised to a common scale prior to analysis. This was followed by a permutation procedure to test the hypothesis of no correlation between the biotic and abiotic similarity matrices. The location labels of the environmental similarity matrix were permuted to effectively destroy any correlation between the biotic and abiotic matrices, and the rank correlation procedure was repeated 9999 times to produce a null distribution of ρ under the null hypothesis. The null hypothesis of no correlation between the two matrices was rejected if ρ_i was found to occur in less than 5% of

permuted procedures. These analyses were performed in PRIMER-E 6.0, and carried out independently for each study species.

Relationship between temperature, body size and longevity

Simple linear regression analyses were performed to examine the relationship between sea surface temperature (SST) and mean size-at-age one, adult body size (mean maximum size), and longevity (mean maximum age) in *O. pullus* and *N. fucicola*. Analyses were performed on parameter values *L(1)*, L_{max} and T_{max}. Assumptions of normality and homogeneity of variance of the observed values and residuals were checked for each analysis using box plots and by examining the relationship between the residuals and predicted values from the regression model fitted. Longevity data for *O. pullus* was cube-root transformed. The presence of outliers and the effect of individual *x*- and *y*-value on the regression model fitted were examined using leverage estimates and Cook's D_i values (Quinn and Keough, 2002). Analyses were performed in STATISTICA 7.1.

Table 4.5: List of life history variables identified and of life history variables retained in the PCA for *Odax pullus* and *Notolabrus fucicola*. Variables are presented by category of demographic information provided. Variables retained in the analysis were those that were correlated by less than 75% to any other variable within a given category. FL: fork length; GW: gutted weight; L(*t*): mean size-at-age *t* as estimated from the re-parameterized Von Bertalanffy Growth Function (rVBGF); IGR_t: instantaneous growth rate-at-age *t*; age and size of smallest male are used as approximations for age- and size-at-sex change (timing of development).

Category	Life history variables identified		Life history variables retained	
	Odax pullus	*Notolabrus fucicola*	*Odax pullus*	*Notolabrus fucicola*
Age	max age, mean max age	max age, mean max age	mean max age	mean max age
Size	max FL, max GW, mean max FL, mean max GW, L(1), L(5), L(9), mean FL of 1 year olds, mean GW of 1 year olds	max FL, max GW, mean max FL, mean max GW, L(1), L(9), L(17)	mean max FL, L(1), L(5), L(9)	mean max FL, L(1), L(9), L(17)
Growth rate	$IGR_{0.5}$, IGR_1, $IGR_{1.5}$, IGR_2, $IGR_{2.5}$, IGR_3	$IGR_{0.5}$, IGR_1, $IGR_{1.5}$, IGR_2, $IGR_{2.5}$, IGR_3	$IGR_{0.5}$	IGR_1
Timing of development	age smallest male, size smallest male	-	age smallest male, size smallest male	-

Geographical variation in size- and age-at-maturity, and -at-sex change

Estimates of size- and age-at-maturity and -at-sex change were plotted with bootstrapped variance estimates to examine similarities: (i) in the timing of sexual maturation (*O. pullus* and *N. fucicola*) across the Hauraki Gulf and Stewart Is populations of both species, and (ii) in the timing of sex reversal (*O. pullus*) across the Hauraki Gulf, D'Urville Is, and Stewart Is populations. Populations used in the analysis were those displaying reproductively active females for estimation of maturation schedules at the time of sampling, and those including transitional individuals (undergoing functional female-to-male sex reversal, see Chapter 3 for histological diagnosis) for examination of the timing of sex change. The slope of the thermal reaction norm for size- and age-at-maturity and -at-sex change was assessed by plotting the relationship between size-at-maturity (parameter L_{50}) or -at-sex change (parameter L_{sc50}) and age-at-maturity (parameter T_{50}) or -at-sex change (parameter T_{sc50}). Comparison of 95% confidence intervals has been shown to provide comparatively more conservative results relative to standard significance testing methods (Schenker and Gentleman, 2001).

4.3 Results

Size, age, and growth

Examination of the relationship between size and age in six populations of *Odax pullus* and in six populations of *Notolabrus fucicola* across New Zealand revealed a large amount of variation in the form of growth within both study species (Fig. 4.3). Variation in the form of growth was observed primarily in terms of: (i) the steepness of the ascending part of the growth trajectory, (ii) asymptotic body size achieved, and (iii) maximum age. The form of growth of *O. pullus* ranged from an asymptotic (determinate) form in the northern populations of Karikari and Hauraki Gulf, where individuals grew fast initially before reaching asymptotic size within the first 40 to 50% of the life span, to an indeterminate form of growth at Stewart Is, where individuals grow more slowly to reach maximum body sizes at ~75% of the life span. In contrast, *N. fucicola* showed an indeterminate form of growth that was relatively consistent across populations sampled, although individuals sampled in the Hauraki Gulf and at D'Urville Is showed comparatively more determinate forms of growth,

with growth rates declining at an earlier age than those at other locations. In *O. pullus*, maximum body size recorded across populations sampled ranged between a minimum of 450 mm FL in Karikari to a maximum of 554 mm FL in Fiordland, while in *N. fucicola,* maximum body size recorded in the samples varied between a minimum of 374 mm FL at the Three Kings Is and a maximum of 487 mm FL in the Hauraki Gulf (Fig. 4.4). These patterns were associated with variation in maximum age across locations sampled. Maximum age recorded for *O. pullus* varied from 10 years at the most northern location sampled (Karikari Peninsula) to 19 years at the most southern location sampled (Stewart Island), showing a two-fold increase in the duration of the maximum life span in individuals sampled at higher latitudes (Fig. 4.5). A similar pattern of increase in maximum age with latitude was found in *N. fucicola*, with maximum ages found ranging between 17 years in the north (Hauraki Gulf) and 26 years in the south (Fiordland) (Fig.4.5). These results indicate the presence within both study species of variation across populations sampled in terms of: (i) growth rate, (ii) adult body size, (iii) longevity, and (iv) the relationship between growth rate, body size and age.

No differences in growth were found between the sexes in any of the populations sampled, in both *O. pullus* and *N. fucicola*. With one exception, for both species and across all locations, the oldest, largest (in fork length) and heaviest (in gutted weight) individuals sampled were consistently female. The exception was in the Hauraki Gulf, where the largest *O. pullus* individual sampled was male (Figs. 4.4 & 4.5).

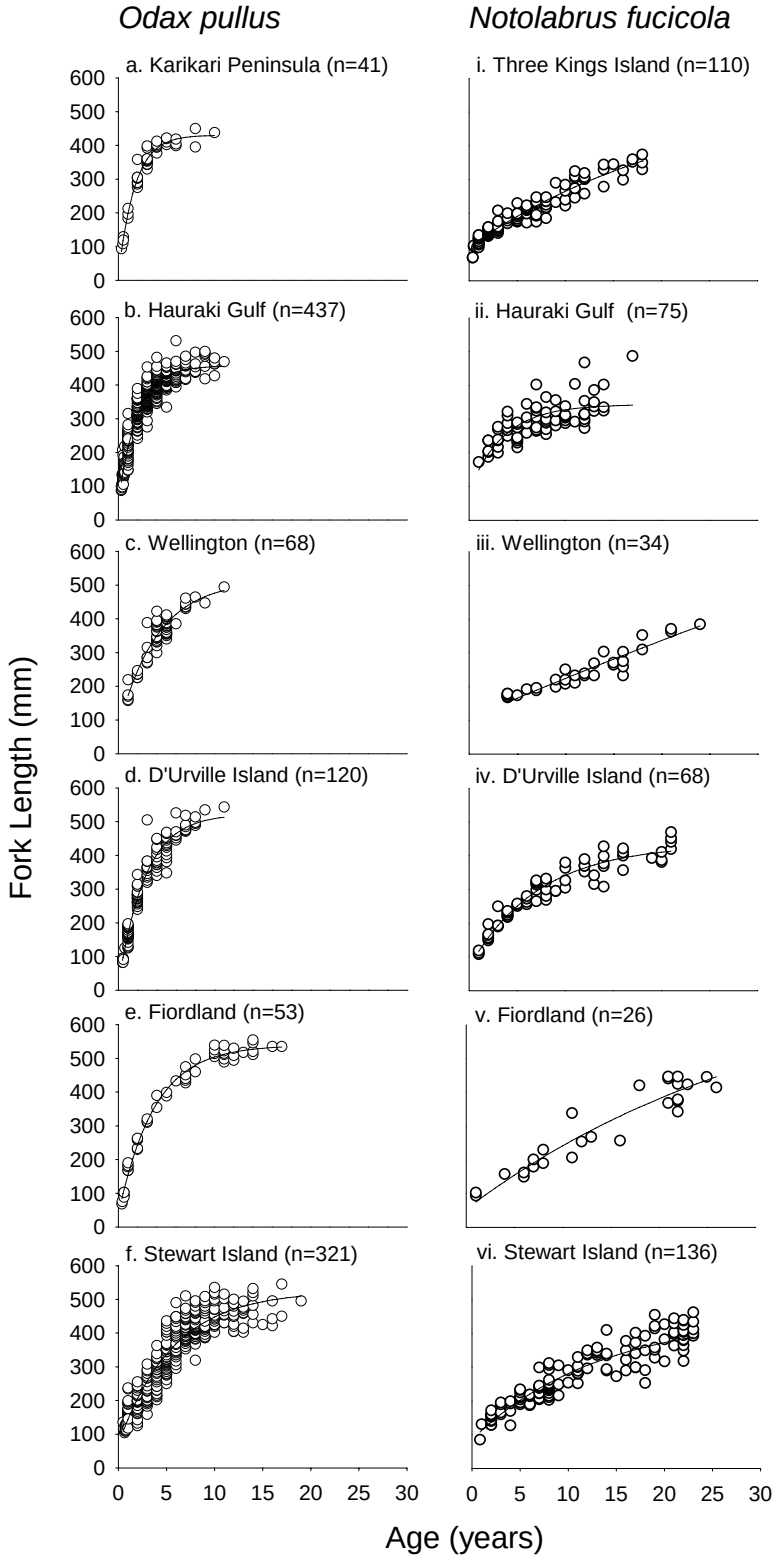

Fig. 4.3: Growth of *Odax pullus* (left panel) and *Notolabrus fucicola* (right panel) across New Zealand. Observed individual size-at-age estimates (open circles) are fitted with the re-parameterized equation of the von Bertalanffy Growth Function (Francis 1988) (solid line).

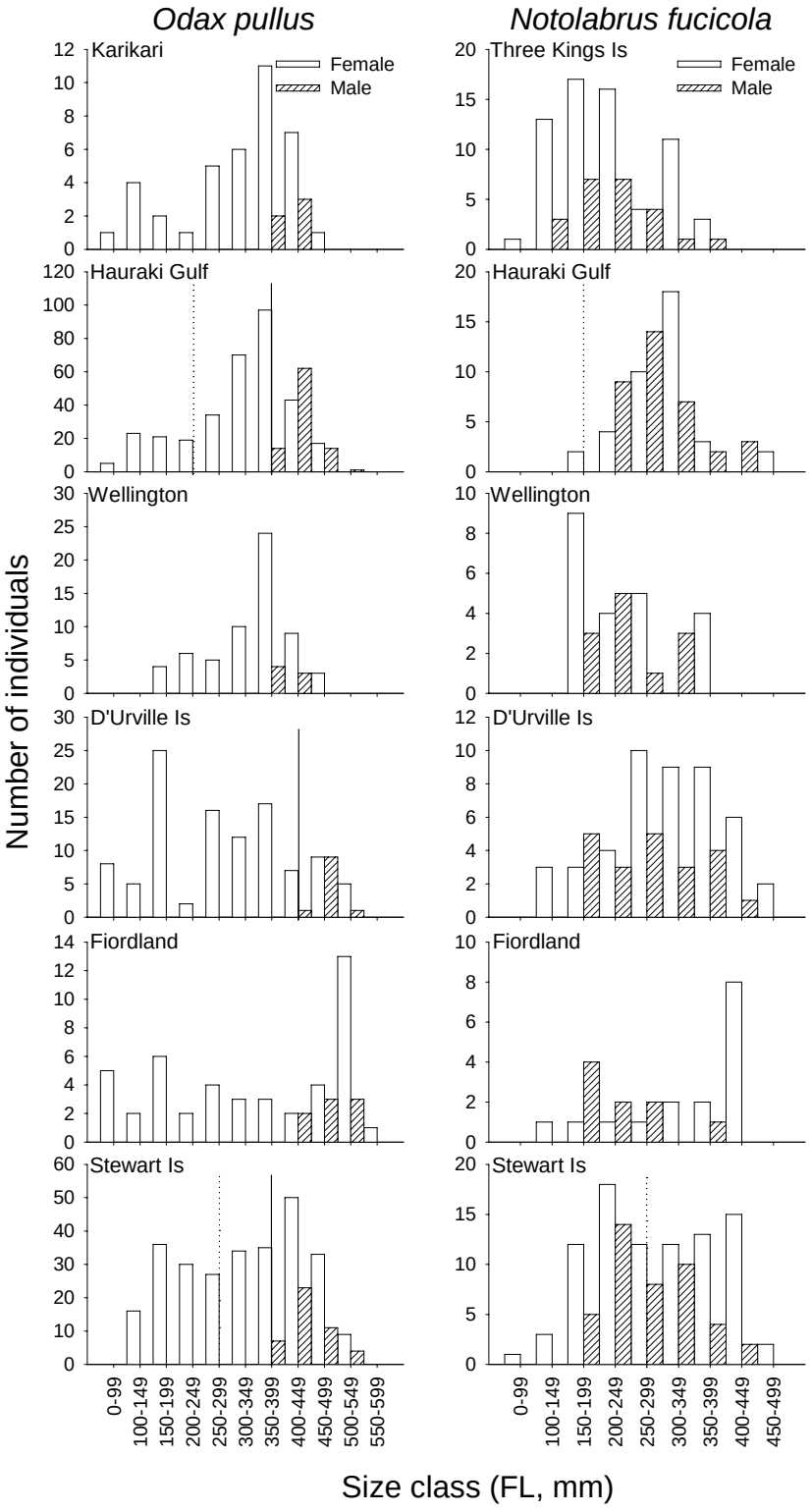

Fig. 4.4: Sex-specific size distribution of *Odax pullus* and *Notolabrus fucicola* across New Zealand, showing number of males (grey bars) and females (white bars) sampled at each location. Dotted line shows age-at-50% female maturity, and solid line shows age-at-50% sex change in *O. pullus*. Note changes in the scale bars. Transitional and bisexual *O. pullus* individuals were excluded; similarly, *N. fucicola* individuals that were identified macroscopically as immature were excluded.

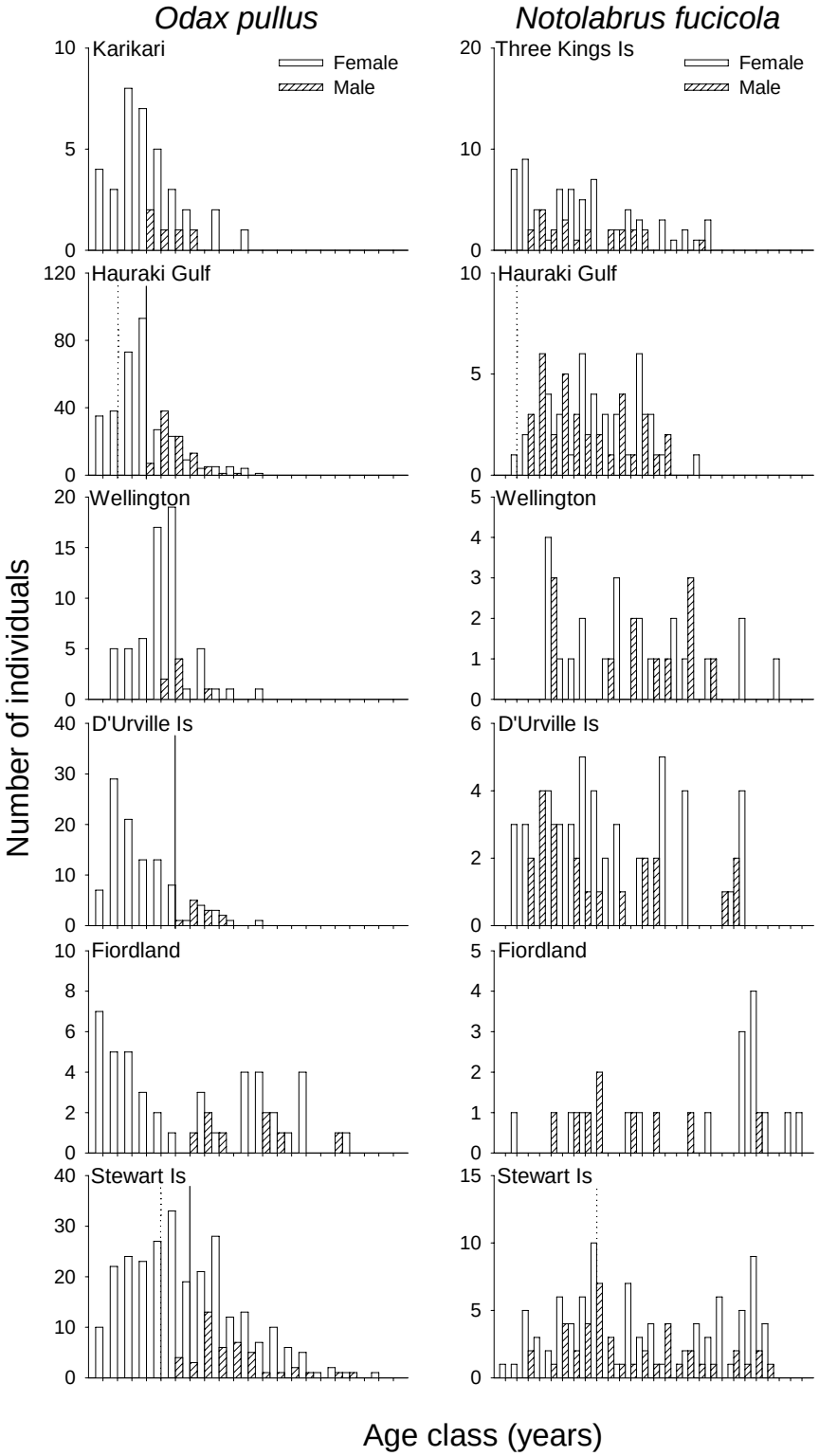

Fig. 4.5: Sex-specific age distribution of *Odax pullus* and *Notolabrus fucicola* across New Zealand, showing number of males (grey bars) and females (white bars) sampled at each location. Dotted line shows age-at-50% female maturity, and solid line shows age-at-50% sex change in *O. pullus*. Note variations in the scale bars. Transitional and bisexual *O. pullus* individuals were excluded; similarly, *N. fucicola* individuals that were identified macroscopically as immature were excluded.

Geographical variation in growth, body size, longevity, and development

PCA ordination of populations sampled across New Zealand confirmed the presence of differences in life history (growth rate, body size, longevity, development rate) across locations within both study species (Fig. 4.6). In both *O. pullus* and *N. fucicola*, locations appeared spread along an overall North-South gradient, from the northern locations of Karikari and the Hauraki Gulf to the southern locations of Fiordland and Stewart Is. Locations showed some spread however, with D'Urville Is and Fiordland separating from the other four locations in *O. pullus*, and Wellington and D'Urville Is separating from the other three locations in *N. fucicola*. The slanted direction of the North-South gradient on the two PCAs indicated that both PC1 and PC2, which together captured 90.8% and 96.2% of the variation in life histories of *O. pullus* and *N. fucicola* respectively, contributed to explaining the patterns of variation in life histories along this gradient. In both species however, PC1 was the primary contributor to explaining the variation across locations (*O. pullus*: 56.2%; *N. fucicola*: 63.6%; Table 4.6).

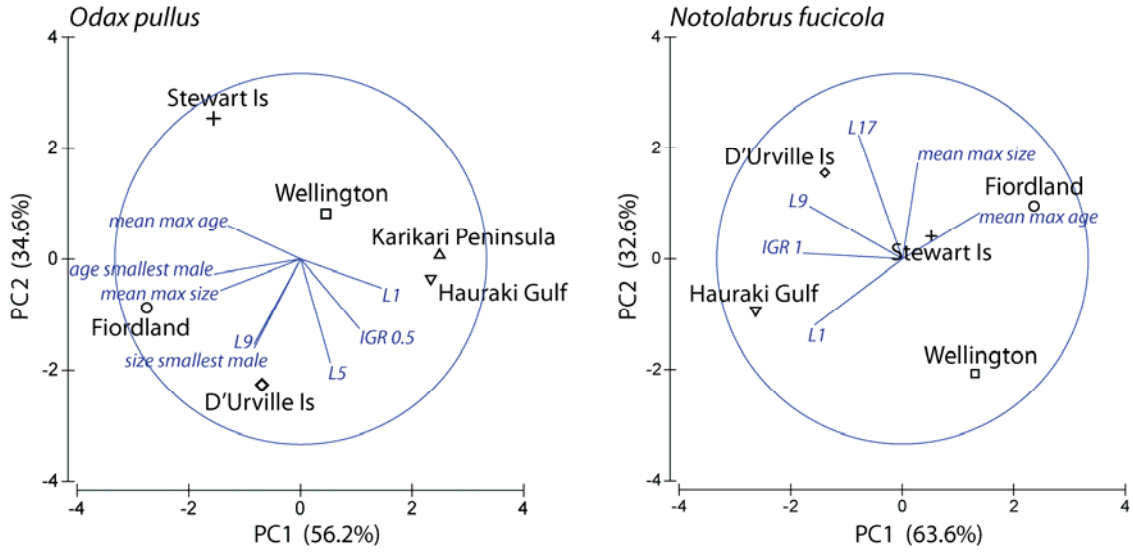

Fig. 4.6: Ordination of life history parameters of populations sampled of *Odax pullus* and *Notolabrus fucicola* across New Zealand using Principal Component Analysis (PCA), showing the direction (eigenvectors) and contribution (relative length of eigenvectors) of the life history variables. Mean max age: longevity; mean max size: adult body size; IGR $_{0.5}$: growth rate-at-age 6 months; IGR $_{1}$: growth rate-at-age 1 year; L1, L5, L9 and L17: mean size-at-age 1, 5, 9, and 17; size and age of smallest male: timing of sex change (as a proxy for development rate). Vector length in relation to circle radius illustrates the proportion of the variation in a given life history variable that is explained by the two principal components plotted (PC1 and PC2); specifically, circle radius indicates vector length of 1 if 100% of the variation in a given life history variable was explained by PC1 and PC2.

In *O. pullus*, the separation across locations along PC1 was best explained by variation in mean maximum age (longevity), mean maximum size (adult body size), size-at-age one, growth rate-at-age 6 months, and age of the smallest male (as a proxy for age-at-stage). PC1 was negatively correlated with longevity, adult body size, and age-at-sex change, and positively correlated with size-at-age one (L1) and growth rate ($IGR_{0.5}$), suggesting that greater maximum ages and greater maximum sizes were associated with reduced early growth and greater age-at-sex change. Locations further separated along PC2, which correlated negatively with size-at-age five (L5), size-at-age nine (L9), and with size of the smallest male (as a proxy for size-at-stage). These results suggest the presence of two groupings in the life history variables, with size-at-age one, longevity, maximum size, and age-at-stage (*i.e.* age-at-maturity or -at sex change) on the one hand, and size-at-age five, nine, and size-at-stage (*i.e.* size-at-maturity or -at sex change) on the other hand, and that these two groupings underlay the separation of the locations in two different directions along PC1 and PC2. Growth rate-at-age six months correlated with both PC1 and PC2 however, suggesting a contribution of growth rate to explaining the differences across locations along both principal axes. Reduced growth correlated with increased longevity, greater maximum body size and increased age-at-stage along PC1, and with smaller size-at-age five, nine and smaller size-at-stage along PC2.

A similar pattern was found in *N. fucicola*, with separation of locations sampled along PC1 correlated with changes in mean maximum age (longevity), size-at-age one (L1), size-at-age nine (L9), and growth rate-at-age one (IGR_1). PC1 was positively correlated with longevity and negatively correlated with size-at-age one, size-at-age nine and growth rate, indicating that longer life spans were associated with reduced early growth and decreased body sizes at the ages of one and nine years. Groupings of life history variables that underlay the separation of locations along PC1 and PC2 resembled that seen in *O. pullus*, with size-at-age one, nine, growth rate, and longevity separating along PC1, and size-at-age seventeen and maximum size separating locations along PC2. *N. fucicola* differed from *O. pullus*, however, in that mean maximum size primarily underlay differences across locations along PC2. PC2 was positively correlated with both mean maximum size and size-at-age seventeen.

Together these results suggested two points. First, longevity, early growth rate, and size-at-age one appeared as the primary drivers underlying the variation in life histories across locations sampled in both study species (separation along PC1). In *O. pullus*, extended

longevities and reduced growth rates were also associated with greater adult body sizes. Second, locations appeared to separate along a secondary axis (PC2), which was explained by changes in body size at intermediate ages (5 and 9 years in *O. pullus*) and in size-at-age 17 and adult body size in *N. fucicola*.

In *O. pullus*, the optimal combination of environmental variables that underlay the patterns of variation in life histories across locations was temperature alone (rank correlation coefficient of $\rho = 0.59$; Table 4.6), although the relationship between the life history variables and temperature was not significant ($p = 0.19$; Table 4.6). The lack of significance of the rank correlation is likely to result from the low number of sampled locations (six), as this suggests that the test is of little power to detect even quite large effects. It is likely that the correlation coefficient value ρ of nearly 0.6 would have indicated a strong relationship were it to have been maintained for a larger number of sites (Clarke, pers. comm.). The next ten best combinations of environmental variables were examined, and the second best subset of environmental variables explaining the patterns of variation in life history of *O. pullus* was identified as a combination of temperature and habitat ($\rho = 0.55$; Table 4.6). Temperature was found to contribute in 80% and habitat in 60% of the first ten best combinations to explaining the patterns of variation in life histories across locations. In contrast, abundance and exposure contributed by 30%, and fishing effort did not contribute to any combination of environmental variables, suggesting temperature and habitat as the environmental variables that best explained the patterns of variation in life histories across latitudes sampled.

In *N. fucicola*, the optimal combination of environmental variables that underlay the patterns of variation in life histories across locations was a combination of temperature and habitat ($\rho = 0.39$; Table 4.6), although the relationship between the life history variables with temperature and habitat was not significant ($p = 0.57$; Table 4.6). As suggested for *O. pullus*, it is likely that the lack of significance of the test may be explained by the small number of locations sampled (five), which provides little power for the analysis. Examination of the direction (Fig. 4.7) and gradient (Fig. 4.8) of temperature and habitat in both *O. pullus* and *N. fucicola* supports the results of the analyses, and suggest that the rank correlation coefficients between the life history and environmental variables would have indicated a significant relationship between the two matrices for a greater number of locations sampled. The next ten best combinations of environmental variables were examined, and the second best subset of environmental variables identified for *N. fucicola* was a combination of temperature and

abundance (ρ = 0.212; Table 4.6). As seen in *O. pullus*, temperature showed the highest contribution to explaining the patterns of variation in life history in *N. fucicola*, with 70% of the first ten optimal combinations of environmental variables including temperature. Abundance contributed to 60% of combinations, while habitat and exposure contributed by 40%, suggesting that temperature and abundance together provide the best explanatory environmental variables for the patterns of variation in life histories in *N. fucicola* across locations sampled.

These results suggest four key points: (1) in both study species, temperature contributed the most to explaining the patterns of variation in life histories across locations sampled; (2) habitat availability and abundance both contributed to explaining the variation in life histories across locations; (3) there was little effect of exposure on the patterns of variation in life histories in both species; and (4) fishing effort did not contribute to explaining the patterns of variation in life history of *O. pullus* across locations.

Table 4.6: Results of global BEST test, showing the first two best single (or combination of) environmental variable(s) that correlate(s) with the patterns of variation in life history in *Odax pullus* and *Notolabrus fucicola* across locations sampled. Estimate of the optimal match between the biological and environmental variables is based on rank correlation coefficient ρ (Rho statistic). *p* values were computed from 9999 permutations. SST is mean annual Sea Surface Temperature.

	Odax pullus		*Notolabrus fucicola*	
Best subset	Variable(s)	ρ	Variable(s)	ρ
1	SST	0.585 (p = 0.19)	SST, Habitat	0.394 (p = 0.57)
2	SST, Habitat	0.546	SST, Abundance	0.212

Examination of the direction of the temperature, habitat, and abundance vectors on the ordination of the life history variables across locations indicated that in both *O. pullus* and *N. fucicola* temperature underlay the separation of the locations along a North-South gradient, from Karikari and the Hauraki Gulf to Stewart Is in *O. pullus* (from right to left on Fig. 4.7), and, similarly, from the Hauraki Gulf to Stewart Is and Fiordland in *N. fucicola* (from left to right on Fig. 4.7). Examination of the temperature gradient on the ordination plot confirmed that locations were ordinated from warmest to coldest temperatures in both species (Fig. 4.8). In both cases, the temperature vector primarily aligned with PC1 (Fig. 4.7), suggesting that increasing temperatures positively correlated with higher growth rates (IGR 0.5 and IGR 1)

and greater size-at-age one (L1), and negatively correlated with longevity (mean maximum age) (Fig. 4.8). In *O. pullus*, increasing temperatures further correlated with decreasing adult body size (mean maximum size) and reduced age-at-stage (Fig. 4.8). Overall, lower temperature locations were associated with reduced growth rate in the early stages of the life span and with greater longevities in both *O. pullus* and *N. fucicola*, and this was associated with greater adult body size (mean maximum size) and delayed age-at-stage (delayed development) in *O. pullus*.

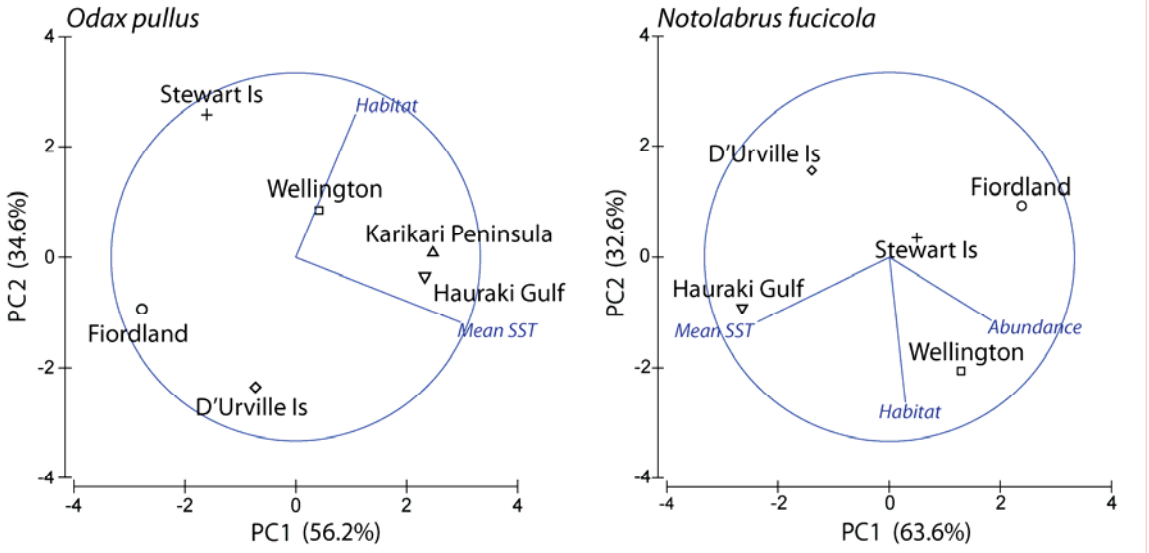

Fig. 4.7: PCA ordination of life history parameters of *Odax pullus* and *Notolabrus fucicola* populations sampled across New Zealand, showing the direction (vectors) and contribution (relative length of the vectors) of the best explanatory environmental variables underlying variation in life histories across locations. Vector length is Spearman's correlation coefficient from rank correlation analysis between environmental and life history resemblance matrices. Circle radius indicates correlation coefficient of 1.
Mean SST: mean annual sea surface temperature (^{o}C); Habitat: total % occurrence of macroalgal species (*Ecklonia radiata*, *Lessonia variegata*, *Carpophyllum maschalocarpum*, *C. flexuosum*, *Macrocystis boryana*); Abundance: density of conspecifics (indiv/300m^2).

In contrast, environmental vectors of habitat (in both *O. pullus* and *N. fucicola*) and abundance (*N. fucicola* only) primarily aligned with PC2 (Fig. 4.7). This suggested that habitat (and abundance) separated the locations along an axis perpendicular to that of temperature, and that these environmental factors contributed to the separation of D'Urville Is and Fiordland in *O. pullus*, and to the separation of D'Urville Is and Wellington in *N. fucicola* (Fig. 4.7). Examination of the gradient in habitat availability on the ordination plots suggested that, in *O. pullus*, D'Urville Is and Fiordland separated from the other four

locations as a result of comparatively lower occurrences of preferred habitat (Fig. 4.8). Similarly, in *N. fucicola* Wellington and D'Urville Is appeared to separate from the other three locations as a result of lower % occurrences of habitat in D'Urville Is and of higher % occurrences of habitat in Wellington (Fig. 4.8). Decreasing availability of preferred habitat appeared to be correlated with increasing size-at-age five (L5) and nine (L9) and with size of the smallest male (size-at-sex change) in *O. pullus*, and, similarly, with increasing size-at-age nine (L9) and seventeen (L17) and mean maximum size (adult body size) in *N. fucicola* (Fig. 4.8).

In both study species, however, habitat availability and abundance were correlated (Pearson's correlation coefficients; *O. pullus*: R = 0.82; *N. fucicola*: R = 0.76), with the abundance of *O. pullus* and *N. fucicola* increasing linearly with the presence of macroalgae (*Ecklonia radiata*, *Lessonia variegata*, *Carpophyllum maschalocarpum*, *C. flexuosum*, *Macrocystis boryana*). This indicates that abundance patterns are likely to underlie (or at least contribute to) the effect of habitat availability on the ordination of the life history variables across locations sampled in both study species. Habitat and abundance vectors aligned primarily with PC2, and suggested that environments of reduced habitat availability and/or of reduced conspecific abundance were correlated with increased body size-at-ages five and nine (*i.e.* a comparatively more asymptotic form of growth), and larger size-at-sex change in *O. pullus*, and with increased size-at-ages nine and seventeen and mean maximum sizes in *N. fucicola*.

Overall, biota-environment linkage analysis of the patterns of variation in life history of *O. pullus* and *N. fucicola* across latitudes in relation to changes in temperature, abundance, exposure, habitat availability, and fishing effort, suggested that (1) temperature, habitat and/or abundance best explained the variation in life histories across populations, (2) exposure had little effect, and there was no effect of fishing in *O. pullus* on the patterns of variation in life history across locations, and (3) that the response of life history variables across the latitudinal gradient sampled was consistent across the two study species. Furthermore, life histories appeared to vary over two spatial scales: with temperature on a broad latitudinal scale, and with habitat and abundance patterns on a local scale; the latter suggesting region-specific patterns in algal community structure. Environmental temperature appeared as the primary driver underlying the differences in life histories across locations, and primarily affected early growth rate, size-at-age one and longevity, as well as age-at-

stage and maximum body size in *O. pullus*, with higher latitudes (colder temperatures) showing slower growth rates, increased life spans, greater maximum sizes, and later age-at-stage (delayed sexual development). Habitat availability and abundance patterns appeared as secondary drivers, underlying separation of locations along an axis perpendicular to that of temperature, and primarily affected size-at-stage (development) and size-at-intermediate ages, individuals achieving larger size-at-ages 5 and 9 (*O. pullus*), and 9 and 17 (*N. fucicola*) in conditions of lower conspecific abundance or reduced habitat availability. In. *O. pullus*, lower abundances were further associated with larger size-at-sex change.

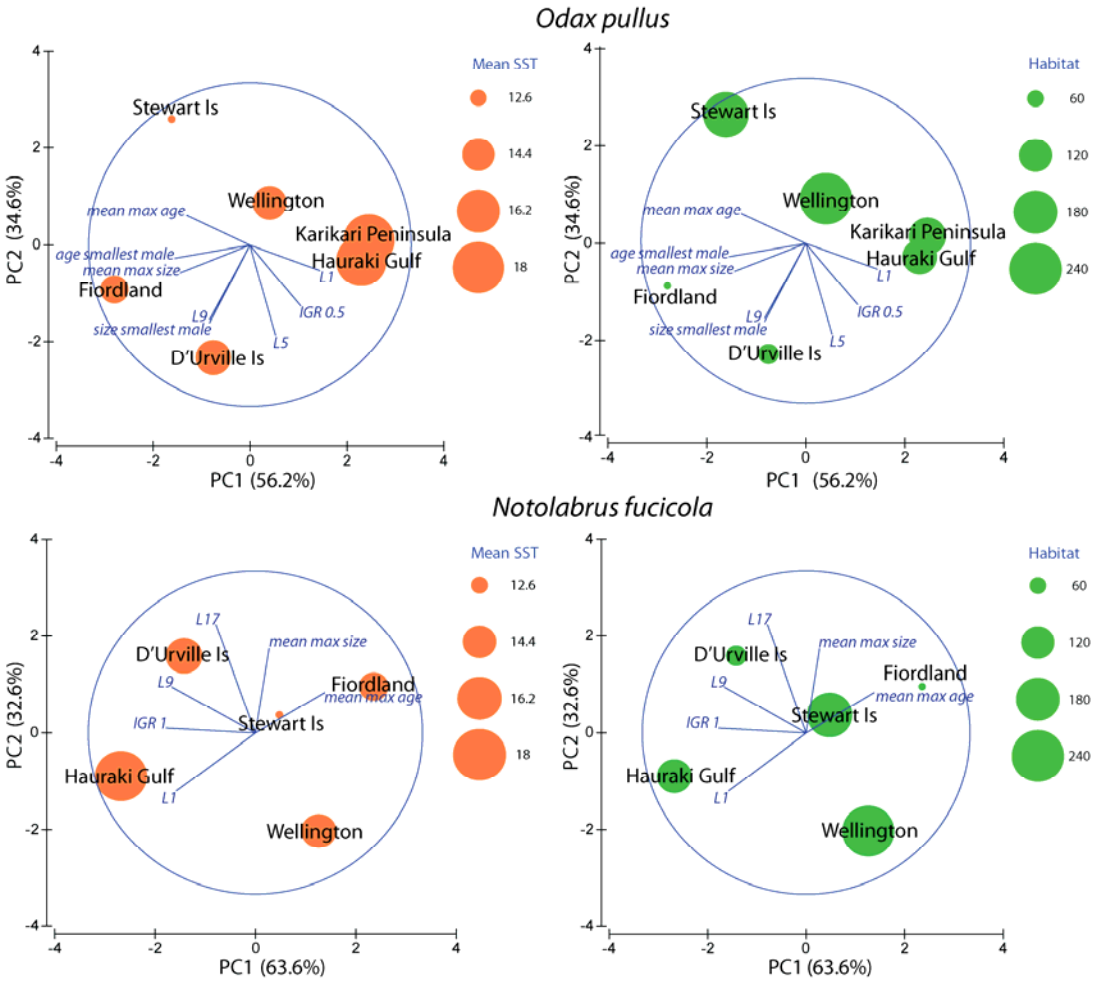

Fig. 4.8: PCA ordination of life history parameters of *Odax pullus* and *Notolabrus fucicola* across locations sampled, showing eigenvectors of life history variables and the shape of the environmental gradients in temperature (Mean SST; left panel) and habitat (right panel). Bubble size represents gradient from lowest to highest values of temperature (^{o}C) and habitat availability (% occurrence of the following macroalgal species: *Ecklonia radiata*, *Lessonia variegata*, *Carpophyllum maschalocarpum*, *C. flexuosum*, *Macrocystis boryana*). Vectors indicate direction and contribution of each life history variable to the ordination of locations sampled.

Environmental temperature and body size, longevity, development, and growth rate

Body size and longevity

Examination of the relationship between sea surface temperature (SST) and size-at-age one (*L(1)*), mean adult body size (L_{max}) and longevity (T_{max}) revealed trends of increasing size-at-age one, decreasing adult body size and decreasing longevity with increasing temperature, and these patterns were consistent across both *O. pullus* and *N. fucicola*. Temperature explained 94 and 42% of the variation in size-at-age one (as a proxy for mean overall growth undertaken over the first year of life), 47 and 35% of the variation in mean maximum size, and 53% and 83% of the variation in longevity across latitudes in *O. pullus* and *N. fucicola*, respectively (Fig. 4.9). There was a significant positive linear relationship between mean size-at-age one and temperature in *O. pullus*, with individuals displaying a larger size-at-age one at warmer locations, and a significant negative linear relationship between longevity and temperature in *N. fucicola* indicating that longevity decreased linearly with increasing temperature across the latitudinal gradient sampled. These trends were consistent across the two study species, although the relationship between temperature and mean size-at-age one, adult body size and longevity was not significant in *N. fucicola* (Fig. 4.9 b), both *O. pullus* (Fig. 4.9 c) and *N. fucicola* (Fig. 4.9 d) and *O. pullus* (Fig. 4.9 e), respectively. These analyses, however, were performed with low statistical power (33, 38, 26 and 44%; Fig. 4.9) associated with a small sample size of six locations.

Overall, these results suggest a pattern of reduced growth, larger adult body size, and increased longevity at colder temperatures (higher latitudes), and that this pattern is consistent between *O. pullus* and *N. fucicola*.

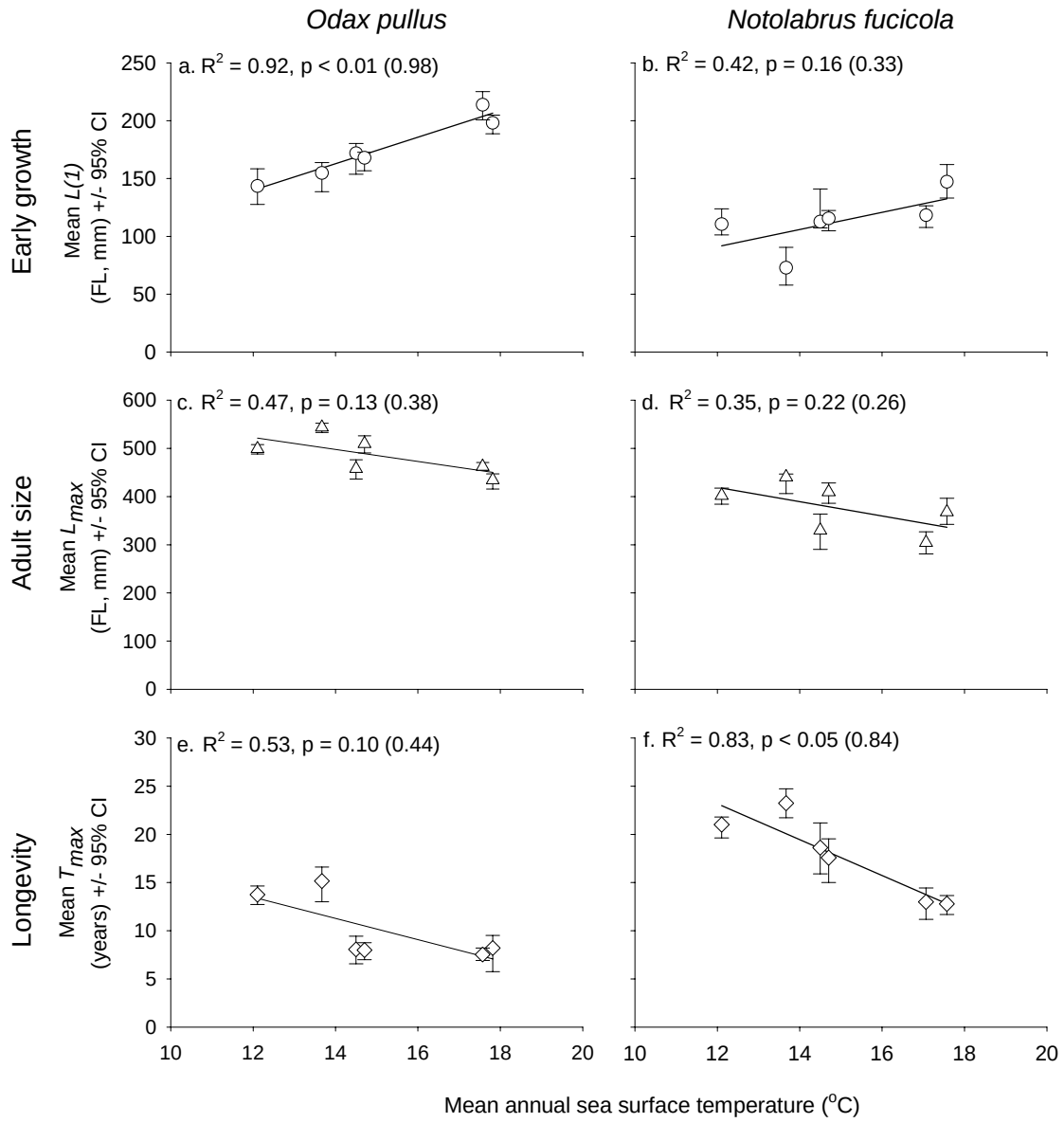

Fig. 4.9: Variation in (a, b) size-at-age one *L(1)*, (c, d) adult body size L_{max} and (e, f) longevity T_{max} with mean annual sea surface temperature in *Odax pullus* and *Notolabrus fucicola* across New Zealand. Mean size-at-age one is best-fit rVBGF (re-parameterized von Bertalanffy Growth Function) parameter. Adult body size and longevity are mean maximum size and age, based on the 10% (*O. pullus*) and 25% (*N. fucicola*) largest and oldest individuals, respectively. Means are presented with 95% percentile confidence intervals on bootstrapped variance estimates (CI). Data are fitted with least-squares regressions:
(a) $y = 11.48\ (\pm\ 1.47) * \mathrm{x} + 2.15\ (\pm\ 22.24)$; (b) $y = 7.45\ (\pm\ 4.38) * \mathrm{x} + 1.58\ (\pm\ 66.01)$; (c) $y = -12.90\ (\pm\ 6.82) * \mathrm{x} + 672.85\ (\pm\ 103.61)$; (d) $y = -11.29\ (\pm\ 7.78) * \mathrm{x} + 577.67\ (\pm\ 117.05)$; (e) $y = -1.10\ (\pm\ 0.52) * \mathrm{x} + 26.69\ (\pm\ 7.92)$; (f) $y = -1.86\ (\pm 0.42) * x + 45.50\ (\pm 6.26)$. Results of regression analyses are presented on each figure with coefficient of determination (R^2), significance level at $\alpha = 0.05$ (p), and result of power analysis on the correlation coefficient at $\alpha_{0.05}$ for sample size of 6 locations (in brackets).

Size- and age-at-maturity

In *O. pullus*, 50% of females in the Hauraki Gulf were sexually mature at 240.7 mm FL [95% percentile CI 228.7 – 264.8], and at 1.2 years [1.1 – 1.5]. At Stewart Is, 50% of *O. pullus* females were sexually mature at 252.1 [246.4 – 264.7] mm FL in body size, and at 3.9 [3.6 – 4.3] years of age. Comparison of variance estimates around the parameter values of size-at-maturity (L_{max}) across populations suggested that females matured at similar body sizes across the two geographically separated locations, ranging between 49.4 and 57.3% of mean maximum body size (Fig. 4.10 A). In contrast, comparison of the variance associated with parameters of age-at-maturity (T_{max}) amongst the two populations revealed that females matured significantly later in the southern location of Stewart Is (26.2 – 31.3% of mean maximum age) relative to those living in the northern location of the Hauraki Gulf (14.6 – 19.9% of mean maximum age) (Fig. 4.10 A).

In contrast, comparison of size- and age-at-maturity of *N. fucicola* from the Hauraki Gulf and Stewart Is, suggested that females matured at significantly larger body sizes and significantly older ages in the southern location of Stewart Is than in the northern location of the Hauraki Gulf (Fig. 4.10 B). 50% of *N. fucicola* females in the Hauraki Gulf were sexually mature at 199.0 mm FL [136.6 – 165.0], and at 1.5 years [1.4 – 1.6], while 50% of *N. fucicola* females in Stewart Is were sexually mature at 250.0 mm FL [225.0 – 272.9], and at 8.3 years [7.3 – 8.7]. Relative size- and age-at-maturity of *N. fucicola* differed between the two locations, and increased from 37.1 – 44.9% of mean maximum size and 10.9 – 12.5% of mean maximum age in the Hauraki Gulf, to 56.0 – 67.9% of mean maximum size and 34.7 – 41.4% of mean maximum age in Stewart Is.

Differing maturation schedules between the Hauraki Gulf and Stewart Is were not associated with intraspecific variation in the patterns of reproductive growth across the two locations within either *O. pullus* or *N. fucicola* (Fig. 4.11). There was no difference between the Hauraki Gulf and Stewart Is in the relationship between ovary weight and female body size of reproductively active females, suggesting no difference in the amount of energy being allocated to reproductive growth for any given size across the two locations. This in turn suggests the absence of a compensatory mechanism in terms of fecundity or reproductive output as a result of delayed sexual maturation.

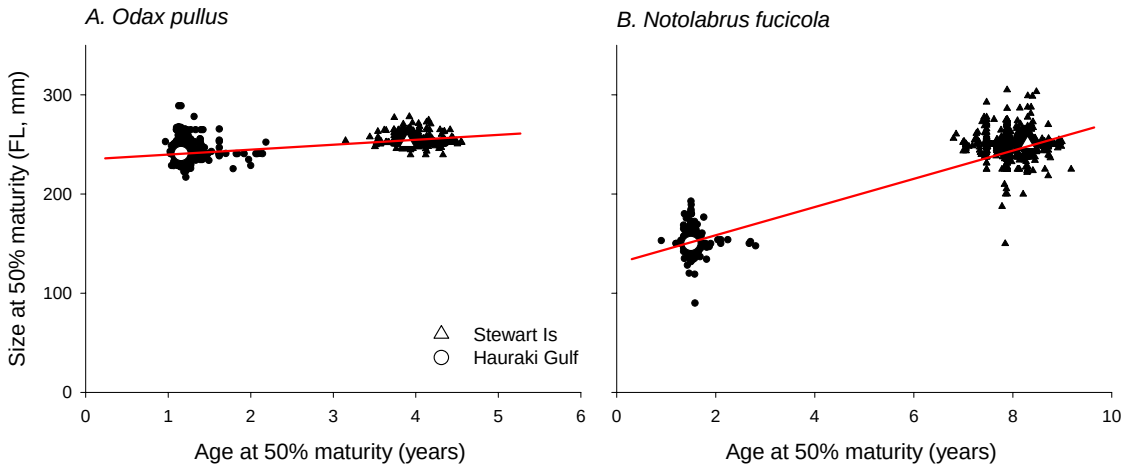

Fig. 4.10: Relationship between size and age at female maturity in (A) *Odax pullus* and (B) *Notolabrus fucicola* across New Zealand (NZ) populations of the Hauraki Gulf (northern NZ) and Stewart Island (southern NZ), showing the thermal reaction norm for size- and age-at-maturity (solid red line). White symbols show bias-adjusted mean parameter values, and black circles (Hauraki Gulf) and triangles (Stewart Island) show bootstrapped variance estimates around each parameter. The relationships between size- and age-at-maturity (thermal reaction norms) are described as: (A) $y = 4.161x + 235.89$; and (B) $y = 14.704x + 127.92$.

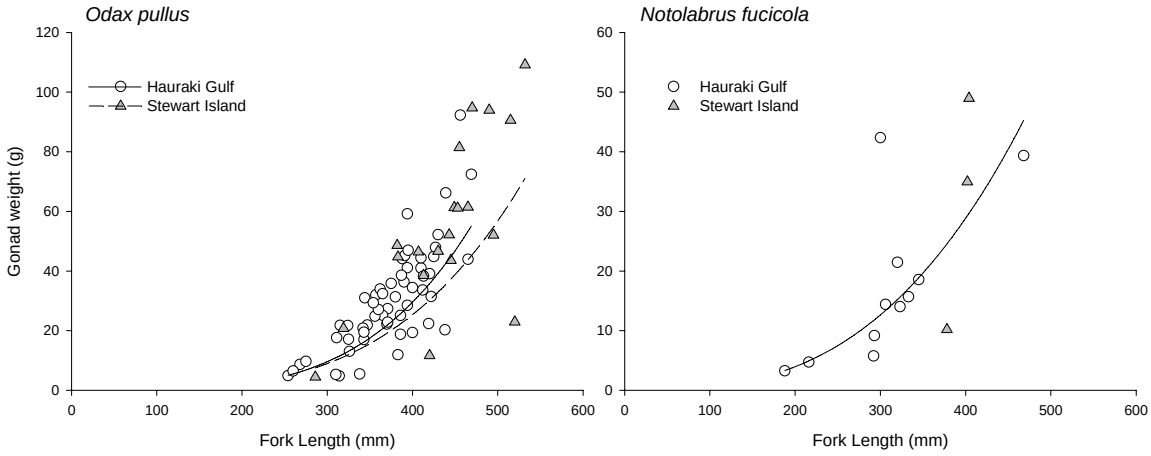

Fig. 4.11: Relationship between ovary weight (as a proxy for reproductive effort) and female body size of reproductively active female *Odax pullus* and *Notolabrus fucicola* in the Hauraki Gulf and Stewart Is.
Solid line represents best-fit exponential regression lines for each location. *O. pullus* Hauraki Gulf: $y = 2^{-9} * x^{3.908}$, $R^2 = 0.65$; Stewart Is: $y = 1^{-8} * x^{3.614}$, $R^2 = 0.53$. *N. fucicola* Hauraki Gulf: $y = 1^{-6} * x^{2.867}$, $R^2 = 0.67$; Stewart Is: no regression line fitted.

Size- and age-at-sex change

A total of eight transitional individuals (undergoing functional female-to-male sex reversal) were found in *O. pullus* at three of the sampling locations, the Hauraki Gulf (2 transitional individuals), D'Urville Is (2) and Stewart Is (4). The schedules of sex change were estimated for the corresponding three *O. pullus* populations.

Mean body sizes of transitional individuals ranged between 369 (+/- 10 SE) mm FL in the Hauraki Gulf, to 446 (+/- 22 SE) mm FL in D'Urville Is, and 416.5 (+/- 34 SE) mm FL in Stewart Is, and there was no difference in body size of transitional individuals across locations (ANOVA, $F_{2,5} = 1.01$, $p = 0.42$; Fig. 4.12 A). This result coincided with that found when comparing parameter and associated variance estimates of size-at-50% sex change L_{sc50} across all three populations (Fig. 4.12 B). 50% sex change was estimated to occur at 398.1 mm FL [95% percentile CI 392.1 – 456.5] in the Hauraki Gulf, 402.3 mm FL [382.2 – 452.8] in D'Urville Is, and 397.1 mm FL [387.1 – 434.7] in Stewart Is, which corresponded to 84.8 – 98.7%, 75.0 – 88.8%, and 77.6 – 87.1% of mean maximum size in the Hauraki Gulf, D'Urville Is, and Stewart Is, respectively, suggesting a similar relative size-at-sex change across locations (ranging between 75 – 99% of mean maximum size).

In contrast, there were significant differences in the age at which sex reversal occurred across the three geographically separated locations. Mean age of transitional individuals was significantly lower in the Hauraki Gulf (2.5 +/- 0.5 SE years) than in Stewart Is (7 +/- 0.9 years), and D'Urville Is individuals (5 +/- 0 SE years) changed sex mid-age range between the Hauraki Gulf and Stewart Is (ANOVA, $F_{2,5} = 6.52$, $p < 0.05$; Fig. 4.12 A). This result coincided with that found when comparing parameter and associated variance estimates of age-at-50% sex change T_{sc50} across all three populations (Fig. 4.12 B). 50% sex change was estimated to occur at 3.1 years [2.9 – 3.6] in the Hauraki Gulf, 5.1 years [4.9 – 5.6] in D'Urville Is, and 6.4 years [6.1 – 7.3] in Stewart Is, which corresponded to 38.7 – 48%, 61.9 – 70.7%, and 44.8 – 53.6% of mean maximum age in the Hauraki Gulf, D'Urville Is and Stewart Is, respectively, suggesting a higher relative age-at-sex change at D'Urville Is while Hauraki Gulf and Stewart Is individuals show similar relative age-at-sex change (38.7 – 53.6% of mean maximum age). There was no overlap in the associated variance around age-at-sex change across all three locations however, suggesting significant differences in the timing of sex reversal across all three locations, sex changing females changing sex later at higher latitudes (Fig. 4.12 B). These results suggest that, in *O. pullus*, sex changing females

delay sex reversal at higher latitudes, and change sex at similar body sizes across a range of latitudes. Examination of the relationship between size- and age-at-sex change showed no slope in the thermal reaction norm for size and age at sex change across populations sampled (Fig. 4.12 B; Simple linear regression: $R^2 = 0.01$, $p = 0.95$).

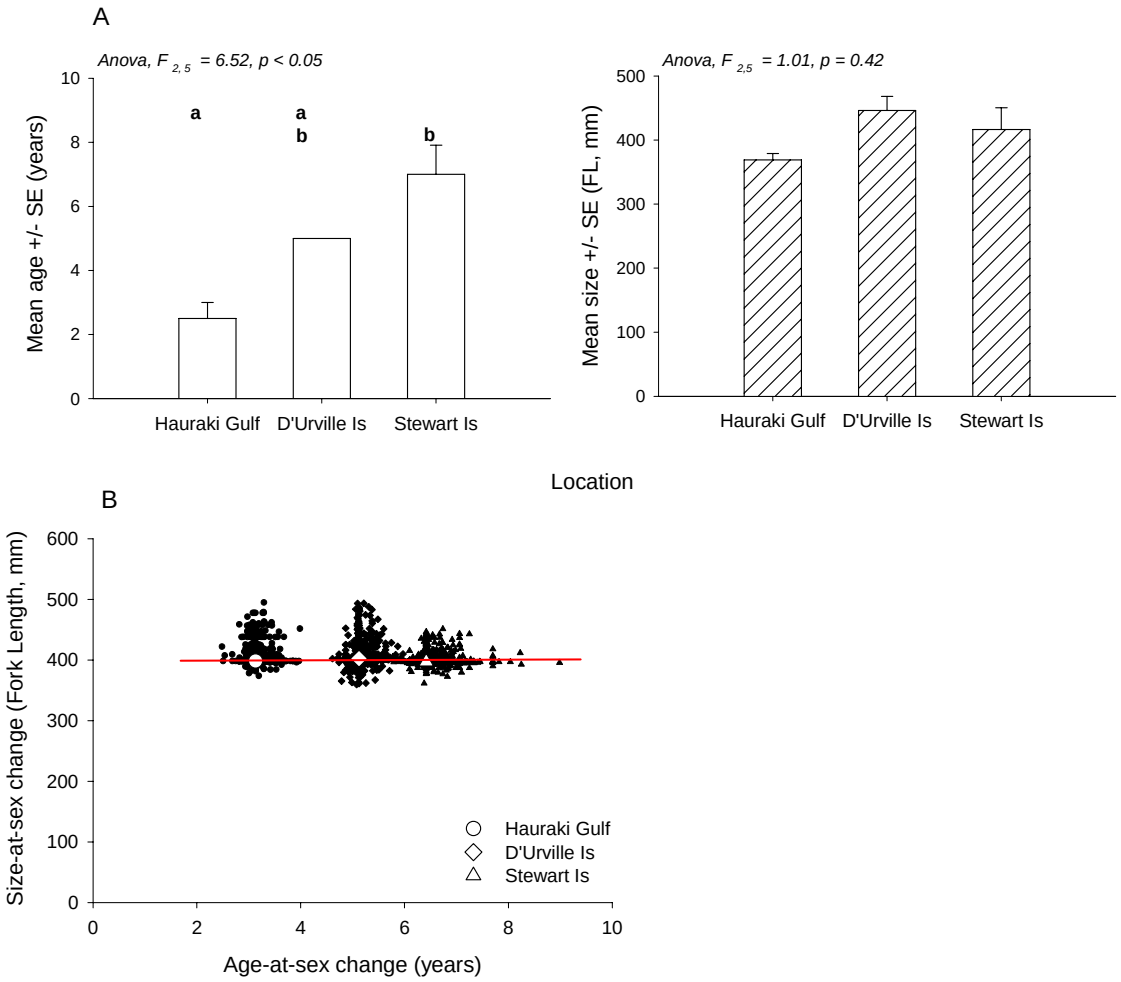

Fig. 4.12: Size- and age-at-sex change in three *Odax pullus* populations across New Zealand (Hauraki Gulf, D'Urville Island, and Stewart Island).
(A) Mean age and size of transitional individuals (undergoing female-to-male sex reversal as determined by histological analysis of gonad material), showing results of one-way ANOVA and homogeneous groupings (a, b) of post-hoc Tuckey Test. Open bars represent mean age of transitional individuals, and striped bars represent mean body size of transitional individuals.
(B) Relationship between size and age at sex reversal in *Odax pullus* across New Zealand, showing the thermal reaction norm for size- and age-at-sex change (solid red line). Open circles, diamonds, and triangles show bootstrapped variance estimates of parameters L_{sc50} (size-at-sex change) and T_{sc50} (age-at-sex change) for Hauraki Gulf, D'Urville Island, and Stewart Island populations, respectively. White crosses and closed circle represent original parameter estimates for all three *O. pullus* populations sampled. The relationship between size- and age-at-sex change (thermal reaction norms) is described as: $y = -0.12\ (\pm 1.66) * x + 399.76\ (\pm 8.43)$.

Growth rate

Examination of growth rate-at-age of *O. pullus* and *N. fucicola* suggested differences in growth rate across locations in both study species (Figs 4.13 & 4.14). Within both species, growth appeared faster in individuals living in the Hauraki Gulf at the ages of 6 months and 1 year than in those living at Stewart Is, indicating faster growth at lower latitudes in both *O. pullus* and *N. fucicola* (Fig. 4.13). Growth rate appeared to decrease at a faster rate in the Hauraki Gulf than at the higher latitude location of Stewart Is, and, by the ages of 2.5 years in *O. pullus* and 4 years in *N. fucicola*, individuals appeared to grow slower in the Hauraki Gulf than in Stewart Is, suggesting that growth reached an asymptote earlier at low latitudes. In comparing the two species at each location, *O. pullus* appeared to display higher average growth rates-at-age than *N. fucicola* individuals at the ages of 6 months, 1 year and 1.5 years, and this was consistent across locations (Fig. 4.14). By the age of two years, the two species showed similar average amounts of growth per unit of body size, suggesting that growth rate of *O. pullus* decreases with age at a faster rate than that of *N. fucicola* within the first two years of life span, which coincides with the comparatively more asymptotic form of growth of *O. pullus*. These differences between the two study species in relative growth rate-at-age were consistent across the Hauraki Gulf and Stewart Is, *O. pullus* individuals appearing to grow faster than *N. fucicola* individuals at the ages of 6 months and 1 year at both lower and higher latitudes.

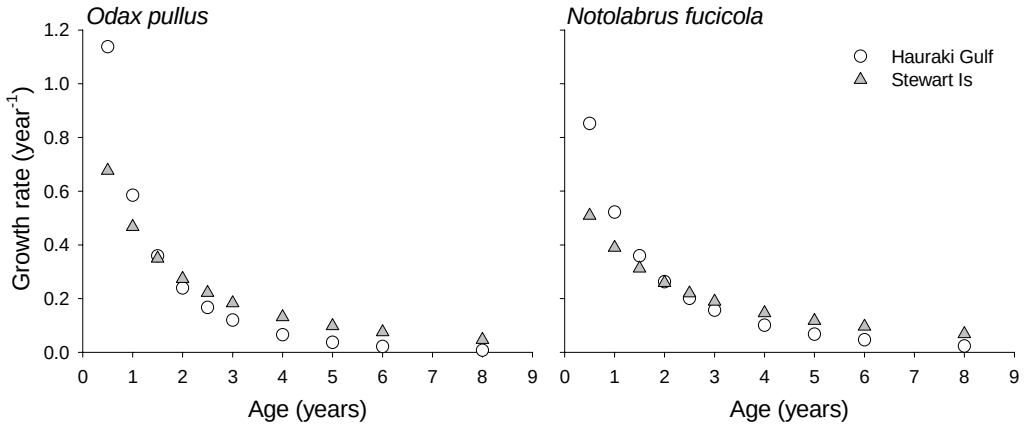

Fig. 4.13: Growth rate-at-age of *Odax pullus* and *Notolabrus fucicola* in the Hauraki Gulf (open symbols) and at Stewart Is (shaded symbols). Growth rate-at-age was scaled by size at each given age (relative instantaneous growth rate *G*).

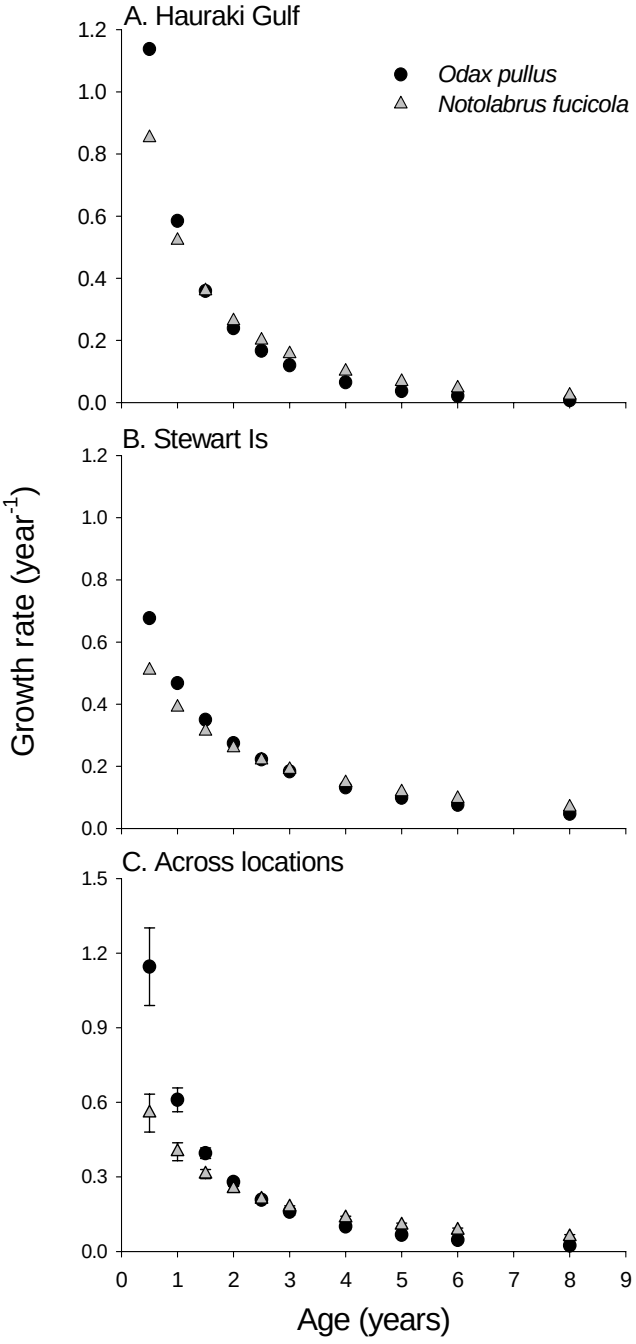

Fig. 4.14: Growth rate-at-age of *Odax pullus* (black symbols) and *Notolabrus fucicola* (shaded symbols), comparing growth rate between the two study species (A) in the Hauraki Gulf, (B) at Stewart Is, and (C) across latitudes sampled (mean growth rate-at-age is presented with Standard Error bars). Growth rate-at-age is relative instantaneous growth rate *G* (scaled by size for each given age).

Relationship between size-at-age one and adult body size

There was an inverse relationship between mean size-at-age one ($L(1)$) and adult body size (mean maximum size L_{max}) across latitudes sampled, and this was consistent in both *O. pullus* and *N. fucicola*. In both species, individuals that reached smaller mean maximum body sizes (L_{max}) appeared larger by the age of one year ($L(1)$), suggesting that faster initial growth was associated with smaller resulting adult body sizes (Fig. 4.15). Conversely, individuals that reached larger mean maximum sizes at higher latitudes appeared smaller at the age of one, indicating that slower initial growth resulted in larger adult body sizes. The inverse relationship between initial growth and adult body size coincides with the predictions of Berrigan and Charnov (1994) in response to temperature, and suggest environmental temperature as the primary driver affecting somatic growth rate.

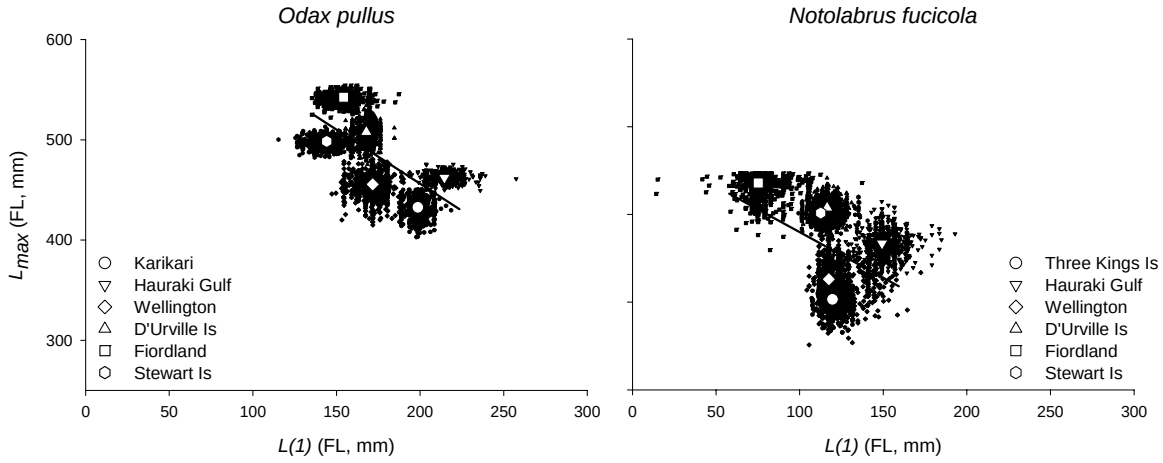

Fig. 4.15: Size-at-age one (*L(1)*) and mean maximum body size (L_{max}) of *Odax pullus* and *Notolabrus fucicola* across New Zealand, showing the relationship between early growth and adult body size. Size-at-age one (*L(1)*) is rVBGF parameter and is used as a proxy for the average amount of growth undertaken between the ages of zero and one year (early growth), and mean maximum body size L_{max} is mean size of 10% (*O. pullus*) and 25% (*N. fucicola*) largest individuals within each sampled population. Mean parameter estimates (open symbols) are presented with bootstrapped variance estimates (black symbols). The relationship between *L(1)* and L_{max} is described as: *O. pullus*: $y = -1.07\ (\pm 0.53) * x + 670.04\ (\pm 94.20)$; *N. fucicola*: $y = -1.14\ (\pm 0953) * x + 504.26\ (\pm 108.04)$.

Linking growth, body size, development, and longevity across latitudes

Relating the above results of growth rate-at-age, body size, longevity, and development rate (size-at-stage) in *O. pullus* and *N. fucicola* across latitudes revealed a

similar response in both study species. Both *O. pullus* and *N. fucicola* responded in a similar fashion over the latitudinal gradient sampled in terms of growth rate within the first year of the life span, adult body size, age-at-maturity, and longevity, with individuals sampled in the southern location of Stewart Is growing slower initially, reaching a larger adult size, maturing (and changing sex in *O. pullus*) later, and living longer than those sampled in the northern latitudes of the Hauraki Gulf. *O. pullus* and *N. fucicola* differed in their response of size-at-maturity across latitudes, with no difference in size-at-maturity (and -at-sex change) across latitudes in *O. pullus*, and an increased size-at-maturity at higher latitudes in *N. fucicola* (Fig. 4.16).

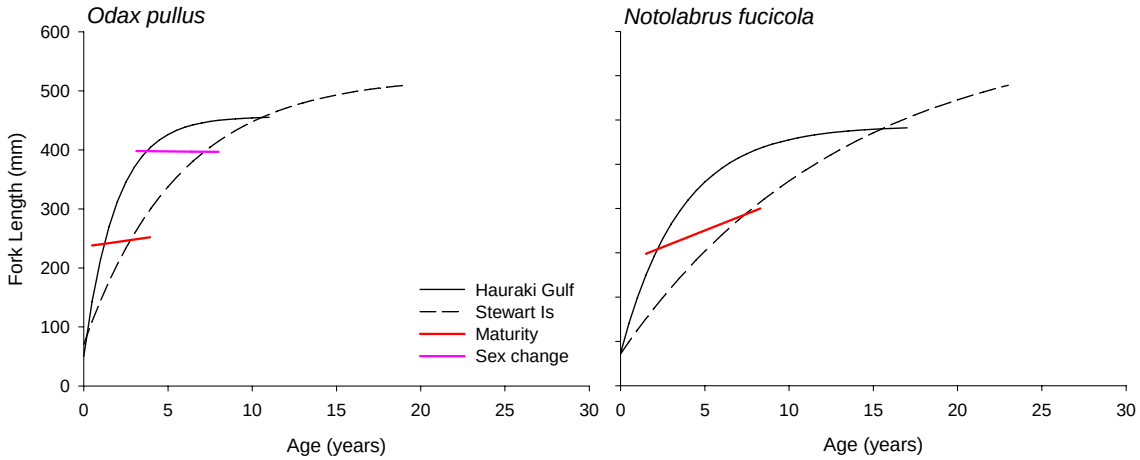

Fig. 4.16: Relationship between growth, life span, and the slope of the reaction norms of sexual maturity (solid red line) and sex change (solid pink line) in *Odax pullus* and *Notolabrus fucicola* at two locations (Hauraki Gulf; Stewart Is) across a geographical gradient of latitude. Black lines are re-parameterized von Bertalanffy Growth Functions (rVBGF) estimated for the Hauraki Gulf and Stewart Island populations, respectively. Size- and age-at-maturity and -at-sex change are size and age at which 50% of females are reproductively mature and at which 50% of sex changing females have changed sex into males, respectively.

4.4 Discussion

Analysis of the life history of two temperate labrids, *Odax pullus* and *Notolabrus fucicola*, identified significant trends in growth rate, developmental rate, body size, and longevity over the main North-South axis of the sampled distributional range. Sampling and analyses spanned over 1,600 km and 13^{o} of latitude, and covered over 85% of the species' latitudinal range. There was a response of faster initial growth, earlier onset of maturity (and of sex change in *O. pullus*), smaller adult body size, and shorter life spans at warmer

temperatures (lower latitudes), a pattern consistent with the "Hotter is smaller" hypothesis suggesting a plastic response of life histories to thermal gradients in the two study species (Kingsolver and Huey, 2008). The responses of growth, body size and maturation rates along environmental gradients, however, may also involve either adaptive or mechanistic processes in response to local environmental conditions (Angilletta, 2009). Both study species were exposed to changes in a number of ecological factors, including variation in local habitat availability, species density patterns, and size-selective mortality rates through fishing (*O. pullus*), which may all affect the responses of life history features across latitudes sampled. The discussion will review the main findings of this section and evaluate the factors that might underlie the observed trends.

The primary findings with respect to latitudinal effects were consistent for *O. pullus* and *N. fucicola*. Specifically, initial growth rates showed a strong positive relationship with temperature, leading to larger body sizes over the first two years of life at the northern sampling sites. Developmental rates (female sexual maturation) were more rapid for northern populations, with maturation being delayed at higher latitude locations (Stewart Is) by three years in *O. pullus* and six years in *N. fucicola*. As faster initial growth at warmer latitudes was coupled with earlier maturation schedules in both species, this resulted in smaller mean maximum sizes in the northern populations sampled. Moreover, a strong demographic signal was seen in the response of life spans, with *O. pullus* and *N. fucicola* achieving maximum ages that were 48% and 35% greater at higher latitudes, respectively. These findings confirm that counter-gradient variation in growth was not a feature in the two study species. Although lower temperature locations were associated with reduced growing seasons, the lower initial growth rates of both species do not provide any evidence for winter-associated size-selective mortality. There was no evidence of the size-specific mortality that provides the selective pressures for enhanced juvenile growth and development rates at higher latitudes.

Increased size-specific mortality rates through fishing may influence the patterns of variation in demographic and life history traits seen in fishes across geographical gradients, including those associated with latitude (Daufresne *et al.*, 2009). If fishing was influencing the life history responses detected across latitudes in *O. pullus*, we would expect greater size-selective removal of older and larger individuals to select for increased growth, earlier maturity, and truncated size and age structures, as well as reduced overall abundances (Conover and Munch, 2002; Hutchings, 2004; Olsen *et al.*, 2004; Conover *et al.*, 2005;

Hamilton *et al.*, 2007). The changes in growth, maturation rates, body size and age structures identified in *O. pullus* across locations sampled, however, showed opposite patterns. Individuals grew faster and matured earlier in regions of lower fishing efforts (Karikari & Hauraki Gulf), whereas individuals living under higher fishing mortality regimes (Wellington & Stewart Is) showed patterns of comparatively slower growth and delayed maturity. This was further coupled with opposing trends in age structures, with shorter life spans identified in regions with comparatively lower levels of fishing mortality. Abundance patterns responded in a similar fashion, with no trend of reduced densities at locations sustaining significant greater levels of fishing mortality (Wellington and Stewart Is) (see Appendices 4.1 & 4.2). Furthermore, population size structure of *O. pullus* recorded in this study also coincided with that seen in archaeological remains from pre-European settlement times (Leach, 2006), indicating that increasing fishing mortality rates sustained over the past century have not significantly affected body size structures to this date (Limburg *et al.*, 2008; Maschner *et al.*, 2008).

Both *O. pullus* and *N. fucicola* showed variation in abundance between locations sampled. In both species, abundances increased with latitude, with lower abundances found in the Hauraki Gulf (low latitudes) than at Stewart Is (high latitudes). Two aspects of these findings are particularly significant: (i) the herbivorous *O. pullus* was more abundant at the southern (colder) margin of its range, and (ii) there was no difference in the trends of variation in abundance across latitudes between the herbivorous *O. pullus* and the carnivorous *N. fucicola*. The finding of increased abundances at higher latitudes in *O. pullus* contradicts the predictions of the temperature-constraint on herbivory, in which a negative effect of temperature on the digestion of algal material would prevent herbivorous fishes from successfully inhabiting high latitudes (Gaines and Lubchenco, 1982; Harmelin-Vivien, 2002; Behrens, 2005; Floeter *et al.*, 2005; Behrens and Lafferty, 2007). The smaller body sizes of *O. pullus* living at lower latitudes (warmer temperatures) are associated with lower abundances, while greater adult body sizes in individuals living at higher latitudes (colder temperatures) was associated with high levels of abundance. It thus appears unlikely that a physiological constraint on the digestive processing of algal material at cold temperatures influences the demographic and life history traits of *O. pullus* over the latitudinal range sampled. In contrast, the responses in growth and abundance patterns across latitudes appeared to reflect the effect of temperature on metabolic rates (Brown *et al.*, 2004).

Locality-specific effects are also likely to play a significant role in the response of demographic and life history traits over latitudinal gradients of temperature (*e.g.* Trip *et al.*, 2008). Increased densities will be associated with smaller adult body sizes due to reduced food resources (Gust *et al.*, 2001; Gust *et al.*, 2002). Reduced species densities in both *O. pullus* (D'Urville Is and Fiordland) and *N. fucicola* (D'Urville Is) were associated with increased body sizes and size-at- maturity, and in greater size-at-sex change in *O. pullus*, as compared with individuals living at similar latitude locations (Wellington and Stewart Is). These results suggest that growth and body size of both *O. pullus* and *N. fucicola* also reflected local patterns of abundance and food availability, but that these ecological effects on the response of life histories were seen on a local spatial scale within given latitudes.

The findings for both *O. pullus* and *N. fucicola* in relation to temperature, species density patterns and size-selective morality regimes (fishing) provide a basis for rejecting the impacts of fishing and density (food availability) as primary explanatory factors of the patterns of variation in life histories on a broad spatial scale across latitudes. The effects of temperature on the patterns of variation in life histories in both *O. pullus* and *N. fucicola* were primarily seen on a broad latitudinal scale, individuals growing more slowly, achieving larger adult body sizes, maturing (and changing sex in *O. pullus*) later, and living longer at colder latitudes. Conspecific abundance patterns also contributed a significant effect to the response of life histories and this was expressed on a local spatial scale, with individuals displaying comparatively more determinate forms of growth and larger size-at-stage in conditions of reduced conspecific densities (higher food availability). Both intrinsic (physiological) and extrinsic (ecological) factors may affect ectotherm growth and maturation rates, and consequently body size over gradients of latitude (Angilletta, 2009). Individual growth and development rates are affected by temperature regardless of ecological mechanisms, but both intraspecific density and predation (changes in mortality rates) will influence development rates and resulting body size (Metabolic Theory of Ecology; Brown *et al.*, 2004). The critical point arising from this is that intrinsic factors such as the response to temperature will occur over broad spatial scales, as seen in the response of ectotherm life spans across latitudes (Munch and Salinas, 2009), and that ecological factors such as density and resource availability will be manifested in a patchy fashion at local spatial scales.

These findings suggest that the thermal reactions norms for body size and maturation rates observed in *O. pullus* and *N. fucicola* are the result of a phenotypic response to

temperature across latitudes ("Hotter is smaller" hypothesis), although the near-universal nature of this trend (Temperature-Size Rule) does indicate some form of selective mechanism underlying the responses of life histories over gradients of latitude (Kingsolver and Huey, 2008). The processes (adaptive or mechanistic) underlying the negative slopes of the reactions norms associated with "Hotter is smaller", however, have yet to be identified, although there is some indication that earlier maturation will result in smaller final body sizes when temperature affects development rate at a faster rate than it affects growth (van der Have and de Jong, 1996). Examination of the genetic structure of the two species across latitudes sampled will provide some insights as to the potential presence of local adaptive mechanisms underlying the differences in life history features across latitudes.

This study contributes to the understanding of broad-scale patterns of variation in ectotherm life histories and specifically in two temperate labrid species. Findings suggest that the main effects of latitude are seen in the phenotypic response of life histories to changes in environmental temperature on a broad spatial scale as predicted by the "Hotter is smaller" hypothesis (Kingsolver and Huey, 2008). Local habitat availability and species densities (i.e. food availability) also affected the responses of life history features in both *O. pullus* and *N. fucicola*, but their effects were primarily seen on a local spatial scale. Furthermore, this study provides the first comprehensive analysis of the life history of an odacine labrid and of a temperate marine herbivore across the majority of the species' distributional range. Results suggest no direct evidence in terms of life history for a temperature-constraint on herbivory at high latitudes, and establish a basis for re-evaluating the assumptions underlying the 'temperature-constraint' hypothesis and its contribution to explaining the biogeographic distribution of herbivory in marine systems (Clements *et al.*, 2009).

Chapter 5. Latitudinal variation in life span: temperature effects on the rate of ageing in a temperate marine fish, *Odax pullus* (Labridae)

5.1 Introduction

Higher metabolic rates at warmer temperatures have been shown to be correlated with higher oxidative stress, the effect of which is thought to intensify the rate of physiological ageing (senescence) and result in shorter life spans ("rate-of-living" hypothesis of ageing; Finkel and Holbrook, 2000). The rate-of-living theory originated in Pearl (1928), who suggested that variation in life span may be due to variation in metabolic rate, with a faster "rate of living" causing increasing cellular damage and earlier death. This hypothesis later developed into the "free-radical" hypothesis of ageing, which proposes that earlier death at warmer temperatures may be linked to an enhanced production of Reactive Oxygen Species (ROS), a by-product of aerobic respiration and metabolic rate (Gershman *et al.*, 1954; Harman, 1956). More recently, this idea was further developed in the "oxidative-stress" hypothesis. This suggests that shorter life spans may be the effect of increased oxidative damage as a result from the combined effects of age-based decreasing anti-oxidant capacities and increasing ROS production rates at higher temperatures (Beckman and Ames, 1998; Finkel and Holbrook, 2000; Monaghan *et al.*, 2009).

The predictions of the oxidative-stress hypothesis of ageing have been successfully applied to explaining interspecific variation in life spans across closely related ectothermic species living at different temperatures, with a comparatively faster rate of ageing in temperate as opposed to polar environments (Philipp *et al.*, 2005a; Philipp *et al.*, 2005b; Philipp *et al.*, 2006). Philipp and colleagues demonstrated that species achieving significantly greater life spans in colder environments displayed slower basal metabolic rates, a comparatively slower rate of oxidative damage accumulation, reduced ROS production (per unit of oxygen consumed), and a less pronounced decrease with age in antioxidant functions. Intraspecific variation in life span over latitudinal gradients of temperature have been demonstrated in an increasing number of fish species, with individuals often living longer at higher latitudes (Meekan *et al.*, 2001; Choat and Robertson, 2002; Choat *et al.*, 2003; Trip *et*

al., 2008). Comparatively little is known, however, as to how oxidative stress may contribute to explaining intraspecific patterns of variation in life spans across wild fish populations.

Intraspecific differences in life span across wild fish populations living in different temperature environments have previously been linked to Pearl's "rate-of-living" theory, based on the fact that reduced life spans at warmer temperatures are often correlated with fast early growth (Gerking, 1957). More recently, some studies have shown that shorter life spans in fish reared at warmer temperatures were correlated with faster rates of oxidative damage accumulation (increased rate of ageing) and faster rates of somatic growth (Valenzano *et al.*, 2006). These patterns coincide with the predictions of the oxidative-stress hypothesis of ageing, and provide support for the idea that the effect of temperature on the rate of oxidative damage accumulation may contribute to explaining intraspecific changes in life span over geographical gradients of latitude.

In fish, greater life spans appear to be systematically correlated with a pattern of slower somatic growth and increased age-at-maturity (increased reproductive life span) (Roff, 1992; Reznick *et al.*, 2002). These consistent correlations of life span with growth and development rates have suggested a trade-off between development rate and life span. It has been hypothesised that fast early growth increases both immediate and long-term mortality risks, thus generating earlier death. The immediate risks of fast growth include, for instance, increased requirements for foraging and hence increased exposure to predation (Bernays, 1997). The underlying mechanisms of an effect of fast growth on long-term mortality risks (senescence-related), however, have yet to be identified (Metcalfe and Monaghan, 2003). Metcalfe and Monaghan (2003) reviewed several hypotheses, many of which suggested that fast growth may increase the rate of metabolically-induced damage (*e.g.* telomere abrasion, protein oxidation or oxidative damage) as a result of increased cellular activity. Furthermore, a correlation between fast early growth and earlier maturity implies that, at least over the first years of the life span, comparatively little energy may be involved in repair mechanisms, in particular those related to cellular damage. These hypotheses imply that growth rate may be directly linked to the rate of senescence (ageing). A corollary of this is that conditions enhancing somatic growth and increasing development rate (earlier age-at-maturity) are likely to be linked with increased intrinsic mortality rates and shorter life spans. In the context of the response of ectotherm life histories to temperature over gradients of latitude ("Hotter is smaller"), we may expect faster somatic growth rates at warmer developmental

temperatures (lower latitudes) to be coupled with a greater rate of ageing (senescence) and to result in shorter life spans.

The Metabolic Theory of Ecology (MTE) proposes that individual life history characteristics (*e.g.* life span, development rate) are governed by a universal effect of temperature and body size on metabolic rate, and that the correlation between temperature, body size and metabolic rate may be used to explain a range of biological and ecological processes including that of intra-specific variation in life histories (Gillooly *et al.*, 2001; Brown *et al.*, 2004; but see Clarke, 2004; Clarke and Fraser, 2004; Gillooly *et al.*, 2006). Munch and Salinas (2009) tested the predictions of the MTE in the context of latitudinal clines in life spans, and demonstrated across a range of ectothermic taxa, including many species of fishes, a consistent intra-specific response of life span to temperature (latitude) as predicted by the effects of temperature on metabolic rate. The authors thus concluded that environmental temperature and its effect(s) on metabolic rate may play a central role in explaining latitudinal gradients in life span in ectotherms.

The present study explores how intrinsic (senescence-related) mortality may contribute to explaining intraspecific patterns of variation in life span across latitudes. Specifically, this chapter examines intraspecific variation in life span in a widely distributed temperate reef fish, *Odax pullus*, over a broad gradient of latitude, and explores the relationship between temperature, metabolic rate, oxidative damage, and population age structure (life span). The MTE provides a tool to explore the hypothesis that increased life spans at higher latitudes in *O. pullus* may be associated with reduced metabolic rates. As the rate of oxidative damage accumulation is a product of metabolic rate (aerobic respiration), the MTE also provides a basis for establishing predictions as to the effects of senescence-related processes (intrinsic mortality) and life span in the study species.

A strong effect of temperature was seen in the response of life span across latitudes in *O. pullus*, and increased life spans at higher latitudes were correlated with slower somatic growth rate, greater age-at-maturity, and larger adult body size (Chapter 4). I first use the predictions of the MTE to explore the relationship between environmental temperature, metabolic rate, development rate, and life span in *O. pullus* (Munch and Salinas, 2009), and compare the response of life spans in *O. pullus* to that of another labrid, *Notolabrus fucicola*, which have been shown to display similar systematic changes in life span and associated life histories with latitude (Chapter 4). It was suggested that the response of life histories (growth,

development rate and body size) to changes in environmental temperature in *O. pullus* and *N. fucicola* is likely to be the result of a plastic response to temperature (Chapter 4) as predicted by the effects of temperature on growth and development rates in ectotherms distributed over wide spatial scales ("Hotter is smaller"; Kingsolver and Huey 2008). Secondly, this study explores the relationship between physiological and chronological age using neurolipofuscin, an age-associated pigment that is thought to be a direct marker of oxidative damage. Lipofuscin is a non-degradable cellular waste mixture of oxidized proteins, lipids, carbohydrates and traces of metals (mainly iron) that accumulates in post-mitotic cells (primarily neurons and cardiac myocytes), and is often considered a hallmark of ageing (Terman and Brunk, 1998; Brunk and Terman, 2002; Terman and Brunk, 2004; Seehafer and Pearce, 2006; Terman and Brunk, 2006). The formation of lipofuscin is thought to be correlated with oxygen metabolism through the effects of reactive oxygen species. Recent work demonstrated a positive relationship between temperature and the rate of age-based neurolipofuscin accumulation, and showed a negative effect of neurolipofuscin accumulation on life span in a short-lived freshwater notobranchiid fish (Valenzano *et al.*, 2006; Terzibasi *et al.*, 2008; Terzibasi *et al.*, 2009). In *O. pullus*, we predicted that systematic changes in population age structure with latitude would be reflected in the accumulation rates of oxidative damage (neurolipofuscin), with greater life spans at higher latitudes being associated with slower accumulation rates of neurolipofuscin. We expected to find a significant effect of environmental temperature on life span as predicted by the MTE, suggesting the presence of metabolically-induced processes underlying the determination of life span in *O. pullus*.

5.2 Materials and Methods

This chapter explores the relationship between chronological and physiological age, and how these traits may be affected by temperature over a gradient of latitude. *Chronological age* is defined as absolute age or total number of calendar years of an individual's life span; *physiological age* is a relative measure of "physiological fitness" or natural physiological state of "ageing" of the cells or tissues (senescence).

Sampling

A total of 1064 *Odax pullus* and 450 *Notolabrus fucicola* were collected at six locations across New Zealand for estimation of chronological age and life span (Karikari Peninsula, Hauraki Gulf, Wellington, D'Urville Is, Fiordland, Stewart Is; see Fig. 4.2 in Chapter 4 for map of sampling sites). Each fish was measured to the nearest millimetre (fork length) and the sagittal pair of otoliths was dissected. Age was estimated for all individuals collected from sectioned sagittal otoliths, as described in Chapter 2 (section 2.2). All age data were presented in Chapter 4 (see section 4.3 for results).

Life span (mean maximum age T_{max}) of *O. pullus* and *N. fucicola* was estimated for each of the six populations sampled as the average age (in years) of the 10% (*O. pullus*) and 25% (*N. fucicola*) oldest individuals within each sample, as described in Chapter 4 (section 4.2). Percent number of oldest individuals included in the estimation of T_{max} of *O. pullus* and *N. fucicola* were chosen so as to account for the differences in sample size between the two species (Claisse *et al.*, 2009). Estimates of life span T_{max} were presented in Chapter 4 (see section 4.3 for results).

Brain samples of *O. pullus* were collected for investigation of physiological age using neurolipofuscin histology at four of the six locations sampled: Hauraki Gulf, D'Urville Is, Fiordland and Stewart Is (Fig. 5.1). Brain samples were collected for a total of 499 individuals (out of the 1064 *O. pullus* sampled), along with the sagittal pair of otoliths and measure of body size (see above). The forebrain (telencephalon) was dissected out (Fig. 5.2), and fixed in FACC (formaldehyde 4%, glacial acetic acid 5%, calcium chloride 1.3%). Formalin-based fixatives have been shown to provide the best results for the detection of lipofuscin fluorescence (Encarnacao and Castro, 2001). The aim of this study was two-fold: (1) to establish the presence of neurolipofuscin in brain tissue of *O. pullus*, and (2) to explore the relationship between neurolipofuscin accumulation and age across latitudes sampled. As neurolipofuscin has been shown to accumulate with age (Valenzano *et al.*, 2006; Terzibasi *et al.*, 2008; Terzibasi *et al.*, 2009), the probability of detecting lipofuscin in the study species was assumed to be higher in older individuals. After determination of age, five individuals were randomly selected within the ~40% oldest age classes recorded at each location. A minimum of at least one individual per age class present was retained so as to allow establishing the relationship between neurolipofuscin and chronological age. This sampling

procedure allowed comparison of lipofuscin accumulation with age across populations over similar proportions of the older end of the life span.

Mean annual sea surface temperature (SST) estimates were obtained for each location sampled from long term satellite-derived SST data from mean monthly SST between January 1985 and December 2007 (see Chapter 4, section 4.2 for details of methods).

Sample sizes and age range of individuals for which brain samples were collected and for which brain histology was undertaken are presented in Table 5.1.

Fig. 5.1: Map of sampling locations of *Odax pullus* across New Zealand, showing sites where brain samples were collected for examination of physiological age.

Table 5.1: Summary table showing coordinates, mean annual sea surface temperature (SST) and total number of brain samples of *Odax pullus* collected across New Zealand. Maximum age and mean maximum age T_{max} (life span), age range of samples for which brains were collected, and age range of individuals for which neurolipofuscin histology was performed at each location are shown. All age estimates are presented in years.

Location	Longitude / Latitude	SST (°C)	Max age	Life span (T_{max})	N brain samples (age range)	Age range for neurolipofuscin histology
Hauraki Gulf	175.3°E, 36.3°S	17.6	11	7.5	276 (0.4 – 10)	6 – 10
D'Urville Is	173.9°E, 40.7°S	14.7	11	7.9	81 (1 – 11)	7 – 11
Fiordland	166.9°E, 45.5°S	13.7	17	15	41 (1 – 17)	11 – 17
Stewart Is	167.9°E, 47°S	12.1	19	13.625	101 (0.7 – 17)	12 – 17
Total	-	-			*499*	

Life span and temperature

The contribution of environmental temperature to explaining intra-specific variation in life span was examined in *O. pullus* and *N. fucicola* across New Zealand, using two approaches. Firstly, separate simple linear regression analyses were performed on (i) maximum age data and (ii) life span estimates (mean maximum age T_{max}) of both study species. Assumptions of normality and homogeneity of variance were checked for each analysis by examining the distribution of the observed values and residuals and by examining the relationship between the residuals and predicted values from the regression model fitted. Maximum age data of *O. pullus* was transformed (fourth-root of natural logarithm) before analysis.

Secondly, the predictions of the Metabolic Theory of Ecology (MTE) were tested on estimates of life span of both *O. pullus* and *N. fucicola* across latitudes sampled, as in Munch and Salinas (2009).

The MTE predicts that biological time t scales with metabolic rate as a function of body mass m and temperature T (Gillooly *et al.*, 2001; Gillooly *et al.*, 2002; Brown *et al.*, 2004) as follows:

$$t \propto m^{1/4} * e^{E/kT} \qquad (1)$$

where E is activation energy, k is Boltzmann's constant ($k = 8.62 \times 10^{-5}\ eV/K$), and T is absolute temperature (in degrees Kelvin). The Boltzman constant k predicts how temperature

affects the rate of reaction by changing the proportion of molecules with sufficient kinetic energy *E*. Activation energy *E* may vary between 0.2 – 1.2 eV and averages between 0.6 – 0.7 eV.

Life span T_{max} may then be expected to scale with temperature as follows:

$$T_{max} \propto m^{1/4} * e^{E/kT} \quad (2)$$

A linear regression approach was used to test the relationship between life span and temperature as predicted by equation (2) (Munch and Salinas, 2009). The following linear regression model was fitted to life span estimates of *O. pullus* and *N. fucicola*, respectively, at each of the six locations sampled across New Zealand. Munch and Salinas (2009) also demonstrated that the exclusion of parameter *m* from the regression did not significantly alter the slope of the fitted model. The following model was fitted to each of the two study species independently:

$$\ln(T_{\max}) = \frac{1}{kT} * E + cst + \varepsilon \quad (3)$$

where activation energy *E* is the slope, *cst* is the intercept, and ε is random error.

The predictions of the MTE (equation (2)) were considered supported when the slope of the least-squares regression (equation (3)) did not significantly differ from the predicted range of values for activation energy *E* ($0.2 < E < 1.2$ eV) (Gillooly *et al.*, 2001). The regression coefficient values (*E*) generated from the regression model were subsequently compared graphically (with 95% confidence intervals) across the two study species.

Development rate

Development time was estimated for *O. pullus* as the time taken (age) to reach body lengths ranging between 80 – 120 mm (fork length, FL). This size range was selected so as to represent development over the first year of life and included all smallest individuals collected across New Zealand (Karikari, Hauraki Gulf, D'Urville Is, Fiordland and Stewart Is). Individuals within the 80 – 120 mm FL size range were aged between 115 and 351 days, with one individual aged 1 year. Few *N. fucicola* individuals sampled were aged one year or

less (see Table 4.2, Chapter 4); as a result, early development rate was not estimated for this species. Development rate δ was calculated as the inverse of development time (year $^{-1}$).

A similar approach as for examination of life span was used to explore the contribution of environmental temperature to explaining variation in early development rate across latitudes in *O. pullus*. Firstly, separate simple linear regression analyses were performed on (i) estimates of development rate, and (ii) estimates of mean size-at-age one year *L(1)* (re-parameterized von Bertalanffy Growth Function parameter, see Chapter 4 for modelling of growth and parameter estimation). Assumptions of normality and homogeneity of variance were checked by examining the distribution of the observed values and residuals and by examining the relationship between the residuals and predicted values from the regression model fitted.

Secondly, the predictions of the MTE were tested on development rate (δ) data of *O. pullus*. Development rate δ may be expected to scale with body mass *m* and temperature *T* as follows (Brown *et al.*, 2004; Munch and Salinas, 2009):

$$\delta \propto m^{-1/4} * e^{-E/kT} \qquad (4)$$

A linear regression approach was used to test the predictions of (4), by fitting the following linear regression model to development rate estimates of *O. pullus* across populations sampled:

$$\ln\left(\delta * m^{1/4}\right) = -\frac{1}{kT} * E + cst + \varepsilon \qquad (5)$$

where activation energy *E* is the slope, *cst* is the intercept, and *ε* is random error.

The predictions of the MTE (equation (4)) were considered supported when the value of activation energy *E*, corresponding to the slope of regression model (5), did not significantly differ from the predicted range of values for activation energy *E* ($0.2 < E < 1.2$ eV) (Gillooly *et al.*, 2001).

Brain histology and neurolipofuscin

Neurolipofuscin is characterised by aldehyde bonds formed across lipid and protein waste compounds that display auto-fluorescent properties, and the detection of lipofuscin auto-fluorescence is best achieved through histology (Hammer and Braum, 1988; Sheehy, 1996). Each of the five forebrain samples collected at each of the four locations was embedded in paraffin and sectioned transversally at the front of the telencephalon through the olfactory bulb region (Fig. 5.2). The olfactory region was found to display highest concentrations of neurolipofuscin fluorescence in a number of crustacean decapods (Sheehy, 1990; Sheehy *et al.*, 1996; Fonseca *et al.*, 2005). No comparable neurolipofuscin concentrations could be found throughout the samples examined in this study. In contrast, fluorescence appeared spread throughout the forebrain region examined (including the olfactory bulb region), and resembled patterns found in Terzibasi et al. (2008; 2009). As a result, sampling of the forebrain of *O. pullus* was designed to survey the front of the telencephalon including the olfactory bulb region so as to provide a mean estimate of neurolipofuscin across the front region of the telencephalon surveyed. Three 5 μm-thick serial sections were taken at each of five equidistant points across the forebrain (between A & B, Fig. 5.2). Points sampled were separated by ~50 μm, resulting in five slides taken per individual fish. Sections were de-waxed and cover-slipped using a xylene-based mountant.

A subset of telencephalon samples from the Hauraki Gulf, D'Urville Is, and Stewart Is were weighed to the nearest 0.1 milligram. Forebrain weight increased linearly with body length and as a power-function with body weight and age. No differences other than those reflecting differences in somatic growth were found in the effects of body length, weight or age on telencephalon weight across locations and between the sexes, suggesting no location- or sex-specific differences in telencephalon growth and/or development (Appendix 3).

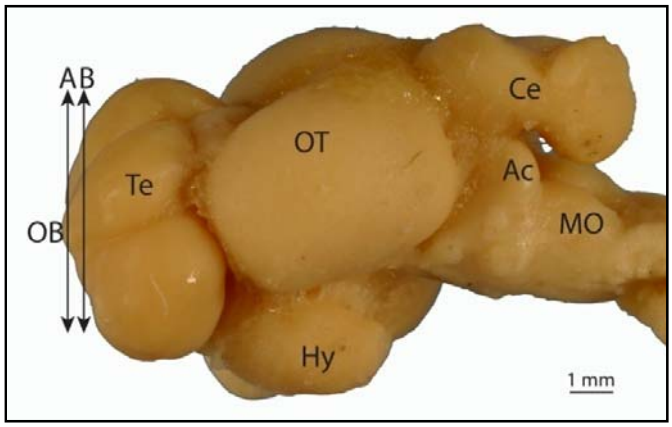

Fig. 5.2: Photomicrograph of the brain of *Odax pullus* (lateral view, left hand side) showing brain anatomy, sectioning plan (arrows) and region sampled for the histology of neurolipofuscin (A-B). Sample shown was fixed in a formalin-based fixative. Ac: acoustico-lateral area; Ce: cerebellum; Hy: hypothalamus; MO: medulla oblongata; OB: olfactory bulb; OT: optic tectum; Te: telencephalon. Brain anatomy adapted from Bauchot et al. (1989) and Kotrschal et al. (1998).

Histochemistry of neurolipofuscin

A control slide was used to confirm the presence of neurolipofuscin material in the fluorescence identified. The slide-mounted section was first photographed under UV light at 100x-objective prior to staining. Sudan black B, a lipophilic stain, was used to stain for lipids, which are characteristic components of lipofuscin, following (Sheehy, 1989). The coverslip was removed in xylene, and the section was re-hydrated through successive ethanol baths (100%, 95% to 70% ethanol) before staining with Sudan black B for 1 hour. Stain was prepared a few weeks prior to staining for optimal staining results (0.5 mg Sudan black B, 100 mL 70% ethanol). Stained slide was rinsed in 70% ethanol and water, counter-stained with Erlich's haematoxylin (3 minutes) and differentiated with acid alcohol 1% (1 dip). Slide was mounted with Aquamount (water-soluble mountant) and coverslipped.

The Sudan-stained section was re-photographed under transmitted light (at 100x-objective), and compared with the fluorescence image (Fig. 5.3). The majority of fluorescing vacuoles (Fig. 5.3a) stained positively to Sudan black B (Fig. 5.3b), confirming the lipophilic character of the fluorescence identified, and suggesting the presence of lipofuscin in the fluorescing vacuoles (Fig. 5.3b).

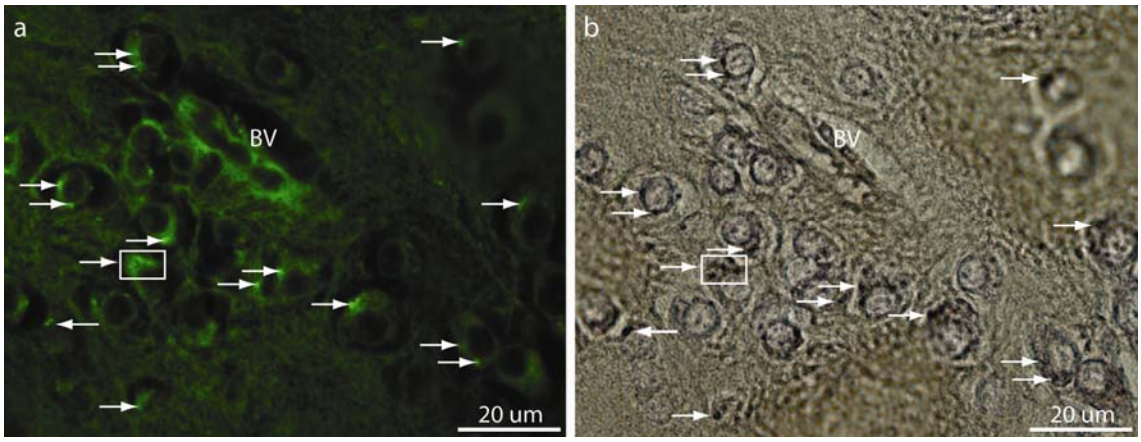

Fig. 5.3: Validation of lipofuscin-fluorescence in the olfactory bulb region of the telencephalon of *Odax pullus* (viewed at 100x). The same frame was photographed (a) under UV light before staining, and (b) after staining with Sudan black B under transmitted light. Arrows indicate position of neurolipofuscin vacuoles. Individual photographed is a 14 year old female from Stewart Is (532 mm FL, 2400 g GW). BV: blood vessel.

Neurolipofuscin quantification

A total of 1000 slide-mounted sections (5 independent sections were taken across the forebrain of each of 5 individuals sampled at the 4 locations) were examined for auto-fluorescence at 100x-oil immersion objective, with an excitation wavelength of 450 – 490 nm (blue) and an emission wavelength of 500 – 550 nm (green). This combination of excitation / emission wavelengths was found to provide the best discrimination of background to lipofuscin-fluorescence ratio. The best section of the three serial sections taken per slide was photographed (Fig. 5.4a), generating five photographs per fish for image analysis. Image analysis was undertaken using image analysis software ImageJ 1.43g. A binary image was taken of each photograph so as to display lipofuscin-fluorescence in black and background tissue in white (Fig. 5.4b). The resulting binary mask and its original colour-photograph were overlaid to check for overlap of the black regions generated in the binary image and the original fluorescing areas (Fig. 5.4c). Total area of fluorescence was calculated as the sum of the areas of all black regions observed (from the binary image) and expressed as a proportion of total brain area photographed for each slide examined (% fluorescence).

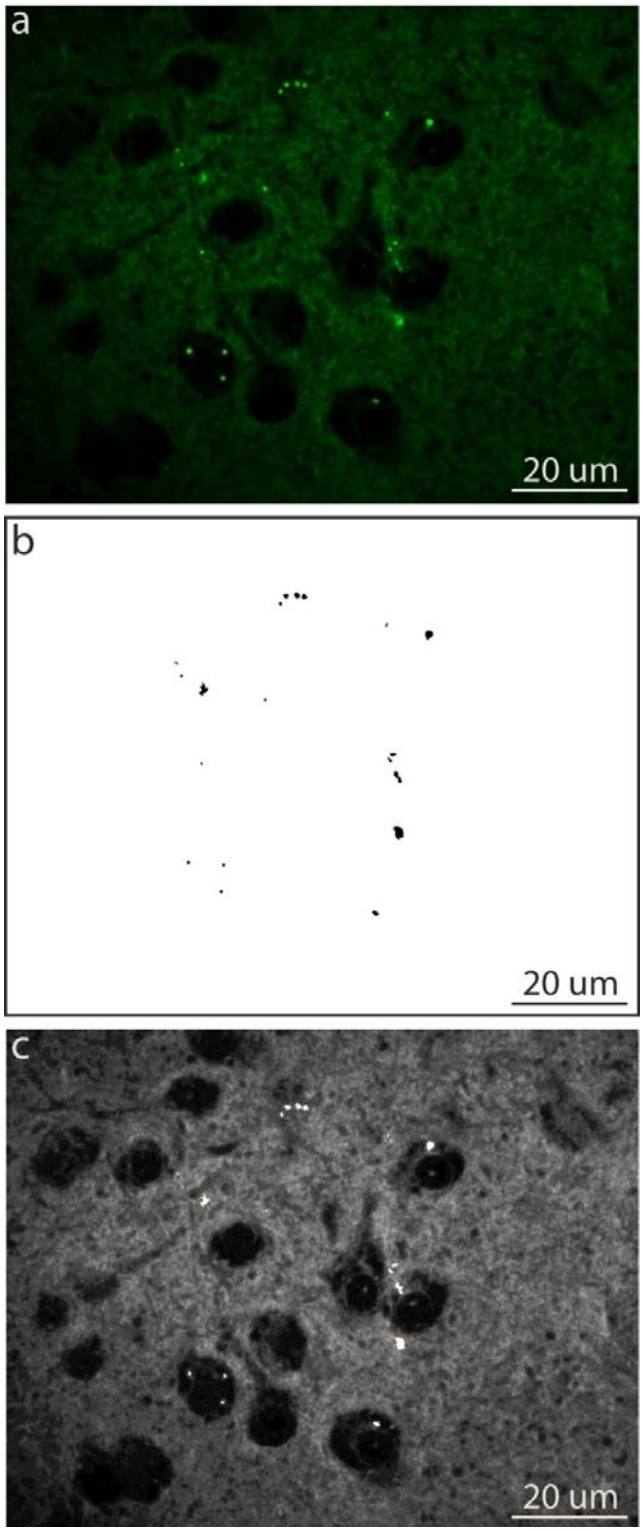

Fig. 5.4: Neurolipofuscin-fluorescence in the olfactory bulb region of the telencephalon of *Odax pullus* (viewed at 100x). (a) photograph under UV light (blue excitation, green emission), (b) thresholded binary mask of (a), and (c) overlay of (a) and (b) (black regions seen in (b) are presented in white). Individual photographed is a 14 year old female from Fiordland (554 mm FL, 2100 g GW).

Analysis: neurolipofuscin accumulation, temperature and development rate

Analysis was aimed at examining the following two questions. Firstly, does neurolipofuscin accumulate with age over the last 40% of the life span? Secondly, is neurolipofuscin accumulation rate affected by temperature and/or development rate?

Analysis of covariance (homogeneity-of-slopes model) was used to compare the slopes of the relationship between percent neurolipofuscin and age (1) across locations sampled, and (2) between regions sampled (North, South) (Quinn and Keough, 2002). Two measures of age were used in two separate ANCOVAs, firstly with age measured as chronological age (in years), and secondly with age estimated as a percentage of mean maximum age, to provide a relative measure of the proportion of life span achieved. Mean maximum age was calculated as the mean age of the 10% oldest individuals at each location (T_{max}, Chapter 4). The oldest 10% was selected as the reference point, rather than the oldest individual, to avoid the possibility that a chance sampling event of a particularly old fish would skew the data. However, as a result of scaling to the mean of the oldest 10% individuals some values for the scaled data will be greater than 100%. Hauraki Gulf and D'Urville Is were in the North, and Fiordland and Stewart Is in the South. The relationship between mean percent area of neurolipofuscin present across the olfactory region and age recorded over the 40% oldest age classes present was established as linear at each location and within both regions, and locations (random) were nested within each region (fixed). Assumptions of normality, homogeneity of variance, independence (between observed values and residuals), linearity (between % lipofuscin and age), and non-colinearity between the categorical factors (location, region) and the covariate (age) were checked, and no transformations of the data were required. Step-wise regression revealed that body size was a significant predictor of % neurolipofuscin independent of age and body size varied across individuals within any given age classes at each of the four locations (see Fig. 4.3 in Chapter 4). In order to examine the effect of body size, mean % neurolipofuscin was scaled to size using an ANCOVA approach, by using the average slope of the relationship between body size and mean % neurolipofuscin to scale neurolipofuscin to the grand mean body size (Packard and Boardman, 1999). A subsequent plot of the relationship between size-scaled mean % neurolipofuscin and body size showed no correlation between the two (Correlation Analysis, $R = 0.05$, $p = 0.84$), confirming that the effect of body size had been effectively removed. Analysis of covariance (homogeneity-of-slopes) was used to compare the slope of

the relationship between size-scaled mean % neurolipofuscin and age, across locations and between regions sampled. All analyses were performed on mean % neurolipofuscin data, *i.e.* mean lipofuscin-fluorescence across all five replicate estimates taken for each individual fish.

Neurolipofuscin accumulation rate (%.year^{-1}) was estimated at each location from the slope of the relationship between mean % neurolipofuscin and chronological age. The effect of temperature (mean annual sea surface temperature) and development rate on neurolipofuscin accumulation rate were estimated using two separate linear regression analyses (high colinearity between temperature and development rate precluded the use of a stepwise multiple regression analysis). Assumptions of normality, homogeneity of variance, linearity and independence were checked by plotting the distribution of the residuals and by examining the relationship between the residuals and predicted values from the regression model fitted. All analyses were performed in STATISTICA 7.1.

5.3 Results

Life span, development rate, and temperature

Over 1000 *Odax pullus* and 450 *Notolabrus fucicola* individuals were used to examine the relationship between life span and temperature in the two study species. Locations sampled spanned over ~13^{o} of latitude over the majority of the species' distributional range, and covered a temperature difference in mean annual Sea Surface Temperature (SST) of ~5.5^{o}C. Examination of the relationship between temperature (SST), maximum age and life span (mean maximum age T_{max}) revealed a significant decrease in both maximum age and life span with temperature in both study species, with individuals living longer at colder temperatures (Fig. 5.5). Similarly, mean size-at-age one and development rate (within the first year of life) both increased significantly with temperature over the latitudinal gradient sampled (Fig. 5.6), suggesting faster growth and development rates at warmer developmental temperatures (lower latitudes). These results coincide with those found for both *O. pullus* and *N. fucicola* in Chapter 4.

The Metabolic Theory of Ecology (MTE) predicts that intra-specific variation in biological times (*e.g.* life span) may be explained by the effect of temperature on metabolic rate when the slope of the relationship between ln(life span) and the inverse of temperature

$^{1}/_{kT}$ corresponds to an activation energy ranging between 0.2 – 1.2 eV and averaging between 0.6 – 0.7 eV (Gillooly *et al.*, 2001; Brown *et al.*, 2004). Examination of the relationship between ln(life span) and $^{1}/_{kT}$ in *O. pullus* and *N. fucicola* across temperature regimes (latitudes) revealed a significant positive relationship between ln(life span) and the inverse of temperature ($^{1}/_{kT}$) (Fig. 5.7 a). The regression coefficient values found for the effect of $^{1}/_{kT}$ on ln(life span) were 0.75 [+/- 0.65 95% CI] in *O. pullus* and 0.80 [+/- 0.31 95% CI] in *N. fucicola*, suggesting that the slopes did not significantly differ from the average range (0.6 – 0.7 eV) of expected values for activation energy E as predicted by the MTE (Fig. 5.7 b). However, the regression coefficient values were associated with substantial amounts of variation in both *O. pullus* and *N. fucicola* (Fig. 5.7), which encompassed not only the predicted average values but also a large range of values other than those within the predicted average limits of 0.6 – 0.7eV. Additionally, two-tailed power analysis comparing the mean and variance of the regression coefficients to the expected mean of 0.65 eV revealed very low statistical power values of 5 and 12% for *O. pullus* and *N. fucicola*, respectively, which are likely to reflect the low sample sizes (six locations) and large variances. The regression coefficients of both species did, however, fall within the expected range of 0.2 – 1.2 eV. These results suggest some support for the predictions of the MTE (equation (2) in section 5.2), indicating the possibility of a link between metabolic rate, temperature and life span, but also indicate that additional mechanistic effects to that of temperature-related changes in metabolic rate are likely to contribute to changes in life span over a gradient of latitude in both *O. pullus* and *N. fucicola* (Irlich *et al.*, 2009).

In *O. pullus*, examination of the relationship between development rate and temperature following the predictions of the MTE revealed a significant linear decrease in ln(development rate*$m^{1/4}$) with increasing $^{1}/_{kT}$ (*i.e.* with decreasing temperature), with a regression coefficient value of 0.49 [+/- 0.37 95% CI]. The regression coefficient value fell within the expected range (0.2 – 1.2 eV) of values for activation energy *E* (Fig. 5.8). The regression coefficient also encompassed the expected average limits of (0.6 – 0.7 eV), although this result was associated with high variance and low power (10%). This result coincides from that found for the effect of temperature on life span, and suggests that temperature-related changes in metabolic rate may, to some extent, contribute to affecting development rate over a gradient of latitude.

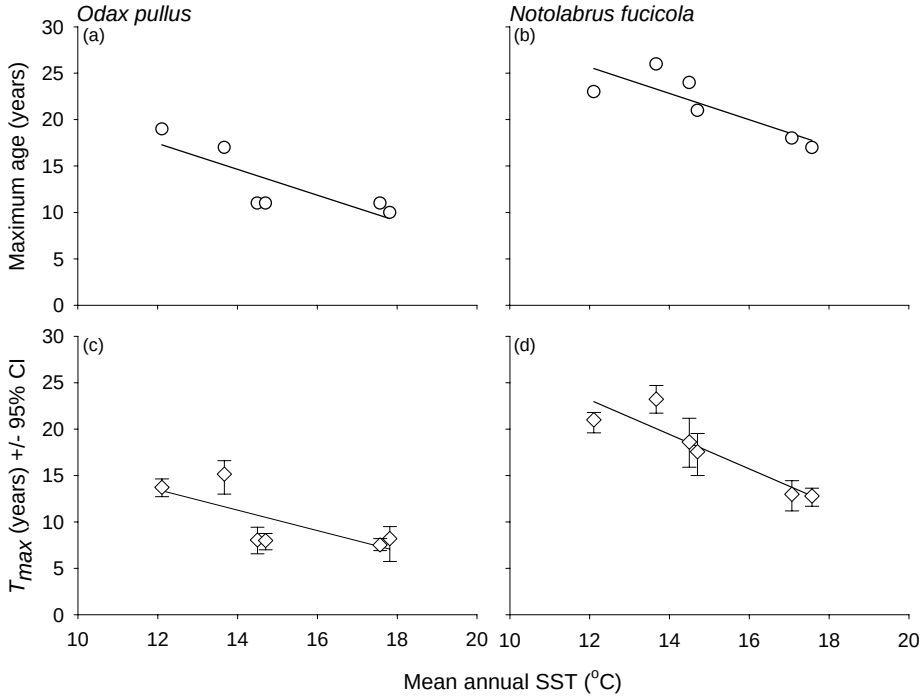

Fig. 5.5: Variation in maximum age and life span (mean maximum age, T_{max}) of *Odax pullus* and *Notolabrus fucicola* with temperature (mean annual sea surface temperature, SST) across New Zealand. Locations sampled are: Three Kings Is (*N. fucicola* only), Karikari (*O. pullus* only), Hauraki Gulf, Wellington, D'Urville Is, Fiorldland, and Stewart Is. Mean maximum age T_{max} was estimated from the 10% (*O. pullus*) and 25% (*N. fucicola*) oldest individuals at each location, and is presented with 95% percentile confidence intervals on bootstrapped variance estimates (CI, see Chapter 4 for description of method used). Data are fitted with least-squares linear regressions: (a) $y = -1.39\ (\pm 0.50) * x - 34.09\ (\pm 7.53)$, $R^2 = 0.66$, $p < 0.05$ (regression analysis performed on fourth-root transformed maximum age); (b) $y = -1.42\ (\pm 0.47) * x - 42.66\ (\pm 7.04)$, $R^2 = 0.70$, $p < 0.05$; (c) $y = -1.10\ (\pm 0.52) * x - 26.69\ (\pm 7.92)$, $R^2 = 0.53$, $p = 0.10$; (d) $y = -1.86\ (\pm 0.42) * x + 45.50\ (\pm 6.26)$, $R^2 = 0.83$, $p < 0.05$.

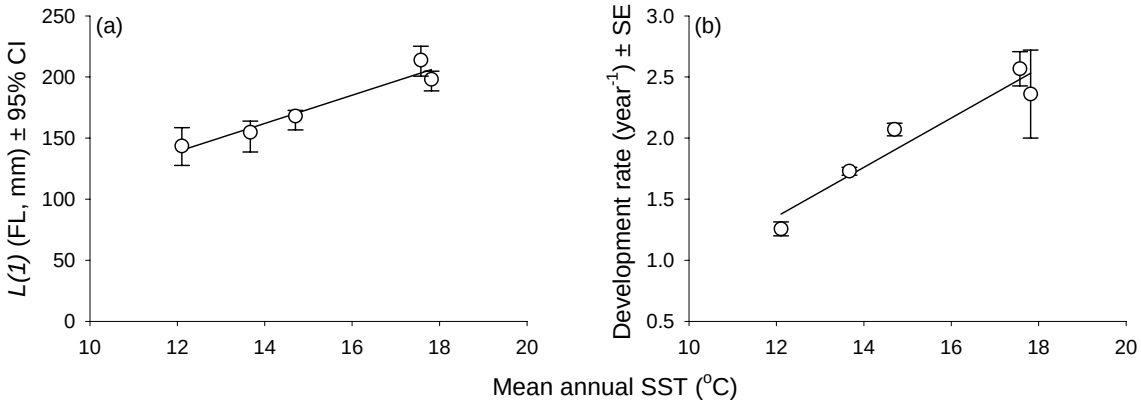

Fig. 5.6: Variation in mean size-at-age one (*L(1)*) and development rate of *Odax pullus* with temperature (mean annual sea surface temperature, SST) across New Zealand. Locations sampled are: Karikari, Hauraki Gulf, D'Urville Is, Fiordland, and Stewart Is. Mean size-at-age one (in years) is best-fit re-parameterized von Bertalanffy Growth Function parameter (see Chapter 4 for modelling of growth and parameter estimation methods), and is presented with 95% percentile confidence intervals on bootstrapped variance estimates (CI). Development rate (year^{-1}) is the inverse of time taken to reach 80 – 120 mm (fork length) as estimated from individuals aged 0 – 1 year. Data are fitted with least-squares linear regressions: (a) $y = 11.48\ (\pm\ 1.47) * \mathrm{x} + 2.15\ (\pm\ 22.24)$, $R^2 = 0.92$, $p < 0.01$; (b) $y = 0.20\ (\pm\ 0.03) * \mathrm{x} - 1.06\ (\pm\ 0.51)$, $R^2 = 0.93$, $p < 0.01$.

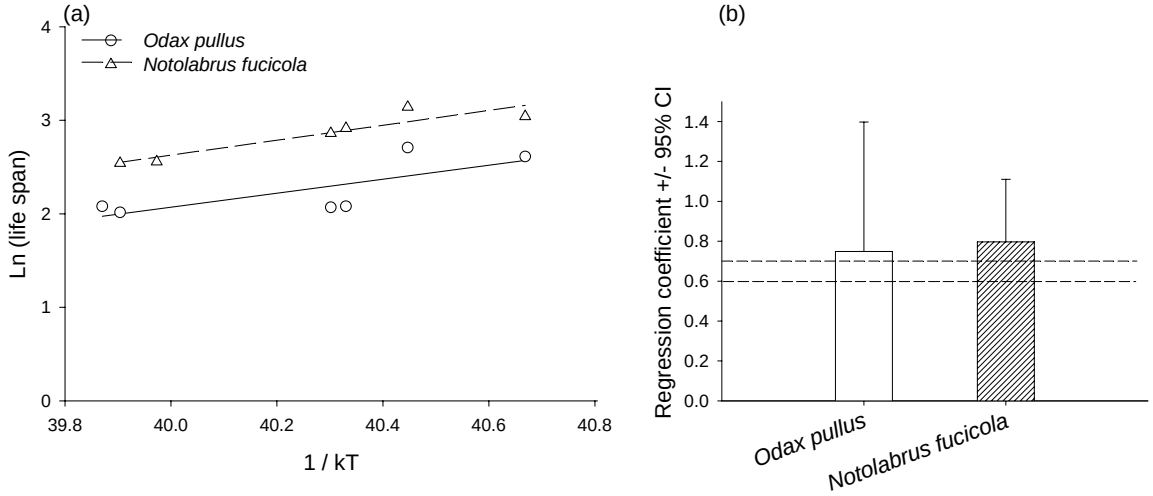

Fig. 5.7: Temperature dependence of life span in *Odax pullus* and *Notolabrus fucicola* across New Zealand, as predicted by the Metabolic Theory of Ecology. (a) Relationship between ln(life span) and temperature (1/kT, in °K): *O. pullus*: $\ln(\text{life span}) = 0.75\ (\pm 0.33) * \left(\frac{1}{kT}\right) - 27.88\ (\pm 13.33)$, $R^2 = 0.56$, $p < 0.1$; *N. fucicola*: $\ln(\text{life span}) = 0.80\ (\pm 0.16) * \left(\frac{1}{kT}\right) - 29.25\ (\pm 6.43)$, $R^2 = 0.86$, $p < 0.01$. (b) Comparison between *O. pullus* and *N. fucicola* of the regression coefficients (slopes) shown in (a). Dashed lines show predicted mean range for activation energy *E* (MTE).

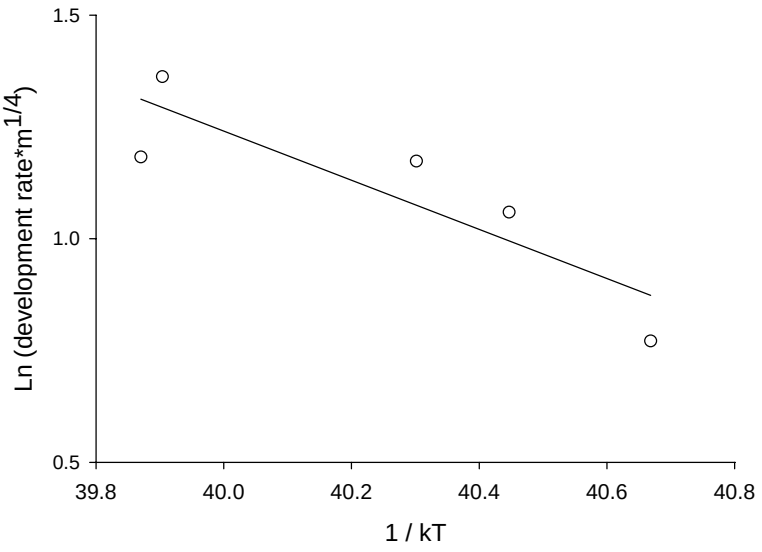

Fig. 5.8: Temperature dependence of early development rate δ (mass-corrected) in *Odax pullus* across New Zealand, as predicted by the Metabolic Theory of Ecology. Development rate (in grams$^{1/4}$.year^{-1}) was estimated as the inverse of time taken to reach 80 – 120 mm (fork length) from individuals aged 0 – 1 year. Temperature is measured in ^{o}K. Least-squares linear regression: $\ln\left(\delta * m^{1/4}\right) = -0.55\ (\pm 0.18) * \left(\frac{1}{kT}\right) + 23.20\ (\pm 7.16)$, $R^2 = 0.76$, $p = 0.054$.

Neurolipofuscin

A total of five older *O. pullus* individuals were processed for neurolipofuscin histology at each of four locations across New Zealand (Hauraki Gulf, D'Urville Is, Fiordland, Stewart Is). Neurolipofuscin-related fluorescence appeared randomly distributed throughout the olfactory region surveyed at the front of the telencephalon (forebrain) (five equidistant points were surveyed for each fish). Histochemistry of the auto-fluorescing vacuoles identified confirmed the presence of lipid compounds, a characteristic component of neurolipofuscin.

Neurolipofuscin fluorescence was identified at all four locations sampled. Analysis of covariance (homogeneity-of-slopes) identified significant differences in mean % neurolipofuscin across age classes (ANCOVA; $F_{1,\ 12} = 179.49$, $p < 0.001$; Table 5.2 A), and neurolipofuscin-fluorescence increased linearly with chronological age across the oldest 40% age classes of the life span (Fig. 5.9 a). The slope of the relationship between neurolipofuscin and age was consistent across all four locations sampled (no significant interaction between age and location(region), Table 5.2 A), suggesting no differences on a local scale in the effect

of age on neurolipofuscin accumulation. In contrast, while there was no difference in overall mean % lipofuscin between regions, the slope of the relationship between neurolipofuscin and age differed significantly between regions ($F_{1, 12} = 16.57$, $p < 0.01$; Table 5.2 A), with faster neurolipofuscin accumulation with age at the two northern locations (Hauraki Gulf, D'Urville Is) than in the two southern locations (Fiordland, Stewart Is) (Fig. 5.9 a).

Maximum ages of *O. pullus* ranged from 11 years in the two northern locations to 17 and 19 years in Fiordland and Stewart Is, respectively (Table 5.1), meaning that the oldest 40% age classes spanned a comparatively greater number of years in populations with greater life spans (greater maximum age) (Fiordland, Stewart Is). This was reflected in similar slopes of neurolipofuscin accumulation across regions when age was measured as a proportion of mean maximum age achieved ($F_{1, 12} = 1.04$, $p = 0.34$; Table 5.2 B), indicating similar rates of neurolipofuscin accumulation over equal proportions of the life span achieved across locations sampled (*i.e.* across temperatures) (Fig. 5.9 b).

Size-scaled mean % neurolipofuscin differed significantly across age classes ($F_{1, 12} = 16.39$, $p < 0.05$; Table 5.2 C), and increased linearly with age at all four locations (Fig 5.9 c). However, the slope of the relationship between size-scaled mean % neurolipofuscin and age did not differ significantly between regions ($F_{1, 12} = 1.26$, $p = 0.36$; Table 5.2 C), suggesting that, when the effect of body size on the relationship between lipofuscin and chronological age was taken into account, there was no difference in neurolipofuscin accumulation rate across locations and regions sampled (*i.e.* across temperatures). Similarly, there was no difference in the slope of the relationship between size-scaled neurolipofuscin and proportion of mean maximum age achieved ($F_{1, 12} = 0.05$, $p = 0.84$; Table 5.2 D), indicating similar rates of neurolipofuscin accumulation per unit of body size over equal proportions of the life span achieved across locations sampled (Fig. 5.9 d). Additionally, individuals aged between 70 and 90 % of mean maximum age (Hauraki Gulf: 6; D'Urville Is: 7; Fiordland: 11 – 13; Stewart Is: 12 years) displayed similar amounts of mean % neurolipofuscin accumulated (one-way ANOVA: $F_{1,3} = 0.69$, $p = 0.61$) (average mean % lipofuscin (70 – 90 % life span) = 0.06 ± 0.006), indicating that older individuals at higher latitude locations show similar amounts of neurolipofuscin accumulated as younger individuals living at lower latitudes.

There was an overall increase in the rate of neurolipofuscin accumulation (slope of the relationship between mean % neurolipofuscin and chronological age) with mean annual sea surface temperature (SST), and SST explained 81% of the variation in neurolipofuscin

accumulation rate across locations, although the effect of SST on neurolipofuscin accumulation was not significant (Fig. 5.10). Similarly, examination of the relationship between neurolipofuscin accumulation rate, development rate and life span showed (i) an overall increase in the rate of neurolipofuscin accumulation with development rate although the relationship was non-significant (Fig. 5.11 a) and (ii) that neurolipofuscin accumulation rate decreased significantly with increasing life span, indicating that faster accumulation rates of neurolipofuscin at warmer temperatures were correlated with shorter life spans (Fig. 5.11 b).

Overall, exploration of the relationship between neurolipofuscin accumulation and chronological age in *O. pullus* revealed four critical points. Firstly, there was a linear increase in neurolipofuscin with age over the second half of the life span (between ~60 & 100% of maximum age), and broad-scale differences in neurolipofuscin accumulation with age were identified along a north – south gradient of latitude, with faster neurolipofuscin accumulation rates in individuals living at warmer temperatures (lower latitudes). Secondly, neurolipofuscin accumulation rate was negatively correlated with life span, with shorter life spans associated with higher neurolipofuscin accumulation rates. Thirdly, neurolipofuscin accumulation rates were affected by differences in body size (growth rate) of individuals across latitudes, suggesting higher neurolipofuscin accumulation associated with faster growth. This was reflected by increasing neurolipofuscin accumulation rates with faster development rates at warmer temperatures (lower latitudes). Fourthly, these results indicate that neurolipofuscin may successfully be used as an age-marker in *O. pullus* for estimation of physiological age (location-specific) and may contribute significantly to the exploration of temperature effects on the relationship between development rate and the rate of ageing (senescence) in this species.

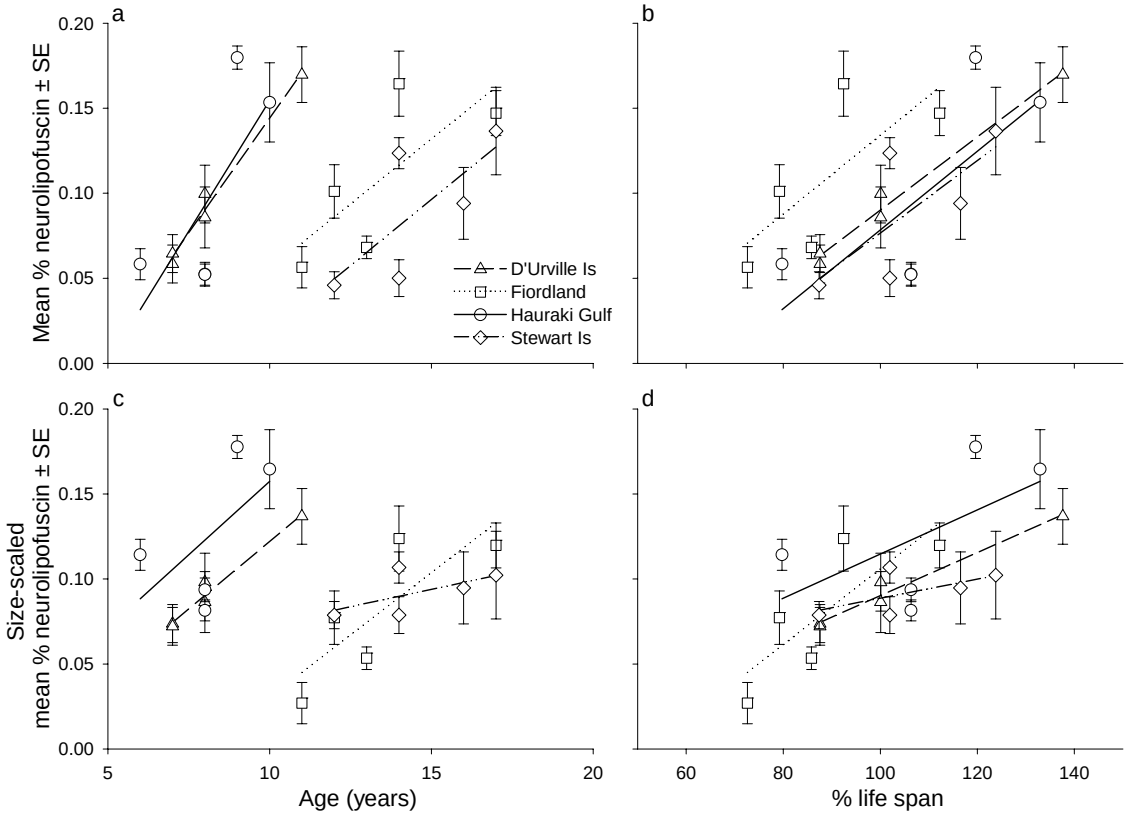

Fig. 5.9: Relationship between neurolipofuscin accumulated in the forebrain of *Odax pullus* and (a, c) chronological age and (b, d) % life span body size across New Zealand. (a, b) show mean % neurolipofuscin and (c, d) show size-scales mean % neurolipofuscin. Mean % neurolipofuscin (presented with standard error) was estimated across five equidistant points within the olfactory region of the telencephalon of each individual fish. Results of analyses of covariance are presented in Table 5.2.

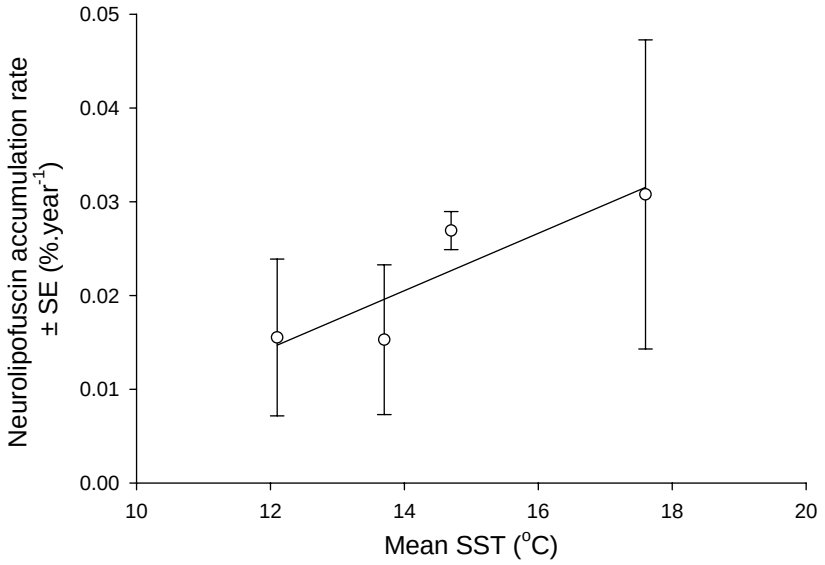

Fig. 5.10: Relationship between neurolipofuscin accumulation rate and mean annual Sea Surface Temperature (SST) in *Odax pullus* across New Zealand. Accumulation rate is estimated from the slope (β) of the relationship between % neurolipofuscin and chronological age found for all four locations examined (Hauraki Gulf: β = 0.0308 ± 0.0165, D'Urville Is: β = 0.0269 ± 0.0020, Fiordland: β = 0.0153 ± 0.0080, and Stewart Is: β = 0.0155 ± 0.0084). Least-squares linear regression is of the form:
$y = 0.0031\ (\pm 0.0011) * x - 0.0227\ (\pm 0.0157)$, $R^2 = 0.81$, $p = 0.10$.

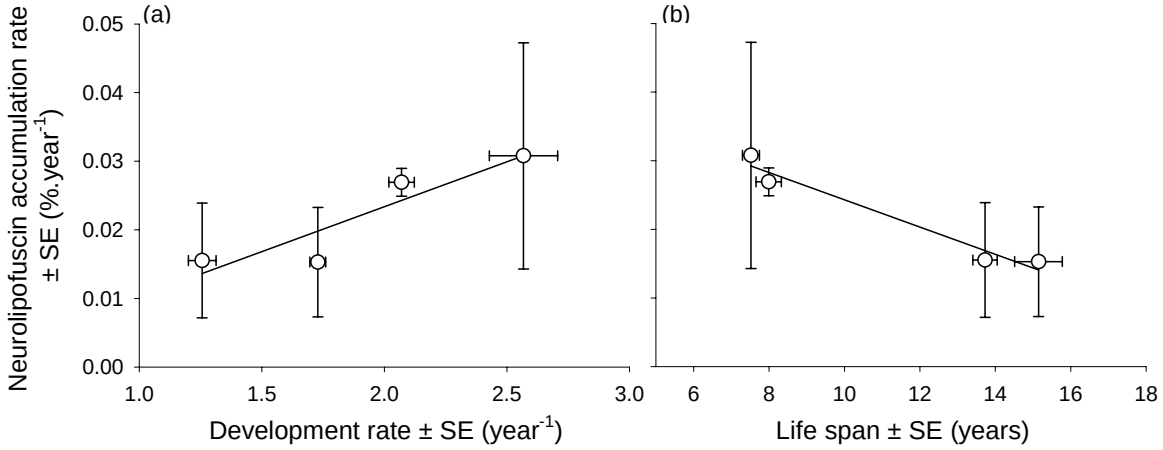

Fig. 5.11: Relationship between neurolipofuscin accumulation rate, (a) development rate and (b) life span (mean maximum age T_{max}) in *Odax pullus* across New Zealand. Neurolipofuscin accumulation rate is the slope (β) of the relationship between % neurolipofuscin and chronological age found for all four locations examined (Hauraki Gulf: β = 0.0308 ± 0.0165, D'Urville Is: β = 0.0269 ± 0.0020, Fiordland: β = 0.0153 ± 0.0080, and Stewart Is: β = 0.0155 ± 0.0084). Least-squares linear regressions are of the form:
(a) $y = 0.0131\ (\pm 0.0041) * x - 0.0029\ (\pm 0.0080)$, $R^2 = 0.84$, $p = 0.085$;
(b) $y = -0.0020\ (\pm 0.0003) * x + 0.0441\ (\pm 0.0034)$, $R^2 = 0.96$, $p < 0.05$.

Table 5.2: Analysis of covariance (homogeneity-of-slopes) examining the relationship between % neurolipofuscin detected in the telencephalon (olfactory region) of *Odax pullus* and (A) age and (B) % of life span across New Zealand.
Two spatial scales are examined: across geographical regions (North, South) and across locations (Hauraki Gulf, D'Urville Is, Fiordland, Stewart Is). Age is chronological age (in years), and % life span is percent of mean maximum age (10% oldest individuals) recorded at each location. Significant results are shown in bold ($p < 0.05$).

Mean % neurolipofuscin

A. Age

Effect	SS	df	F	*p*
Intercept	0.00706	1	57.36	< ***0.001***
Region	0.00005	1	0.43	*0.53*
Location (region)	0.00012	2	0.05	*0.95*
Age	0.02455	1	179.49	< ***0.001***
Age * Region	0.00227	1	16.57	< ***0.01***
Age * Location (region)	0.00007	2	0.03	*0.97*
Error	0.01456	12		

B. % Life span

Effect	SS	df	F	*p*
Intercept	0.00706	1	57.36	< ***0.001***
Region	0.00005	1	0.43	*0.53*
Location (region)	0.00012	2	0.05	*0.95*
% life span	0.22342	1	172.06	< ***0.001***
% life span * Region	0.00000	1	0.0009	*0.98*
% life span * Location (region)	0.00004	2	0.015	*0.99*
Error	0.01456	12		

Size-scaled mean % neurolipofuscin (.mm FL^{-1})

C. Age

Effect	SS	df	F	*p*
Intercept	0.00049	1	0.97	*0.42*
Region	0.00003	1	0.054	*0.84*
Location (region)	0.00100	2	0.79	*0.48*
Age	0.00843	1	16.39	< ***0.05***
Age * Region	0.00065	1	1.26	*0.36*
Age * Location (region)	0.00101	2	0.79	*0.48*
Error	0.00766	12		

D. % Life span

Effect	SS	df	F	*p*
Intercept	0.00049	1	0.97	*0.42*
Region	0.00003	1	0.05	*0.84*
Location (region)	0.00100	2	0.79	*0.48*
% life span	0.00804	1	13.40	< ***0.05***
% life span * Region	0.00001	1	0.02	*0.89*
% life span * Location (region)	0.00119	2	0.93	*0.42*
Error	0.00766	12		

5.4 Discussion

This chapter explored the relationship between life span, the rate of physiological ageing (senescence) and environmental temperature in *Odax pullus*, over ~13^{o} of latitude. A strong demographic signal was identified in the response of life span to temperature in this

species, with extended life spans at higher latitudes. The effect of temperature on life span was consistent with the predictions of the Metabolic Theory of Ecology (MTE), suggesting that greater life spans at higher latitudes (colder temperatures) may be linked to the underlying effect(s) of temperature on metabolic rate in this species (Gillooly *et al.*, 2001; Brown *et al.*, 2004). Examination of the effect of temperature on neurolipofuscin accumulation rate, a measure of metabolically-induced oxidative damage, suggested a comparatively slower rate of ageing (neurolipofuscin accumulation) over the last 40% of the life span in individuals living at colder temperatures (higher latitudes). Slower rates of oxidative damage accumulation at higher latitudes were correlated with reduced development rates, with individuals developing faster in the initial part of the life span, ageing faster and displaying shorter life spans at warmer temperatures, a pattern coinciding with the "oxidative stress" hypothesis of ageing (Pearl, 1928; Finkel and Holbrook, 2000). These results provide support for the presence of a mechanistic (physiological) response of life spans to temperature (latitude) as a contributing factor underlying the patterns of intra-specific variation in longevity across latitudes. The discussion will review the association of senescence, life span and temperature in *O. pullus*, and consider the relationship between life span and latitude in the context of the responses in growth and development rates to temperature.

A significant correlation between life span and temperature was identified in *O. pullus*, with individuals achieving maximum ages up to 48% greater at colder temperatures (higher latitudes). Comparison of the two species revealed a similar response of increased longevity (up to 35% greater maximum ages) at higher latitudes in *Notolabrus fucicola*. The relationship between life span and latitude was consistent with the predictions of the MTE in both *O. pullus* and *N. fucicola*, with activation energy values that fell within the predicted range of 0.2 – 1.2 eV, suggesting that reduced metabolic rates at colder temperatures may play a role in shaping the pattern of increased life spans at higher latitudes in the study species. In ectotherms, metabolic rates are influenced by environmental temperature regimes, with individuals living at colder temperature generally displaying reduced metabolic rates. Although there is some debate as to some of the assumptions of the MTE, primarily with regard to a unifying mechanistic principle that would explain the effect of temperature on all aspects of metabolism (and ensuing biological rates), the use of the MTE has proven, in many cases, to be useful in predicting the response of biological rates to temperature (Gillooly *et al.*, 2001; Brown *et al.*, 2004; Clarke and Fraser, 2004; Clarke, 2006; Gillooly *et al.*, 2006;

Irlich *et al.*, 2009). As the relationship between life span and temperature in both study species was consistent with the predictions of the MTE, we may hypothesise that increased life spans at higher latitudes may be linked to reduced metabolic rates at colder temperatures, a result which coincides with a ubiquitous pattern seen across a range of ectothermic taxa, including many species of fishes (Munch and Salinas, 2009).

Aerobic metabolism is intrinsically associated with the production of oxidative damage, which is thought to contribute to the physiological processes of ageing (senescence), and the positive correlation between oxidative damage and intrinsic mortality rate (rate of ageing) is at the basis of the "oxidative-stress" hypothesis of ageing (Finkel and Holbrook, 2000). A corollary of this is that we may expect lower metabolic rates at colder temperatures to be associated with reduced oxidative stress, and thus to result in lower rates of senescence and extended life spans. Examination of the patterns of accumulation of the age-pigment neurolipofuscin in *O. pullus* revealed significant differences in the rate of oxidative damage accumulation along a broad north – south geographical scale, with comparatively slower rates of neurolipofuscin accumulation in the southern regions (Fiordland and Stewart Is) than in northern locations (Hauraki Gulf and D'Urville Is). If metabolic rates are reduced at lower temperatures (higher latitudes) as suggested by the predictions of the MTE, these findings suggest that reduced metabolic rates at colder temperatures may be correlated with a slower rate of ageing in *O. pullus*. Neurolipofuscin accumulation rate was also negatively correlated with life span, a pattern which coincides with the suggestion that reduced senescence rates may play a role in increasing life spans at higher latitudes.

Senescence may be defined as an "age-specific decline in the probability of survival or reproduction caused by a progressive physiological deterioration" (Reznick, 1997). In this context, increased life spans at higher latitudes may be the result of (i) a deferred onset of senescence, by which the onset of the decrease in survival and reproductive functions is delayed, (ii) the result of a decrease in the rate of senescence, whereby the rate at which survival and reproductive functions decrease with age is comparatively lower, or (iii) a combination of these two mechanisms. Examination of neurolipofuscin accumulation over the last 50% of the life span in *O. pullus* suggested the presence of similar amounts across latitudes of oxidative damage accumulated at 50 – 75% of the life span (maximum age). As individuals achieved significantly different maximum ages across latitudes, however, this timing corresponded to different absolute (chronological) ages, suggesting that *O. pullus*

individuals of six and seven years of age living in the northern locations (Hauraki Gulf, D'Urville Is) showed similar amounts of oxidative damage as 11 – 13 year old individuals living the southern locations of Stewart Is and Fiordland. These patterns were associated with significant differences in the rate of neurolipofuscin accumulation over the oldest 40% age classes of the life span along a north – south gradient, with comparatively slower rates of neurolipofuscin accumulation in individuals living at the southern end of the species' distributional range. Although the first 50% of the life spans were not examined in this study, the present initial exploration of the patterns of neurolipofuscin accumulation in *O. pullus* indicate that increased life spans at higher latitudes (colder temperatures) may be the result of a combination between a delay in the onset of senescence-related physiological processes and a reduction in the rate at which oxidative damage accumulated with age in the study species.

Intrinsic mortality rates are likely to reflect a range of physiological conditions other than those directly relating to environmental temperature, including that of reproductive growth, dietary restriction, or somatic growth and development rates, which have all been shown to correlate with life span (Metcalfe and Monaghan, 2003; Partridge and Brand, 2005; Ruttenberg *et al.*, 2005). Ruttenberg et al. (2005) showed that temperature-mediated reproductive outputs were a cause of increased adult mortality rates, thereby suggesting that greater reproductive expenditures at warmer temperatures may underlie reduced life expectancy. No differences were detected in the amount of energy allocated to reproductive growth across latitudes in *O. pullus*, however, with similar ovary weights for any given body size across latitudes sampled (Chapter 4), suggesting that changes in reproductive effort are unlikely to be directly linked to the pattern of reduced life spans at lower latitudes in the study species. Alternatively, it has been proposed that dietary restriction extends life expectancy by delaying the onset of senescence-related damage and decreasing the rate of ageing (Partridge and Brand, 2005; Partridge *et al.*, 2005b). If longer life spans were associated with conditions of dietary restriction in *O. pullus*, we would expect conditions of lower food availability or increased nutrient stress at higher latitudes (colder temperatures). There was no evidence in the study species, however, for the presence of a reduction in the abundance of preferred food items or for the presence of a temperature-constraint on the digestion of herbivorous material at higher latitudes (Chapter 4), indicating that dietary restriction is unlikely to play a role in extending life spans at higher latitudes in *O. pullus*. Furthermore, preliminary analyses of the nutritional ecology of this species suggest no

changes in nutrient ratios across latitudes, particularly in terms of protein-to-carbohydrate ratios, which have been proposed to affect life spans in other ectotherms (Lee *et al.*, 2008).

The rate of neurolipofuscin accumulation (rate of ageing) was positively correlated with development rate, with individuals living at warmer temperature growing faster, maturing earlier, and ageing faster, and differences in growth across latitudes directly affected the rate of neurolipofuscin accumulation. This finding coincides with the pattern found across many ectothermic species, and provides support for the hypothesis of a trade-off between development rate, in terms of somatic and/or reproductive growth, and life span (Metcalfe and Monaghan, 2003; Partridge *et al.*, 2005a). Although the proximate mechanisms underlying the correlation between development (growth) rate and life span have yet to be resolved, two principal lines of thought are developing (Metcalfe and Monaghan, 2003; Partridge *et al.*, 2005a; Monaghan *et al.*, 2009). First, it is hypothesised that, in the context of a trade-off in resource allocation to the functions of growth, reproduction, and maintenance (including repair mechanisms), fast growth and earlier maturation at warm temperatures may divert energy from that available to maintenance processes, thus increasing the accumulation of senescence-related damage and leading to earlier death. An alternative view is that the physiological processes associated with reproduction directly incur somatic damage and cause earlier death (Barnes and Partridge, 2003; Harshman and Zera, 2007). Disentangling the possibilities of a direct effect of temperature on life span (senescence-related processes; oxidative stress hypothesis) on the one hand, and of an indirect effect via temperature-related consequences of development rate (somatic or reproductive growth) on damage accumulation processes (ageing) on the other will provide a rewarding field for future research.

This study identified intraspecific changes in life span in *O. pullus* over a gradient of latitude and explored the hypothesis that temperature-mediated ageing processes (senescence) may contribute to explaining latitudinal changes in mortality schedules. Differences in oxidative damage (neurolipofuscin) accumulation rates were identified on a broad latitudinal scale, with individuals living in the southern regions ageing at a slower rate, a trend which was associated with life spans that were extended by over 40%. Increased rates of ageing and shorter life spans at lower latitudes (warmer temperatures) were correlated with faster development rates and earlier maturity in *O. pullus*, a pattern which coincides with the concept central to the oxidative-stress hypothesis of ageing, that of “live fast – die young”. As oxidative damage is the product of a balance between the rate of Reactive Oxygen Species

(ROS) production per unit of oxygen consumed and the capacity to neutralise the effects of ROS production (anti-oxidant), further analysis of the contribution of oxidative damage to intraspecific changes in life spans over gradients of latitude will need to be coupled with the examination of the relationship between metabolic rate, ROS production and anti-oxidant capacities (Monaghan *et al.*, 2009). It will also prove interesting to identify predation pressures for *O. pullus*, and to examine the contribution of predation levels to shaping the response of life spans in this species (Ricklefs, 2008).

Chapter 6. General Discussion

This thesis addressed two primary issues concerning the demography and life history of *Odax pullus*: firstly, the response of ectotherm life history traits to environmental temperature over a gradient of latitude, and secondly, that of the demographic performance of an herbivorous ectotherm in response to varying temperature. The demography and life history of *O. pullus* was examined across ~13^{o} of latitude (1,600 km) and covered ~5^{o}C in mean annual sea surface temperature difference and over 85% of the species' distributional range. The analysis was age based following the successful validation of both annual and daily growth increments (Chapter 2). In Chapter 3, I combined gonad histology and age-based demographic information to establish the sexual ontogeny, patterns of male and female recruitment, and schedules of sexual maturation and reproductive development of *O. pullus* to establish monandric protogynous sex change. Chapters 2 & 3 thus provided essential information for the comparative analysis of size- and age-based life histories across latitudes (Chapter 4) and for the analysis of the relationship between chronological and physiological age (rate of ageing), life span, and latitude (Chapter 5). I first highlight the key findings of my thesis and discuss their significance, and then identify what I consider to be priority areas for future research.

Key findings & significance

Comparative analysis of the response of life history traits of *O. pullus* to latitude identified significant trends over the main North-South axis of the sampled distributional range (Chapter 4). There was a response of slower growth, delayed development (increased age-at-maturity and at-sex change), greater adult body size, and extended life span at higher latitudes. The main effects of latitude were seen in the phenotypic response of life histories to changes in environmental temperature on a broad latitudinal scale, a pattern which is described by the "Hotter is smaller" rule (Kingsolver and Huey, 2008). These responses coincided with the slope of the thermal reactions norms for growth, development, body size, and longevity documented in a majority of ectothermic taxa (Atkinson, 1994; Angilletta, 2009; Munch and Salinas, 2009). Similar trends were also identified in a phylogenetically related species *Notolabrus fucicola*, a temperate labrid which is exclusively carnivorous. The responses in growth, development, and body size of *O. pullus* provided no support for the

temperature-based constraint on herbivory at high latitudes suggested by Gaines and Lubchenco (1982), Harmelin-Vivien (2002), Behrens (2005), Floeter *et al.* (2005), and Behrens and Lafferty (2007). My findings thus establish a basis for re-evaluating the presence of a 'temperature-constraint' in ectothermic herbivores living at high latitudes (cold temperatures), and for re-considering the contribution of the temperature-constraint hypothesis to explaining the biogeographic distribution of herbivory in marine systems (Clements *et al.*, 2009).

Greater life expectancies at higher latitudes were associated with a slower rate of ageing (Chapter 5), suggesting that temperature-mediated ageing processes are likely to contribute to latitudinal changes in mortality schedules. This result is significant in that it represents a novel approach to the examination of intraspecific latitudinal gradients in life span and provides support for the hypothesis that temperature (and its effects on metabolic and/or development rates) plays a critical role in the determination of life spans in ectotherms as suggested in Munch and Salinas (2009). Furthermore, the present study provides grounds for further investigation of the relationship between life span and metabolically- and growth-induced changes in ageing-related processes, particularly in terms of the contribution of development- and temperature-related senescence processes to changes in mortality schedules in species distributed over wide spatial scales. As life spans are intrinsically linked with development rate (age-at-maturity) and impact on generation time and lifetime reproductive output (and ultimately on population increase), these results have direct implications for our understanding of the proximate mechanisms underlying the response of ectotherm life history traits over gradients of latitude.

The sampling regime of this study covered the majority of the species distributional range and examined the effects of a range of environmental and ecological factors, including temperature, abundance, food and habitat availability, exposure, and extrinsic mortality pressure, which have all been shown to affect life histories at a range of spatial scales (Gust *et al.*, 2001; Meekan *et al.*, 2001; Choat and Robertson, 2002; Gust *et al.*, 2002; Choat *et al.*, 2003; Robertson *et al.*, 2005; Ruttenberg *et al.*, 2005; Trip *et al.*, 2008). This allowed me to distinguish the effects of environmental temperature across latitudes from those of potentially confounding factors. A critical point arising from this study is that the effects of intrinsic (*e.g.* physiological response(s) to temperature) and extrinsic (*e.g.* density and resource availability) factors on the response of life history traits are seen over different spatial scales. While

changes in environmental temperature will be apparent over broad gradients of latitude, as seen in the response of ectotherm life spans across latitudes (Munch and Salinas, 2009), ecological factors will be manifested in a patchy fashion at local or regional spatial scales (*e.g.* Ruttenberg *et al.*, 2005). Moreover, an integrative approach that investigated all key aspects of the study species' life history (somatic growth, development, body size and life span) provided a basis for interpreting the dynamics underlying the response to latitudinal change. Additionally, this work also provides the first comprehensive analysis of the life history and reproductive biology of an odacine labrid, an important endemic herbivorous element of the south-eastern hemisphere fish fauna.

Future directions

A central aspect of this thesis is the use of a life history approach to explore the paradigm that herbivorous fishes are constrained by temperature at higher latitudes. The idea of a temperature-based constraint on herbivory was first suggested by Gaines and Lubchenco (1982) to explain the relative rarity of herbivorous fishes in temperate and polar environments, and this view has since become widespread (*e.g.* Harmelin-Vivien, 2002; Behrens, 2005; Floeter *et al.*, 2005; Behrens and Lafferty, 2007). This hypothesis is based on a number of assumptions, however, which have largely drawn from the literature on terrestrial herbivorous ectotherms, and the processes governing herbivory in marine systems are likely to differ from those in terrestrial environments (Choat and Clements, 1998; Clements *et al.*, 2009). Firstly, algae differ from terrestrial plants in the proportion of structural carbohydrates present as well as in biochemical composition, and there is no evidence to suggest that algae provide a 'low-quality' diet (*e.g.* Smit *et al.*, 2006). Second, the presence of fermentative processes involved in the digestion of algal material has been hypothesised to be limiting at cooler temperatures (*e.g.* Behrens 2005). However, while many herbivorous terrestrial ectotherms (*e.g.* lizards) rely heavily on the presence of gut endosymbionts for the digestion of algal material, the presence of fermentative processes in herbivorous fishes varies greatly among species (Mountfort *et al.*, 2002; Choat *et al.*, 2004; Crossman *et al.*, 2005; Skea *et al.*, 2005; 2007; Clements *et al.*, 2009). Third, the stability of the thermal environment and the constancy of food availability are greater in marine than in terrestrial systems, indicating that 'adaptation or acclimation of gastrointestinal communities is likely to be far less of a problem for marine herbivorous fishes than terrestrial herbivorous

ectotherms' (Clements *et al.*, 2009). In this thesis, no support was found for the hypothesis of a temperature-based constraint on herbivory in the marine herbivorous fish *O. pullus*. This finding adds to the emerging body of work on herbivory in marine ectotherms and to the view of Clements et al. (2009) that an integrative understanding of the nutritional ecology is needed before conclusions can be made as to the processes underlying the biogeography and evolution of marine herbivorous fishes. Examination of the nutritional ecology of *O. pullus* over its distributional range will provide new insights into the understanding of herbivory in marine systems. It will be particularly interesting to establish whether nutrient intake and assimilation patterns of *O. pullus* differ across latitudes, whether cooler latitudes are associated with a shift in the nutrient-ratios targeted, and whether higher latitudes are coupled with differences in the gastrointestinal communities or in the degree to which individuals rely on hindgut fermentation. It will also prove particularly interesting to relate the diet, nutrient intake and assimilation patterns to the patterns of variation in life history traits shown in this work, particularly in terms of the patterns of growth and maturation rates.

Understanding the nutritional processes underlying herbivory in marine systems will provide critical information for assessing the impact of herbivorous fishes, a subject which has received great amounts of attention particularly in the context of coral reefs (Clements *et al.*, 2009). *O. pullus* is a conspicuous herbivorous fish within New Zealand temperate reef systems, and may play an important role in shaping the local and regional distribution of large brown algal populations (Taylor and Schiel, 2009). A number of questions, however, remain to be answered regarding the ecology of this species, particularly in terms of the relationship between abundance and distribution patterns, short- and long-term changes in algal communities (habitat and food availability), recruitment and/or settlement success and mortality rates. Identifying the principal causes of extrinsic mortality (*e.g.* predator species) and how these may affect different life history stages (juvenile and adult mortality) will also help provide insights into the contribution of extrinsic environmental factors to shaping the patterns seen in the responses of growth and maturation rates, body size and life span across spatial scales. Furthermore, a genetic analysis of the population structure of O. *pullus* will provide information as to the patterns of larval dispersal and the possibility of adaptive and/or phenotypic factors driving the life history patterns seen in this study.

The processes underlying the thermal reaction norms of growth, body size, development and life span (rate of ageing), whether reflecting local adaptive differences or

plastic physiological responses, have yet to be resolved. This thesis highlights two main challenges that have been previously identified: firstly, that of the mechanism(s) underlying the inverse relationship between growth rate and body size in response to changes in temperature ("life history puzzle") (Angilletta *et al.*, 2004). This challenge is significant as it is at the basis of the Temperature-Size Rule ("Hotter is smaller"), a response which is shared amongst a majority of ectothermic taxa (Atkinson, 1994; Angilletta, 2009). A number of hypotheses have been proposed, amongst which the possibility that fast growth may result in small final size as a result of differential thermal sensitivities in growth and development rate (van der Have and de Jong, 1996; de Jong and van der Have, 2009), or as the result of a differential effect of temperature on the rates of cell division and cell growth (Partridge *et al.*, 1994; Partridge and French, 1996; van Voorhies, 1996). Secondly, while considerable advances have been made as to the understanding of the deleterious effects of ageing on a molecular and cellular level (*e.g.* oxidative damage, lipid peroxidation, telomere abraison), comparatively little is known about (i) the processes (*e.g.* environmental) which govern the production and accumulation of ageing-related damage and (ii) how these affect mortality rates and life spans, particularly in wild ectothermic populations distributed over wide spatial scales.

Partridge and Gems (2002) explored the link between life span (rate of ageing) and the insulin/Insulin-like Growth Factor (IGF) signalling pathway. The authors showed that increased rates of insulin/IGF production lead to an increase in the rate of ageing and earlier death, and that this mechanism is likely to be mediated by environmental factors (*e.g.* dietary restriction) through a trade-off between reproductive rate and life span, in both ectotherms and mammals. The IGF system is also thought to be involved in mediating a trade-off between growth rate and life span, by which growth rate may directly affect the rate of ageing (Metcalfe and Monaghan, 2003). In fish, the Growth Hormone/IGF (GH/IGF) system is involved in larval development, somatic growth, and gonad maturation (Duan, 1997; Mommsen, 2001; Wood *et al.*, 2005), while in mammals, IGF levels have been shown to increase with age until maturity followed by a subsequent fall throughout adulthood (Juul *et al.*, 1994). A critical point arising here is that the GH/IGF signalling pathway appears to be involved in a number of aspects of the latitudinal response of ectothermic life histories to temperature ("Hotter is smaller"), namely those of somatic growth rate, maturation rate (development), and the rate of ageing (life span or intrinsic mortality). In the context of this study, we may thus hypothesise a scenario by which increased production of GH/IGF at

warmer temperatures (lower latitudes) may be intrinsically linked with a response of faster growth and maturation rates, thus leading to earlier maturity, smaller adult body size, and a faster rate of ageing (earlier death). Partridge and colleagues proposed that a better understanding of the mechanisms underlying the GH/IGF signalling pathway may allow greater insight into the evolution of ageing. Here, we may hypothesise that exploration of the relationship between the GH/IGF signalling pathway, growth, development, body size and ageing-related processes in wild populations of widely distributed ectotherms may help understand the response of life histories over gradients of latitude in ectotherms. Additionally, examination of the response of the GH/IGF pathway to environmental changes in both food availability and temperature may provide valuable new research directions for the investigation of the differential responses in growth rate and body size to those two environmental cues ("life history puzzle", Berrigan and Charnov 1994).

Finally, the links between nutrition, temperature, and the rate of ageing, and how these relate to reproductive performance and development rate represent an important area for future research. Temperature and nutrition are both strong predictors of reproductive rate and life span, but the underlying functional and mechanistic effects of these two environmental cues have yet to be resolved. In particular, disentangling the differential effects of nutrient intake on lifetime reproductive output and on the rate of ageing in species distributed over wide spatial scales will provide essential information for our understanding of how these interact with the effects of environmental temperature, and, ultimately, of the dynamics underlying the trade-off between life span and reproduction over gradients of latitude (Simpson and Raubenheimer, 2007; Lee *et al.*, 2008). The life history data reported in this thesis are linked to a study in which nutrient intake, assimilation, and utilisation efficiencies were measured for the same fish included in the present analyses. Examination of the relationship between nutrition, development rate, oxidative damage accumulation rate (rate of ageing) and associated life history traits across latitudes may shed some light in the near future on this question for temperate marine fishes.

Appendices

Appendix 1: Mean abundance of *Odax pullus* and *Notolabrus fucicola* across New Zealand. (A) Abundance estimates collected in this study at Karikari, Poor Knights Is, Hauraki Gulf, D'Urville Is, and Stewart Is; and (B) Abundance estimates from Choat and Ayling (1987) in Wellington; and Schiel and Hickford (2001) in Fiordland. Abundance is expressed in number of individuals per 300 m^2 with Standard Error (SE). Number of transects performed at each location are presented in brackets.

A.

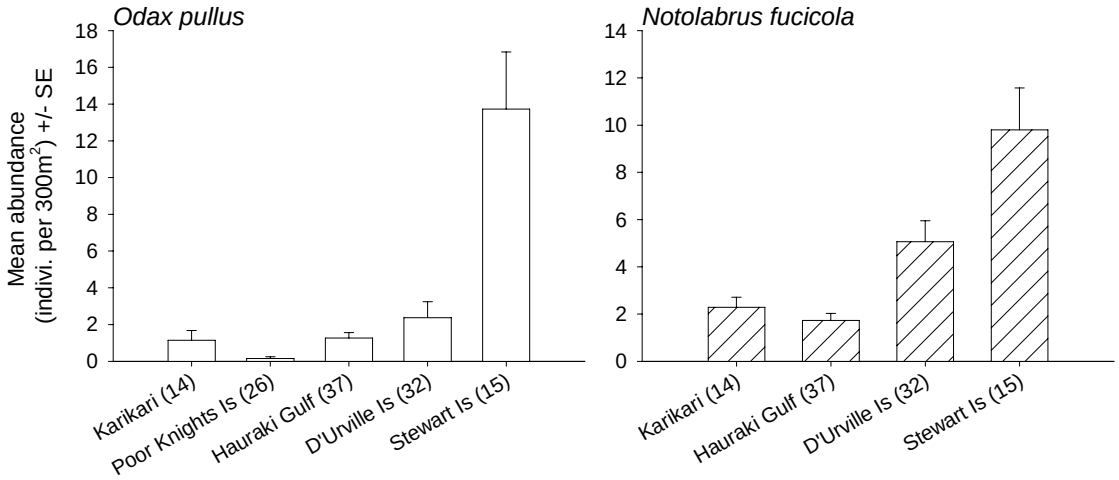

B.

Location	Mean abundance (indiv. per 300 m^2) +/- SE		Source
	Odax pullus	*Notolabrus fucicola*	
Wellington	11.2 +/- 3.1	10.9 +/- 2.6	Choat and Ayling (1987)
Fiordland	0.06 +/- 0.02	9.5 +/- 1.5	Schiel and Hickford (2001)

Appendix 2: Estimated commercial and recreational fishing effort for *Odax pullus* across locations sampled.
Data presented were taken from the New Zealand Ministry of Fisheries report 2008. The Poor Knights Islands have been a no-take marine reserve since 1981.

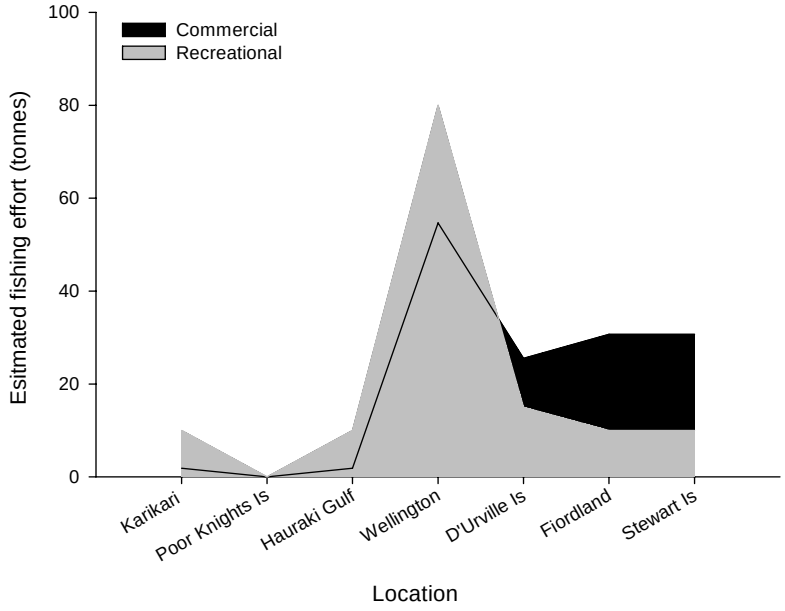

Appendix 3: Relationship between forebrain (telencephalon) weight and (a) body size, (b) gutted weight, and (c) age across locations (left hand panel) and between the sexes (right hand panel) in *Odax pullus* across New Zealand.

Best-fit least-squares regression lines are fitted: (a) Hauraki Gulf: $y = 0.00042\,x - 0.060$ ($r^2 = 0.79$); D'Urville Is: $y = 0.00043\,x - 0.059$ ($r^2 = 0.82$); Stewart Is: $y = 0.00039\,x - 0.040$ ($r^2 = 0.78$); (b) Hauraki Gulf: $y = 0.0031\,x^{0.54}$ ($r^2 = 0.75$); D'Urville Is: $y = 0.0033\,x^{0.53}$ ($r^2 = 0.88$); Stewart Is: $y = 0.0067\,x^{0.42}$ ($r^2 = 0.80$); (c) Hauraki Gulf: $y = 0.044\,x^{0.60}$ ($r^2 = 0.79$); D'Urville Is: $y = 0.040\,x^{0.71}$ ($r^2 = 0.82$); Stewart Is: $y = 0.031\,x^{0.68}$ ($r^2 = 0.76$). (i) Females: $y = 0.00040\,x - 0.049$ ($r^2 = 0.81$); Males: $y = 0.00045\,x - 0.067$ ($r^2 = 0.48$); (ii) Females: $y = 0.0047\,x^{0.47}$ ($r^2 = 0.84$); Males: $y = 0.0041\,x^{0.49}$ ($r^2 = 0.49$); (iii) Females: $y = 0.0040\,x^{0.59}$ ($r^2 = 0.73$); Males: $y = 0.062\,x^{0.42}$ ($r^2 = 0.31$).

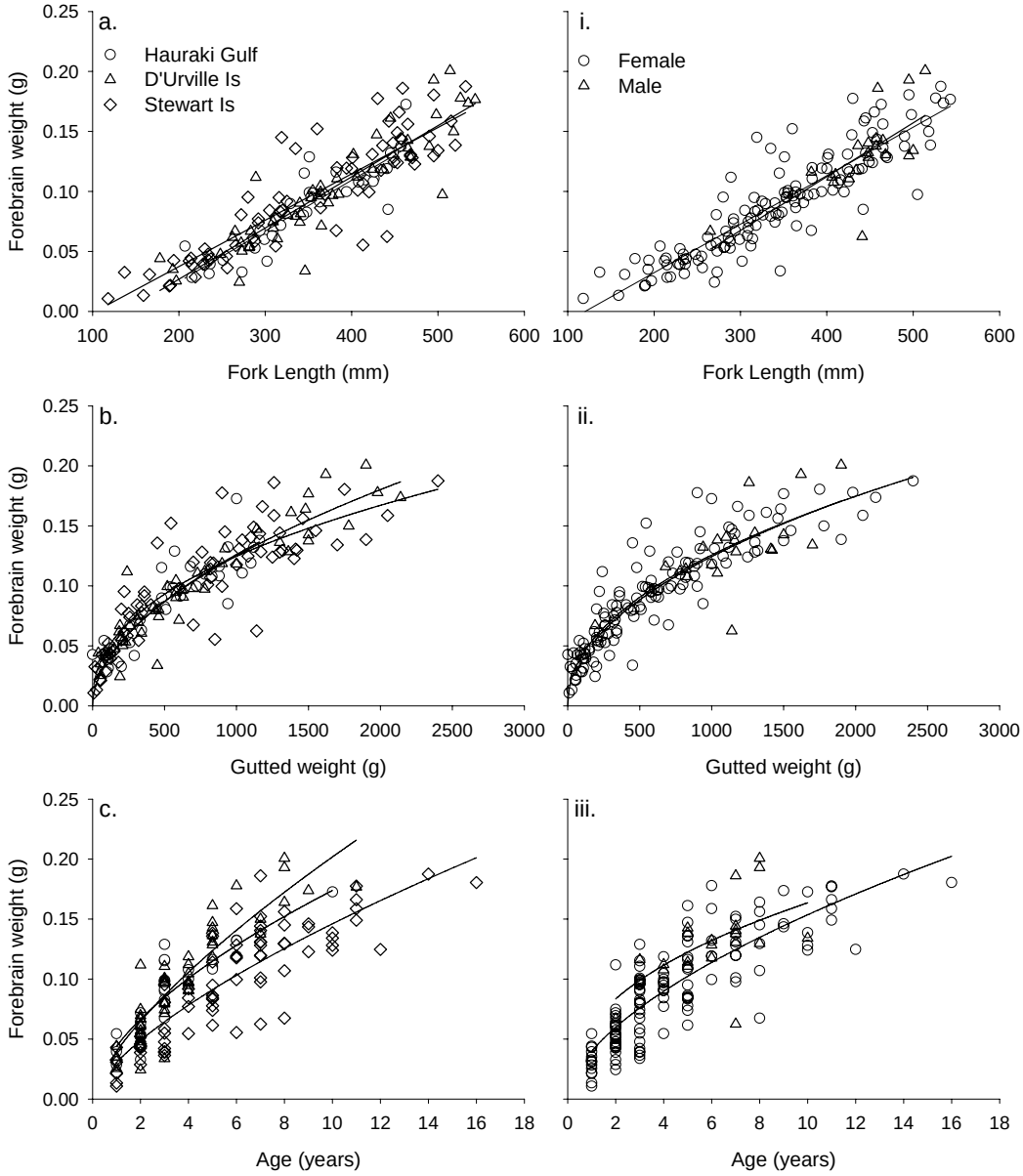

References

Adams, S. & Choat, J. H. (2002). The reproductive ecology of epinepheline Serranids. *Program booklet for the reproductive analysis of harvested epinepheline serranids, Sultanate of Oman, 3-28 June 2002*.

Allsop, D. J. & West, S. A. (2003a). Changing sex at the same relative body size. *Nature* **425**, 783-784.

Allsop, D. J. & West, S. A. (2003b). Constant relative age and size at sex change for sequentially hermaphroditic fish. *Journal of Evolutionary Biology* **16**, 921-929.

Allsop, D. J. & West, S. A. (2004). Sex change and relative body size in animals - Reply. *Nature* **428**, 2.

Angilletta, M. J. (2009). Thermal adaptation: a theoretical and empirical synthesis. *Oxford University Press, New York, USA*.

Angilletta, M. J., Sears, M. W. & Steury, T. D. (2004). Temperature, growth rate, and body size in ectotherms: Fitting pieces of a life history puzzle. *Integrative and Comparative Biology* **44**, 498-509.

Arendt, J. D. & Wilson, D. S. (1999). Countergradient selection for rapid growth in pumpkinseed sunfish: Disentangling ecological and evolutionary effects. *Ecology* **80**, 2793-2798.

Ashton, K. G. & Feldman, C. R. (2003). Bergmann's rule in nonavian reptiles: turtles follow it, lizards and snakes reverse it *Evolution* **57**, 1151-1163.

Asoh, K. & Yoshikawa, T. (2003). Gonadal development and an indication of functional protogyny in the Indian damselfish (*Dascyllus carneus*). *Journal of Zoology* **260**, 23-39.

Atkinson, D. (1994). Temperature and organism size - a biological law for ectotherms? *Advances in ecological research* **25**, 1-58.

Atkinson, D. (1996). Ectotherm like history responses to developmental temperature. *In: Animals and Temperature, Johnston IA & Bennett AF (Eds), Cambridge University Press, Cambridge (UK)*.

Atkinson, D. & Sibly, R. M. (1997). Why are organisms usually bigger in colder environments - making sense of a life history puzzle. *Trends in Ecology & Evolution* **12**, 235-239.

Bader, C. (1998). The ecology of the butterfish *Odax pullus* around the Kaikoura Peninsula. *MSc thesis, University of Canterbury, New Zealand*.

Barnes, A. I. & Partridge, L. (2003). Costing reproduction. *Animal Behaviour* **66**, 199-204.

Barrett, N. S. (1995). Aspects of the biology and ecology of six temperate reef fishes (Families: Labridae and Monacanthidae). *PhD Thesis, University of Tasmania, Australia*.

Bauchot, R., Ridet, J.-M. & Bauchot, M.-L. (1989). The brain organization of butterflyfishes. *Environmental Biology of Fishes* **25**, 205-219.

Beamish, R. J. & McFarlane, G. A. (1983). The forgotten requirement for age validation in fisheries biology. *Transactions of the American Fisheries Society* **112**, 735-743.

Beamish, R. J. & McFarlane, G. A. (1987). Current trends in age determination methodolgy. *In: Age and Growth of fish. Summerfelt, R.C. & Hall, G.E. (Eds), Iowa State University Press, Ames, Iowa, USA*.

Beckman, D. W. & Wilson, C. A. (1995). Seasonal timing of opaque zone formation in fish otoliths. *In: Recent developments in fish otolith research. Secor, D.H., Dean, J.M. and Campana, S.E. (Editors). The Belle W. Baruch library in Marine Science Number 19. University of South Carolina.*, 27-43.

Beckman, K. B. & Ames, B. N. (1998). The free radical theory of aging matures. *Physiological Reviews* **78**, 547-581.

Begg, G. A., Campana, S. E., Fowler, A. J. & Suthers, I. M. (2005). Fish otolith research and application: current directions in innovation and implementation. *Marine and Freshwater Research* **56**, 477-483.

Behrens, M. D. (2005). Evidence for physiological drivers of herbivorous fish diversity. *PhD Thesis, University of California, Santa Barbara (USA)*.

Behrens, M. D. & Lafferty, K. D. (2007). Temperature and diet effects on omnivorous fish performance: implications for the latitudinal diversity gradient in herbivorous fishes. *Canadian Journal of Fisheries and Aquatic Sciences* **64**, 867-873.

Bergmann, C. (1847). Ueber die Verhaltnisse der Warmeokonomie der Thiere zu ihrer Grosse. *Gottinger studien* **3**, 595-708.

Berkeley, S. A., Chapman, C. & Sogard, S. M. (2004). Maternal age as a determinant of larval growth and survival in a marine fish, *Sebastes melanops*. *Ecology* **85**, 1258-1264.

Bernays, E. A. (1997). Feeding by lepidopteran larvae is dangerous. *Ecological Entomology* **22**, 121-123.

Berrigan, D. & Charnov, E. L. (1994). Reaction norms for age and size at maturity in response to temperature: a puzzle for life historians. *Oikos* **70**, 474-478.

Berumen, M. L. (2005). The importance of juveniles in modelling growth: butterflyfish at Lizard Island. *Environmental Biology of Fishes* **72**, 409-413.

Blackburn, T. M., Gaston, K. J. & Loder, N. (1999). Geographic gradients in body size: A clarification of Bergmann's rule. *Diversity & Distributions* **5**, 165-174.

Boehlert, G. (1985). Using objective criteria and multiple regression models for age determination in fishes. *Fisheries Bulletin* **83**, 103-117.

Brown, J. H., Gillooly, J. F., Allen, A. P., Savage, V. M. & West, G. B. (2004). Toward a metabolic theory of ecology. *Ecology* **85**, 1771-1789.

Brunk, U. T. & Terman, A. (2002). Lipofuscin: Mechanisms of age-related accumulation and influence on cell function. *Free Radical Biology and Medicine* **33**, 611-619.

Buston, P. M., Munday, P. L. & Warner, R. R. (2004). Sex change and relative body size in animals. *Nature* **428**, 1.

Campana, S. E. (2001). Accuracy, precision and quality control in age determination, including a review of the use and abuse of age validation methods. *Journal of Fish Biology* **59**, 197-242.

Candi, G., Castriota, L., Andaloro, F., Finoia, M. G. & Marino, G. (2004). Reproductive cycle and sex inversion in razor fish, a protogynous labrid in the southern Mediterranean Sea. *Journal of Fish Biology* **64**, 1498-1513.

Cerrato, R. M. (1990). Interpretable Statistical Tests for Growth Comparisons Using Parameters in the Von Bertalanffy Equation. *Canadian Journal of Fisheries & Aquatic Sciences* **47**, 1416-1426.

Cerrato, R. M. (1991). Analysis of Nonlinearity Effects in Expected-Value Parameterizations of the Von Bertalanffy Equation. *Canadian Journal of Fisheries & Aquatic Sciences* **48**, 2109-2117.

Charnov, E. L. (1993). Life history invariants, some explorations of symmetry in evolutionary ecology. *Oxford University Press, New York, USA*.

Charnov, E. L. & Gillooly, J. F. (2004). Size and temperature in the evolution of fish life histories. *Integrative and Comparative Biology* **44**, 494-497.

Chen, Y., Jackson, D. A. & Harvey, H. H. (1992). A comparison of von Bertalanffy and polynomial functions in modelling fish growth data. *Canadian Journal of Fisheries and Aquatic Sciences* **49**, 1228-1235.

Choat, J. H., Axe, L. M. & Lou, D. C. (1996). Growth and longevity in fishes of the family Scaridae. *Marine Ecology Progress Series* **145**, 1-3.

Choat, J. H. & Ayling, A. M. (1987). The Relationship between Habitat Structure and Fish Faunas on New-Zealand Reefs. *Journal of Experimental Marine Biology and Ecology* **110**, 257-284.

Choat, J. H. & Clements, K. D. (1998). Vertebrate herbivores in marine and terrestrial environments: A nutritional ecology perspective. *Annual Review of Ecology and Systematics* **29**, 375-403.

Choat, J. H., Robbins, W. D. & Clements, K. D. (2004). The trophic status of herbivorous fishes on coral reefs - II. Food processing modes and trophodynamics. *Marine Biology* **145**, 445-454.

Choat, J. H. & Robertson, D. R. (1975). Protogynous hermaphroditism in fishes of the family Scaridae. *In: Intersexuality in the animal kingdom. Reinboth R (Ed), Springer-Verlag, Berlin*, 263-283.

Choat, J. H. & Robertson, D. R. (2002). Age-based studies on coral reef fishes. *In: Coral reef fishes, dynamics and diversity in a complex ecosystem.* **Sale PF (ed.), Academic Press, New York, USA**.

Choat, J. H., Robertson, D. R., Ackerman, J. L. & Posada, J. M. (2003). An age-based demographic analysis of the Caribbean stoplight parrotfish *Sparisoma viride*. *Marine Ecology-Progress Series* **246**, 265-277.

Claisse, J. T., Kienzle, M., Bushnell, M. E., Shafer, D. J. & Parrish, J. D. (2009). Habitat- and sex-specific life history patterns of yellow tang *Zebrasoma flavescens* in Hawaii, USA. *Marine Ecology Progress Series* **389**, 245-255.

Clarke, A. (2004). Is there a Universal Temperature Dependence of metabolism? *Functional Ecology* **18**, 252-256.

Clarke, A. (2006). Temperature and the metabolic theory of ecology. *Functional Ecology* **20**, 405-412.

Clarke, A. & Fraser, K. P. P. (2004). Why does metabolism scale with temperature? *Functional Ecology* **18**, 243-251.

Clarke, K. R. (1993). Nonparametric Multivariate Analyses of Changes in Community Structure. *Australian Journal of Ecology* **18**, 117-143.

Clarke, K. R. & Ainsworth, M. (1993). A Method of Linking Multivariate Community Structure to Environmental Variables. *Marine Ecology-Progress Series* **92**, 205-219.

Clarke, K. R., Somerfield, P. J. & Gorley, R. N. (2008). Testing of null hypotheses in exploratory community analyses: similarity profiles and biota-environment linkage *Journal of Experimental Marine Biology and Ecology* **366**, 56-69.

Clements, K. D. (1985). Feeding in two New Zealand herbivorous fish, the butterfish *Odax pullus* and the marblefish *Aplodactylus arctidens*. *MSc Thesis, University of Auckland, New Zealand*.

Clements, K. D. (2003). Herbivorous fishes. *In: The living reef - The ecology of New Zealand's rocky reefs. Craig Potton Publishing, Nelson, New Zealand*, 128-135.

Clements, K. D., Alfaro, M. E., Fessler, J. L. & Westneat, M. W. (2004). Relationships of the temperate Australasian labrid fish tribe Odacini (Perciformes; Teleostei). *Molecular Phylogenetics and Evolution* **32**, 575-587.

Clements, K. D. & Choat, J. H. (1993). Influence of season, ontogeny and tide on the diet of the temperate marine herbivorous fish *Odax pullus* (Odacidae). *Marine Biology* **117**, 213-220.

Clements, K. D., Raubenheimer, D. & Choat, J. H. (2009). Nutritional ecology of marine herbivorous fishes: ten years on. *Functional Ecology* **23**, 79-92.

Conover, D. O. (1990). The relation between capacity for growth and length of growing season: Evidence for and implications of countergradient variation. *Transactions of the American Fisheries Society* **19**, 416-430.

Conover, D. O., Arnott, S. A., Walsh, M. R. & Munch, S. B. (2005). Darwinian fishery science: lessons from the Atlantic silverside (*Menidia menidia*). *Canadian Journal of Fisheries & Aquatic Sciences* **62**, 730-737.

Conover, D. O., Brown, J. J. & Ehtisham, A. (1997). Countergradient variation in growth of young striped bass (*Morone saxatilis*) from different latitudes. *Canadian Journal of Fisheries and Aquatic Sciences* **54**, 2401-2409.

Conover, D. O. & Munch, S. B. (2002). Sustaining fisheries yields over evolutionary time scales. *Science* **297**, 94-96.

Conover, D. O. & Present, T. M. C. (1990). Countergradient variation in growth rate: compensation for length of the growing season among Atlantic silversides from different latitudes. *Oecologia* **83**, 316-324.

Conover, D. O. & Schultz, E. T. (1995). Phenotypic similarity and the evolutionary significance of countergradient variation. *Trends in Ecology & Evolution* **10**, 248-252.

Coulson, P. G., Hesp, S. A., Hall, N. G. & Potter, I. C. (2009). The western blue groper (*Achoerodus gouldii*), a protogynous hermaphroditic labrid with exceptional longevity, late maturity, slow growth, and both late maturation and sex change. *Fisheries Bulletin* **107**, 57-75.

Crabb, P. L. (1993). Reproduction in greenbone, *Odax pullus* (Teleostei, Odacidae). *MSc thesis, University of Otago, Dunedin, New Zealand*.

Craig, P. C. (1999). The Von Bertalanffy Growth Curve: When a good fit is not good enough. *Naga, The ICLARM Quaterly* **22**, 28-29.

Crossman, D. J., Choat, J. H. & Clements, K. D. (2005). Nutritional ecology of nominally herbivorous fishes on coral reefs. *Marine Ecology Progress Series* **296**, 129-142.

Daufresne, M., Lengfellner, K. & Sommer, U. (2009). Global warming benefits the small in aquatic ecosystems. *Proceedings of the National Academy of Sciences of the United States of America* **106**, 12788-12793.

de Jong, G. & van der Have, T. M. (2009). Temperature dependence of development rate, growth rate and size: from biophysics to adaptation. *In: Phenotypic plasticity of insects: mechanisms and consequences. Whitman D. W. & Ananthakrishnan T. N. (Eds). Science Publishers, Enfield, NH.*, 461-526.

Denny, C. M. & Schiel, D. R. (2001). Feeding ecology of the banded wrasse *Notolabrus fucicola* (Labridae) in southern New Zealand: prey items, seasonal differences, and ontogenetic variation. *New Zealand Journal of Marine and Freshwater Research* **35**, 925-933.

Denny, C. M. & Schiel, D. R. (2002). Reproductive biology and population structure of the banded wrasse, *Notolabrus fucicola* (Labridae) around Kaikoura, New Zealand. *New Zealand Journal of Marine and Freshwater Research* **36**, 555-563.

Duan, C. (1997). The insulin-like growth factor system and its biological actions in fish. *American Zoologist* **37**, 491-503.

Encarnacao, P. & Castro, M. (2001). The effect of fixatives in the quantification of morphological lipofuscin as an age index in crustaceans. *Hydrobiologia* **449**, 301-305.

Ewing, G. P., Welsford, D. C., Jordan, A. R. & Buxton, C. (2003). Validation of age and growth estimates using thin otolith sections from the purple wrasse, *Notolabrus fucicola*. *Marine and Freshwater Research* **54**, 985-993.

Fennessy, S. T. & Sadovy, Y. (2002). Reproductive biology of a diandric protogynous hermaphrodite, the serranid *Epinephelus andersoni*. *Marine and Freshwater Research* **53**, 147-158.

Finkel, T. & Holbrook, N. J. (2000). Oxidants, oxidative stress and the biology of ageing. *Nature* **408**, 239-247.

Fletcher, W. J. (1991). A test of the relationship between otolith weight and age for the pilchard *Sardinops neopilchardus*. *Canadian Journal of Fisheries & Aquatic Sciences* **48**, 35-38.

Floeter, S. R., Behrens, M. D., Ferreira, C. E. L., Paddack, M. J. & Horn, M. H. (2005). Geographical gradients of marine herbivorous fishes: patterns and processes. *Marine Biology* **147**, 1435-1447.

Fonseca, D. B., Sheehy, M. R. J., Blackman, N., Shelton, P. M. J. & Prior, A. E. (2005). Reversal of a hallmark of brain ageing: Lipofuscin accumulation. *Neurobiology of Aging* **26**, 69-76.

Francis, M. P. (2001). Coastal fishes of New Zealand, an identification guide. *Reed Publishing Ltd, Birkenhead, New Zealand*.

Francis, M. P., Williams, M. W., Pryce, A. C., Pollard, S. & Scott, S. G. (1993). Uncoupling of otolith and somatic growth in *Pagrus auratus* (Sparidae). *Fisheries Bulletin* **91**, 159-164.

Francis, R. I. C. C. (1988). Are Growth Parameters Estimated from Tagging and Age-Length Data Comparable. *Canadian Journal of Fisheries & Aquatic Sciences* **45**, 936-942.

Francis, R. I. C. C. (1990). Back-calculation of fish length: a critical review. *Journal of Fish Biology* **36**, 883-902.

Francis, R. I. C. C. & Campana, S. E. (2004). Inferring age from otolith measurements: a review and a new approach. *Canadian Journal of Fisheries and Aquatic Sciences* **61**, 1269-1284.

Francis, R. I. C. C., Harley, S. J., Campana, S. E. & Doering-Arjes, P. (2005). Use of otolith weight in length-mediated estimation of proportions at age. *Marine and Freshwater Research* **56**, 735-743.

Gaines, S. D. & Lubchenco, J. (1982). A unified approach to marine plant-herbivore interactions. II. Biogeography. *Annual Review of Ecology & Systematics* **13**, 111-138.

Gerking, S. D. (1957). Evidence of Aging in Natural Populations of Fishes. *Gerontologia* **1**, 287-305.

Gershman, R., Gilbert, D. L., Nye, S. W., Dwyer, P. & Fenn, W. O. (1954). Oxygen poisoning and X-irradiation - a mechanism in common *Science* **119**, 623-626.

Ghiselin, M. T. (1969). The evolution of hermaphroditism among animals. *Quaterly review of biology* **44**, 189-208.

Gillanders, B. M. (1995). Reproductive biology of the protogynous hermaphrodite Achoerodus viridis (Labridae) from south-eastern Australia. *Australian Journal of Marine and Freshwater Research* **46**, 999-1008.

Gillooly, J. F., Allen, A. P., Savage, V. M., Charnov, E. L., West, G. B. & Brown, J. H. (2006). Response to Clarke and Fraser: effects of temperature on metabolic rate. *Functional Ecology* **20**, 400-404.

Gillooly, J. F., Brown, J. H., West, G. B., Savage, V. M. & Charnov, E. L. (2001). Effects of size and temperature on metabolic rate. *Science* **293**, 2248-2251.

Gillooly, J. F., Charnov, E. L., West, G. B., Savage, V. M. & Brown, J. H. (2002). Effects of size and temperature on developmental time. *Nature* **417**, 70-73.

Gotz, A., Kerwath, S. E., Attwood, C. G. & Sauer, W. H. H. (2008). Effects of fishing on population structure and life history of roman *Chrysoblephus laticeps* (Sparidae). *Marine Ecology-Progress Series* **362**, 245-259.

Grier, H. J. (1981). Cellular organization of the testis and spermatogenesis in fishes. *American Zoologist* **21**, 345-357.

Gust, N., Choat, J. H. & Ackerman, J. L. (2002). Demographic plasticity in tropical reef fishes. *Marine Biology* **140**, 1039-1051.

Gust, N., Choat, J. H. & McCormick, M. I. (2001). Spatial variability in reef fish distribution, abundance, size and biomass: a multi-scale analysis. *Marine Ecology-Progress Series* **214**, 237-251.

Haddon, M. (2001). Modelling and quantitative methods in fisheries. *Chapman & Hall / CRC Press, Noca Raton, Florida, USA*.

Hamilton, R. J., Adams, S. & Choat, J. H. (2008). Sexual development and reproductive demography of the green humphead parrotfish (*Bolbometopon muricatum*) in the Solomon Islands. *Coral Reefs* **27**, 153-163.

Hamilton, S. L., Caselle, J. E., Standish, J. D., Schroeder, D. M., Love, M. S., Rosales-Casian, J. A. & Sosa-Nishizaki, O. (2007). Size-selective harvesting alters life histories of a temperate sex-changing fish. *Ecological Applications* **17**, 2268-2280.

Hammer, C. & Braum, E. (1988). Quantification of Age Pigments (Lipofuscin). *Comparative Biochemistry and Physiology B-Biochemistry & Molecular Biology* **90**, 7-17.

Harman, D. (1956). Aging: a theory based on free radical and radiation chemistry. *Journal of Gerontology* **11**, 298-300.

Harmelin-Vivien, M. L. (2002). Energetics and fish diversity on coral reefs. *in: Coral reef fishes, dynamics and diversity in a complex ecosystem, Sale P.F. (Ed), Academic Press, Elsevier Science (USA)*, 265-274.

Harshman, L. G. & Zera, A. J. (2007). The cost of reproduction: the devil in the details. *Trends in Ecology & Evolution* **22**, 80-86.

Heibo, E., Magnhagen, C. & Vollestad, L. A. (2005). Latitudinal variation in life-history traits in Eurasian perch. *Ecology* **86**, 3377-3386.

Hernaman, V., Munday, P. L. & Schlappy, M. L. (2000). Validation of otolith growth-increment periodicity in tropical gobies. *Marine Biology* **137**, 715-726.

Horn, M. H. (1989). Biology of marine herbivorous fishes. *Oceanography and Marine Biology. An annual review* **27**, 167-272.

Hunter, J. R. & Macewicz, B. J. (1985). Rates of atresia in the ovary of captive and wild northern anchovy, *Engraulis mordax*. *Fisheries Bulletin* **83**, 119-136.

Hutchings, J. A. (2004). Evolutionary biology - The cod that got away. *Nature* **428**, 899-900.

Imsland, A. K., Foss, A., Naevdal, G., Cross, T., Bonga, S. W., Ham, E. V. & Stefansson, S. O. (2000). Countergradient variation in growth and food conversion efficiency of juvenile turbot. *Journal of Fish Biology* **57**, 1213-1226.

Irlich, U. M., Terblanche, J. S., Blackburn, T. M. & Chown, S. L. (2009). Insect rate - temperature relationships: environmental variation and the Metabolic Theory of Ecology. *American Naturalist* **174**, 819-835.

James, F. C. (1970). Geographic size variation in birds and its relationship to climate. *Ecology* **51**, 365-390.

Jones, G. P. (1986). Food availability affects growth in a coral reef fish. *Oecologia* **70**, 136-139.

Juul, A., Bang, P., Hertel, N. T., Main, K., Dalgaard, P., Jorgensen, K., Muller, J., Hall, K. & Skakkebaek, N. E. (1994). Serum insulin-like growth factor-I in 1030 healthy children, adolescents, and adults: relation to age, sex, stage of puberty, testicular size, and body mass index. *Journal of Clinical Endocrinology and Metabolism* **78**, 744-752.

Kimura, D. K. (1980). Likelihood methods for the Von Bertalanffy growth curve. *Fisheries Bulletin* **77**, 765-776.

Kingsolver, J. G. & Huey, R. B. (2008). Size, temperature, and fitness: three rules. *Evolutionary Ecology Research* **10**, 251-268.

Kingsolver, J. G., Shlichta, J. G., Ragland, G. J. & Massie, K. R. (2006). Thermal reaction norms for caterpillar growth depend on diet. *Evolutionary Ecology Research* **8**, 703-715.

Knight, W. (1968). Asymptotic growth: an example of nonsense disguised as mathematics. *Journal Fisheries research board of Canada* **25**, 1303-1307.

Kokita, T. (2003). Potential latitudinal variation in egg size and number of a geographically widespread reef fish, revealed by common-environment experiments. *Marine Biology* **143**, 593-601.

Kokita, T. (2004). Latitudinal compensation in female reproductive rate of a geographically widespread reef fish. *Environmental Biology of Fishes* **71**, 213-224.

Kotrschal, K., van Staaden, M. J. & Huber, R. (1998). Fish brains: evolution and environmental relationships. *Reviews in Fish Biology and Fisheries* **8**, 373-408.

Kozlowski, J. (1992). Optimal allocation of resources to growth and reproduction: implications for age and size at maturity. *Trends in Ecology & Evolution* **7**, 15-19.

Kritzer, J. P., Davies, C. R. & Mapstone, B. D. (2001). Characterizing fish populations: Effects of sample size and population structure on the precision of demographic parameter estimates. *Canadian Journal of Fisheries & Aquatic Sciences* **58**, 1557-1568.

Leach, F. (2006). Fishing in pre-european New Zealand. *New Zealand Journal of Archaeology and archaeofauna* **15**.

Lee, K. P., Simpson, S. J., Clissold, F. J., Brooks, R., Ballard, J. W. O., Taylor, P. W., Soran, N. & Raubenheimer, D. (2008). Lifespan and reproduction in Drosophila: New insights from nutritional geometry. *Proceedings of the National Academy of Sciences of the United States of America* **105**, 2498-2503.

Limburg, K. E., Walther, Y., Hong, B., Olson, C. & Stora, J. (2008). Prehistoric versus modern Baltic Sea cod fisheries: selectivity across the millennia. *Proceedings of the Royal Society B-Biological Sciences* **275**, 2659-2665.

Liu, M. & Sadovy, Y. (2004). Early gonadal development and primary males in the protogynous epinepheline, *Cephalopholis boenak*. *Journal of Fish Biology* **65**, 987-1002.

Liu, M. & Sadovy, Y. (2009). Gonad development during sexual differentiation in hatchery-produced orange-spotted grouper (*Epinephelus coioides*) and humpback grouper (*Cromileptes altivelis*) (Pisces: Serranidae, Epinephelinae). *Aquaculture* **287**, 191-202.

Maklakov, A. A., Simpson, S. J., Zajitschek, F., Hall, M. D., Dessmann, J., Clissold, F., Raubenheimer, D., Bonduriansky, R. & Brooks, R. C. (2008). Sex-specific fitness effects of nutrient intake on reproduction and lifespan. *Current Biology* **18**, 1062-1066.

Manickchand-Heileman, S. C. & Phillip, D. A. T. (2000). Age and growth of the yellowedge grouper, *Epinephelus flavolimbatus*, and the yellowmouth grouper, *Mycteroperca interstitialis*, off Trinidad and Tobago. *Fisheries Bulletin* **98**, 290-298.

Martell, D. J., Kieffer, J. D. & Trippel, E. A. (2005). Effects of temperature during early life history on embryonic and larval development and growth in haddock. *Journal of Fish Biology* **66**, 1558-1575.

Maschner, H. D. G., Betts, M. W., Reedy-Maschner, K. L. & Trites, A. W. (2008). A 4500-year time series of Pacific cod (Gadus macrocephalus) size and abundance: archaeology, oceanic regime shifts, and sustainable fisheries. *Fisheries Bulletin* **106**, 386-394.

Mayr, E. (1956). Geographical character gradients and climatic adaptation. *Evolution* **10**, 105-108.

McBride, R. S. & Johnson, M. R. (2007). Sexual development and reproductive seasonality of hogfish (Labridae : *Lachnolaimus maximus*), an hermaphroditic reef fish. *Journal of Fish Biology* **71**, 1270-1292.

McBride, R. S. & Thurman, P. E. (2003). Reproductive biology of *Hemiramphus brasiliensis* and *H. balao* (Hemiramphidae): maturation, spawning frequency and fecundity. *Biological Bulletin* **204**, 57-67.

McMillan, D. B. (2007). Fish histology: female reproductive systems. *Springer (Ed.), Dordrecht, The Netherlands*.

Meekan, M. G., Ackerman, J. L. & Wellington, G. M. (2001). Demography and age structures of coral reef damselfishes in the tropical eastern Pacific Ocean. *Marine Ecology-Progress Series* **212**, 223-232.

Meekan, M. G., Vigliola, L., Hansen, A., Doherty, P. J., Halford, A. & Carleton, J. H. (2006). Bigger is better: size-selective mortality throughout the life history of a fast-growing clupeid, *Spratelloides gracilis*. *Marine Ecology-Progress Series* **317**, 237-244.

Metcalfe, N. B. & Monaghan, P. (2003). Growth versus lifespan: perspectives from evolutionary ecology. *Experimental Gerontology* **38**, 935-940.

Mommsen, T. P. (2001). Paradigms of growth in fish. *Comparative Biochemistry and Physiology B-Biochemistry & Molecular Biology* **129**, 207-219.

Monaghan, P., Metcalfe, N. B. & Torres, R. (2009). Oxidative stress as a mediator of life history trade-offs: mechanisms, measurements and interpretation. *Ecology Letters* **12**, 75-92.

Moore, S. E., Hesp, S. A., Hall, N. G. & Potter, I. C. (2007). Age and size compositions, growth and reproductive biology of the breaksea cod *Epinephelides armatus*, a gonochoristic serranid. *Journal of Fish Biology* **71**, 1407-1429.

Moulton, P. L., Walker, T. I. & Saddlier, S. R. (1992). Age and growth studies of Gummy Shark *Mustelus antarcticus* Gunther, and School Shark *Galeorhinus galeus* (Linnaeus), from Southern Australian waters. *Australian Journal of Marine and Freshwater Research* **43**, 1241-1267.

Mountfort, D. O., Campbell, J. & Clements, K. D. (2002). Hindgut fermentation in three species of marine herbivorous fish. *Applied and Environmental Microbiology* **68**, 1374-1380.

Mousseau, T. A. (1997). Ectotherms follow the converse to Bergmann's rule. *Evolution* **51**, 630-632.

Munch, S. B. & Salinas, S. (2009). Latitudinal variation in lifespan within species is explained by the metabolic theory of ecology. *Proceedings of the National Academy of Sciences of the United States of America* **106**, 13860-13864.

Munday, P. L., Buston, P. M. & Warner, R. R. (2006a). Diversity and flexibility of sex-change strategies in animals. *Trends in Ecology & Evolution* **21**, 89-95.

Munday, P. L., Hodges, A. L., Choat, J. H. & Gust, N. (2004). Sex-specific growth effects in protogynous hermaphrodites. *Canadian Journal of Fisheries & Aquatic Sciences* **61**, 323-327.

Munday, P. L., Kingsford, M. J., O'Callaghan, M. & Donelson, J. M. (2008). Elevated temperature restricts growth potential of the coral reef fish *Acanthochromis polyacanthus*. *Coral Reefs* **27**, 927-931.

Munday, P. L., Ryen, C. A., McCormick, M. I. & Walker, S. P. W. (2009). Growth acceleration, behaviour and otolith check marks associated with sex change in the wrasse Halichoeres miniatus. *Coral Reefs* **28**, 623-634.

Munday, P. L., White, J. W. & Warner, R. R. (2006b). A social basis for the development of primary males in a sex-changing fish. *Proceedings of the Royal Society B-Biological Sciences* **273**, 2845-2851.

Munoz, R. C. & Warner, R. R. (2003). A new version of the size-advantage hypothesis for sex change: Incorporating sperm competition and size-fecundity skew. *American Naturalist* **161**, 749-761.

Olsen, E. M., Heino, M., Lilly, G. R., Morgan, M. J., Brattey, J., Ernande, B. & Dieckmann, U. (2004). Maturation trends indicative of rapid evolution preceded the collapse of northern cod. *Nature* **428**, 932-935.

Packard, G. C. & Boardman, T. J. (1999). The use of percentages and size-specific indices to normalize physiological data for variation in body size: wasted time, wasted effort?

Comparative Biochemistry and Physiology a-Molecular and Integrative Physiology **122**, 37-44.
Pannella, G. (1971). Fish otoliths: daily growth layers and periodical patterns. *Science* **173**, 1124-1127.
Partridge, L., Barrie, B., Fowler, K. & French, V. (1994). Evolution and development of body size and cell size in *Drosophila melanogaster* in response to temperature. *Evolution* **48**, 1269-1276.
Partridge, L. & Brand, M. D. (2005). Special issue on dietary restriction: Dietary restriction, longevity and ageing-the current state of our knowledge and ignorance. *Mechanisms of Ageing and Development* **126**, 911-912.
Partridge, L. & French, V. (1996). Thermal evolution of ectotherm body size: why get big in the cold? In: Animals and Temperature - Phenotypic and Evolutionary Adaptation. Johnston Ian A. and Bennett Albert F. (Ed). Cambridge University Press. 265-292.
Partridge, L. & Gems, D. (2002). Ageing: A lethal side-effect. *Nature* **418**, 921-921.
Partridge, L., Gems, D. & Withers, D. J. (2005a). Sex and death: What is the connection? *Cell* **120**, 461-472.
Partridge, L., Pletcher, S. D. & Mair, W. (2005b). Dietary restriction, mortality trajectories, risk and damage. *Mechanisms of Ageing and Development* **126**, 35-41.
Partridge, L. & Sibly, R. (1991). Constraints in the evolution of life histories. *Phil. Trans. R. Soc. London B.* **332**, 3-13.
Paul, L. P. (1998). Butterfish - slippery, but they've got plenty of customers. *Seafood New Zealand*, 25-27.
Paul, L. P., Maolagain, C. O., Francis, M. P., Dunn, A. & Francis, R. I. C. C. (2000). Age, growth, mortality, and yield per recruit of butterfish (*Odax pullus*) in Cook Strait, New Zealand. *New Zealand Fisheries Assessment Report* **2000/6**, 30p.
Pawson, M. G. (1990). Using Otolith Weight to Age Fish. *Journal of Fish Biology* **36**, 521-532.
Pearl, P. (1928). The rate of living. *University of London, London*.
Pears, R. J., Choat, J. H., Mapstone, B. D. & Begg, G. A. (2006). Demography of a large grouper, *Epinephelus fuscoguttatus*, from Australia's Great Barrier Reef: implications for fishery management. *Marine Ecology-Progress Series* **307**, 259-272.
Perrin, N. (1995). About Berrigan and Charnov's life history puzzle. *Oikos* **73**, 137-139.
Philipp, E., Brey, T., Heilmayer, O., Abele, D. & Portner, H. O. (2006). Physiological ageing in a temperate and a polar swimming scallop. *Marine Ecology-Progress Series* **307**, 187-198.
Philipp, E., Brey, T., Portner, H. O. & Abele, D. (2005a). Chronological and physiological ageing in a polar and a temperate mud clam. *Mechanisms of Ageing and Development* **126**, 598-609.
Philipp, E., Portner, H. O. & Abele, D. (2005b). Mitochondrial ageing of a polar and a temperate mud clam. *Mechanisms of Ageing and Development* **126**, 610-619.
Pickard, R. (2000). Fetch effect analysis computer program, version 1.01:E. Villouta.
Porch, C. E., Wilson, C. A. & Nieland, D. L. (2002). A new growth model for red drum (*Sciaenops ocellatus*) that accommodates seasonal and ontogenic changes in growth rates. *Fisheries Bulletin* **100**, 149-152.
Quinn, G. P. & Keough, M. J. (2002). Experimental design and data analysis for biologists. *Cambridge University Press, Cambridge (UK)*.
Ray, C. (1960). The application of Bergmann's and Allen's rules to the poikilotherms. *Journal of Morphology* **106**, 85-108.

Reinboth, R. (1962). Morphologische und funktionelle Zweigeschlechtigkeit bei marinen Teleostiern (Serranidae, Sparidae, Centracanthidae, Labridae). *Zoologische Jahrbucher Physiologie Bd* **69**, 405-480.
Reinboth, R. (1967). Biandric teleost species. *General and Comparative Endocrinology* **9**, 486.
Reinboth, R. (1968). Protogynia in Parrot Fish (Scaridae). *Zeitschrift Fur Naturforschung Part B-Chemie Biochemie Biophysik Biologie Und Verwandten Gebiete* **B 23**, 852-&.
Reinboth, R. (1970). Intersexuality in fishes. *Memoirs of the Society for Endocrinology* **18**, 515-543.
Reinboth, R. (1975). Spontaneous and hormone-induced sex reversion in wrasses (Labridae). *Pubblicazioni della Stazione Zoologica di Napoli* **39 (Suppl.)**, 82-86.
Rensch, B. (1938). Some problems of geographical variation and species-formation. *Proceedings of the Linnean Society of London* **150**, 275-285.
Reznick, D., Ghalambor, C. & Nunney, L. (2002). The evolution of senescence in fish. *Mechanisms of Ageing and Development* **123**, 773-789.
Reznick, D., Lindbeck, E. & Bryga, H. (1989). Slower growth results in larger otoliths, an experimental test with guppies *Poecilia reticulata*. *Canadian Journal of Fisheries & Aquatic Sciences* **46**, 108-112.
Reznick, D. N. (1997). Life history evolution in guppies (*Poecila reticulata*): Guppies as a model for studying the evolutionary biology of aging. *Experimental Gerontology* **32**, 245-258.
Ricklefs, R. E. (2008). The evolution of senescence from a comparative perspective. *Functional Ecology* **22**, 379-392.
Ritchie, L. D. (1969). Aspects of the biology of the butterfish *Coridodax pullus* (Forster). *MSc thesis, Victoria University, Wellington, New Zealand*.
Robertson, D. R., Ackerman, J. L., Choat, J. H., Posada, J. M. & Pitt, J. (2005). Ocean surgeonfish *Acanthurus bahianus*. I. The geography of demography. *Marine Ecology-Progress Series* **295**, 229-244.
Robertson, D. R. & Warner, R. R. (1978). Sexual patterns in the Labroid fishes of the western Caribbean, II: the parrotfishes (Scaridae). *Smithsonian contributions to zoology* **255**, 1-26.
Rochet, M.-J. (2000). A comparative approach to life-history strategies and tactics among four orders of teleost fish. *Journal of Marine Science* **57**, 228-239.
Roff, D. A. (1980). A motion for the retirement of the Von Bertalanffy function. *Canadian Journal of Fisheries & Aquatic Sciences* **37**, 127-129.
Roff, D. A. (1984). The Evolution of Life-History Parameters in Teleosts. *Canadian Journal of Fisheries and Aquatic Sciences* **41**, 989-1000.
Roff, D. A. (1992). The evolution of life histories, theory and analysis. *Chapman & Hall, New York, USA*.
Roff, D. A. (2000). Trade-offs between growth and reproduction: an analysis of the quantitative genetic evidence. *Journal of Evolutionary Biology* **13**, 434-445.
Roff, D. A. & Fairbairn, D. J. (2007). The evolution of trade-offs: where are we? *Journal of Evolutionary Biology* **20**, 433-447.
Russell, B. C. (1988). Revision of the labrid fish genus *Pseudolabrus* and allied genera *Records of the Australian Museum* **9**, 1-76.
Ruttenberg, B. I., Haupt, A. J., Chiriboga, A. I. & Warner, R. R. (2005). Patterns, causes and consequences of regional variation in the ecology and life history of a reef fish. *Oecologia* **145**, 394-403.
Sadovy, Y., Kulbicki, M., Labrosse, P., Letourneur, Y., Lokani, P. & Donaldson, T. J. (2003). The humphead wrasse, *Cheilinus undulatus*: synopsis of a threatened and poorly known giant coral reef. *Reviews in Fish Biology and Fisheries* **13**, 327-364.

Sadovy, Y. & Liu, M. (2008). Functional hermaphroditism in teleosts. *Fish and Fisheries* **9**, 1-43.
Sadovy, Y. & Shapiro, D. Y. (1987). Criteria for the Diagnosis of Hermaphroditism in Fishes. *Copeia*, 136-156.
Schenker, N. & Gentleman, J. F. (2001). On judging the significance of differences by examining the overlap between confidence intervals. *American Statistician* **55**, 182-186.
Schiel, D. R. & Hickford, M. J. H. (2001). Biological structure of nearshore rocky subtidal habitats in southern New Zealand. *Science for conservation* **182**, 1-54.
Schnute, J. & Fournier, D. (1980). A new approach to length-frequency analysis - growth structure. *Canadian Journal of Fisheries & Aquatic Sciences* **37**, 1337-1351.
Schultz, E. T., Lankford, T. E. & Conover, D. O. (2002). The covariance of routine and compensatory juvenile growth rates over a seasonality gradient in a coastal fish. *Oecologia* **133**, 501-509.
Secor, D. H., Dean, J. M. & Campana, S. E. (1995). Recent developments in fish otolith research. *University of South Carolina Press, USA*.
Seehafer, S. S. & Pearce, D. A. (2006). You say lipofuscin, we say ceroid: Defining autofluorescent storage material. *Neurobiology of Aging* **27**, 576-588.
Shapiro, D. Y. & Rasotto, M. B. (1993). Sex-differentiation and gonadal development in the diandric protogynous wrasse *Thalassoma bifasciatum* (Pisces, Labridae). *Journal of Zoology* **230**, 231-245.
Shears, N. T. & Babcock, R. C. (2007). Quantitative description of mainland New Zealand's shallow subtidal reef communities. *Science for conservation* **280**, 1-126.
Sheehy, M. R. J. (1989). Crustacean Brain Lipofuscin - an Examination of the Morphological Pigment in the Fresh-Water Crayfish Cherax-Cuspidatus (Parastacidae). *Journal of Crustacean Biology* **9**, 387-391.
Sheehy, M. R. J. (1990). Individual Variation in, and the Effect of Rearing Temperature and Body Size on, the Concentration of Fluorescent Morphological Lipofuscin in the Brains of Fresh-Water Crayfish, Cherax-Cuspidatus (Crustacea, Parastacidae). *Comparative Biochemistry and Physiology a-Physiology* **96**, 281-286.
Sheehy, M. R. J. (1996). Quantitative comparison of in situ lipofuscin concentration with soluble autofluorescence intensity in the crustacean brain. *Experimental Gerontology* **31**, 421-432.
Sheehy, M. R. J., Shelton, P. M. J., Wickins, J. F., Belchier, M. & Gaten, E. (1996). Ageing the European lobster Homarus gammarus by the lipofuscin in its eyestalk ganglia. *Marine Ecology-Progress Series* **143**, 99-111.
Sibly, R. M. & Atkinson, D. (1994). How rearing temperature affects optimal adult size in ectotherms. *Functional Ecology* **8**, 486-493.
Simpson, S. J. & Raubenheimer, D. (2007). Caloric restriction and aging revisited: The need for a geometric analysis of the nutritional bases of aging. *Journals of Gerontology Series a-Biological Sciences and Medical Sciences* **62**, 707-713.
Skea, G. L., Mountfort, D. O. & Clements, K. D. (2005). Gut carbohydrases from the New Zealand marine herbivorous fishes *Kyphosus sydneyanus* (Kyphosidae), *Aplodactylus arctidens* (Aplodactylidae) and *Odax pullus* (Labridae). *Comparative Biochemistry and Physiology B* **140**, 259-269.
Skea, G. L., Mountfort, D. O. & Clements, K. D. (2007). Contrasting digestive strategies in four New Zealand herbivorous fishes as reflected by carbohydrase activity profiles. *Comparative Biochemistry and Physiology A* **146**, 63-70.
Smale, D. A. & Wernberg, T. (2009). Satellite-derived SST data as a proxy for water temperature in nearshore benthic ecology. *Marine Ecology Progress Series* **387**, 27-37.

Smit, A. J., Brearley, A., Hyndes, G. A., Lavery, P. S. & Walker, D. I. (2006). delta N-15 and delta C-13 analysis of a *Posidonia sinuosa* seagrass bed. *Aquatic Botany* **84**, 277-282.
Smith, T. B. (2008). Temperature effects on herbivory for an Indo-Pacific parrotfish in Panama: implications for coral-algal competition. *Coral Reefs* **27**, 397-405.
Stearns, S. C. (1989). Trade-offs in life-history evolution. *Functional Ecology* **3**, 259-268.
Stearns, S. C. (1992). The evolution of life histories. *Oxford University Press, New York.*
Stearns, S. C. & Koella, J. C. (1986). The evolution of phenotypic plasticity in life history traits - predictions of reaction norms for age and size at maturity. *Evolution* **40**, 893-913.
Stillwell, R. C., Wallin, W. G., Hitchcock, L. J. & Fox, C. W. (2007). Phenotypic plasticity in a complex world: interactive effects of food and temperature on fitness components of a seed beetle. *Oecologia* **153**, 309-321.
Summerfelt, R. C. & Hall, G. E. (1987). Age and growth of fish. *Iowa State University Press, USA*.
Taylor, D. I. & Schiel, D. R. (2009). Algal populations controlled by fish herbivory across a wave exposure gradient on southern temperate shores. *Ecology* **In press**.
Terman, A. & Brunk, U. T. (1998). Lipofuscin: Mechanisms of formation and increase with age. *Apmis* **106**, 265-276.
Terman, A. & Brunk, U. T. (2004). Lipofuscin. *International Journal of Biochemistry & Cell Biology* **36**, 1400-1404.
Terman, A. & Brunk, U. T. (2006). Oxidative stress, accumulation of biological 'garbage', and aging. *Antioxidants & Redox Signaling* **8**, 197-204.
Terzibasi, E., Lefrancois, C., Domenici, P., Hartmann, N., Graf, M. & Cellerino, A. (2009). Effects of dietary restriction on mortality and age-related phenotypes in the short-lived fish *Nothobranchius furzeri*. *Aging Cell* **8**, 88-99.
Terzibasi, E., Valenzano, D. R., Benedetti, M., Roncaglia, P., Cattaneo, A., Domenici, L. & Cellerino, A. (2008). Large differences in aging phenotype between strains of the short-lived annual fish *Notobranchius furzeri*. *PLoS ONE* **3**, 1-13.
Thorrold, S. R. & Milicich, M. J. (1990). Comparison of larval duration and presettlement and postsettlement growth in 2 species of damselfish, *Chromis atripectoralis* and *Pomacentrus coelestis* (Pisces, Pomacentridae), from the Great Barrier Reef. *Marine Biology* **105**, 375-384.
Tracey, D. M. & Horn, P. L. (1999). Background and review of ageing orange roughy (*Hoplostethus atlanticus*, Trachichthyidae) from New Zealand and elsewhere. *New Zealand Journal of Marine & Freshwater Research* **33**, 67-86.
Trip, E. L., Choat, J. H., Wilson, D. T. & Robertson, D. R. (2008). Inter-oceanic analysis of demographic variation in a widely distributed Indo-Pacific coral reef fish. *Marine Ecology-Progress Series* **373**, 97-109.
Valenzano, D. R., Terzibasi, E., Cattaneo, A., Domenici, L. & Cellerino, A. (2006). Temperature affects longevity and age-related locomotor and cognitive decay in the short-lived fish Nothobranchius furzeri. *Aging Cell* **5**, 275-278.
van der Have, T. M. & de Jong, G. (1996). Adult size in ectotherms: temperature effects on growth and differentiation. *Journal of Theoretical Biology* **183**, 329-340.
van Voorhies, W. A. (1996). Bergmann size clines: a simple explanation for their occurrence in ectotherms. *Evolution* **50**, 1259-1264.
Walker, S. P. W., Ryen, C. A. & McCormick, M. I. (2007). Rapid larval growth predisposes sex change and sexual size dimorphism in a protogynous hermaphrodite, *Parapercis snyderi* Jordan & Starks 1905. *Journal of Fish Biology* **71**, 1347-1357.
Wallace, R. A. & Selman, K. (1981). Cellular and dynamic aspects of oocyte growth in Teleosts. *American Zoologist* **21**, 325-343.

Warner, R. R. (1975). Reproductive biology of the protogynous hermaphrodite *Pimelometopon pulchrum* (Pisces; Labridae). *Fisheries Bulletin* **73**, 262-283.
Warner, R. R. (1984). Mating behavior and hermaphroditism in coral reef fishes. *The American Scientist* **72**, 128-136.
Warner, R. R. & Robertson, D. R. (1978). Sexual patterns in the Labroid fishes of the western Caribbean, I: the wrasses (Labridae). *Smithsonian contributions to zoology* **254**, 1-25.
Wellenreuther, M., Syms, C. & Clements, K. D. (2008). Body size and ecological diversification in a sister species pair of triplefin fishes. *Evolutionary Ecology* **22**, 575-592.
Welsford, D. C. (2003). Interpretation of otolith microstructure in the early life history stages of two temperate reef wrasses (Labridae). *Marine & Freshwater Research* **54**, 69-75.
Welsford, D. C., Jordan, A. R. & Smolenski, A. J. (2004). Description and genetic identification of the early life-stages of *Notolabrus fucicola* and *N. tetricus* from Tasmanian waters, Australia, with notes on their newly-settled juveniles. *New Zealand Journal of Marine & Freshwater Research* **38**, 267-277.
Welsford, D. C. & Lyle, J. M. (2005). Estimates of growth and comparisons of growth rates determined from length- and age-based models for populations of purple wrasse (*Notolabrus fucicola*). *Fisheries Bulletin* **103**, 697-711.
West, G. (1990). Methods of assessing ovarian development in fishes: a review. *Australian Journal of Marine and Freshwater Research* **41**, 199-222.
Westneat, M. W. & Alfaro, M. E. (2005). Phylogenetic relationships and evolutionary history of the reef fish family Labridae. *Molecular Phylogenetics and Evolution* **36**, 370-390.
Williams, A. J., Currey, L. M., Begg, G. A., Murchie, C. D. & Ballagh, A. C. (2008). Population biology of coral trout species in eastern Torres Strait: Implications for fishery management. *Continental Shelf Research* **28**, 2129-2142.
Williams, A. J., Davies, C. R. & Mapstone, B. D. (2005). Variation in the periodicity and timing of increment formation in red throat emperor (*Lethrinus miniatus*) otoliths. *Marine and Freshwater Research* **56**, 529-538.
Wood, A. W., Duan, C. M. & Bern, H. A. (2005). Insulin-like growth factor signaling in fish. *International Review of Cytology* **243**, 215-285.
Yamahira, K. & Conover, D. O. (2002). Intra- vs. interspecific latitudinal variation in growth: Adaptation to temperature or seasonality? *Ecology* **83**, 1252-1262.
Young, P. C. & Martin, R. B. (1982). Evidence for Protogynous Hermaphroditism in Some Lethrinid Fishes. *Journal of Fish Biology* **21**, 475-484.
Zar, J. H. (1999). Biostatistical analysis (4th edition). *Prentice-Hall International Inc, Upper Saddle River, New Jersey, USA*.